PROCEEDINGS OF THE 23rd ANNUAL INTERNATIONAL CONFERENCE ON SOIL, WATER, ENERGY & AIR

Volume 1

Proceedings of the 23rd Annual International Conference on Soil, Water, Energy & Air

Volume 1

Bioremediation
Engineered Remediation
Hydrocarbons
Metals
Modeling
Site Characterization

Selected manuscripts from the
23rd Annual International Conference on Soil, Water, Energy & Air
San Diego, CA
March 18 - 21, 2013

Editors

Paul T. Kostecki
Edward J Calabrese
Christopher M. Teaf
David F. Ludwig

ISBN 978-0-9888932-0-7

AEHS Foundation, Inc., and Amherst Scientific Publishers
150 Fearing Street, Suite 21
Amherst, MA 01002
www.AEHSFoundation.org

Table of Contents

Contributing authors *i*

Foreword *iv*

About the Editors *v*

Part I: Bioremediation

1. **BIOLOGICAL TREATMENT OF PCB-CONTAMINATED SOIL INOCULATED WITH RHIZOSPHERE ORGANISMS AND PLANTED WITH CHROMOLAENA ODORATA (L) KING & ROBINSON** 1
Harrison Ifeanyichukwu Atagana

2. **PHYTOREMEDIATION OF ESCRAVOS (NIGERIA) LIGHT CRUDE OIL CONTAMINATED SOIL USING LEGUMES** 24
Maryam Lami Ibrahim, Udeme Josiah J. Ijah, Lawal S. Bilbis and Shuaibu Bala Manga

Part II: Engineered Remediation

3. **REMEDIATION OF MTBE & TBA IN GROUNDWATER USING A FLUIDIZED BED BIOREACTOR** 42
Joseph E. O'Connell

4. **NANOMAGNETITE - ZEOLITE COMPOSITES TO BE USED IN ENVIRONMENTAL REMEDIATION OF ANIONIC CONTAMINANTS IN WATER BODIES** 60
Carmen Pizarro, María Fernanda Albornoz, Daniela Muñoz, José Domingos Fabris, Mónica Antilén, and Mauricio Escudey

Part IV: Hydrocarbons

5. **FORMATION OF OIL-LIKE PRODUCTS BY HYDROUS PYROLYSIS OF SCRAP TIRES AT TEMPERATURES FROM 150^{O}C TO 350^{O}C** 68
Ahmed I. Rushdi, Abdulgader Y. BaZeyad, Abdurahman S. Al-Awadi, Khalid F. Al-Mutlaq and Bernd R. T. Simoneit

6. **TREATMENT OF 1,4-DIOXANE IN GROUNDWATER** 80
Randy Putnam and Susan Welt

Part V: Metals

7. **TRACE METAL CONTENTS OF FERTILIZERS MARKETED IN LEBANON** 98
Isam Bashour, Rita Wakim, Nay Dia and Jessica El Asmar

8. **IS IT CHROMIUM III OR CHROMIUM VI? ARE YOU SURE?** 113
Robert Wellbrock, and Anthony Rattonetti

Part VI: Modeling

9. **MODELING OF CONTAMINANT TRANSPORT IN POROUS MEDIA UNDER FLUCTUATING WATER TABLE CONDITION USING COMSOL MULTIPHYSICS® PLATFORM** 125
S. Lukman and M.S. Al-Suwaiyan

10. **SIMULATION MODELING OF ARSENIC DYNAMICS & REMOVAL IN CONTAMINATED GROUNDWATER** 137
Michael Miyittah, James Jones, Samuel Adiku, Dean Rhue, Craig Stanley and Jack Rechcigl

11. **BIODEGRADATION KINETICS OF PETROLEUM DERIVATIVES IN WASTEWATER THROUGH RESPIROMETRY DATA MODELING** 145
Renato N. Montagnolli, Paulo Renato M. Lopes, Ivo S. Tamada, Jaqueline M. Cruz, Mariana L. Sousa, and Ederio D. Bidoia

12. **A QSAR MODEL FOR THE PREDICTION OF DRUG BINDING AFFINITIES TO HUMAN SERUM ALBUMIN** 162
Serli Onlu, Gulcin Tugcu, and Melek Türker Saçan

Part VII: Site Characterization

13. **LNAPL INVESTIGATION AND BEHAVIOR IN A SAPROLITE AQUIFER** 173
Christopher J. Mulry, and Don A. Lundy

14. **DETERMINATION OF MERCURY IN ENVIRONMENTAL SAMPLES** 194
Anthony Rattonetti, Mike Salvato, Grant Mays, Mike Nguyen, and Steven Z. Wen

Index 211

Contributing Authors:

Samuel Adiku, University of Ghana, Soil Science Department, P.O. Box 245, Legon, Accra, Ghana
Abdurahman S. Al-Awadi, Department of Chemical Engineering, College of Engineering, King Saud University, Riyadh 11451, Saudi Arabia
Khalid F. Al-Mutlaq, Chair of Green Energy Research and Plant Protection Department, College of Food and Agricultural Sciences, King Saud University, P.O. Box 2460, Riyadh 11451, Saudi Arabia
Mohammad Al-Suwaiyan, KFUPM, Dhahran, Saudi Arabia, 31261
María Fernanda Albornoz, Universidad de Santiago de Chile, Av. L. Bernardo O'Higgins 3363, Santiago, Chile, 725475
Mónica Antilén, Pontificia Universidad Católica de Chile, Av. L. B. O'Higgins 3363, Santiago, Chile, 7820436
Harrison Atagana, University of South Africa, Institute for Science and Technology Education, P.O. Box 392 UNISA, South Africa, 3
Isam Bashour, American University of Beirut, Faculty of Agricultural and Food Sciences, Bliss Street, Beirut, Lebanon, 11-0236
Abdulgader Y. BaZeyad, Chair of Green Energy Research and Plant Protection Department, College of Food and Agricultural Sciences, King Saud University, P.O. Box 2460, Riyadh 11451, Saudi Arabia
Ederio D. Bidoia, São Paulo State University, Avenida 24 A, 1515, Rio Claro, SP, Brazil, 13506-900
Lawal S. Bilbis, Usmanu Danfodiyo University, Sokoto, Nigeria, PMB 2346
Jaqueline M. Cruz, São Paulo State University, Avenida 24 A, 1515, Rio Claro, SP, Brazil, 13506-900
Nay Dia, American University of Beirut, Faculty of Agricultural and Food Sciences, Bliss Street, Beirut, Lebanon, 11-0236
Jessica El Asmar, American University of Beirut, Faculty of Agricultural and Food Sciences, Bliss Street, Beirut, Lebanon, 11-0236
Mauricio Escudey, Universidad de Santiago de Chile, Av. L. B. O'Higgins 3363, CEDENNA. Av. L. B. O'Higgins 3363, Santiago, Estación Central, Chile, 725475
José Domingos Fabris, Universidade Federal de Minas Gerais, Minas Gerais, Brazil, 31270-901
Maryam Lami Ibrahim, Usmanu Danfodiyo University, Sokoto, Nigeria, PMB 2346
Udeme Josiah J. Ijah, Federal University of Technology, Niger, Nigeria, PMB 65
James Jones, University of Florida, 289 Frazier Rogers Hall, P.O. Box 110570, Gainesville, FL, 32611-0570
Paulo Renato M. Lopes, São Paulo State University, Avenida 24 A, 1515, Rio Claro, SP, Brazil, 13506-900
Salihu Lukman, KFUPM, Dhahran, Saudi Arabia, 31261
Don A. Lundy, P.G, Groundwater & Environmental Services, Inc., 6655 Peachtree Dunwoody Road, Atlanta, GA, 30328, USA
Shuaibu Bala Manga, Usmanu Danfodiyo University, Sokoto, Nigeria, PMB 2346
Grant Mays, Southeast Laboratory San Francisco Public Utilities Commission, 750 Phelps Street, San Francisco, California, USA, 94124

Michael Miyittah, University of Cape Coast, Department of Environmental Science, Cape Coast, Ghana
Renato N. Montagnolli, São Paulo State University, Avenida 24 A, 1515, Rio Claro, SP, Brazil, 13506-900
Christopher J. Mulry, Groundwater & Environmental Services, Inc., 1350 Blair Drive, Suite A, Odenton, MD, 21113, USA
Mike Nguyen, Southeast Laboratory San Francisco Public Utilities Commission, 750 Phelps Street, San Francisco, California, USA, 94124
Joseph E. O'Connell, Cardno ERI, 25371 Commercentre Drive, Suite 250, Lake Forest, CA 92630
Serli Onlu, Bogazici University, Institute of Environmental Sciences, 34342, Bebek, Istanbul, Turkey
Carmen Pizarro, Universidad de Santiago de Chile, Av. L. Bernardo O'Higgins 3363, Santiago, Chile, 725475
Randy Putnam, EnviroGroup, A Geosyntec Company, 7009 S. Potomac Street, Suite 300, Centennial, CO, 80112
Anthony Rattonetti, Southeast Laboratory San Francisco Public Utilities Commission, 750 Phelps Street, San Francisco, California, 94124, USA
Jack Rechcigl, University of Florida, Gulf Coast Research and Education Center, 14625 CR 672, Wimauma, FL, 33598
Dean Rhue, University of Florida, Soil and Water Science Department, P. O. Box 110290, Gainesville, FL, 32611
Ahmed I. Rushdi, Chair of Green Energy Research and Plant Protection Department, College of Food and Agricultural Sciences, King Saud University, P.O. Box 2460, Riyadh 11451, Saudi Arabia and Department of Geosciences, Oregon State University, Corvallis, OR, 97331, U.S.A.
Mike Salvato, Southeast Laboratory San Francisco Public Utilities Commission, 750 Phelps Street, San Francisco, California, USA, 94124
Bernd R. T. Simoneit, King Saud University, College of Food and Agricultural Sciences, P.O. Box 2460, Riyadh 11451, Saudi Arabia and Department of Chemistry, Oregon State University, Corvallis, OR, 97331, U.S.A.
Mariana L. Sousa, São Paulo State University, Avenida 24 A, 1515, Rio Claro, SP, Brazil, 13506-900
Craig Stanley, University of Florida, Gulf Coast Research and Education Center, 14625 CR 672, Wimauma, FL, 33598
Ivo S. Tamada, São Paulo State University, Avenida 24 A, 1515, Rio Claro, SP, Brazil, 13506-900
Gulcin Tugcu, Bogazici University, Institute of Environmental Sciences, 34342, Bebek, Istanbul, Turkey
Melek Türker Saçan, Bogazici University, Institute of Environmental Sciences, 34342, Bebek, Istanbul, Turkey
Rita Wakim, American University of Beirut, Faculty of Agricultural and Food Sciences, Bliss Street, Beirut, Lebanon, 11-0236

Robert Wellbrock, Southeast Laboratory San Francisco Public Utilities Commission, 750 Phelps Street, San Francisco, CA, 94124
Susan Welt, EnviroGroup, a Geosyntec Company, 26 Century Hill Drive, Suite 205, Latham, NY, 12110
Steven Z. Wen, Southeast Laboratory San Francisco Public Utilities Commission, 750 Phelps Street, San Francisco, California, USA, 94124

Foreword

The International Conference on Soil, Water, Energy, and Air had its beginnings in petroleum contaminated soils in 1990, supported by a few interested parties. It has evolved to encompass a broad range of important contaminants in different media, drawing interest from around the world. This prestigious annual conference, with its East Coast sibling, is among the most significant and influential environmental conferences in the world. It regularly draws more than 200 presenters, and as many as 700 participants, from nearly all 50 states, and over 40 countries worldwide.

What is common logic for addressing all types of sites that exhibit the environmental contamination of soils, groundwater, surface water and sediments? Everyone reading this volume knows from their personal and professional perspective how the fundamental process operates. Put together a conceptual picture of the issues, understand the site-specifics of the contaminant distribution and magnitude in the various environmental matrices, research the present and future constraints on uses of the property, formulate the appropriate remediation methods, and develop the cleanup engineering plan. It's a tried and tested process that has helped clean up contaminated sites throughout North America and around the globe.

The papers that are included in this volume, reflecting a number of presentations from the 23rd Annual West Coast Conference, mirror the logic of the process for addressing contaminated media. The articles in the Modeling and Site Characterization section provide the conceptual foundations related to site investigation and fate/transport, those in the Metals and Organics element address site-specific chemistry at various common types of sites, while the Bioremediation and Engineered Remediation papers describe various aspects of the state-of-the-art in cleanup methodologies and approaches.

Taken together as an integrated volume, this edition provides a valuable and representative snapshot of the existing state of environmental response science and engineering, as reflected by participants at the 23rd Annual Conference, developed and coordinated by AEHS Foundation, Inc. As the latest product from a long-running series of symposia, these proceedings discuss and document the potential problems, effective solutions, and remarkable innovations that have allowed our field of practice to make substantive progress in managing environmental issues for a cleaner, safer, and richer future.

David F. Ludwig, Ph.D.
Arcadis U.S.

Christopher M. Teaf, Ph.D.
Florida State University

About the Editors

Dr. Paul T. Kostecki's professional career has focused on research, education and training in environmental contamination with an emphasis on human and ecological risk assessment and risk management of soils. His work includes soil ingestion estimates for children and adults; establishment of scientifically sound cleanup levels for soil; bioavailability of soil contaminants; fish as toxicological models for contamination assessment; and assessment and management of petroleum contaminated soils. Dr. Kostecki has developed and conducted over 55 conferences, workshops and courses both nationally and internationally, and has made presentations at over 100 national and international meetings. Since 1985, his conference at the University of Massachusetts Amherst on Contaminated Soils, Sediments and Water has attracted over 10,000 environmental professionals from over 50 countries. Dr. Kostecki has published over 100 articles and reports, co-edited/co-authored 35 Books and secured over $15M in research support.

Dr. Kostecki co-created the Association for Environmental Health and Sciences (AEHS) in 1989 and served as its Executive Director until 2009. In 2009, he established the AEHS Foundation. He helped found Amherst Scientific Publishers and co-created seven peer-reviewed journals: Journal of Soil and Sediment Contamination (1990); Human and Ecological Risk Assessment (1994); Journal of Phytoremediation (1998); Journal of Environmental Forensics (1999); Journal of Children's Health (2003); Non-Linearity Journal (2003); and Journal of Medical Risks (2004). In addition, Dr. Kostecki co-created the International Society for Environmental Forensics in 2002.

Dr. Kostecki served as Vice Provost for Research and Vice Chancellor for Research and Engagement at the University of Massachusetts Amherst from 2003 to 2009. He served as Special Advisor for the Clean Energy China Initiative, Office of the President, University of Massachusetts from 2009–2011. He briefly left the University of Massachusetts Amherst to establish the online education program for Simmons College, Boston, MA (2011 -2012). He is presently xi Professor of Environmental Health in the School of Public Health and Health Sciences, University of Massachusetts, Amherst.

Dr. Edward J. Calabrese is a Professor of Toxicology at the University of Massachusetts, School of Public Health and Health Sciences, Amherst. Dr. Calabrese has researched extensively in the area of host factors affecting susceptibility to pollutants, and is the author of over 750 papers in scholarly journals, as well as more than 10 books, including Principles of Animal Extrapolation; Nutrition and Environmental Health, Vols. I and II; Ecogenetics; Multiple Chemical Interaction; Air Toxics and Risk Assessment; and Biological Effects of Low Level Exposures to Chemical and Radiation. Along with Mark Mattson (NIH) he is a co-editor of the recently published book entitled Hormesis: A Revolution in Biology, Toxicology and Medicine. He has been a member of the U.S. National Academy of Sciences and NATO Countries Safe Drinking Water committees, and on the Board of Scientific Counselors for the Agency for Toxic Substances and Disease Registry (ATSDR). Dr. Calabrese also serves as Chairman of the Biological Effects of Low Level Exposures (BELLE) and as Director of the Northeast Regional Environmental Public Health Center at the University of Massachusetts. Dr. Calabrese was awarded the 2009 Marie Curie Prize for his body of work on hormesis. He was the recipient of the International Society for Cell Communication and Signaling-Springer award for 2010. Dr. Calabrese will receive an honorary Doctor of Science from McMaster University, Hamilton, Ontario 2013. Over the past 20 years Professor Calabrese has redirected his research to

understanding the nature of the dose response in the low dose zone and underlying adaptive explanatory mechanisms. Of particular note is that this research has led to important discoveries which indicate that the most fundamental dose response in toxicology and pharmacology is the hormetic-biphasic dose response relationship. These observations are leading to a major transformation in improving drug discovery, development, and in the efficiency of the clinical trial, as well as the scientific foundations for risk assessment and environmental regulation for radiation and chemicals.

Dr. David F. Ludwig is a systems ecologist by training and a risk assessor by trade. He took an undergraduate Bachelor of Science degree from Rutgers University, a Master's in Marine Biology at the Virginia Institute of Marine Sciences, and a PhD in Systems Ecology at the University of Georgia Institute of Ecology. His career linked environmental consulting with university teaching. He worked in academia, the private sector, and for regulatory agencies, a breadth of background the gives him unique perspectives on environmental matters.

Dave's career spanned the globe. He worked in mainland Asia, Pacific Oceania, the Middle East, Europe, the Caribbean, and throughout North America. He is broadly published in the technical literature, and co-author of books on urban ecology and the ecology and toxinology of true viper snakes. He provides weekly insights regarding environmental sustainability in a column published on the AEHS Foundation web site, titled "PeopleSystems and Sustainability: This Week in the Global Environment".

Dr. Christopher M. Teaf is a Board-certified toxicologist with broad experience in evaluation of potential effects from chemical exposures related to industrial facilities, agriculture, waste management facilities, power generation, educational institutions, and products in general commerce. Dr. Teaf has served on the faculty of the Center for Biomedical & Toxicological Research at Florida State University since 1979, and as Director of Toxicology for Hazardous Substance & Waste Management Research since 1985.

Chris' areas of interest include risk assessments under environmental and occupational elements of federal, state or local regulations, risk communication, and development of risk-based targets to guide remedial actions. He has extensive experience in evaluation of environmental fate and potential health effects from petroleum, solvents, metals, pesticides, pharmaceuticals, biological agents (e.g., mold, microbes) and physical agents (e.g., particulates, asbestos. For over 30 years, he has directed or conducted research in environmental and occupational toxicology for the World Health Organization, NATO, U.S. EPA, U.S. Air Force, U.S. Department of Agriculture (USDA), Florida Department of Environmental Protection, Florida Department of Health, Florida Department of Community Affairs, and Agency for Toxic Substances & Disease Registry (ATSDR), among others. He served as Toxicologist for the Florida Landfill Technical Advisory Group and the state Petroleum Technical Advisory Committee. He served on the Florida Governor's Financial and Technical Advisory Committee and was Chair of the Toxic Substances Advisory Council for the Florida Department of Labor. Chris has organized and taught many graduate and undergraduate courses and technical seminars for presentation to universities as well as international, federal, state and local agencies. He has served as Chair of the Dog Island Conservation District since 2004.

Dr. Teaf has served on editorial boards or as peer reviewer for a variety of journals and is Senior Editor for Human Health of the international journal *Human & Ecological Risk Assessment*. In addition to training, research and advisory services to many environmental

agencies and private sector firms, he has provided environmental and toxicological services to the U.S. Attorney, Florida State Attorney, and Attorneys General of FL, OK, and WA. Chris has been qualified as an expert in federal and state courts, as well as administrative proceedings, in a number of states regarding toxicology, health risk assessment, and environmental chemistry.

PART I: Bioremediation

Chapter 1

BIOLOGICAL TREATMENT OF PCB-CONTAMINATED SOIL INOCULATED WITH RHIZOSPHERE ORGANISMS AND PLANTED WITH CHROMOLAENA ODORATA (L) KING & ROBINSON

Harrison Ifeanyichukwu Atagana[§]
Institute for Science and Technology Education, University of South Africa, P.O. Box 392, Pretoria 0003, South Africa

ABSTRACT

Soil containing Aroclor-1260 (10%, 30% and 50%) and transformer oil (10%, 20% and 30%) with known polychlorinated biphenyl (PCB) congeners was inoculated with enriched rhizosphere organisms and planted with *Chromolaena odorata* to study the phytoextraction of PCB from the soil under greenhouse conditions. Moisture was maintained at 60%. NPK fertilizer (5%) was applied, and the experiment was kept in a greenhouse with temperature control for ten weeks. Plant growth, enzyme activities and PCB concentration in soil and plant tissues were measured. Rhizosphere microorganisms were characterized by16S rDNA base sequencing. PCB did not affect plant growth in the 10% and 30% Aroclor-1260 and 10% and 20% transformer oil experiments. However, Aroclor-1260 at 50% and transformer oil at 30% impeded plant growth. Enzyme activities in the soil increased in the Aroclor-1260 and the 10% transformer oil experiments from week 1. Enzyme activities were slower in the 20% and 30% transformer oil experiments. There was a significant difference in the reduction of PCB in the Aroclor-1260 and transformer oil experiments. There was between 47% and 87% reduction in the Aroclor-1260 experiments and between 42% and 82% in the transformer oil experiments. There was a higher concentration of PCBs in the

[§] Corresponding Author: Harrison Atagana, Institute for Science and Technology Education, University of South Africa, P.O. Box 392, Pretoria 0003, South Africa, 124293903, atagahi@unisa.ac.za

roots of all experimental plants than in the shoots. Overall, plants in the Aroclor experiments showed higher levels of PCBs in the tissues than those in transformer oil experiments. Experiments inoculated with rhizosphere organisms did not show any significant difference in growth, PCB reduction in soil, or concentration in plant tissues when compared to non-inoculated experiments. Although *Chromolaena odorata* has demonstrated the ability to grow in and extract PCB from contaminated soil, it is not clear whether degradation of PCB occurred in plant tissues or in the soil. However, the difference in PCB recovered from the soil and plant may be due to biodegradation, volatilization or translocation, or a combination of two or all three processes. This study has demonstrated that *Chromolaena odorata* shows potential for further investigation as a phytoremediation agent for PCB contaminated soil.

Keywords: Aroclor-1260, phytoremediation, rhizosphere organisms, soil, transformer oil.

1. INTRODUCTION

Polychlorinated biphenyls (PCBs) are a group of compounds produced commercially by direct chlorination of biphenyl molecules (two connecting benzene rings) (Figure 1) with one or more chlorine atoms replacing the carbon atoms of the biphenyl nucleus (Annema *et al*., 1995). PCBs consist of 209 congeners with the empirical formula $C_{12}H_{10-n}CL_n$ (n=1-10) (Larsson *et al*., 2000; Gray, 2004; Gray *et al*., 2005). Aroclor 1254 and 1260 are commercial examples of PCBs, although other brand names exist. The first two digits designate the number of carbon atoms in the molecule while the last two indicate chlorine weight by percentage in each type (Cogliano, 1998).

Environmental contamination by PCBs became obvious when Jenson reported a high level of PCBs in a white-tailed sea eagle found dead on the Stockholm archipelago in 1966 (Andersson, 2000). Since then, PCBs have been found in all environmental compartments including water, soil, and air, even in the Polar Regions. The main channels through which PCBs enter the environment include dumps, landfills, combustion and application in many industrial and domestic appliances, which results in exposure to wildlife and humans (Giesy and Kannan, 1998; Safe, 1994; Van den Berg *et al*., 1998). The toxicity of PCBs became known to the public as a result of the Yusho incident in Japan in 1968, where more than 1800 persons suffered from toxicity due to consumption of contaminated rice oil (Kuratsune *et al*., 1996). Subsequently, the production of PCBs in Sweden and many other industrial countries has been restricted since the 1970s (Andersson, 2000).

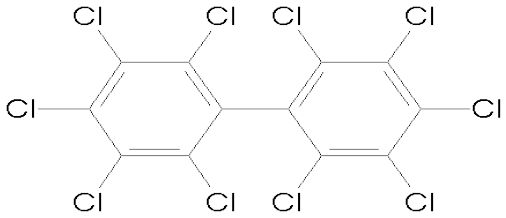

Figure 1. Structure and arrangement of chlorine atoms in PCB (Fiedler, 1998).

Remediation of PCBs in the environment is usually by incineration (Rodriguez and Lafuente, 2002), which is an expensive method and produces toxic compounds as by-products (Erickson *et al*., 1989; in Keun Lee *et al*., 2000). The degradability or transformation of PCBs in the environment is dependent on the degree of chlorination of the biphenyl molecule as well as isomeric substitution pattern (Bhandari, 2007). Currently the most common biological approaches for treating environment contaminated by organics including PCBs is the application of biochemical abilities of microorganisms to transform or degrade such contaminants (Idris and Ahmed, 2003), which is dependent on factors such as the structure of the compound, the presence of exotic substituents and their position in the molecule, solubility of the compound, and concentration of the pollutant (Dobbins, 1995). The shift to biological methods of PCB remediation was necessitated by the aforementioned disadvantages of chemical and physical methods of disposal.

Phytoremediation is the application of biological processes inherent in plants to treat contaminated environment *in situ*. Phytoremediation is a growing technology that can be used to manage pollution (Singh *et al*., 2009). Phytoremediation includes phytodegradation (phytotransformation), phytostabilization (immobilization of contaminants), phytovolatilization, rhizofiltration, rhizodegradation (phytostimulation) and phytoextraction. While many of these options have been exploited for PCB remediation, limited attention has been given to research on phytoextraction (Aken *et al*., 2010; Ficko *et al*., 2010) and rhizodegradation. Food crops have been used extensively in phytoextraction of organic contaminants including PCBs in the environment (Zeeb et al., 2006; Mattina *et al*., 2007; Ficko *et al*., 2011). Phytoextraction essentially involves the uptake of contaminants from soil or water by plant roots and possibly translocating them into above ground tissues for storage. The effectiveness of phytoextraction depends on a number of factors including the

ability to be propagated and cultivated with simple agronomic methods, relative inexpensiveness of the plants, self-sustainability, possession of a root system that facilitates uptake of materials from a wide coverage of the soil or water, and the ability to grow in a variety of environments (Singh *et al*., 2009; Ficko *et al*., 2010, 2011; Atagana, 2011a; Atagana, 2011/b).

For a plant to be considered for phytoremediation, it should possess the following characteristics; high germination rates, ability to be propagated vegetatively, growth in different types of soil, survival under stress, accumulation of high biomass, concentration its absorbed compound in the shoot, and perhaps be perennial, as well as have the potential to be invasive and dominate native vegetation at any new environment (Singh et al., 2009; Atagana, 2011b; Tanhan, 2011). *Chromolaena odorata*, an invasive weed of tropical to neo tropical environments possess some of these characteristics such as growing perennially under a wide variety of soil types, surviving in poor nutrient soil and near drought conditions, easily dominating native vegetation and the ability to be propagated vegetatively. These characteristics are responsible for Chromolaena's success as an invasive plant in new environments. These are the same factors that make *Chromolaena odorata* a potential plant for phytoremediation of PCB-contaminated soil.

The rhizosphere is the region of soil immediately bordering and directly influenced by the root of a plant, its secretions, and associated soil microorganisms. The rhizosphere contains many bacteria that feed on *rhizodeposition* (sloughed-off plant cells) and proteins and sugars exuded by roots. Other organisms such as protozoa and nematodes that graze on bacteria are very abundant in the rhizosphere. The nutrient cycling and disease suppression needed by plants occurs immediately adjacent to roots. Soil microorganisms, including plant root associated free-living, as well as symbiotic rhizobacteria and mycorrhizal fungi in particular, are an integral components of the rhizosphere biota. This microbial community is essential in the phytoremediation processes that take place in the soil. Rhizosphere microorganisms include free-living and symbiotic rhizobacteria and mycorrhizal fungi. Rhizosphere supports alarge and active microbial population is capable of exerting beneficial, neutral and detrimental effects on the plants (Kumar *et al*., 2012). Rhizobacteria (root colonizing bacteria) that exert beneficial effects on the growth of the host plant via direct or indirect mechanisms are called plant growth promoting rhizobacteria (PGPR), which are divided into free-living and symbiotic forms. The plant-microbe interactions in the rhizosphere are responsible for increasing plant health and soil fertility (Kumar *et al*., 2012). The PGPR enhance plant growth by atmospheric nitrogen fixation, phytohormone production, specific enzymatic activity, plant protection from diseases by producing anti-biotic and other pathogen-depressing substances such as siderophores and chelating agents (Khan,

2005). The *in situ* applicability of phytoremediation is constrained by the root zone, i.e., confined to a few decimeters or meters from the soil surface, and often by the relatively long time required to achieve the remedial target.

PGPR have been associated with improved growth in inoculated plants in metal contaminated soil, and the subsequent uptake of essential elements and increased efficiency of phytoremediation (Karami and Shamsuddin 2010). There are, however, safety concerns regarding the use of PGPR for phytoremediation purposes, as some of such organisms may present health risks (Lee *et al*., 2008), despite their abilities to increase the efficiency of phytoremediation. It has been demonstrated that during degradation of anthropogenic compounds the composition of the rhizosphere microbial consortia involved in degradation might be influenced by the plant species (MarschGraff and Conrad, 2005; Leigh et al., 2006; Carnegie et al., 2007). The same research also suggests that successful degradation may be determined by the relationship between rhizosphere microorganisms and plant species (Carnegie et al., 2007).

The aim of this study is to investigate the potential of *C. odorata* plants inoculated with consortia of improved rhizosphere organisms to grow in Aroclor and transformer oil-contaminated soil, anduptake of the compounds under greenhouse conditions.

2. MATERIALS AND PROCEDURE

2.1 Soil

Soil was collected from a grass field at the University of KwaZulu-Natal to a depth of 30 cm. The soil was homogenized by hand to remove pebbles, stone and gravel and air dried before it was put in cellophane bags and stored at $4^{o}C$ before use. About 250g were used for soil characterization at a private laboratory. The soil is a loamy sand with the following characteristics: sand 63.5%, silt 18.5%, clay 8%, pH 6.1, total organic carbon 8, total N 0.04%, total P 4.5mg/kg^{-1}, K 21 mg/kg^{-1}, Ca 81 mg/kg^{-1}, Mg 17 mg/kg^{-1}, Al 0.1 meq 100 g^{-1} soil, Fe 58.6 mg/kg^{-1}, total exchangeable cations 4.55 cmol L^{-1}, exchange acidity 0.20 cmol L^{-1}, thermal conductivity 0.2 $Wm^{-2/}k^{-1}$, soil density 1.25 g/cm^{-1}.

2.2 Plants

Chromolaena odorata plants were collected from the University of KwaZulu-Natal Pietermaritzburg and propagated by stem cuttings. Carbon, nitrogen and phosphates values (CNP) of the soil were analyzed at a private laboratory. Stem cuttings were planted in soil a bed, as described by Clark *et al*.

(1999). Plant rooting hormone "Indole Butyric Acid" IBA, obtained from Plantland Malanseuns, a commercial supplier in South Africa, was applied to the stem cuttings, to aid rooting. The soil was watered to maintain 70% moisture at field capacity and the plants were allowed to root and grow for three months before being used for subsequent propagation and experimentation. Growth of plants in the experiments was measured by enumerating the number of fully opened leaves and by measuring the height of the plants every week. Plant biomass accumulation was measured by standard methods.

2.3 Chemicals

Commercial Aroclor-1260 was obtained from Sigma Aldreich. Transformer oil containing 560 ppm Aroclor was obtained from City Power, Johannesburg, South Africa.

2.4 Experimental Procedure

Thirty-six kilograms of soil, as described above, were used for the experiment. The soil was sterilized by gamma irradiation and 1 kg of the soil was put in each of 36 PVC pots. The pots were divided into two groups (A and B) of 18 pots each. Pots in group A were divided into three subgroups, and each subgroup was separately amended with Aroclor-1260 to give final concentrations of 10%, 30% and 50%, respectively. Pots in group B were also divided into three groups and each group was amended with transformer oil containing 560 mg/L^{-1} Aroclor-1260 to give final concentrations of 10%, 20% and 30%, respectively. All pots were planted with one 3-month-old *C. odorata*. Soil around the roots of the plants was carefully removed and the roots washed with water to ensure that the roots did not have soil microorganisms attached before transplanting. Pots in groups A and B that were planted and amended with Aroclor-1260 and transformer oil were further subdivided into two subgroups, and one of the groups was inoculated with 100 mL of the enrichment culture of the rhizosphere microorganisms. All pots in both groups were treated with 100 mL of 5% solution NPK fertilizer. All treatments were set up in triplicate and incubated in a tunnel with automatic cooling fans set to a control temperature of $25^{O}C$.

2.5 Mineral Salts Medium (MSM)

The mineral salts medium contained per liter: K_2HPO_4, 1.5 g; $MgCl_2 \cdot 6H_2O$, 0.2 g; $NaH_2PO_4 \cdot 2H_2O$, 0.85 g; Na_2SO_4, 1.4 g; NH_4Cl, 0.9 g; $NaHCO_3$, 0.5 g; Na_2CO_3, 0.2 g; 1 mM solution of $NiCl_2 \cdot 6H_2O$, 1 ml; vitamin solution, 1 ml; Trace Elements Solution A, 1 mL; and Trace Elements Solution B, 1 mL. The vitamins solution contained (mg L^{-1} distilled water): Biotin, 10; p-aminobenzoic

acid, 10; folic acid, 10; pyroxidine HCl, 20; thiamine, 20; riboflavin, 30; nicotinic acid, 50. The Trace Elements Solution A contained (mg/L−1distilled water): $FeCl_2 \cdot H_2O$, 1500; NaCl, 9000; $MnCl_2 \cdot 4H_2O$, 197; $CaCl_2$, 900; $CoCl_2 \cdot H_2O$, 238; $CuCl_2 \cdot H_2O$, 17; $ZnSO_4$, 287; $AlCl_3$, 50; H_3BO_3, 62; $NiCl_2 \cdot 6H_2O$, 24; Conc. HCl, 10ml. Trace Elements Solution B (mg L−1 distilled water): $Na_2MoO_4 \cdot 2H_2O$, 48.4; $NaSeO_3 \cdot xH_2O$ (31% Se), 2.55; $Na_2WO_4 \cdot 2H_2O$, 3.3. The medium was prepared in three stages. Stage 1: All components of the medium except Na_2CO_3, $NaHCO_3$, trace element solutions A and B, and vitamins were dissolved in distilled water and diluted to 900 ml. This solution was dispensed into flasks and stoppered with cotton wool bungs wrapped in aluminum foil and autoclaved at 121C◦ for 15 min. In stage 2: $NaHCO_3$ and Na_2CO_3 were dissolved in 97 ml of distilled water and autoclaved as in stage 1. In stage 3: Trace element solutions A and B and vitamins were filter sterilized through 0.2 μm millipore membrane filters and 1mL of each were added to the medium before use. All solutions were stored at 4C◦ before being dispensed under aseptic conditions using sterile glassware on a laminar flow bench.

2.6 Enrichment of Rhizosphere Microorganisms Capable of Utilizing PCB

To 100 mL sterile MSM in 250 mL flasks, 15 g of soil from the rhizosphere of mature *C. odorata* was added. The flasks were spiked with 10 mg of Aroclor-1260. The flasks were stoppered with cotton wool bung and incubated in the dark at 30 ± 2°C on a rotary shaker at 150 rpm for 21 days. Following incubation, 1 mL from the flask was aseptically sub-cultured into another 250 mL flask containing 100 mL MSM spiked with Aroclor-1260, as described above, and incubated for a secondary 21 day period at 30 ± 2°C in a rotary shaker in the dark. The sub-culturing was repeated 5 times. For the final culture (the fifth culture), 5 mL each were transferred into two 1 L flasks each containing 500 mL MSM and incubated as described above. Cultures from these flasks were used as inoculum for the potted plants. At the end of each incubation period, samples were withdrawn from each flask for determination of concentrations of the PCB by gas chromatography and for plate counts of total heterotrophs and hydrocarbon degraders.

2.7 Enumeration of PCB Degrading Bacteria

One gram of soil taken from the rhizosphere of experimental plant was analyzed for total PCB-degrading microorganisms by using standard dilution plating techniques on a modified version of the Organization for Economic Co-operation and Development (OECD) medium containing 30 mL Aroclor-1260 as the sole carbon source. The OECD medium was prepared by adding 17 g agar, 4mL $FeCl_3$ (0.25 g/L^{-1}), 1ml each of $MgSO_4.7H_2O$ (22.5g L^{-1}), $CaCl_2$ (27.5g L^{-1}) and $(NH_4)_2SO_4$ 40g L^{-1} to 2 ml of the following mixture: KH_2PO_4 (8.5 g/L^{-1}), K_2HPO_4 (21.75 g/L^{-1}), NaH_2PO_4 $.7H_2O$ (33.4 g/L^{-1}) and NH_4Cl (1.7 g/L^{-1}), and diluting to one litre with distilled water. The mixture was autoclaved at 121^{O} C for 20 minutes and cooled. Aroclor-1260 was filtered through a hydrophilic membrane (0.4 µm) pore filter and agar was added to it before the plates were poured.

2.8 Enzyme Measurement

Extraction of Mn-dependent peroxidase (MnP) was done by mixing 5 g of soil with 10 mL of phosphate buffer (50 mM, pH 7.0), incubating it on ice for 1 h, centrifuging it at 15,000 x g for 15 min at 15C◦, and then the supernatant was centrifuged at 5,000 x g for 15 min at 15C◦, assayed in succinate-lactate buffer (100 mM, pH 4.5), and measured by spectrophotometer (Baldrian,2000).

2.9 Genomic DNA Extraction of the Rhizosphere Bacteria

Genomic DNA was extracted with Cetyltrimethyl Ammonium Bromide (CTAB). Sample of soil from the rhizosphere were put in a microcentrifuge (Eppendorf Minispin plus, 12 x 1.5/2.0 mL) and centrifuged at 14,000 rpm for 5 min. The pellets were suspended in 567 µL of tris ethylene diamine tetraactic acid buffer (tris EDTA), 30 µL of 10% sodium dodecyl sulphate (SDS), 3 µl of proteinase K (20 mg/mL), and incubated in Accu block digital dry bath incubator at 65^{o}C for 1 h. The DNA pellets and 100 µL of TE buffer were added to the dried DNA pellets, which were incubated at 37 ^{o}C for 60 min to dissolve the DNA pellets. Then 1 µL of RNAase was added to the tubes and was incubated at 37 ^{o}C for 60 min. The concentration of DNA template was separated electrophoretically with ethidium bromide (0.1 µg/mL)-stained 1% agarose gel running at 80 V for 60 min using TAE Electrophoresis buffer. The DNA templates were visualised by UV fluorescence to determine the success of the extraction process.

2.10 Polymerease Chain Reaction (PCR) and Sequencing

PCR was performed using MJ Mini Thermal Cycler (Bio-Rad, Hercules, CA, USA). The PCR reagent contained in 50 µL; buffer 5 µL, $MgCl_2$ 1.5 µL, primer 1: 2 µL (forward, 16S-P1 PCR 5′AGAGTTTGATCCTGGCTCAG3′), primer 2: 2 µL (reverse, 16S-P2 PCR 5′AAGGAGGTGATCCAGCCGCA3′), dNTP mix 1 µL, Dream Taq 0.25 µL, sterile sabax water 35.25 µL, and DNA template 3 µL. The cycling conditions were (a) initial denaturation 10 minutes at 95^{O}C for 1 cycle. (b) denaturation at 95^{O}C for 30 seconds, (c) Annealing cycling at 94^{O}C for 30 seconds, (d) elongation at 54^{O}C for 2 min. All steps in denaturation, annealing and elongation were for 35 cycles, with (e) the final elongation 10 min at 72^{O}C for 1 cycle. The reaction was held at 4^{O}C for 1 h in the thermal cycler. The PCR products were separated electrophoretically with ethidium bromide (0.1 µg/mL)-stained 1% agarose gel running at 80 V for 60 mins, using TAE Electrophoresis buffer. PCR product was visualized by UV fluorescence to determine the size of the amplified bands. PCR products (20 µL each) were later cleaned up using 160 µl of 13% polyethylene glycol (PEG) 8000, 20 µl of 5M NaCl solutions, and 200 µL of 70% ethanol.

2.11 Basic Local Alignment Search Tool (BLASTing) of DNA Sequences

The sequences of the 16S rDNA region obtained were edited using BioEdit software. The edited sequences were copied in a fasta format. Blasting was done on National Center for Biotechnology Information (NCBI) website. This was to check and compare the sequences with those on the database.

2.12 Determination of PCB Concentrations in Soil and Plant Tissues

Extraction of PCB from contaminated soil was done in a Microwave Extraction Unit. Ten grams of soil were put into 40 mL of a 1:9 acetone/hexane mixture in Teflon-lined extraction vessels. The vessels were microwaved at 110^{O}C for 10 min at 100% power (1000 W) and allowed to cool to room temperature before opening. Ten mills of the extract were then transferred into 40 ml hexane and filtered into amber vials through 0.2 µm filter, discarding the first 2–3 ml of the filtrate, and retaining the remainder for analysis. Gas chromatographic analysis of Aroclor 1260 was performed using a Varian 3800 GC coupled with Mass Spectrometer. The column was temperature programmed at 80^{O}C as an initial (0.1 min), followed with two ramps at 15 ^{O}C/ min to 180^{O}C/min and 4^{O}C/min to 300^{O}C/min. Injector and detector temperatures were maintained at 270 ^{O}C and 330^{O}C, respectively. The column was operated with a

helium carrier gas at a flow rate of 1.3 mL/min. The detector makeup and anode purge gases consisted of 5% methane and 95% argon. The run time was set at 37 min. Total Aroclor 1260 levels were quantified using area counts of 10 major peaks of a 0.8 mg/kg Aroclor 1260 standard (Lopez-Avila et al, (1995). For extraction of PCB from plant tissues, the plant parts were homogenized before extraction in a mixture of acetone/hexane.

2.13 Statistical Analysis of Values

Results were analyzed by analysis of variance using SPSS.

3. RESULTS AND DISCUSSION

The effects of the different concentrations of Aroclor-1260 and transfornmer oil containing 560 mg/kg^{-1} Aroclor-1260 on the growth of *Chromolaena odorata* were assessed by weekly enumeration of fully opened leaves and measurement of increases in plant height, with the determination of biomass at the end of experimentation. The results showed that the plants grown in the experiments containing 10% and 30% Aroclor-1260, and those containing 10% and 20% transformer oil did not significantly impede the growth of the plants during the experimental period. The number of leaves and height of the plants in these experiments increased significantly during the period of experimentation (Table, 1-4). The highest number of leaves (51) was recorded in the 10% direct Aroclor-1260 treatment inoculated with enriched rhizosphere microorganisms, while the least number of leaves (23) was recorded in the 30% transformer oil treatment not inoculated with enriched rhizosphere microorganisms. There was no significant difference at p=0.05 in biomass accumulation between the three Aroclor-1260 treatments; however, there was a significant difference between the experiments inoculated with enriched rhizoorganisms and those not inoculated. In the transformer oil experiments, the concentrations of PCB and the rhizosphere microorganisms affected biomass accumulation. The results also showed that the presence of enriched rhizosphere organisms in the experimental soil significantly enhanced the growth of the plants, which was shown by a higher number of leaves, and taller and more profusely branched plants. However, Aroclor 1260 at 50% concentration impeded plant growth significantly at p=0.05 during the first six weeks of growth. Although growth started to improve in the later stages of the experimental period, the plants were lower in height and accumulated less biomass at the end of experimentation (Fig 2).

Table 1. Number of leaves in plants grown in soil ameded with different concentrations of Aroclor-1260 and inoculated/not inoculated with enriched rhizosphere microorganisms. Values are means of 3 + Standard Deviation.

Treatment →	10% Aroclor-1260				30% Aroclor-1260				50% Aroclor-1260			
Weeks	Inoculated	Std. Dev.	Not Inoculated	Std. Dev.	Inoculated	Std. Dev.	Not Inoculated	Std. Dev.	Inoculated	Std. Dev.	Not Inoculated	Std. Dev.
0	8	0,3	9	0,1	8	0,4	7	0,9	8	0,9	7	1
1	13	0,5	6	0,3	13	0,5	9	0,6	10	0,5	5	0,4
2	17	0,3	10	0,3	16	0,8	10	0,5	14	0,6	7	0,5
3	21	0,2	12	0,3	18	0,8	11	1,4	17	1,2	10	1,3
4	25	0,4	13	0,2	23	1,3	11	0,8	21	0,3	15	1,8
5	29	0,5	15	0,8	26	1,4	15	0,4	25	1,3	14	0,5
6	34	0,3	18	1,4	30	0,8	18	1,2	27	1,4	12	0,9
7	38	2,1	25	1,2	35	0,9	20	1,6	33	1,9	16	1,2
8	42	1,5	33	1,4	38	0,5	31	1,3	37	1,2	20	1,5
9	45	2,3	37	0,8	42	2,5	35	1,2	40	1,8	26	1,2
10	51	1,3	42	1,6	49	2,2	40	1,5	45	1,8	33	1,8

Table 2. Number of leaves in plants grown in soil ameded with different concentrations of transformer oil and inoculated/not inoculated with enriched rhizosphere microorganisms. Values are means of 3 + standard deviation.

Treatment→	10% Aroclor-1260				20% Aroclor-1260				30% Aroclor-1260			
Weeks	Inoculated	Std. Dev.	Not Inoculated	Std. Dev.	Inoculated	Std. Dev.	Not Inoculated	Std. Dev.	Inoculated	Std. Dev.	Not Inoculated	Std. Dev.
0	8	0,5	8	0,3	9	0,1	10	1	8	0,1	7	0,4
1	13	0,5	10	0,5	12	0,3	8	0,4	11	0,3	5	0,5
2	15	0,6	12	0,3	14	0,3	8	0,5	14	0,3	8	0,8
3	18	0,7	15	0,2	15	0,3	10	1,3	17	0,3	10	0,8
4	21	0,3	17	0,4	18	0,2	13	1,8	20	0,2	8	1,3
5	25	1,3	17	0,5	23	0,8	17	0,5	23	0,8	10	1,4
6	27	1,4	20	0,3	27	1,4	20	0,9	26	1,4	10	0,8
7	35	1,9	21	0,7	31	1,2	18	1,2	29	1,2	12	0,9
8	40	1,2	25	1,5	33	1	23	1,5	32	1	15	0,5
9	43	0,9	31	0,8	36	0,8	26	1,2	35	0,8	20	1,3
10	42	1,5	35	1,3	37	1,1	30	1,8	37	1,1	23	1,5

Unlike the 30% Aroclor-1260, which did not impede plant growth, the 30% PCB in transformer oil significantly affected growth of *C. odorata.* This observation was believed to be the combined effects of oil and PCB rather than PCB alone. The results obtained for biomass accumulation showed that Aroclor 1260 had less adverse effects on the plants than the transformer oil. In general, plants grown in the transformer oil amended soil were more adversely affected by the PCB than the direct Aroclor 1260 application. Oil impacted soils have been reported to inhibit growth of plants due to closure of air pores in the soil, and also depletion of oxygen and build-up of carbon dioxide in the soil. Anoxic conditions are common occurences in oil impacted soil due to respiratory activities of roots and soil microbes (Chekol et al 2004; Balcom and Crowley 2010). The relatively greater adverse effects of the transformer oil treatments compared to the direct Aroclor-1260 treatment is thus a combined effect of oil and PCB, both of which have inhibitory effects on plant growth at elevated concentrations.

PCBs as exotic, substituted hydrocarbons are expected to inhibit plant growth and development, and the activities of soil microorganisms present in the rhizosphere. Compounds with aromatic structures have been reported to inhibit plant growth and microbial activities in the soil (Bona et al 2011). The extent of inhibition increases with an increase in aromaticity, the number and nature of the substitutions, and the position of the substition. However, the relative ease with which the subsitutions are oxidised by microbial actions is suggested to be the factor that decreases the rate of inhibition in plants and microorganisms by these compounds. This process also accounts for the reduction in the concentration of PCB congeners in soil. Biological reductive dechlorination under anaerobic conditions preferentially dechlorinates higher chlorinated PCB congeners, transforming them to lower-chlorinated congeners (Magar et al 2003).

Table 3. Height of plants grown in soil amended with different concentrations of Aroclor-1260 and inoculated/not inoculated with enriched rhizosphere microorganisms. Values are means of 3 + Standard Deviation.

Treatment→	10% Aroclor-1260				30% Aroclor-1260				50% Aroclor-1260			
Weeks	Inoculated	Std. Dev.	Not Inoculated	Std. Dev.	Inoculated	Std. Dev.	Not Inoculated	Std. Dev.	Inoculated	Std. Dev.	Not Inoculated	Std. Dev.
0	1	2,3	18	3,4	15	1,2	16	0,9	18	1	15	1
1	2	1,5	18	2,1	19	1,2	18	1,4	20	1	15	1
2	2	2,1	21	2	25	1,7	18	1,2	23	1	18	1
3	3	3	25	2,1	28	1	20	2,5	25	1	20	1
4	3	3,3	27	3	31	1,6	23	2,1	27	2,3	21	1
5	4	2,5	29	1,5	35	2,1	26	2,9	30	1,4	23	1,9
6	4	2,1	33	2,3	38	2,3	30	3,2	34	1,3	25	2,4
7	5	2	35	1,1	41	2,9	35	3,5	37	1	27	2,3
8	5	3,8	39	1,5	44	1,7	35	2,2	42	2	30	1,8
9	6	3,1	42	4,1	51	1,9	38	2,5	48	3	33	2,1
10	6	2,9	42	3,1	57	2,2	42	3,4	55	2,7	35	2,5

The succesful growth of *C. odorata* in the PCB-contaminated soil in this study can be further attributed to the action of rhizosphere microorganisms on the PCB

molecules, which may have rendered them available and susceptible to phytoextraction and possibly, phytodegradation. PCBs are used as dispersants for pesticides in agriculture and have been found to persist in agricultural soil with no detectable adverse effects on soil microorganisms and plants, and as a results microorganisms that have the ability to grow and metabolise in PCB have developed over the years.

Table 4. Height of plants grown in soil amended with different concentrations of transformer oil and inoculated/not inoculated with enriched rhizosphere microorganisms. Values are means of 3 + Standard Deviation.

Treatment→	10% Aroclor-1260				20% Aroclor-1260				30% Aroclor-1260			
Weeks	Inoculated	Std. Dev.	Not Inoculated	Std. Dev.	Inoculated	Std. Dev.	Not Inoculated	Std. Dev.	Inoculated	Std. Dev.	Not Inoculated	Std. Dev.
0	15	0,9	17	1	15	0,9	15	0,5	16	1,2	17	0,9
1	18	0,9	18	1	17	0,5	15	0,7	18	1	17	0,7
2	21	1	19	1	20	0,7	16	1	21	1,4	17	0,7
3	25	1	20	1	24	1,9	17	1	24	0,9	19	1
4	27	1	23	1	27	1,2	19	1	26	0,5	21	0,2
5	30	1,7	27	1,2	31	1,1	21	0,9	28	1	23	0,5
6	34	2,1	31	1,5	37	1	21	0,4	31	1	24	1
7	38	2,2	32	2,4	39	1	25	1,4	33	0,6	25	1
8	41	3	35	1,2	41	2,3	27	1,3	35	1	27	1,8
9	45	1,2	38	0,5	45	2,5	31	1,8	37	0,5	27	1,5
10	52	1,5	38	1,3	48	1,5	33	2	38	1,3	28	1

The results of the measurement of PCB concentration in the experimental soil showed that PCB was reduced between 47% and 87% in the Aroclor 1260 treated experiments (Figure 3), and between 42% and 82% in the transformer oil treated soil (Figure 4). There was no statistically significant difference between the inoculated and un-inoculated experiments in terms of PCB accumulation with the exception of plants in the 50% Aroclor treatments where concentrations of PCB was consistently higher in the un-inoculated soil.

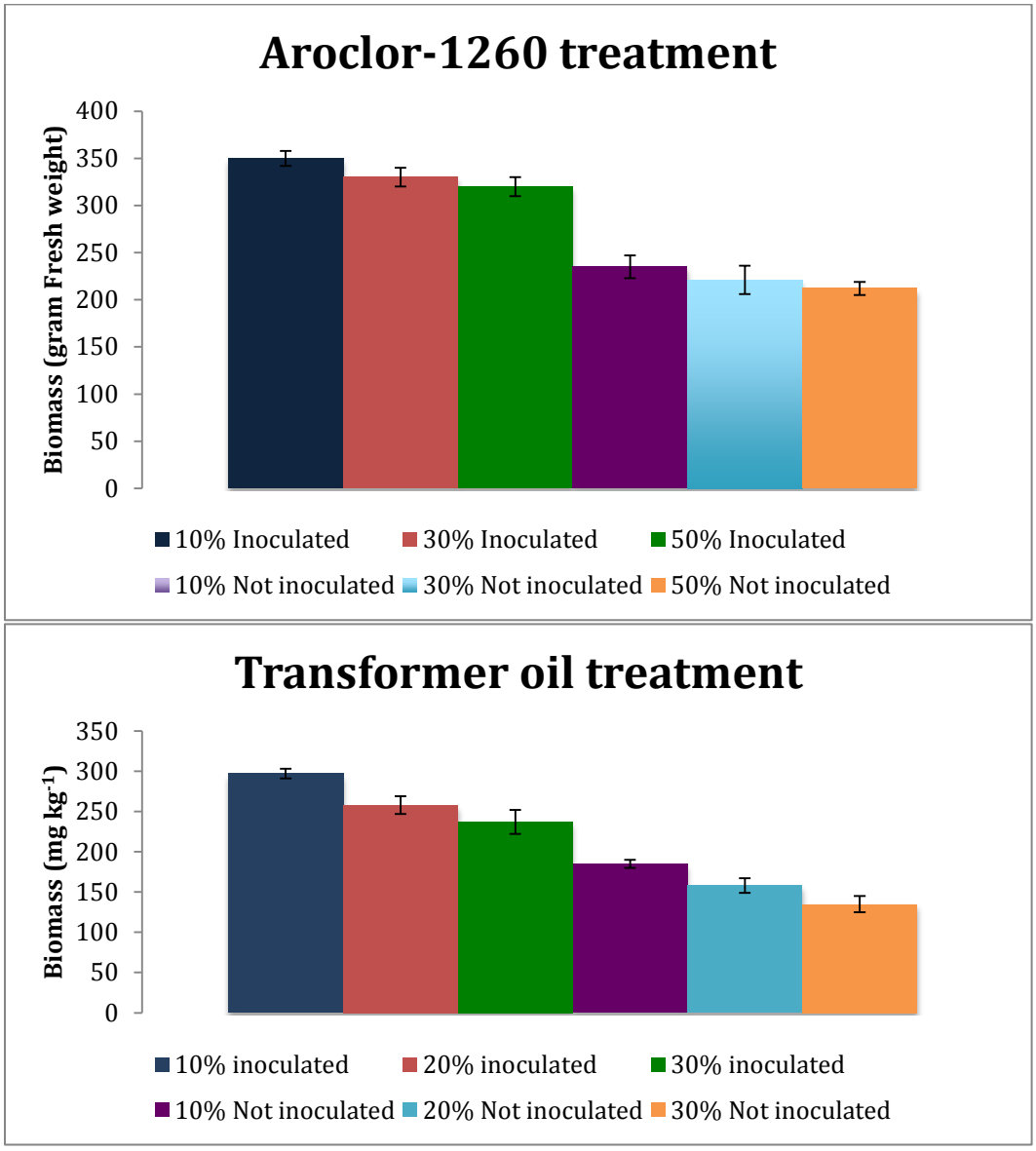

Figure 2. Biomass of plants grown in soil contaminated with different concentrations of PCB and inoculated/not inoculated with enriched rhizosphere organisms. Values are means of 3 ± Standard Deviation.

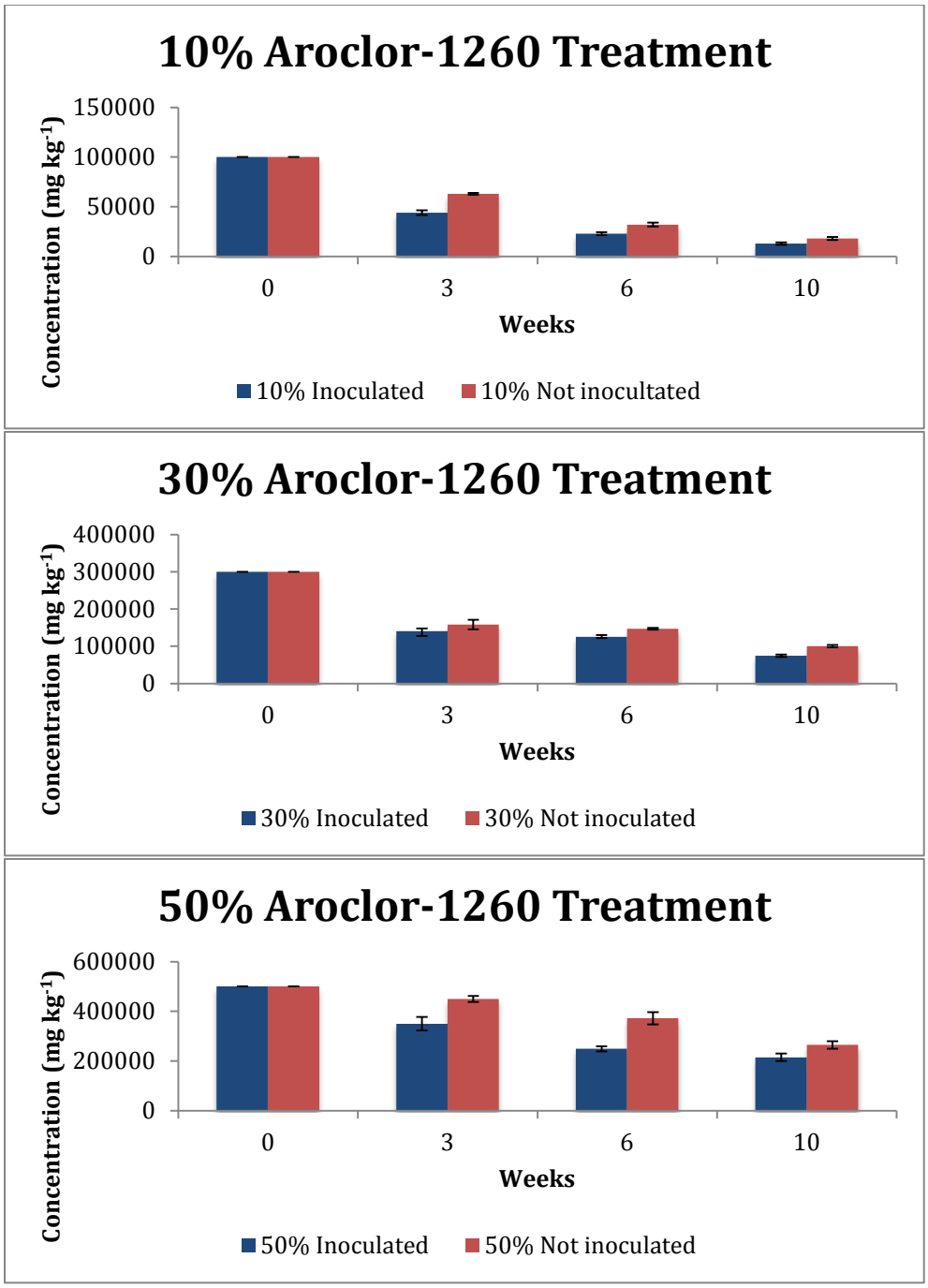

Figure 3. Changes in concentrations of PCB in soil treated with Aroclor1260 and inoculated/not inoculated with enriched rhizosphere organisms. Values are means of 3 ± Standard Deviation.

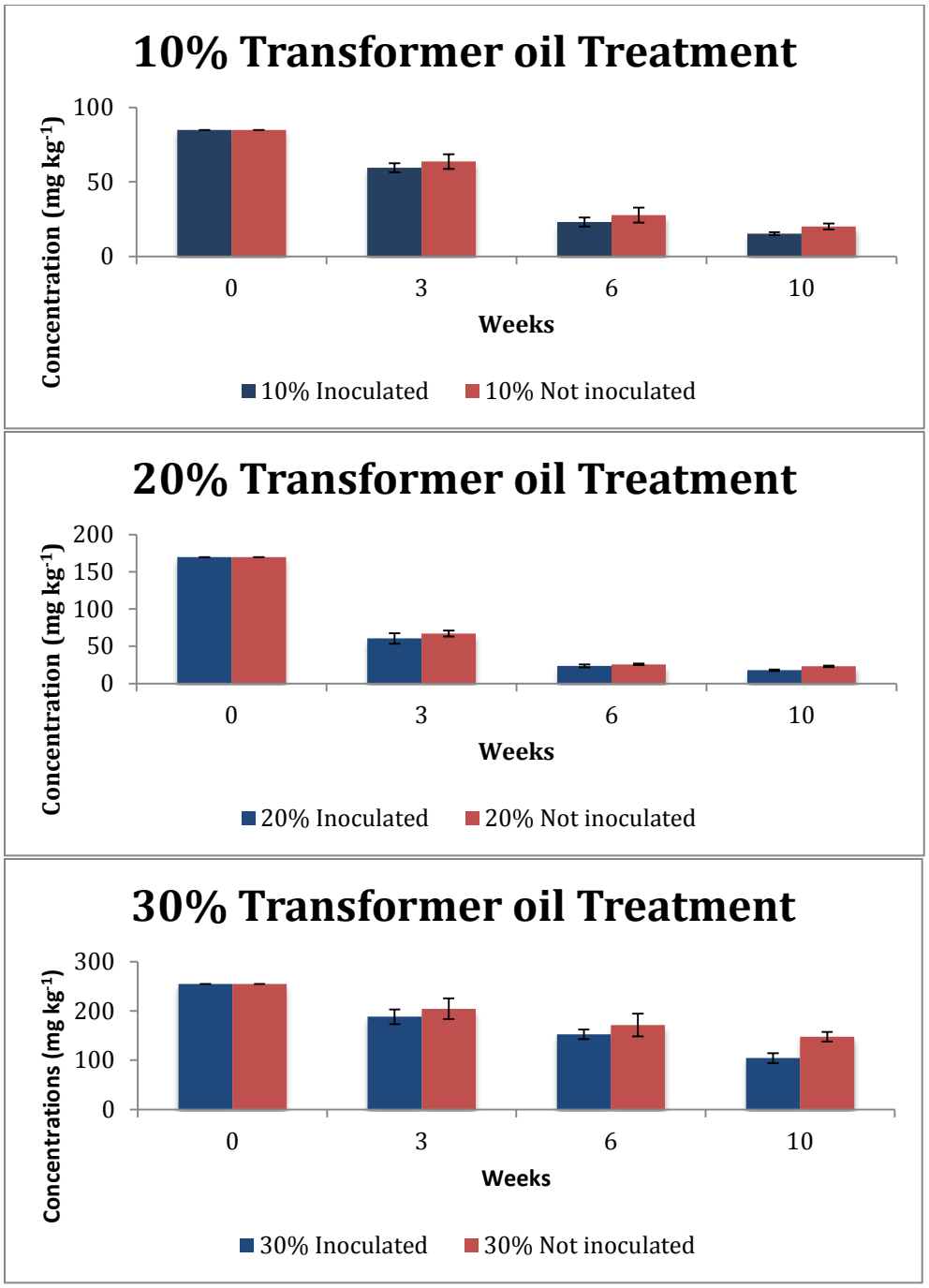

Figure *4*. Changes in concentrations of PCB in soil treated with transformer oil and inoculated/not inoculated with enriched rhizosphere organisms. Values are means of 3 ± Standard Deviation.

Reduction in soil PCB levels in both the inoculated and the un-inoculated soil showed that *C. odorata* is capable of taking up PCBs from the soil. Experiments inoculated with enriched rhizosphere microorganisms showed relatively higher PCB reduction compared to those un-inoculated. In the plant tissues, substantial amounts of PCBs were recovered from the roots and shoots of the plants grown in the experimental soil. In the Aroclor treatments, there was more PCB accumulation in the roots than in the shoots of the plants. There were also higher amounts of PCBs in plants grown in higher concentrations than those grown in low PCB concentrations. In the Aroclor-1260 treatments, plants accumulated between 1320 to 22000 μg, and between 321 to 773 μg were accumulated in the transformer oil treatment. The low accumulation of PCB in the tissues of plants grown in transformer experiments is associated with the presence of oil.

In the transformer oil amended soil, plants also accumulated more PCB in the roots than in the shoots. However, while the amounts of PCB accumulated in the roots increased with a concentration increase, the amounts accumulated in the shoots decreased with an increase in concentration.

Results of the measurement of manganese peroxidase (MnP) activities in the experimental soil and counts of soil microorganisms in the rhizosphere capable of utilizing PCB shows that the soil inoculated with enriched rhizhosphere microorganisms had consistently higher activity than the un-inoculated ones. Although the soil was sterilized, significant numbers of microbial cells were found in the un-inoculated soil, albeit very low compared to the inoculated soil. Manganese peroxidase (MnP) activity was not significantly different in the treatments containing the three Aroclor 1260 concentrations (Figure 5). There were, however, significant differences at p=0.05 between the transformer oil treatments inoculated with enriched rhizosphere organisms and those not inoculated. The enzyme activity in the inoculated soil was significantly higher in all experiments. In both the Aroclor 1260 and transformer oil experiments, enzyme activity continued to increase throughout the end of the experimental period.

The presence of enzyme activity in the un-inoculated experiments was confirmed by the high number of microorganisms found in the experiments. Counts of microorganisms were consistently higher in the inoculated experiments throughout the entire period of the experiment (Figure 6).

It was not clear how much degradation of the PCB was achieved by the rhizosphere microorganism and in the plant tissues, as the PCB congener that was used for the experiments was detected in the plant tissues. However, the deficit in the amounts of PCB recovered from the soil and the plant tissues, and the initial concentration of PCB applied, suggests that some amounts of PCB were degraded or volatilized, or both. This suggests that the interaction between *C. odorata* with

rhizosphere microorganisms provides a medium for PCB degradation and removal from the soil. The presence of a limited amount of PCB and a few other compounds in the plant tissues, which are yet to be identified, suggests that some of the compound may have been metabolized in the plant tissues or transformed into other compounds. Earlier reports have suggested the metabolism of different PCB congeners in plant cells (Wilkens et al 2009).

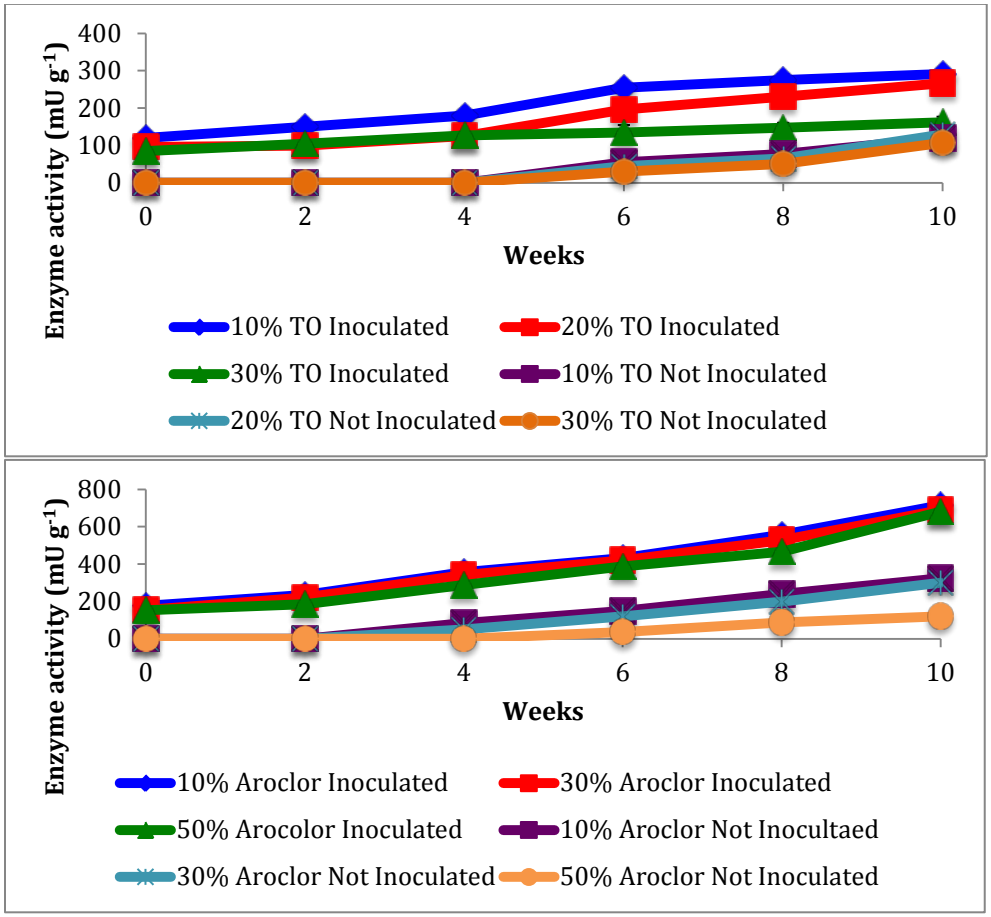

Figure 5. Changes in manganese peroxidase (MnP) activities in experimental soil. Values are means of 3 ± Standard Deviation.

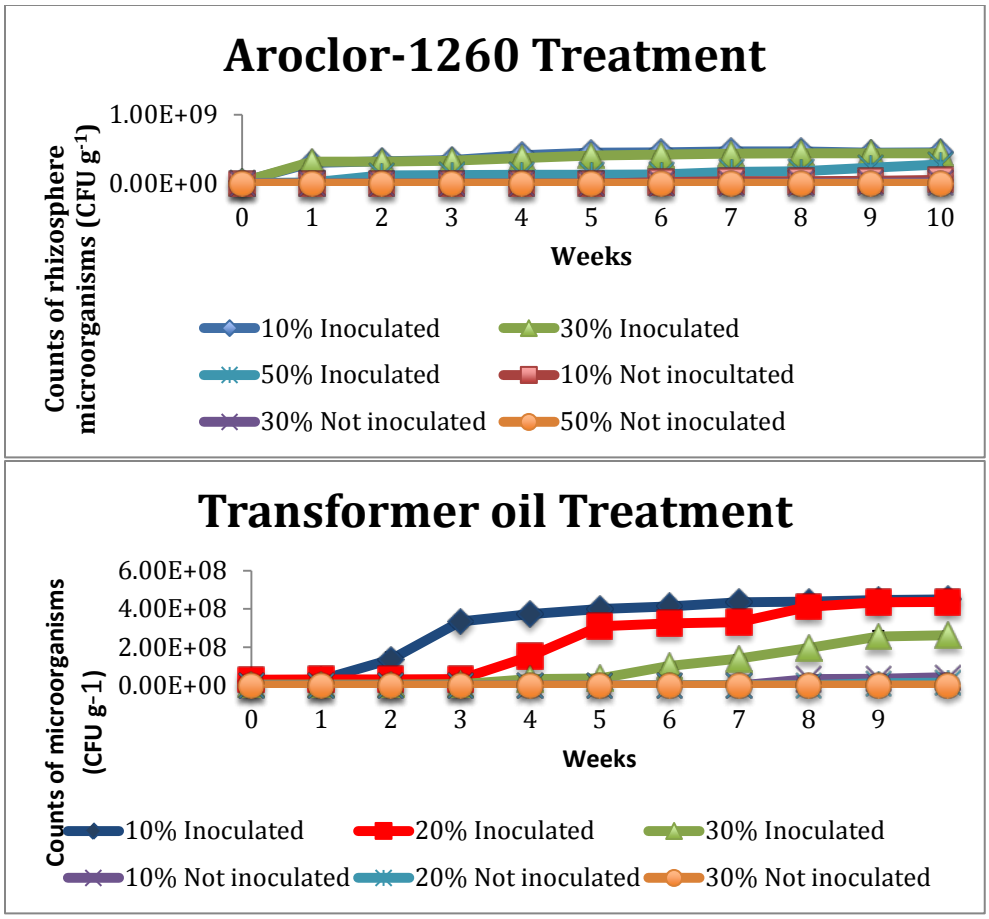

Figure 6. Changes in counts of microorganisms in experimental soil. Values are means of 3 ± Standard Deviation.

In both the Aroclor 1260 and the transformer oil treatments, rhizosphere microorganisms were detected in the un-inoculated experiments, albeit in small numbers. The numbers increased during the experiments, but did not grow high enough to exert the effects observed in the inoculated experiments (Figure 6). Microorganisms in the un-inoculated soil are attributed to contamination from the environment and the result of deposition of plant activities, which will normally promote the growth of microorganisms (Meggo and Schnoor, 2013).

Characteristics of bacterial species that were represented by individual DNA bands in the DGGE gels were determined by excising the bands and DNA sequencing. Analysis of rhizosphere consortia showed three bacterial species each, one with sequence homologies to the known species of *Bacillus* (99%),

Pseudomonas (99%) and *Arthrobacter* (99%), the second with homologies to *Brevibacillus* (99%) *Streptococcus* (99%), *Pseudomonas* (99%), and *Bacillus* (99%) genera and the third comprised of bacteria with 16S rRNA gene homology to *Rhizobium* (99%), *Agrobacterium* [99%]), *Streptomyces* (99%). The PCB enrichment cultures yielded *Pseudomonas, Proteus, Norcadia, Acidobacterium* and *Geothrix*.

4. CONCLUSIONS

This experiment demostrates that *Chromolaena odorata* has the capabilities to grow in soil contaminated with different concentrations of PCBs. It has also shown that rhizosphere microorganisms are important in the uptake of PCBs by *C. odorata* in contaminated soil. However, it has shown that *C. odorata* can continue to take up PCBs in the envirnment in the absence of rhizosphere microorganisms albeit in a relatively smaller amounts. The growth and development of *C. odorata* in contaminated soil can continue up to certain contrations where inhibition may set in due to toxicity of the PCBs to the plants.

It is recommended that the fate of PCBs in *C. odorata* tissues be further investigated to determine whether degradation occurs at the cellular level in the plant.

5. REFERENCES

Aken, B.V., Correa, P.A., and Schnoor, J.L. 2010. Phytoremediation of polychlorinated biphenyls: new trends and promises. Environ. Sci. Technol. 44, 2767-2776.

Andersson, P. 2000. Physico-chemical characteristics and quantitative structure-activity relationships of PCBs. Department of Environmental chemistry, Umea University Sweden. 1-10.

Annema, J.A., Beurskens, J.E.M., and Bodar, C.W.M. (Eds.). 1995. Evaluation of PCB Fluxes in the Environment. Bilthoven-The Netherlands. RIVM Report 601014011, 33.

Atagana, H.I. 2011. Bioremediation of co-contamination of crude oil and heavy metals in soil by phytoremediation using Chromolaena odorata (L). King & H.E. Robinson. Water Air Soil Poll. 215, 261-271.

Atagana, H.I. 2011. The potential of Chromolaena odorata (L) to decontaminate used engine oil impacted soil under greenhouse conditions. Int. J. Phytorem. 13, 627-641.

Balcom, I.N., and Crowley, D.E. 2010. Isolation and Characterization of Pyrene Metabolizing Microbial Consortia from the Plant Rhizoplane, Inter J. of Phytorem. 12(6), 599-615.

Bhandary, A. 2007. Remediation technologies for soil and groundwater. US Environmental Council. Science. 17-23.

Chekola, T., Voughb, L.R., and Chaneyc, R.L. 2004. Phytoremediation of polychlorinated biphenyl-contaminated soils: the rhizosphere effect. Environment International 30, 799– 804.

Clark, D.G., Gubrium, E.K., Barrett, J.E., Nell, T.A., and Klee, H.J. 1999. Root formation in ethylene-insensitive plants. Plants Physiol. 121, 53-59

Cogliano, V.J. 1998. Assessing the cancer risk from environmental PCBs. Environ. Health Pespect. 106, 317-323.

Dobbins, D.C. 1995. Biodegradation of pollutants. Encyclopeadia of environmental biology, 1, Academic Press Inc., 22, 63.

Erickson, M.D., Swanson, S.E., Flora Jr., J.D., and Hinshaw, G.D. 1989. Polychlorinated debenzofuran and other thermal combustion products and dielectric fluids containing polychlorinated biphenyls. Environ. Sci. Technol. 23, 462-469.

Ficko, S.A., Rutter, A., and Zeeb, B.A. 2010. Potential for phytoextraction of PCBs from contaminated soils using weeds. Sci. Total. Environ. 408, 3469-3476.

Geisy, J.P. and Kinnan, K. 1998. Dioxin-like and non dioxin-like toxic effects of polychlorinated biphenyls (PCBs): implication for risk assessment. Critic. Rev. Toxicol. 28, 511-569

Gray, K.A., Klebanoff, M.A., Brock, J.W., Zhou, H., Darden, R., Needham, L. and Longnecker, M.P. 2005. In utero exposure to background levels of polychlorinated biphenyls and cognitive functioning among school-age children. Am. J. Epidemol. 162, 17-26.

Idris, A., and Ahmed, M. 2003. Treatment of polluted soil using bioremediation – A review. Faculty of Chemical and Environmental Engineering. University of Putra, Malaysia. 1-18.

Karami, A., and Shamsuddin, Z. H. 2010. Phytoremediation of heavy metals with several efficiency enhancer methods. Afr. J. Biotechnol. 9(25), 3689-3698.

Khan, A.G. 2005. Role of soil microbes in the rhizospheres of plants growing on trace metal contaminated soils in phytoremediation. J.Trace Elem. Med. Biol. 18, 355-64.

Kumar, A., Kumar, A., Devi, S., Patil, S., Payal, C., and Negi, S. 2012. Isolation, screening and characterization of bacteria from Rhizospheric soils for different plant growth promotion (PGP) activities: an in vitro study. Recent Res. Sci. Technol. 4(1), 01-05

Kuratsune, M., Yoshimura, H., Hori, Y., Okumura, M. and Matsuda, Y. 1996. Yusho- a human disaster caused by PCB and related compounds. Kyushu University Press, Fukuoka. 361, 91.

Larsson, P., Andersson, A., Broman, D., Nordback, J. and Lundberg, E. 2000. Persistent organic pollutants (POPs) in pelagic systems. Ambiol. 29, 202-209.

Lee, C.S., Lee, H.B, Cho, Y.G., Park, J.H., Lee, H.S. 2008. Hospital-acquired Burkholderia cepacia infection related to contaminated benzalkonium chloride. J. Hosp. Infect. 68, 280-282.

Leigh, M.B., Fletcher, J., Nagle, D., Kucerova, P., Mackova, M. and Macek, T. 2006. Rhizosphere remediation of PCBs based on field studies in the Czech Republic. Int Biodeteriol. Biodegrad. 53, 260-271.

Lopez-Avila, V., Benedicto, J., Charan, C., Young, R. 1995. Determination of PCBs In soils/sediments by microwave-assisted extraction and GC/ECD or ELISA. J. Environ.

Sci. Technol. 29, 2709– 12.
Mattina, M.J.I., Berger, W.A. and Eitzer B.D. 2007. Factors affecting the phytoaccumulation of weathered, soil-borne organic contaminants: analyses at the ex Planta and in Planta sides of the plant root. Plant Soil. 291, 143–54.
Rodriguez, J.G., and Lafuente, A. 2002. A new advanced method for heterogeneous catalyzed dechlorination of polychlorinated biphenyls in hydrocarbon solvent. Tetrahedron Lett. 43, 9581–9583.
Safe, S.H. 1994. Polychlorinated biphenyls (PCBs); environmental impacts, biochemical and toxic responses and implication for risk assessment, Critic. Rev. Toxicol. 24, 87-149.
Singh, S., Thorat, V., Kaushik, C.P., Raj, K. and D'Souza, S.F. 2009. Potential for *Chromolaena odorata* for phytoremediation of ^{137}Cs from solution and low level nuclear waste. J. Hazard. Mat. 162, 743-745
Tanhan, p., Pokethitiyook, P., Kruatrachue, M., Chaiyarat, R. and Upatham, S. 2011. Effects of soil amendments and EDTA on lead uptake by *Chromolaena odorata*: Greenhouse and Field Trial Experiments. Inter. J. Phytorem. 13, 897-911
Van Den Berg, M., Birnbaum, L., Bosveld, A.T., Brunstrom, B., Cook, P., Feeley, M., Geisy, J.P., Hanberg, A., Hasengawa, R., Kennedy, S.W., Kubiak, T., Larsen, J.C., Van Leeuwen, F.X., Liem, A.K., Nolt, C., Peterson, R.E., Poellinger, L., Safe, S., Schienk, D., Tillitt, D., Tysklind, M., Younes, M., Waem, F. and Zacharewski, T. 1998. Toxic equivalent factors (TEFs) for PCBs, PCDDs, PCDFs for humans and wildlife, Environ. Health Perspect. 106, 775-792.
Zeeb, B.A., Amphlett, J.S., Rutter, A., and Reimer, K.J. 2006. Potential for phytoremediation of polychlorinated biphenyls-(PCB)-contaminated soil. Int. J. Phytorem. 8, 199-221

Chapter 2

PHYTOREMEDIATION OF ESCRAVOS (NIGERIA) LIGHT CRUDE OIL CONTAMINATED SOIL USING LEGUMES

Maryam Lami Ibrahim[1§], Udeme Josiah J. Ijah[2], Lawal S. Bilbis[3] and Shuaibu Bala Manga[1]

[1]Department of Microbiology, Usmanu Danfodiyo University Sokoto, PMB 2346 Sokoto, Nigeria, [2]Department of Microbiology, Federal University of Technology Minna, Niger, Nigeria, [3]Department of Biochemistry, Usmanu Danfodiyo University Sokoto, PMB 2346, Sokoto, Nigeria.

ABSTRACT

A sustainable approach for rehabilitation of petroleum contaminated soil is phytoremediation, the use of plants and their associated microorganisms to metabolize and degrade chemicals in place. This study evaluated three legumes for their phytoremediation potential by conducting plant growth inhibition assessment and contaminant degradation studies in the rhizosphere of the legumes. Three legume species ((*Arachis hypogea*, *Cajanus cajan* and *Lablab purpureus*) with three replications each were grown singly and mixed in varying concentrations (0.1%, 1%, 5%, 10% and 15%) of crude oil contaminated and uncontaminated soil in a completely randomized design. Microbes associated with the rhizosphere of the legumes were enumerated using a plate dilution technique and characterized. Degradation in the root zone of the plants was estimated gravimetrically. *A. hypogea* was the most tolerant species of the three legumes as biomass growth was stimulated at the highest crude oil concentration (15%). Nodule formation was significantly ($P< 0.05$) reduced in all crude oil

§ Corresponding Author: Maryam Lami Ibrahim, Usmanu Danfodiyo University, Sokoto, PMB 2346, Nigeria, 234803504-2282, marlamibrahim@hotmail.com

contaminated soil compared to the control. There were significant ($P< 0.05$) differences in populations of heterotrophic and crude oil degrading bacteria in the rhizosphere of the legumes. Crude oil degraders being the highest in the contaminated rhizosphere of *Cajanus cajan*, ranging between $1.9\pm 0.09 \times 10^7$ and $2.0\pm0.26 \times 10^8$cfu/g. Weight loss of crude oil ranged from 55.6% to 99.8% after 2 months and statistical analysis indicated significant differences ($P< 0.05$) between the legumes. The results show that the legumes were tolerant to varying concentrations of crude oil and exhibit potential for phytoremediation of petroleum hydrocarbon polluted soils.

Keywords: phytoremediation, rhizosphere, mixed planting, petroleum hydrocarbons

1. INTRODUCTION

Several oil producing countries are faced with the problem of environmental pollution resulting from exploration and exploitation activities of the petroleum industries. Soil and sediment contamination with petroleum products is a concern for ecological and human health because of their persistence, bioaccumulation and potential toxicity (Weber *et al*., 2008; Cui *et al*., 2013). Clean up technologies are often expensive, and most countries, such as Nigeria, cannot afford them. However, one technology that can be affordably and easily implemented is phytoremediation. Phytoremediation is the use of plants and their associated microorganisms to extract, sequester and/or detoxify pollutants. It is an efficient, environmentally friendly and cost effective method (Cunningham *et al*., 1996; Khan *et al*., 2000; Singh and Jain, 2003; Gerhardt *et al*., 2009). Because phytoremediation depends on natural synergistic relationships among plants, microorganisms and the environment, it does not require intensive engineering techniques.

Not all plants prove to be useful in phytoremediation processes. Depending on the type and age of contaminants present in the soil, plants are selected based on the application (mechanism) and the contaminant of concern. Plants used for phytoremediation of petroleum hydrocarbons must be tolerant of different concentrations of the contaminant (Kirk *et al*., 2002; Huang *et al*., 2004; Lin and Mendelssohn, 2008) and it has been reported that some plant species are more tolerant of petroleum hydrocarbons in soil than others (Chaineau *et al*., 1997; Robson *et al*., 2004). Many plant species are sensitive to petroleum contaminants, with some species experiencing adverse effects while others are positively stimulated. Most studies reported growth reduction in response to crude oil contamination (Lewis *et al*., 2011; Sodré *et al*., 2013) while others (Lin and Mendelsshon, 1996; Merkl *et al*., 2004;) reported plant growth stimulation.

Merkl *et al*. (2004) evaluated two grasses and six legume species for tolerance to crude oil added at 3% and 5% to savannah soil and concluded that enhanced growth in the presence of crude oil contamination was observed. Similarly, Ogbo (2009) studied the effects of diesel fuel contamination on seed germination of four crop plants-*Arachis hypogea*, *Vigna unguiculata*, *Sorghum bicolor* and *Zea mays* and concluded that *Zea mays* and *A. hypogea* were more tolerant due to their ability to withstand different degrees of contamination.

Phytoremediation has been reported to be facilitated through the rhizosphere effect; plants exude organic compounds through their roots that influence the abundance, diversity or activity of potential hydrocarbon degrading microorganisms in the zone surrounding the roots (Anderson *et al*., 1993; Phillips *et al*., 2012). Most studies on phytoremediation have been limited to the use of single plant treatments nevertheless, the use of mixed plant species (in most cases mixture of grasses and legumes) have reported the potential to increase soil heterogeneity and microbial diversity for effective pollutant removal (Phillips *et al*., 2009). Legumes confer more advantage when grown in an oil spill site because of their ability to fix atmospheric nitrogen. Therefore, it was the aim of this study to assess the tolerance of some legumes grown in single and mixed treatments to varying concentrations of crude oil by determining the effect of crude oil on some plant growth parameters and enumerating the bacteria associated with the rhizosphere of the legumes in relation to the varying concentrations of crude oil. The study also investigated biodegradation of the crude oil in the rhizosphere of the legumes.

2. MATERIAL AND METHODS

2.1 Sample Collection

Escravos (Nigeria) light crude oil was collected from the Kaduna Refinery and Petrochemical Company (KRPC), Kaduna, Nigeria. Plant seeds were obtained from the National Animals Production Research Institute (NAPRI), Zaria, Kaduna State, Nigeria. Soil samples were collected randomly using a hand dug soil auger at a depth of about 10-15 cm from the botanical garden of Usmanu Danfodiyo University, Sokoto, Nigeria. Samples were collected by augring different random spots and pooling them together to form composite samples.

2.2 Soil Preparation and Planting

Soil samples were air dried and passed through 2mm mesh to remove surface litter and large debris. Escravos light crude oil was used to contaminate the soil before transferring into planting pots. The pots were treated with five

different levels of crude oil with the following percentage soil contamination: 0.1%, 1%, 5%, 10% and 15% and control treatments in which one was left uncontaminated but planted and the other contaminated but not planted. Each treatment had three replications. The pots were left undisturbed for 7 days to allow for adsorption of the contaminant into the soil pores. The planting pots were perforated at the bottom and sides to allow for aeration and drainage of excess water; however, this was done after the interval of seven days. Pre-planting irrigation was done for a period of five days after crude oil contamination. The irrigation continued throughout the experimental period and was applied using watering cans such that each treatment option received a daily irrigation depth of 3.5 mm. Fertilizer (15-15-15 NPK) was applied to all pots (including controls) to improve the nutrient content of the soils. The application rate was 100 mg per pot; this was done on the third week after planting (Ayotamuno and Kogbara, 2007).

Seeds of three legume species, *Cajanus cajan, Arachis hypogea* and *Lablab purpureus* were surface-sterilized using the method of Kirk *et al*. (2005). Seeds were surface-disinfected by shaking at 200 rpm at room temperature for 15 min in a solution of 5.25% sodium hypochlorite in distilled water. Seeds were rinsed five times with distilled water and germinated in the dark at room temperature on sterile filter paper soaked in 5 ml of sterilized deionized water. Ten seedlings per pot were planted and later thinned to two strands per pot and monitored for 8 weeks.

2.3 Sampling

Plants were harvested and indices of plant performance such as shoot length, root length, root nodules and dry weight of biomass were determined to evaluate the tolerance level of the plant to the oil contaminants. Plants were uprooted from the planting pots and shaken to dislodge loose soil from the roots. Shoot length was assessed with a measuring tape from soil level to terminal bud. Radicles (root lengths) were rinsed with deionized water and the length measured. Plants were dried at 100°C for dry weight measurement.

Rhizosphere soil from all the treatments was collected for the assessment of microbial numbers and total petroleum hydrocarbons. Plants were uprooted from the contaminated and uncontaminated soils and shaken to dislodge excess soil adhering to the roots, defined here as rhizosphere soil.

2.4 Enumeration of Bacteria

Total heterotrophic and crude oil utilizing bacteria were determined using the plate dilution technique (Ibrahim *et al.,* 2008). One gram from each of the soil samples was serially diluted and aliquots (1 ml) were inoculated into sterile Nutrient Agar (NA) and Oil Agar (OA) for enumeration of total heterotrophic and

crude oil utilizing bacteria. The oil agar contained the following composition in g/l: NaCl 1.0; NH_4Cl 4.0; K_2HPO_4 1.8; KH_2PO_4 1.2; $MgSO_4.7H_2O$ 0.2; $FeSO_4.7H_2O$ 0.02, 2% crude oil, 20g agar in 1000 ml of distilled water. The pH was adjusted to 7.4. The NA and OA plates were incubated at 30 ^oC for 24 hours and 5 days, respectively. After incubation, colonies that developed on the plates were counted and recorded as colony forming units per gram (cfu/g) of soil. Pure cultures of the isolates were obtained by repeated subculturing on fresh media used for primary isolation. The pure cultures were maintained on agar slants at 4^oC for further characterization and identification.

2.5 Characterization and Identification of Isolates

Bacterial isolates were identified on the basis of microscopic examination, cultural characteristics, morphological characteristics and gram staining reaction. Relevant biochemical tests were also carried out including production of catalase, coagulase, oxidase, indole, utilization of citrate, fermentation of sugars, presence of spores, H_2S test, production of gas, motility and methyl red-Voges proskauer test. Confirmatory identities of the microorganisms were made using the schemes of Bergey's Manual of Determinative Bacteriology (Holt *et al*., 1994).

2.6 Rate of Degradation of Crude Oil in Soil

Crude oil degradation was determined using the method of Diab (2008). Ten grams of air dried soil samples were mixed with equal amount of anhydrous sodium sulphate (Na_2SO_4) to remove moisture. Petroleum hydrocarbons were soxhlet extracted with 30 ml chloroform for 8 hours. The chloroform extract was evaporated in a pre-weighed dish and the amount of total petroleum hydrocarbons (TPHs) was determined. The weight loss (%) of TPHs was then calculated using the formula:

Weight loss% = Amount of crude oil degraded / amount of crude oil added X 100

2.7 Statistical Analysis

Statistical tests were carried out using SPSS software (SPSS 16.0). Analysis of variance (ANOVA) was used to examine treatment effects for the overall data set. Duncans' multiple range test was used to compare means ($P \leq 0.05$) if significant differences existed between treatments.

3.0 RESULTS

3.1 Plant Performance

3.1.1 Shoot Length

Observations of the effect of crude oil contamination on legumes planted singly or mixed showed a high rate of survival across varying concentrations with a few notable exceptions. Shoot length (Figure 1) assessed in lower oil concentrations (0.1% and 1%) indicated that there was significant ($P \leq 0.05$) reduction for all the legumes grown in crude oil contaminated soil compared to uncontaminated soil. Though single treatments of *C. cajan* and *L. purpureus* were most affected in lower crude oil doses, the effect in the mixed plant treatment was not significant ($P \geq 0.05$). Both plants survived and even had a shoot length that was in some cases not significantly ($P \leq 0.05$) different from the control. *L. purpureus* which did not emerge in single planting at 0.1% and 1%, survived in the same concentrations in mixed planting with a shoot length (20.67 ± 4.33 cm at 1%) that was not significantly ($P \geq 0.05$) different from the control (21.33 ± 4.70 cm) (Figure 1). Similarly, *C. cajan* was unable to grow at 1.0% crude oil contamination when planted singly, but germinated and grew under a mixed planting regime with a highest shoot length of 16.00 ± 4.51 cm. Increasing oil pollution level to 5% for legumes grown singly did not produce any significant ($P \leq 0.05$) increase when compared with the control. In the mixed planting, however, *A. hypogea* had the highest shoot length that was significantly ($P \leq 0.05$) different from the control and the single treatment. Shoot length for *C. cajan* (13.33 ± 0.33 cm) and *L. purpureus* (13.00 ± 1.15 cm) differed significantly ($P \leq 0.05$) from the control (40.33 ± 2.40 cm and 36.67 ± 0.88 cm for *C. cajan* and *L. purpureus*, respectively.

In contrast to the other species, *A. hypogea* had a greater shoot length at higher oil doses (10 and 15%) in both single and mixed planting that was significantly ($P \leq 0.05$) different from the control (Figure 1). *C. cajan* and *L. purpureus* grown singly had a reduced shoot length compared to their respective controls, but did not differ significantly from each other. In the mixed planting, a negative effect for *C. cajan* and *L. purpureus* was observed as both plants were inhibited. *L. purpureus* could not germinate in either crude oil concentration.

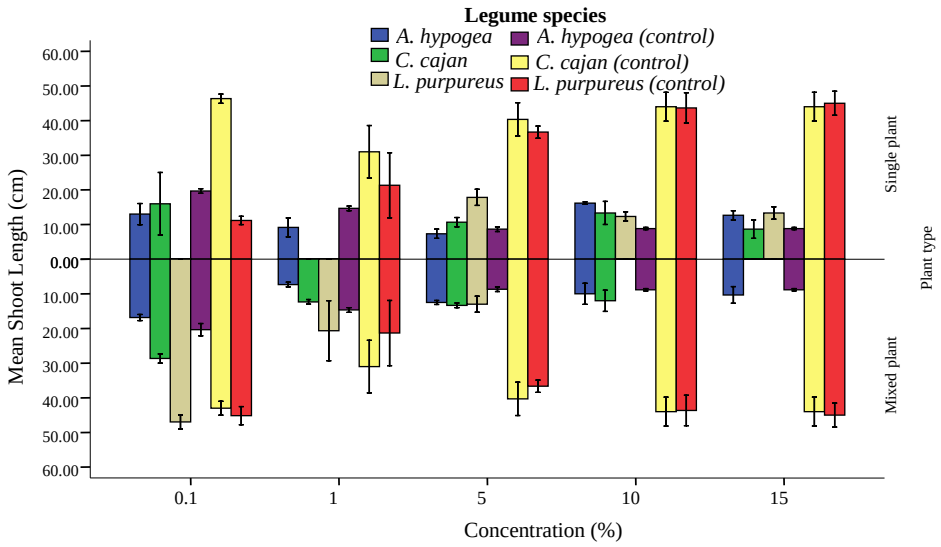

Figure 1. Shoot length (cm) of the legume species at different concentrations for single and mixed plant treatments.

3.1.2 Root Length

Generally, contamination caused a significant (P< 0.05) decrease in the root length of legumes grown singly in all the oil treatments compared to the control (Figure 2). Nonetheless, variations were observed in the performance of the legumes. At lower (0.1% and 1%) oil concentrations the highest root length was observed in *A. hypogea*, though there was no significant (P≥ 0.05) difference with the control. Contrary to the single treatment, root length in the mixed planting for both concentrations showed significant (P< 0.05) increase for *C. cajan* and *L. purpureus* which did not show any growth in the single planting. Root length in the mixed planting showed slight decrease for *A. hypogea*. Slight increase in root length was observed for *A. hypogea* and *L. purpureus* in moderately (5%) contaminated soil, although they were not significantly (P≥ 0.05) different when compared with their controls (Figure 2). Mixing the legumes however, caused additional influence in the root length for *A. hypogea* and *C. cajan*, while *L. purpureus* had shorter root length in mixed planting in comparison to single planting. Increasing oil concentration to 10% and 15% indicated that there was no apparent toxicity due to high crude oil concentration in the root length of either single and mixed plants with the exception of *L. purpureus* which was inhibited (Figure 2). Reduction effect that was significantly (P< 0.05) different with the control was observed for legumes grown singly whereas, the mixed plants indicated *A. hypogea* to be the most tolerant species since its root length was significantly (P< 0.05) increased (Figure 2). *C. cajan* and *L. purpureus* were

more affected by the 15% crude oil treatment as no growth of the two species was observed (Figure 2).

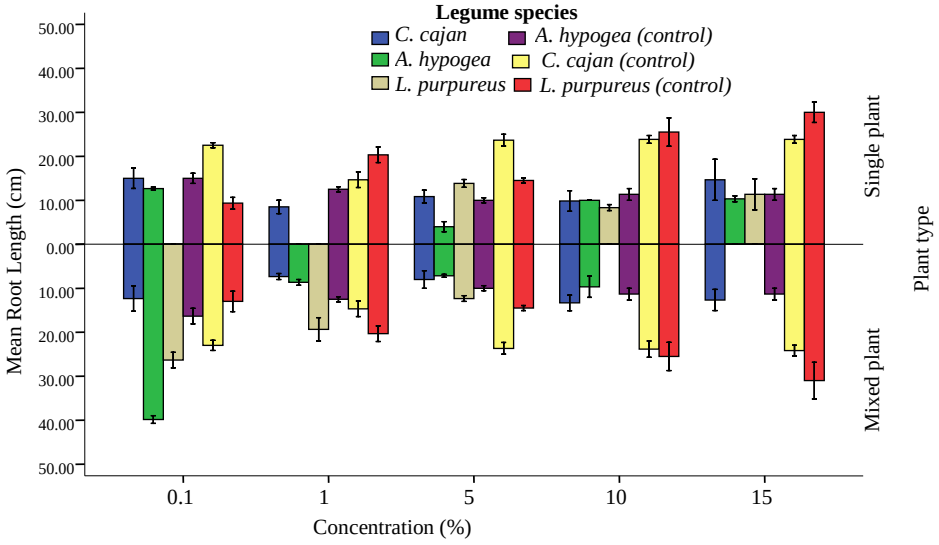

Figure 2. Root length (cm) of the legume species at different concentrations for single and mixed plant

3.1.3 Dry Weight of Plants

Results for the dry weight of plants are presented in Table 1. Significant ($P<0.05$) reduction in the dry weight of the legume species grown singly across all oil contamination levels was observed except in *A. hypogea*, which was grown in 5% and 10% crude oil treatments. The highest plant biomass in the crude oil contaminated soil was observed in *A. hypogea* grown in 10% crude oil while the lowest biomass was observed in *C. cajan* grown in 5% crude oil.. Conversely, in the mixed planting, a significant ($P< 0.05$) increase was observed in only *A. hypogea* grown in the 5% crude oil level, while all other treatments showed a reduction effect compared to the uncontaminated controls (Table 1).

3.1.4 Root Nodulation by Legumes

Root nodulation was significantly reduced by the presence of crude oil for the three species (Table 2) in most treatments. *A. hypogea* showed a significant ($P< 0.05$) increase in root nodulation in all the oil concentrations except in the 1% treatment compared to the control (Table 2). Fewer nodules (0.33 ± 0.33) were observed in the *C. cajan* treatment and only occurred in the 5% oil concentration. For *L. purpureus* only 5% and 15% crude oil contaminations produced a significant ($P< 0.05$) increase in root nodules, whereas nodulation reduced significantly ($P> 0.05$) in a 15% oil pollution level. All other crude oil treatments (0.1%, 1% and 10%) inhibited nodulation (Table 2). The species performance in the mixed planting indicated that the number of nodules in *A. hypogea* increased significantly ($P< 0.05$) in 0.1% and 15% compared to the uncontaminated control.

Table 1. Dry weight (kg) of legumes grown in different crude oil pollution levels in soil for single and mixed plant treatments.

Legume species	Crude oil concentration (%)				
	0.1	1	5	10	15
	Single plant treatment				
A. hypogea	$0.82^{d} \pm 0.02$	$0.99^{b} \pm 0.07$	$1.74^{c} \pm 0.35$	$1.86^{a} \pm 0.43$	$1.07^{cd} \pm 0.35$
A. hypogea (control)	$2.31^{b} \pm 0.16$	$2.01^{a} \pm 0.02$	$1.54^{c} \pm 0.07$	$0.22^{b} \pm 0.03$	$2.38^{a} \pm 0.30$
C. cajan	$0.36^{de} \pm 0.17$	0.00 ± 0.00	$0.10^{d} \pm 0.01$	$0.19^{b} \pm 0.00$	$0.29^{d} \pm 0.03$
C. cajan (control)	$1.49^{c} \pm 0.33$	$1.79^{a} \pm 0.36$	$2.40^{b} \pm 0.29$	$2.11^{a} \pm 0.03$	$2.06^{abc} \pm 0.32$
L. purpureus	$0.00^{e} \pm 0.00$	0.00 ± 0.00	$1.50^{c} \pm 0.01$	$0.51^{b} \pm 0.06$	$1.35^{bc} \pm 0.50$
L. purpureus (control)	$2.88^{a} \pm 0.01$	$2.27^{a} \pm 0.21$	$3.20^{a} \pm 0.20$	$2.35^{a} \pm 0.25$	$2.27^{ab} \pm 0.06$
	Mixed plant treatment				
A. hypogea	$0.90^{b} \pm 0.33$	$0.74^{b} \pm 0.14$	$2.48^{b} \pm 0.03$	$0.69^{b} \pm 0.09$	$1.10^{b} \pm 0.06$
A. hypogea (control)	$2.39^{a} \pm 0.24$	$2.18^{a} \pm 0.13$	$1.18^{c} \pm 0.37$	$0.29^{cd} \pm 0.03$	$2.38^{a} \pm 0.30$
C. cajan	$1.41^{ab} \pm 0.53$	$0.24^{b} \pm 0.04$	$0.42^{d} \pm 0.06$	$0.46^{bc} \pm 0.08$	$0.00^{c} \pm 0.00$
C. cajan (control)	$1.77^{ab} \pm 0.26$	$1.89^{a} \pm 0.31$	$2.30^{b} \pm 0.14$	$2.21^{a} \pm 0.03$	$2.06^{a} \pm 0.32$
L. purpureus	$2.10^{ab} \pm 0.75$	$0.44^{b} \pm 0.02$	$1.27^{c} \pm 0.06$	$0.00^{d} \pm 0.00$	$0.00^{c} \pm 0.00$
L. purpureus (control)	$2.49^{a} \pm 0.20$	$2.33^{a} \pm 0.18$	$3.20^{a} \pm 0.20$	$2.42^{a} \pm 0.22$	$2.27^{a} \pm 0.06$

Values are mean ± standard error of 5 replications

^{a,b,c} means in a column with different superscripts are significantly different ($P<0.05$)

The number of nodules formed by *A. hypogea* grown in 10% crude oil contaminated soil was not significantly ($P> 0.05$) different from the control. Although nodulation in *C. cajan* was highly affected by crude oil in both the single and mixed treatments, better performance was observed in the mixed planting for this legume than the single planting, particularly at 0.1% and 5%

crude oil (Table 2). Increased oil concentration also affected nodule formation for *L. purpureus*, causing a significant ($P< 0.05$) reduction in all the oil treatments compared to the controls.

3.2 Heterotrophic Count of Bacteria

Figure 3 shows the results for the heterotrophic count of bacteria isolated from the rhizosphere soil of the legumes. The results revealed that the mean count in the rhizosphere of the legumes significantly ($P\leq 0.05$) decreased in comparison with the control, especially *A. hypogea* and *L. purpureus* grown in 0.1% and 1% treatments, respectively. At 5% crude oil contamination, the mean counts were similar ($4.37\pm0.32 \times 10^7$ and $4.63\pm0.12 \times 10^7$ cfu/g) in the rhizosphere of *A. hypogea* and *L. purpureus* respectively and were not significantly ($P\geq 0.05$) different from each other. However, at higher crude oil doses (10% and 15%), heterotrophic bacterial count significantly ($P\leq 0.05$) increased in the rhizosphere of *L. purpureus* in comparison with the control. *A. hypogea* and *C. cajan* were mostly affected by high crude oil treatments (10% and 15%). *A. hypogea* had a count that was significantly ($P\leq 0.05$) different from the control at the highest (15%) crude oil contamination.

Table 2. Counts of root nodules of legumes grown in different crude oil pollution levels in soil for single and mixed planting treatments.

Legume species	Crude oil concentration (%)				
	0.1	1	5	10	15
	Single plant treatment				
A. hypogea	$17.33^{a} \pm 0.67$	$6.33^{b} \pm 2.73$	$18.67^{a} \pm 0.88$	$19.00^{a} \pm 0.58$	$32.33^{a} \pm 1.45$
A. hypogea (control)	$5.67^{b} \pm 0.33$	$13.00^{a} \pm 1.00$	$16.67^{b} \pm 0.88$	$8.67^{b} \pm 0.33$	$16.67^{b} \pm 0.88$
C. cajan	$0.00^{c} \pm 0.00$	$0.00^{c} \pm 0.00$	$0.33^{e} \pm 0.33$	$0.00^{e} \pm 0.00$	$0.00^{f} \pm 0.00$
C. cajan (control)	$5.67^{b} \pm 0.33$	$5.67^{b} \pm 0.67$	$6.67^{d} \pm 0.67$	$6.33^{c} \pm 0.33$	$6.67^{d} \pm 0.67$
L. purpureus	$0.00^{c} \pm 0.00$	$0.00^{c} \pm 0.00$	$15.00^{b} \pm 0.00$	$0.00^{e} \pm 0.00$	$3.00^{e} \pm 0.58$
L. purpureus(control)	$17.00^{a} \pm 0.58$	$6.33^{b} \pm 0.67$	$9.67^{c} \pm 0.33$	$3.67^{c} \pm 0.88$	$10.33^{c} \pm 0.33$
	Mixed plant treatment				
A. hypogea	$39.33^{a} \pm 0.67$	$4.67^{b} \pm 0.33$	$7.67^{c} \pm 0.33$	$8.67^{a} \pm 0.33$	$19.00^{a} \pm 0.58$
A. hypogea (control)	$5.83^{de} \pm 0.17$	$13.00^{a} \pm 1.00$	$16.67^{a} \pm 0.88$	$8.33^{a} \pm 0.33$	$16.33^{b} \pm 1.20$
C. cajan	$5.67^{e} \pm 0.67$	$0.00^{c} \pm 0.00$	$0.67^{e} \pm 0.33$	$0.00^{d} \pm 0.00$	$0.00^{e} \pm 0.00$
C. cajan (control)	$8.00^{d} \pm 0.58$	$5.67^{b} \pm 0.67$	$6.67^{c} \pm 0.67$	$6.33^{b} \pm 0.33$	$7.00^{d} \pm 0.58$
L. purpureus	$11.33^{c} \pm 0.67$	$5.67^{b} \pm 0.67$	$3.67^{d} \pm 0.88$	$0.00^{d} \pm 0.00$	$0.00^{e} \pm 0.00$
L. purpureus (control)	$14.33^{b} \pm 1.20$	$6.33^{b} \pm 0.67$	$9.67^{b} \pm 0.33$	$4.00^{c} \pm 0.58$	$11.00^{c} \pm 0.58$

Values are mean ± standard error of 5 replications

^{a,b,c} means in a column with different superscripts are significantly different ($P<0.05$)

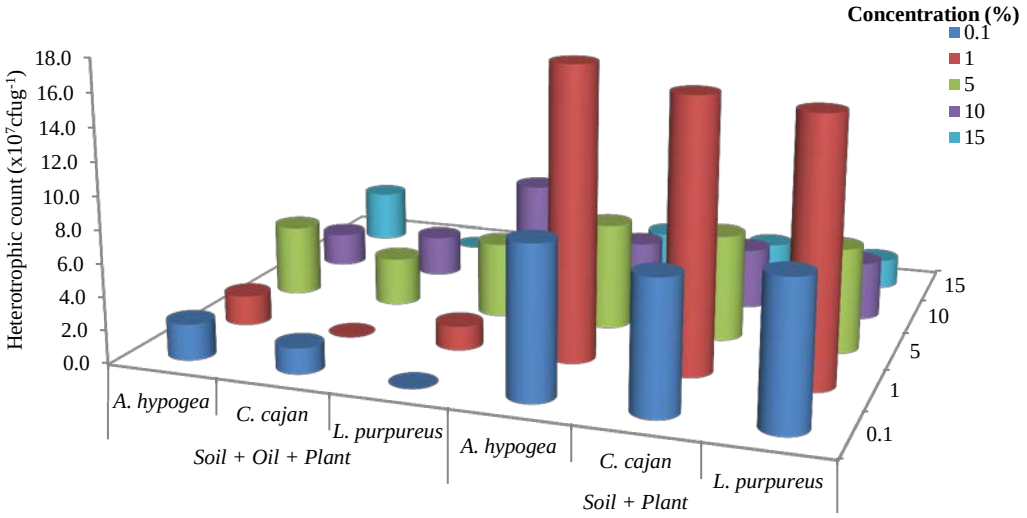

Figure 3. Heterotrophic bacterial count in the rhizosphere soil of legumes grown in different concentrations of crude oil.

3.3 Crude Oil Degrading Bacterial Count and Identity

The results for counts of crude oil degrading bacteria are shown in Figure 4. At lower oil concentrations (0.1 and 1%) crude oil degraders were significantly more abundant in the contaminated rhizosphere soil, especially in the 1% crude oil treatment. The results revealed that *C. cajan* harbored the highest counts of crude oil degraders ranging from $7.4 \pm 0.40 \times 10^7$ to $9.0 \pm 0.61 \times 10^7$cfu/g, which was slightly lower than the uncontaminated control. The total mean counts of bacteria in the contaminated rhizosphere of A. *hypogea* ranged from $1.63 \pm 0.15 \times 10^7$ to $7.0 \pm 0.07 \times 10^7$ cfu/g compared to control, which ranged between 2.8×10^7 and 8.3×10^7 cfu/g. *L. purpureus* had the lowest counts of crude oil degraders ranging from $1.00 \pm 0.08 \times 10^7$ to $3.53 \pm 0.43 \times 10^7$ cfu/g. Higher crude oil contamination (10 and 15%) clearly stimulated microbial numbers in the rhizosphere of *C. cajan.* Crude oil degrading bacteria were identified as *Actinobaicllus equuli, Bacillus alvei, Staphylococcus sciuri, Bacillus coagulans, Proteus mirabilis, Micrococcus kristinae, Bacillus megaterium, Proteus vulgaris, Morganella morganii, Bacillus thuringiensis, Bacillus firmus, Bacillus anthracis* and *Staphylococcus chromogenes.*

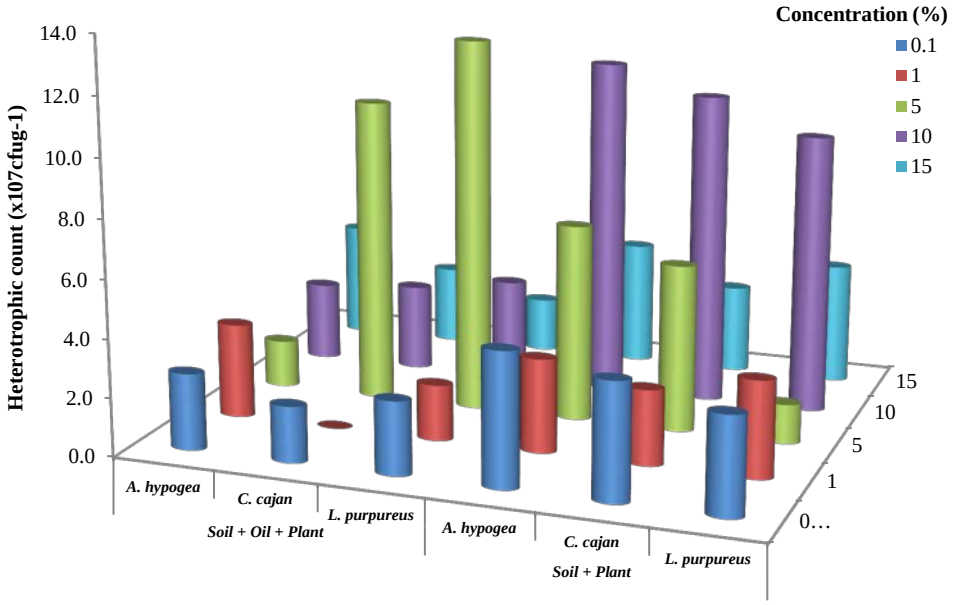

Figure 4. Crude oil degrading bacterial counts in the rhizosphere of the legumes.

3.4 Biodegradation of Crude Oil in Soil

Residual oil obtained from the rhizosphere of the legumes showed variation in the reduction of the total petroleum hydrocarbon (TPH) concentrations (Fig 4). The results showed that in the 0.1% treatment, crude oil was reduced by 55.6% in both rhizosphere soils of *A. hypogea* and *C. cajan. Mean*while, degradation in the rhizosphere of *L. purpureus* was 48.8% in comparison with the unplanted contaminated control, which had 66.7% oil degradation after 8 weeks. Similarly, at 1% crude oil contamination, *C. cajan* had the highest degradation rate of 90.2%. *A. hypogea* and *L. purpureus* also had higher rate (>80%) of crude oil degradation than the control (65%). Crude oil reduction at 5% pollution level was 98% in the rhizosphere of *A. hypogea* whereas 91.5% and 89.4% oil reduction in the rhizosphere of *C. cajan and L. purpureus* respectively was observed, in comparison, only a 40.4% reduction was observed in unplanted control after 8 weeks. At higher pollution levels of 10% and 15%, the relatively higher oil degradation (98.0%) was observed in *A. hypogea* than the other legumes (*C. cajan* and *L. purpureus*) in comparison to 60.8% oil degradation in the control after 8 weeks (Figure 5).

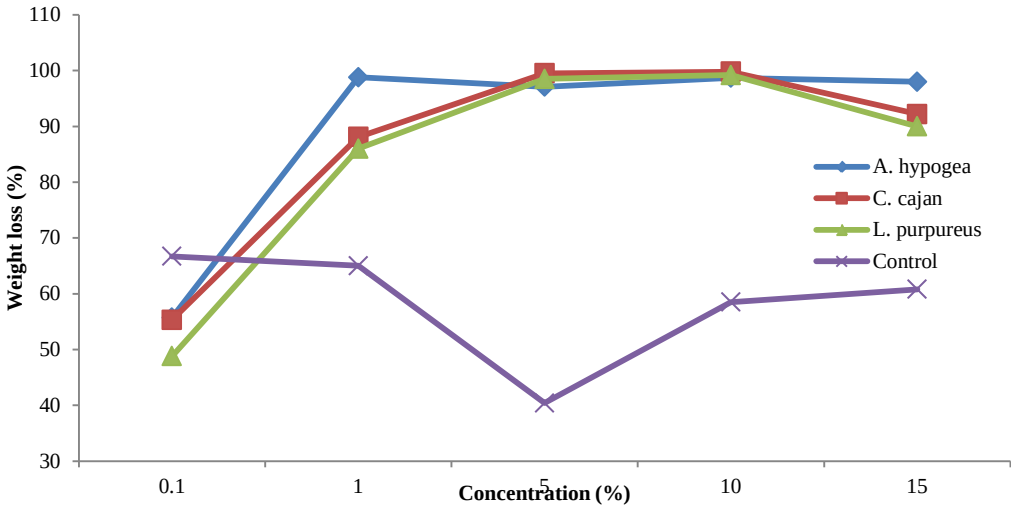

Figure 5. Weight loss (%) of crude oil in the rhizosphere and non rhizosphere of legumes after 8 weeks growth period.

4. DISCUSSION

Plant tolerance to petroleum hydrocarbons assessed in the present study indicates plant sensitivity to the contaminants in varying capacities. Growth reduction in the three legumes (*A. hypogea*, *C. cajan* and *L. purpureus*) observed may be attributed to the toxicity of the petroleum compounds. A number of studies have indicated the toxic effect of crude oil on plants such as decreasing plant height, biomass and crop yield (Chaineau *et al*., 1997; Wiltse *et al*., 1998; Kirk *et al*., 2002; Merkl *et al*., 2004; Phillips *et al*., 2006; Ogbo, 2009). Our results show that *A. hypogea* was the most tolerant of the three legume species assessed due to the lack of adverse growth effect in the presence of varying concentrations of crude oil.. According to Cai *et al*. (2009), plants exhibit responses to toxic compounds only after being exposed to the 'threshold concentration' which varies for different compounds and plant species. A similar effect of reduced shoot length was observed by Gaskin (2008) for *B. decumbens* at 0.5% and 1% diesel oil contamination. Ehiagbonare *et al*. (2011) observed reduced shoot length for *Arachis hypogea* and *Zea mays* grown in five levels (1-5%) of crude oil contamination, with the highest shoot length being recorded in 1% oil pollution level.

Contrary to the findings in this study, some phytoremediation studies (Vwioko and Fashemi, 2005; Muratova *et al*., 2009) reported reduced biomass growth or even plant death at elevated concentrations of petroleum hydrocarbons. *A. hypogea* was not only able to survive but had growth stimulation of both shoot

and root length at the highest oil concentration (15%) used in this study. This may be due to the response of the plant to stress imposed by the oil, or due to activity of microorganisms residing in the rhizosphere that aided the plant in reducing the toxicity of the more volatile compounds found in the crude oil. Similar findings were reported by Gaskin (2008) who observed significant stimulatory effect of diesel/oil contamination on the growth of *C. ambiguus* at concentration of 1%. Merkl *et al*. (2004) also observed growth stimulation for shoot length of *M. camporum* and shoot biomass of *S. capitata.*

L. purpureus could not grow at 0.1% and 1% of crude oil, and similarly, *C. cajan* could not grow at 0.1%. However, in the mixed planting involving these two species, the two plants grew at the two oil concentrations (0.1% and 1%). The reason could be that at these oil concentrations biodegradation was fast and some of the resultant products may be inhibitory to the plants. The results obtained are in agreement with the findings of Song *et al*. (2005) stating that the lowest observable concentration (10mg/kg) of phenanthrene affected green onion, whereas pyrene at a concentration of 50 mg/kg affected wheat. Early on, Salanitro *et al.* (1997) found that toxicity may not be the only factor contributing to growth inhibition, but other factors such as soil properties, hydrocarbon type, microbial load and genetic diversity in plant communities may also contribute. It was also observed in this study that the highest shoot length for *L. purpureus* was observed in a 5% oil concentration. This concentration, may be the optimal concentration that the plant could be exposed to. Spiares and Kenworthy (2001) made a similar observation.

Even though mixed planting did not seem to influence plant performance in the contaminated soil, *C. cajan* and *L. purpureus* were stimulated having enhanced shoot and root length in 0.1% treatment when compared with the control. This suggests that the effect of contamination was reduced due to the presence of other plants. This finding is consistent with that of Ogbo (2009) that higher plant density improved performance of the weed *Paspalum scrobiculatum* L. against stress imposed by crude oil contamination. The author also reported that wild chipilín was the most sensitive because the concentrations of 50,000 mg/kg^{-1} fresh oil and 79,457 mg/kg^{-1} weathered oil inhibited vegetative growth and consequently the formation of biomass. This report corresponds with the findings in this study because *L. purpureus* and *C. cajan* were only able to resist 5% and 15% (for *L. purpureus*) and 5% (for *C. cajan*) of crude oil contamination.

Nodulation in legumes was significantly reduced in all the oil treatments probably due to crude oil toxicity, which may have affected the nitrogen-fixing microorganisms. Other studies (Merkl *et al*., 2004b; Rivera-Crutz *et al*., 2005) have reported the effect of PHCs on nodule formation in legumes. Hernandez (1997) observed that kerosene reduced the number of nodules of *Phaseolus vulgaris* and found that the concentration of 2500 mg/kg of kerosene did not

result in a reduction of 10 times the number of nodules on the plants established in the control soil. All crude oil concentrations grown with *A. hypogea* favored nodule formation with the the exception of 1% oil treatment, which was possibly due to unfavorable soil conditions. Atlas and Bartha (2002) reported that under favorable conditions in the soil *Rhizobium* can invade the root hairs under the influence of some bacterial products. All leguminous rhizobia are sensitive to low pH and cannot establish infections in acidic soils (Rivera-Crutz *et al*., 2005); therefore, it may be that the pH of the rhizosphere soil in this oil concentration was acidic due to the crude oil biodegradation process or plant root exudates. This may also explain why the shoot length of this legume was found to be the lowest since formation of nodules increase the nitrogen content of crude oil-impacted soil. Suominen *et al.* (2000) observed that higher concentrations (500 ppm) of m-toluate in the soil blocked the formation of nodules in *Galega orientalis.* Contrary to the observation in this study, the report by de Farias *et al*. (2009) found that the nodule quantities in roots exposed to petroleum tend to decrease as the oil concentrations increase.

For *C. cajan* and *L. purpureus,* most of the oil treatments (0.1, 1, 10 and 15%) inhibited nodulation while others (5 and 15%) reduced the number of nodules that were likely the result from reduced activity of the genus *rhizobium* due to the presence of an oil contaminant. Werner *et al*. (1998) reported that polyaromatics derived from petroleum could possibly inhibit nodulation by reducing rhizobial growth and/or activity, or disturb the chemical exchange of messenger molecules between symbiont and host, which is essential for the localization of the host by the symbiont and the infection process. Rivera-Cruz *et al*. (2005) also reported that petroleum concentrations higher than 50,000 mg/kg inhibited the development of nodules in *Crotalaria Scop, Leucaena* Benth. and *Mimosa pudica* Mill.

Generally, plant specific differences in total heterotrophic and crude oil degrading counts of bacteria were observed across all the legumes in comparison with the planted control, thus suggesting the effect of the contamination and its intensity. *C. cajan* exhibited greater rhizosphere effect that may indicate the plant's capacity to exude substances which stimulate microbial number and activity. Diab (2008) reported that highest oil degraders were observed in the rhizosphere soil of *Vicia faba* (62.4%) as compared to *Zea mays* (19.9%) and *Triticum aestivum* (17.6%). Early on, Radwan *et al*. (2005) observed that the total number of oil degrading bacteria increased in the rhizosphere of the *Vicia faba* plant and a higher degradation of hydrocarbons in sand close to the root.

In the present study, six genera of bacteria belonging to the species of *Actinobacillus, Bacillus, Staphylococcus, Proteus, Micrococcus* and *Morganella* were identified. Most of these isolates have been implicated in biodegradation of petroleum hydrocarbons, especially the *Bacillus* species (Frick *et al*., 1999; Ijah

and Antai, 2003), which had the highest frequency of occurrence. Our results are consistent with that of Frick *et al.* (1999), which listed 25 genera of crude oil degrading bacteria including all the genera isolated in the current study.

The weight loss of residual crude oil extracted from the rhizosphere of the legumes showed an enhanced loss of the contaminant, which may indicate the effectiveness of the legumes in providing favorable conditions for their associated microorganisms to enhance biodegradation. Different plant species have been reported to be effective in rhizoremediation of petroleum hydrocarbons especially grasses and legumes (Yeteem *et al*., 2000; Merkl *et al*., 200b; Kirk et al., 2005; Diab, 2008; Gaskin, 2008; Tang, 2010). The highest degradation rate was observed at a moderate concentration (5%) for all three legumes (especially *A. hypogea*) screened in this study. This concentration may be less toxic to plants and therefore more favorable for microbial growth and activity. Similar observations were made by Spaires and Kenworthy (2001) and Tang *et al*. (2010).

Similarly, at higher (10 and 15%) crude oil treatments, the degradation rate was up to 98% for all legumes in comparison with control. The reason may be that the microorganisms in the rhizosphere of the legumes have adapted to the high crude oil content, thus serving as a carbon and energy source to the microorganisms leading to an increased number and activity. However, this observation contrasts that of Tang *et al*. (2010) which suggests that high TPH content inhibits plant growth and microbial activity in the rhizosphere hence, low TPH degradation.

5. CONCLUSION

Our results suggest that the effect of contamination was plant-specific and not dose-dependent. While *A. hypogea* was not impaired by high crude oil contamination, *C. cajan* and *L. purpureus* were sensitive to a low oil dose. No significant differences in plant performance for single and mixed planting were observed; however, differences in crude oil degradation by the legumes were noted and plant survival may have contributed to this potential. Therefore, plant tolerance to varying crude oil treatments may serve as a screening criterion for the use of for phytoremediation in crude-oil impacted soil.

6. REFERENCES

Anderson, T.A., Guthrie, E.A., and Walton, B.T. 1993. Bioremediation in the rhizosphere: plant roots and associated microbes clean contaminated soil. Environ. Sci. Technol. 27, 2630–2636.

Atlas, R.M and Bartha, R. 2002. *Microbial Ecology and Environmental Microbiology*. Madrid: Pearson. 4, 677.

Ayotamuno, J.M. and Kogbara, R.B. 2007. Determining the tolerance level of *Zea mays* (maize) to a crude oil polluted agricultural soil. Afr. J. Biotechnol. 6(11),1332-1337.

Chaıneau, C.H., Morel, J.L. and Oudot, J. 1997. Phytotoxicity and plant uptake of fuel oil hydrocarbons. J. Environ. Qual. 26, 12174-12180.

Cui, X., Mayer, P. and Gan, J. 2013. Methods to assess bioavailability of hydrophobic organic contaminants: Principles, operations and limitations. Environ. Pollut. 172, 223-234.

Cunningham, S.D., Anderson, T.A., Schwab, A.P. and Hsu, F.C. 1996. Phytoremediation of soils contaminated with organic pollutants. Adv. Agron. 56, 55-114.

de Farias, V., Maranho, L.T., de Vasconcelos, E.C., da Silva Carvalho Filho, M.A., Lacerda, L.G., Azevedo, J.A.., Pandey, A. and Soccol, C.R. 2009. Phytodegradation potential of *Erythrina crista-galli* L., Fabaceae, in petroleum-contaminated soil. Appl. Biochem. Biotechnol. 157, 10-22.

Diab, E.A. 2008. Phytoremediation of oil contaminated desert soil using the rhizosphere effects of some plants. Res. J. Agric. Biol. Sci. 4(6), 604-610.

Ehiagbonare, J.E., Obayuwana, S., Aborisade, W.T. and Asogwa, I. 2011. Effect of unspent and spent diesel fuel on two agricultural crop plants: *Arachis hypogea* and *Zea mays*. Sci. Res. Essays. 6(11), 2296-2301.

Frick, C.M., Farrell, R.E and Germida, J.J. 1999. Assessment of phytoremediation as an in-situ technique for cleaning oil-contaminated sites: Petroleum Technology Alliance of Canada. Available at: http://www.rtdf.org/public/phyto/phylinks.htm

Gaskin, S.E. 2008. *Rhizoremediation of Hydrocarbon Contaminated Soil Using Australian Native Grasses*. Ph.D Thesis. Flinders University of South Australia, Australia.

Hernandez, A.E. 1997. Influence of Complex Hydrocarbons on Rhizosphere Populations and Growth of Beans Variety Michoacan 12-A3. PhD Thesis, Graduate College status, Montecillo, Mexico.

Holt, J.D. 1994. Bergey's Manual of Determinative Bacteriology, 9th Edition. Williams and Wilkias CO. Baltimore. 983.

Huang, X., El-Alawi, Y., Penrose, M., Glick, B.R. and Greenberg, B.M. 2004. Responses of three grass species to creosote during phytoremediation. Environ. Pollut. 130, 453-463.

Ibrahim, M.L., Ijah, U.J.J., Manga, S.B. and Rabah, A.B. 2008. Occurrence of hydrocarbon utilizing bacteria in the rhizosphere of *Eucalyptus camaldulensis, Lablab purpureus* and *Moringa oleifera*. Int. J. Appl. Sci. 2, 21-26.

Ijah, U.J.J. and Antai, S.P. 2003. The potential use of chicken-drop microorganisms for oilspill remediation. The Environmentalist. 23, 89-95.

Khan, A.G., Kuek, C., Chaudhry, T.M., Khoo, C.S. and Hayes, W.J. 2000. Role of plants, mycorrhizae and phytochelators in heavy metal contaminated land remediation. Chemosphere. 41, 197-207.

Kirk, J.L., Klironomos, J.N., Lee, H. and Trevors, J.T. 2002. Phytotoxicity assay to assess plant species for phytoremediation of petroleum contaminated soil. Bioremed. J. 6, 57-63.

Kirk, J.L., Klironomos, J.N., Lee, H. and Trevors, J.T. 2005. The effects of perennial ryegrass and alfalfa on microbial abundance and diversity in petroleum contaminated soil. Environ. Pollut. 133, 455–465.

Lewis, M., Pryor, R. and Wilking, L. 2011. Fate and effects of anthropogenic chemicals in mangrove ecosystems: a review. Environ. Pollut. 159, 2328-2346.

Lin, Q. and Mendelssohn, I.A. 2008. Determining the tolerance limits for restoration and phytoremediation with *Spartina Patens* in crude oil-contaminated sediment in greenhouse. Arch. Agron. Soil. Sci. 54(6), 681-690.

Merkl, N., Schultz-Kraft, R. and Infante, C. 2004. Assessment of tropical grasses and legumes for phytoremediation of petroleum-contaminated soils. Water, Air Soil Pollut. 165, 195-209.

Merkl, N., Schultz-Kraft, R. and Infante, C. 2004b. Phytoremediation in the tropics- The effect of crude oil on the growth of tropical plants. Bioremed. J. 8, 177-184.

Muratova, A., Golubeva, S., Wittenmayer, L., Dmitrievaa, T., Bondarenkovaa, A., Hircheb, F., Merbach, W. and Turkovskayaa, O. 2009. Effect of the polycyclic aromatic hydrocarbon phenanthrene on root exudation of *Sorghum bicolor* (L.) Moench. Environ. Exp. Bot. 66, 514–521.

Ogbo, E.M. 2009. Effects of diesel fuel contamination on seed germination of four crop plants- *Arachis hypogaea, Vigna unguiculata, Sorghum bicolor* and *Zea mays.* Afric. J. Biotechnol. 8(2), 250-253.

Phillips, L.A., Greer, C.W., Farrell, R.E. and Germida, J.J. 2009. Field-scale assessment of weathered hydrocarbon degradation by mixed and single plant treatments. Appl. Soil Ecol. 42, 9-17

Phillips, L.A., Greer, C.W., Farrell, R.E. and Germida, J.J. 2012. Plant root exudates impact the hydrocarbon degradation potential of a weathered-hydrocarbon contaminated soil. Appl. Soil Ecol. 52, 56-64.

Rivera-Cruz, M.C., Trujillo-Narcia, A., Cruz, M.A.M. and Chavez, E.M. 2005. Toxicological evaluation of petroleumcontaminated soil via test with legumes. Interciencia 30, 326-331.

Robson, D.B., Germida, J.J., Farell, R.E. and Knight, J.D. 2004. Hydrocarbon tolerance correlates with seed mass and relative growth rate. Bioremed. J. 8, 185-199.

Salanitro, J. P., Dorn, P. B., Huesemann, M. H., Moore, K. O., Rhodes, I. A., Jackson, L. M. R., Vipond, T. E., Western, M. M., and Wisniewski, H. L. 1997. Crude oil hydrocarbon bioremediation and soil ecotoxicity assessment. Environ. Sci. Technol. 31, 1769-1776.

Singh, O.V. and Jain, R.K. 2003. Phytoremediation of toxic aromatic pollutants from soil. Appl. Microbiol. Biotechnol. 63, 128-135.

Sodré, V., Caetano, V.S., Rocha, R.M., Carmo, F.L., Medici, L.O., Peixoto, R.S., Rosado, A.S. and Reinert, F. 2013. Physiological aspects of mangrove (Laguncularia racemosa) grown in microcosms with oil – degrading bacteria and oil contaminated sediment. Environ. Pollut. 172, 243-249

Song, Y.F., Gong, P., Zhou, Q.X. and Sun, T.H. 2005. Phytotoxicity assessment of phenanthrene, pyrene and their mixtures by a soil-based seedling emergence test. J. Environ. Sci. 17, 580-583.

Spaires, J.D., Kenworthy, K.E. and Rhykerd, R.L. 2001. Root and shoot biomass of plants seeded in crude oil contaminated soil. Texas. J. Agiric. Nat. Res. 14, 117-124.

Suominen, L., Jussila, M.M., Makelainen, K., Romantschuk, M. and Lindstrum, K. 2000. Evaluation of the Galega-*Rhizobium galegae* system for the bioremediation of oil contaminated soil. Environ. Pollut. 107, 239-244.

Tang, J., Wang, R., Niu, X., Wang, M. and Zhou, Q. 2010. Characterization on the rhizoremediation of petroleum contaminated soil as affected by different influencing factors. Biogeosci. Discuss. 7, 4665-4688

Vwioko, D.E. and Fashemi, D.S. 2005. Growth response of *Ricinus comminus* L. (castor oil) in spent lubricating oil polluted soil. J. Appl. Sci. Environ. Manag. 9, 73-79.

Weber, R., Gaus, C., Tysklind, M., Johnston, P., Forter, M., Hollert, H., and Heinisch, E. 2008. Dioxin- and POP-contaminated sites-contemporary and future relevance and Challenges. Environ. Sci. Pollut. Res. 15, 363-393.

Wiltse, C.C., Rooney, W.L., Chen, Z., Schwab, A.P., and Banks, M.K. 1998. Greenhouse evaluation of agronomic and crude oil-phytoremediation potential among alfalfa genotypes. J. Environ. Qual. 27, 169-217.

PART II: Engineered Remediation

Chapter 3

REMEDIATION OF MTBE & TBA IN GROUNDWATER USING A FLUIDIZED BED BIOREACTOR

Joseph E. O'Connell [§]
Cardno ERI, 25371 Commercentre Drive, Suite 250, Lake Forest, CA 92630

ABSTRACT

Biological fluidized bed reactors are being used at over 30 sites around the country to remove the fuel oxygenates tertiary-butyl alcohol (TBA) and methyl tertiary-butyl ether (MTBE) from groundwater and convert them to carbon dioxide and water. Most of the systems operate in California, where rainfall is scant and groundwater is at a premium. The basic system has been adapted for use in a variety of conditions around the country. In New Hampshire accommodation was made for freeze protection and for iron and manganese found in the incoming water. A bioreactor in Maryland required pH adjustment for increased pH when the groundwater was exposed to oxygen. Since start-up, the system in Maryland has processed water containing 10,000 parts per billion (ppb) of MTBE and TBA at a rate exceeding 25 gallons per minute (gpm) to obtain a stream containing less than 10 ppb of MTBE and less than 15 ppb of TBA, which is suitable for discharge into a local stream. A bioreactor operated at a service station site in South Florida for about one and a half years until the site was cleaned up. In many cases, bioreactors have been picked up and moved to another site when remediation was complete. At a site in the Los Angeles basin, pH adjustment was required to reduce the pH when the groundwater was exposed

§ Joseph O'Connell, Sc.D., P.E., Cardno ERI, 25371 Commercentre Drive, Suite 250, Lake Forest, CA 92630, (949) 457-8950, joe.oconnell@cardno.com

to oxygen. In some cases, like the site in New Hampshire and the one in Florida, the water exiting the bioreactor has been re-injected into an impacted area of the site, thus promoting an *in-situ/ex-situ* operation and speeding up the final clean-up. This paper describes the bioreactor operating principles, process, equipment, and field experiences. Analytical data for the water being treated at the various sites are presented and capital and operating costs are reviewed.

Keywords: bioremediation, TBA, MTBE, groundwater, fuel oxygenates

1. INTRODUCTION

Cardno ERI (formerly Environmental Resolutions, Inc.), in conjunction with Drs. Kate Scow, Edward Schroeder, and Daniel Chang at the University of California at Davis (UC Davis), has developed a biological treatment process for removing fuel oxygenates, such as methyl tertiary butyl ether (MTBE) and tertiary butyl alcohol (TBA), from water. The original source of the biomass was a vapor-phase biofilter located at the Joint Water Pollution Control Plant in Carson, California, used in 1997 to remove volatile organic compounds (VOCs) and odors in the off-gas from a sewage treatment plant. After about 370 days, the biomass adapted to consume MTBE. The culture was harvested in 1998 and further developed by UC Davis, who isolated the active microbes and named them *Methylobium petroleophilum*, or PM-1.

UC Davis then applied the culture to MTBE biodegradation in a bench-scale four-inch-diameter trickling bed filter. In 1999, Cardno ERI set up a pilot plant with eight 16-inch-diameter trickling bed filters at a service station site in Healdsburg, California, and began the development of a high surface area fluidized bed bioreactor in Orange County, California. Cardno ERI's first prototype fluidized bed bioreactor began operating in 2000 at a site in Palo Alto, California. Since that time, Cardno ERI fluidized bed bioreactors have been put into operation at over 30 other sites in California, New Hampshire, Maryland, and Florida.

Although MTBE is no longer used in gasoline, past fuel releases may have introduced enough MTBE and TBA into the subsurface to affect groundwater quality for years to come. Bioreactors offer a green solution that permanently destroys these compounds, converting them to carbon dioxide and water, rather than merely transferring them to another medium, such as air or granular activated carbon (GAC).

2. MATERIAL AND METHODS

2.1 Fluidized Bed Bioreactor Principles

This bioreactor is a two-phase system (solid - sand and liquid - water, no gas) with a recirculating water stream. The biomass is confined to the reaction vessel by its adherence to fine sand. The biomass is distributed within the bioreactor by fluidization with an upward flow of recirculating water. The water passes upward through the sand where the biomass removes VOCs as the water passes by. The reaction on any given pass is limited by the amount of oxygen available in the water. Oxygen solubility in water is a function of the temperature and the partial pressure of oxygen as shown in Table 1. Experience to date indicates that the bioreactor operates best between 10°C and 35°C (50°F and 95°F) at a partial pressure of oxygen above 0.21 atmospheres.

Table 1. Dissolved Oxygen (mg/L) in Water vs. Temperature and Oxygen Partial Pressure. Temperatures are shown in metric (no parentheses) and American (parentheses) units.

	Temp °C (°F)						
	5 (41)	**10 (50)**	**15 (59)**	**20 (68)**	**25 (77)**	**30 (86)**	**35 (95)**
Partial Pressure 0.21 atmosphere	12.8	11.3	10.1	9.1	8.3	7.7	7.0
Partial Pressure 0.40 atmosphere	24.3	21.5	19.2	17.3	15.8	14.6	13.3

The bioreactor is capable of complete reaction in one pass through the fluidized bed as long as the dissolved oxygen (DO) is not consumed completely and sufficient nutrients, such as nitrogen, phosphorus, and potassium (N, P, and K) are available. In addition, pH needs to be in the range of 6.5 to 8.5 standard units. The required oxygen loading is approximately three pounds of oxygen per pound of fuel oxygenates and petroleum hydrocarbons. Oxygen demands for relevant compounds are shown in Table 2.

Table 2. Oxygen Demand for Selected Fuel Constituents.

	Compound					
	TBA	**MTBE**	**Benzene**	**Toluene**	**Xylene or Ethylbenzene**	**Saturated Hydrocarbons**
Required mass of O_2/ Mass fuel constituent	2.59	2.73	3.08	3.13	3.17	3.43

PM-1 is a naturally occurring bacterium, or consortium of bacteria, that has been identified at locations in California, New York, and Europe. It has been

found at both contaminated and uncontaminated sites. PM-1 is characterized by a very slow growth rate. Its doubling time is on the order of weeks rather than on the order of hours, as is typical for many other common aerobic bacteria. The slow growth results in a low yield, meaning very little biomass is produced per pound of organic material consumed. This is advantageous in that excess biomass (sludge) requiring removal from the system is rarely generated. On the other hand, it means that a bioreactor should be started up with a large amount of biomass to avoid delays while waiting for the population to grow. Generally, a bioreactor is started up with half the biomass that will ultimately be needed so that within several weeks the population will be sufficiently large. PM-1 consumes TBA, ethers, and petroleum hydrocarbons as food, breathing oxygen in the process. Photomicrographs of PM-1 are included in Figure 1.

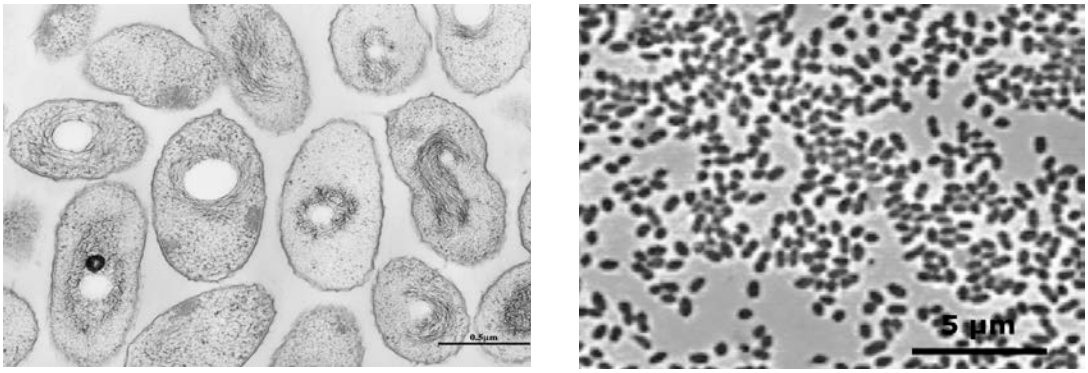

Figure 1. Photomicrographs of PM-1.

The bacterial consortia, while capable of consuming fuel oxygenates, actually prefer to dine on BTEX and other petroleum hydrocarbons. If high concentrations of petroleum hydrocarbons are present in the water being treated, petroleum hydrocarbon degraders that may be present will tend to out-compete the fuel oxygenate degraders, and the bioreactor may lose the ability to degrade MTBE and TBA. If the total concentration of BTEX and other petroleum hydrocarbons exceeds half the total fuel oxygenates concentration, pretreatment using GAC or air stripping is generally recommended ahead of the bioreactor for removal of these more easily metabolized compounds. The fuel oxygenates will break through the GAC or air stripping unit and enter the bioreactor for treatment. This strategy keeps the bacteria focused on consuming the fuel oxygenates.

2.2 Bioreactor Operation

The key to bioreactor sizing and operation is contaminant mass loading, which is the product of the flow rate of groundwater from the site recovery wells times the average total VOC concentration in the groundwater from the site recovery wells. As an example, bioreactor operation for a system to process 10 gallons per minute (gpm) containing 5,000 parts per billion (ppb) or micrograms per liter (µg/L) of MTBE and 5,000 µg/L of TBA (10,000 µg/L total) is shown schematically in Figure 2. The mass loading in this example is 10 gpm times 10,000 µg/L, or 100,000 gpm-µg/L. (this is the equivalent to 1.3 pounds/day.) The constant recirculation rate for this bioreactor to keep the sand media fluidized, is 50 gpm. Well water enters the feed tank where it is diluted with 40 gpm of clean treated water to achieve a diluted MTBE/TBA concentration of 2,008 µg/L and a DO of about eight mg/L. Fifty gpm of the mixture of influent and treated water are pumped into the bottom of the fluidized bed. After spending 15 minutes in the bioreactor, water exiting the top of the bioreactor has low DO and non-detectable MTBE/TBA (<10 µg/L). The treated water passes through an oxygenator where it is replenished with DO. An exit flow of 10 gpm leaves 40 gpm to dilute the incoming 10 gpm stream and cycle through the fluidized bed.

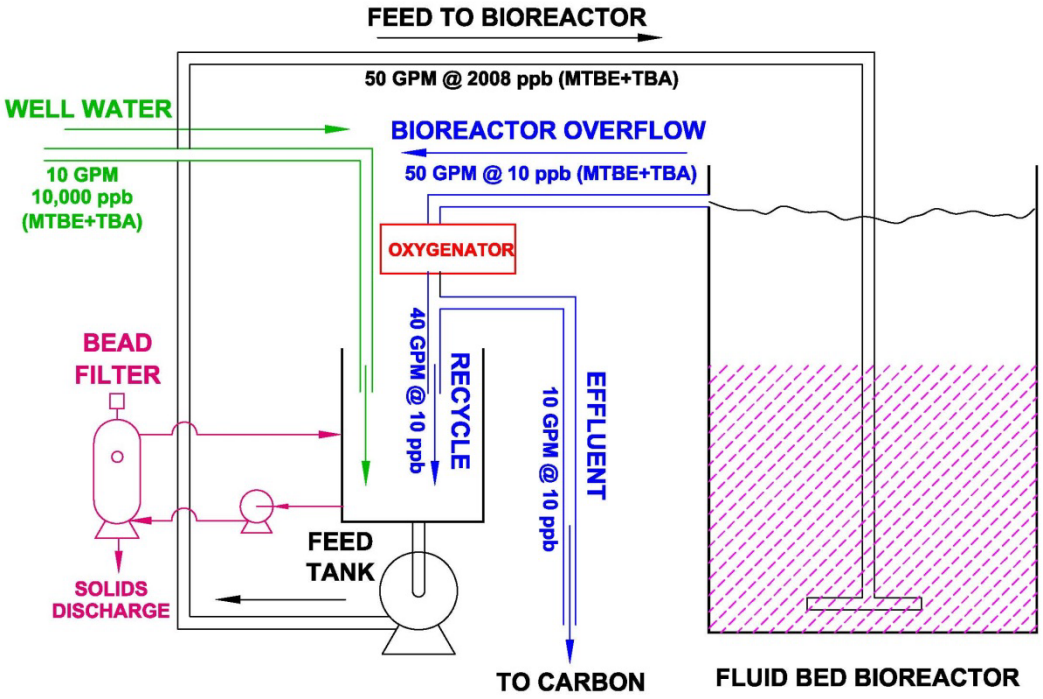

Figure 2. Schematic Flow Diagram.

Higher concentrations of MTBE/TBA can be handled by reducing the influent flow rate from the recovery wells so the mass loading on the system is maintained at 100,000 gpm-µg/L. Another alternative would be to add an oxygen booster. With increased oxygenation from an oxygen booster, the mass loading can be raised to 240,000 gpm-µg/L (three pounds per day).

Treated effluent can be discharged back to groundwater, surface water, or a publicly owned treatment works (POTW). The concentrations of MTBE and TBA exiting the fluidized bed are typically below the detection limit of the laboratory method being used. For most Regional Water Quality Control Boards in California, a detection of 10 µg/L is satisfactory. However, some require a limit of less than five µg/L. For those, the laboratory modifies the procedure and finds the process will deliver ND <5 µg/L for TBA and MTBE.

Most bioreactors are followed by GAC contactors to adsorb VOCs in the event of an upset or overloading of the bioreactor. Typically, the GAC is changed out very infrequently (e.g., every one or two years), if at all.

2.3 Solids Removal

When water is oxygenated, sticky solids can form from the interaction of the biomass with precipitates formed from dissolved iron, manganese, and/or hardness. A filter containing spherical polyethylene beads is used to remove solids from the system (see Schematic Flow Diagram - Figure 2). A separate recycle loop is passed through the filter in up-flow mode until enough solids accumulate on the filter beads to require a backwash. The filter is then isolated with a three-way valve and a motorized agitator is activated to knock the accumulated material off of the beads. When the agitation stops, the beads rise and the solids settle to the bottom of the filter chamber where they are drawn off as a slurry. About five to seven gallons of slurry are accumulated for each backwash. Backwashing frequency varies with the solids loading, but most systems require backwashing less than once per week. A few start-ups, with very heavy solids loading, required a three-day backwash frequency for the first several weeks.

2.4 Bioreactor Size and Application

Either of two off-the-shelf Cardno ERI bioreactors (a five-foot diameter unit or a two-foot diameter unit) can accommodate a wide range of mass loadings. For a custom design, the sizing is changed by altering the footprint of the bioreactor vessel, leaving the height relatively constant. The recirculation flow rate is then adjusted to maintain bed fluidization and a hydraulic residence time of approximately 15 minutes.

The five-foot diameter bioreactor fits on a 10-foot by six-foot skid and stands about 11.5 feet tall. The empty weight is about 3,800 pounds, and when loaded with sand and water, the total weight is about 18,000 pounds. This bioreactor is designed to metabolize about 1.3 pounds of VOCs per day (or 100,000 gpm-µg/L). The mass loading can be increased to three pounds per day with an oxygen booster.

The two-foot diameter bioreactor fits on a four-foot by four-foot skid and stands about 10.5 feet tall. The empty weight is about 400 pounds. Sand and water bring the total weight to about 3,000 pounds. This bioreactor is designed to metabolize 0.2 pounds of VOCs per day (or 20,000 gpm-µg/L). The mass loading can be increased to 0.4 pounds per day with an oxygen booster.

Both of these bioreactors are commercially available and can be delivered and set up virtually anywhere. Clearly some precautions must be taken when the unit is to be operated in extremely cold or hot climates to keep the biomass in the optimal temperature range of 50 to 95^{o}F (10 to 35^{o}C). Once the biomass is established, it generally self regulates the pH at 7.5 $\pm$ 0.5 by generating carbon dioxide, which produces a bicarbonate buffer. At several sites, this was not the case and the pH fell below 6.5 or rose above 8.5. An inexpensive automatic pH adjustment system

was added to regulate the pH by adding either acid or base as needed. Based on performance of the bioreactor in New Hampshire, iron and manganese do not appear to have any deleterious effect on the performance of the biomass; however, these metals exert an oxygen demand. Copper is a known biocide and should be avoided.

3. RESULTS

3.1 Bioreactor Performance in the Field

Cardno ERI fluidized bed bioreactors have operated at gas station sites in California, New Hampshire, Maryland, and Florida. Some of these bioreactors are discussed below.

3.1.1 Palo Alto, California

Data from the operation at Palo Alto, Cardno ERI's first full-scale fluidized bed bioreactor, are shown in Table 3. At this site, MTBE in groundwater was originally being treated with GAC and was then discharged to a POTW via a sanitary sewer. Initially, there was no TBA restriction on the discharge, so TBA values were not routinely measured. BTEX concentrations were very low. The bioreactor was started up in early August 2000 as a side stream treating a portion of the 20 gpm being processed by the GAC system. The first effluent sample, collected on August 9th, indicated complete reaction. The incomplete reaction of August 29th was due to a depletion of essential nutrients, which was corrected by supplementing with N, P, and K on a regular basis. The incomplete reaction of September 22nd was due to overfeeding (164,000 gpm-µg/L, well above the 100,000 gpm-µg/L design mass loading). This was cured by adding an oxygen booster.

On November 9th, with the oxygen booster in operation, the loading was 204,000 gpm-µg/L and reaction was complete for both MTBE and TBA. The oxygen booster was turned off in February 2001 as concentrations appeared to be dropping, and then on February 14th, a surge in concentration required the booster to be turned back on. The booster was restarted in mid-February and ran until it was turned off in September 2001. With the exception of May 8, 2002, TBA was not detected. Over 26 million gallons of water were treated by this bioreactor in the three years it was used. Carbon was not changed out in the last 1.5 years of operation.

Table 3. Performance Data for Five-Foot Fluidized Bed Bioreactor – Palo Alto, California. Demonstration of Basic Bioreactor Principles.

Date	Flow Rate (gpm)	MTBE Influent (µg/L)	MTBE Effluent (µg/L)	TBA Influent (µg/L)	TBA Effluent (µg/L)
9-Aug-00	10	6,200	ND<2.5	NA	NA
29-Aug-00	10	8,000	2,330		
19-Sep-00	10	7,600	ND<2.5		
22-Sep-00	12	13,700	30.6		
26-Oct-00	17	9,670	6.1	980	ND<4
9-Nov-00	17	12,000	ND<0.5	300	ND<5
21-Nov-00	17	5,300	1.2	120	ND<5
20-Dec-00	19	3,600	0.7	260	ND<5
8-Feb-01	19	4,300	ND<2		
14-Feb-01	19	7,600	300		
22-Feb-01	19	4,700	ND<2		
7-Sep-01	16	2,300	ND<2	1,000	ND<5
4-Oct-01	15	1,300	ND<2	740	ND<5
6-Nov-01	14	1,300	ND<2	530	ND<5
6-Dec-01	17	1,100	ND<2	1,100	ND<5
8-May-02	15	710	6	2,100	15
7-Aug-02	15	670	3.6	1,100	ND<20
4-Sep-02	15	3,600	1.1	1,500	ND<20
2-Oct-02	15	4,200	0.8	1,100	ND<5
6-Nov-02	15	900	1	2,000	ND<5
4-Mar-03	12	120	ND<0.5	1100	ND<5
8-May-03	10	49	ND<0.5	570	ND<5
6-Aug-03	11	23	ND<0.5	150	ND<5

NA=not analyzed

The concentrations of oxygenates in site groundwater seemed to rise and fall until the tank tops and dispenser piping were exposed and repaired in January 2003. Vapor leaks were found and corrected. After those repairs, the concentrations of oxygenates dropped steadily until they reached target levels agreed to by the regulating authorities. The bioreactor was moved to another site in September of 2003. Bioreactor treatment was followed by a period of pump and treat with GAC only, and then a period of monitored natural attenuation (MNA), which is on-going.

3.1.2 Milpitas, California

Data for the bioreactor operating in Milpitas is summarized in Table 4. The initial design called for a system to treat 10 gpm with a concentration (MTBE+TBA) of 10,000 µg/L – (100,000 gpm-ppb). In this case, the bioreactor turned out to be considerably oversized for the loading actually produced from the recovery wells. The highest loading occurred on February 22, 2002 and was two gpm with 787 µg/L MTBE plus 194 µg/L TBA, which is just under 2,000 gpm-ppb. The bioreactor had difficulty sustaining a biomass at 2% of design loading and a supplemental feed was required. A small amount of MTBE was added to the nutrient feed drum to maintain a concentration in the bioreactor of 100 µg/L. The bioreactor was employed to meet the five µg/L limit for discharge of TBA to the storm water system in Milpitas. The data shows that these limits were met in the effluent from the bioreactor in each case. This case points out the importance of carrying out a sufficiently long pumping test (e.g., at least 24 hours long in a sandy environment, and longer in a less permeable setting) to properly estimate the mass loading from the site based on approximate steady-state flow rate contaminant concentrations determined after a number of hours of pumping. The large bioreactor has been moved to another location, and this site has been closed, but a smaller bioreactor could have done the job for less cost.

Table 4. Performance Data for Five-Foot Fluidized Bed Bioreactor – Milpitas, California. Demonstration of the Need for Adequate Pretesting (flow-concentration).

Date	Flow Rate (gpm)	MTBE Influent (µg/L)	MTBE Effluent (µg/L)	TBA Influent (µg/L)	TBA Effluent (µg/L)
19-Dec-01	2	420	300	NA	NA
18-Jan-02	2	530	27	NA	NA
15-Feb-02	2	797	0.8	65	ND<5
22-Feb-02	2	787	ND<0.5	194	ND<5
01-Mar-02	2	513	0.6	105	ND<5
08-Mar-02	2	613	0.7	11	ND<5
15-Mar-02	2	737	ND<0.5	24	ND<5
09-Sep-02	2	120	ND<0.5	6	ND<5
22-Oct-02	2	61	ND<0.5	6	ND<5
19-Nov-02	2	73	ND<0.5	16	ND<5
12-Dec-02	2	69	ND<0.5	ND<5	ND<5
16-Dec-02	2	73	ND<0.5	ND<5	ND<5

3.1.3 Stanton, California

At the Stanton site, MTBE appeared to be converted to TBA in the subsurface. The bioreactor was able to metabolize very high concentrations of MTBE/TBA and eventually clean up the site. MTBE concentrations were observed to drop from 200,000 µg/L in 1998 to 2,000 µg/L in 2002. However, the concentration of TBA rose from 65,000 µg/L in 2000, when it was first measured, to 1,300,000 in 2003 just before bioreactor treatment began. TBA concentrations were not being measured in 1998, so a comparison with MTBE concentrations over the entire time period was not possible. A five-foot-diameter bioreactor with an oxygen booster is installed and started in June of 2003. Operating data from this bioreactor are summarized in Table 5.

Extraction of water was limited during the start-up phase due to the wells having concentrations lower than 60,000 µg/L. Once a significant biomass was established after about three months of operation, the well having a TBA concentration of 1,300,000 µg/L was introduced into the system. Care was exercised to restrict flow from this well into the bioreactor so as not to deplete the available oxygen. A small amount of biomass had to be removed from the system periodically. About one 55-gallon drum of biomass was removed during the first nine months of operation.

Table 5. Performance Data for Five-Foot Fluidized Bed Bioreactor – Stanton, California. Demonstration of the Ability to Treat High Concentration of Oxygenates.

Date	Flow Rate (gpm)	MTBE Influent (µg/L)	MTBE Effluent (µg/L)	TBA Influent (µg/L)	TBA Effluent (µg/L)
12-June-03	0.25	160	5	35,000	ND<10
24-Jun-03	1.1	590	3	62,000	ND<10
23-Jul-03	1.3	1,100	1.6	53,000	ND<10
17-Sep-03	2.0	550	ND<1	25,000	ND<10
15-Oct-03	2.5	460	1.8	37,000	ND<10
13-Nov-03	2.7	320	ND<1	20,000	ND<10
18-Dec-03	2.7	220	ND<1	17,000	ND<10
22-Jan-04	2.7	170	ND<1	8,700	ND<10
16-Apr-04	2.0	99	ND<1	6,670	ND<10
13-Jul-04	2.0	9	ND<1	2,520	ND<10
13-Oct-04	1.1	72	ND<1	7,520	ND<10
25-Jan-05	2.0	72	ND<1	13,400	ND<10
11-Oct-05	4.0	100	ND<1	3,600	ND<10
19-Jan-06	4.0	NA	NA	3,000	ND<10
5-Apr-06	5.4	NA	NA	3,500	ND<10
7-Jul-06	5.6	NA	NA	2,000	ND<10
7-Oct-06	1.9	NA	NA	1,100	ND<10
14-Mar-07	1.5	NA	NA	560	ND<10
13-Jul-07	1.8	NA	NA	490	ND<10
31-Aug-07	1.9	NA	NA	480	ND<10

After decreasing steadily over the first year and a half, the TBA concentration leveled off and then actually rose again with the intense rain in Southern California in early 2005. A new release was not indicated because the MTBE values remained very low. The bioreactor could handle five times the current flow rate of three gpm at the concentrations then encountered. Three additional wells were installed in 2005. One produced two gpm with 15,000 µg/L of TBA, and the other two did not yield significant flow. TBA impact was reduced to less than 500 µg/L and a period of monitored natural attenuation was entered. The site is now closed.

3.1.4 Bedford, New Hampshire

At the Bedford site, the small Bio-500 bioreactor was introduced to freezing temperatures, high iron (30 mg/L as Fe), and high manganese (10 mg/L as Mn), in addition to the usual TBA, MTBE, and BTEX. The treatment train consisted of an air stripper to remove BTEX and iron (not shown), a bioreactor to remove MTBE and TBA (green), and activated carbon (gray) for a final polish. The bioreactor was

enclosed in a heated building, the iron was removed in the stripper, and the manganese precipitated out in a separate layer in the bioreactor. The biomass adapted to perform well at groundwater temperatures as low as 49°F, the lowest groundwater temperature measured at the site. The increased solubility of oxygen in cold water is believed to partially offset the slowdown in metabolism expected with cooler temperatures.

Figure 3. Small Bio-500 Located in New Hampshire.

When BTEX concentrations in the incoming groundwater decreased to less than those of MTBE and TBA, the stripper was replaced with an ion exchange unit to control the iron and manganese. Eventually the iron and manganese concentrations decreased to 10 mg/l iron and five mg/L manganese and the ion exchange system was removed. Finally, the carbon polishing unit was taken out of service. The system was then operated as an *in-situ*/*ex-situ* bioremediation treatment unit. Water pumped from the wells down gradient of the source area and was treated in the bioreactor to produce water meeting the discharge requirements for the State of New Hampshire. A portion of that water was infiltrated upgradient from the source and the rest was discharged to surface waters. Remediation at the site is nearly complete. Water discharged from the bioreactor has consistently been reduced from 7,000 µg/L to less than 20 µg/L of TBA, the discharge limit for this site.

3.1.5 Hollywood, Florida

A five-foot diameter bioreactor was set up in Hollywood, Florida to treat a groundwater stream containing TBA at an initial concentration of 100,000 µg/L, with trace amounts of BTEX (<500 µg/L) and some MTBE. The system was set up to re-inject treated water downgradient of the impacted zone. An attempt was made to start the system in August, but the hot weather proved problematic. In addition, regulatory requirements mandated batch analysis prior to discharge. Long laboratory turnaround times would have resulted in a high volume of effluent generated before the receipt of laboratory results. Therefore, the bioreactor was placed in recycle mode during samplings. The weather was so hot that the biomass kept overheating during periods of recirculation.

During one of the recirculation periods, the temperature of the fluidized bed reached 103^{o}F and the biomass lost much of its activity, requiring partial replacement. To overcome the overheating problem, special provisions were made with the agency to allow re-injection of partially treated groundwater into the source area. This continuous flow of groundwater through the bioreactor kept the internal bioreactor temperature down and allowed the biomass to develop in a few weeks.

Re-injection of treated groundwater into the source area also introduced oxygenated water, with a DO of approximately seven mg/l, promoting *in-situ* bioreaction in the subsurface and reducing the lifecycle of the system. The bioreactor operation combined with the re-injection reduced TBA concentrations in groundwater to monitoringlevels only (concentrations decreased by 99.6%) within one year of system activation.

3.1.6 Norwalk California

Two five-foot diameter bioreactors were set up in Norwalk, California to treat up to 25 gpm each (for a total of 50 gpm) of water containing 1,200 µg/L of TBA and 400 µg/L MTBE, as well as containing 2,500 µg/L of BTEX. Sacrificial carbons are used ahead of the bioreactors to remove most of the BTEX allowing the bioreactor system to focus on metabolism of the TBA and MTBE.

The groundwater is unusually hard at this site (hardness of 800 to 1200 ppm as CaCO3). When groundwater is contacted with air in the bioreactor, the pH rises and solids precipitate clogging the injectors, the circulating piping, and the final polishing carbons. A pH control system was installed to keep the pH below 7.2, which pretty well eliminated the solids problem. A picture of the site is shown in Figure 4.

Figure 4. Bioreactor System in Norwalk, California showing an incoming process water surge tank (dark green), bioreactors (light green), HCl storage tank (white), and Nutrient and MTBE feed drums (blue).

During the last year and a half, over 12 million gallons of water have been processed, achieving discharge concentrations of <5 µg/L TBA and <5 µg/L MTBE. At present the groundwater through-put is limited by the filtration rate on the incoming stream. The solids to be removed are gummy in nature and appear to be biological. Current efforts are being directed at finding a system to control or reduce the bio solids (perhaps with a biocide), while protecting the biomass that is needed to metabolize the TBA and MTBE.

4. DISCUSSION

4.1 Bioreaction in the Presence of Surfactants

Pilot studies have confirmed that these bioreactors are able to metabolize hydrocarbons and oxygenates in the presence of surface active materials like detergents.

4.1.1 Deliberate Addition of Biodegradable Surfactant

A current bioreactor user wanted to inject a citrus based biodegradable surfactant to enhance the recovery of non-polar hydrocarbons (BTEX) from the subsurface. A pilot study was run on a two-foot diameter bioreactor in Cardno ERI's laboratory to determine the effect of added surfactant. The results showed no foaming in the bioreactor and after a short period of acclimation, the BTEX and oxygenates were consumed at previous rates obtained before surfactants were added.

4.1.2 Reaction of BTEX in Presence of Alkyl Benzene Sulfonates

Surfactants (suspected to be alkyl benzene sulfonates) were present from previous land use with groundwater containing high concentrations of benzene (>30,000 ppb). Air sparging at the site produced foam in the groundwater wells. Groundwater extraction for treatment with carbon was ineffective because the surfactants solubilized the benzene and it went right through the carbon. As an alternative, a three-week pilot study in a two-foot diameter bioreactor using groundwater from the site confirmed that the benzene could be metabolized in the presence of the surfactants to yield an exit concentration of less than one ppb.

4.2 Bioreactor Costs

Current cost information for the two off-the-shelf Cardno ERI bioreactors is summarized below in Table 6. Incremental operation and maintenance (O&M) costs are estimated on the assumption that O&M is already required at the site for other purposes. Some costs not included in the table tend to be site-specific and will vary. Not included below are site-specific costs for transportation, installation, system enclosure, groundwater extraction, GAC and other filters, underground piping, effluent discharge, sampling and analysis, or project management.

Table 6. Bioreactor Cost Information.

Cost Item	Two-Foot Bioreactor	Five-Foot Bioreactor
Bioreactor, sand, and biomass	$40,000	$70,000
Oxygen booster (optional)	$3,500	$3,500
On-site O&M labor (hours/week)	1.5-2.5	4-5
Power for bioreactor (kilowatts)	0.9	1.5
Materials, chemicals, parts, solids disposal	$100/month	$200/month

5. CONCLUSIONS

The use of fluidized bed reactors to treat fuel oxygenates and petroleum hydrocarbons offers the following features and benefits:

- The process actually destroys fuel oxygenates and petroleum hydrocarbons, mineralizing them to carbon dioxide and water, rather than merely transferring them to another medium.
- The partial recycle loop in the bioreactor provides operational flexibility allowing the bioreactor to treat extremely contaminated groundwater.
- The technology has been proven in full-scale operation at over 30 sites.
- The process uses naturally occurring microorganisms.
- The biomass is extremely resilient, adapting well to gradual changes in contaminant concentrations, temperature, and other conditions.
- Because of its slow growth rate, excess biomass is rarely generated.
- The biomass performs well at temperatures ranging from 50^{o}F to 90^{o}F.
- The process provides one of the very few treatment options for TBA.
- Groundwater extraction and treatment can provide hydraulic control at the site and is often a good strategy for dealing with soluble non-adsorptive contaminants, such as MTBE and TBA.
- The cleaned, aerated, and bacterially seeded effluent can be re-injected to flush the smear zone and promote *in-situ* bioremediation.
- The bioreactors can be scaled to any mass loading.
- Two off-the-shelf sizes are available and larger sizes can be custom manufactured.
- The bioreactors are minimally impacted by clogging and precipitates compared to other technologies. In particular, high manganese concentrations are well tolerated.
- The bioreactors are compact, quiet, and odor-free.
- When remediation is complete, the bioreactor may be reused at the next site.

6. REFERENCES

Keller, A.A., Sandall, O.C., Rinker, R.G., Mitani, M.M., Bierwagen, B., and Snodgrass, M.J. 2003. Cost and performance evaluation of treatment technologies fir MTBE contaminated water. Health and Environmental Assessment of MTBE, Vol. 5. University of California Toxic Substances Research and Training Program, Davis CA.

Schmidt, R., Klemme, D.A., Scow, K., and Hristova, K. 2012. Microbial biosafety of pilot-scale bioreactor treating MTBE and TBA-contaminated drinking water supply. Hazardous Mat. 209-210.

Chapter 4

NANOMAGNETITE - ZEOLITE COMPOSITES TO BE USED IN ENVIRONMENTAL REMEDIATION OF ANIONIC CONTAMINANTS IN WATER BODIES

Carmen Pizarro[1,2§], María Fernanda Albornoz[1,2], Daniela Muñoz[1,3], José Domingos Fabris[4,5], Mónica Antilén[2,6], and Mauricio Escudey[1,2]

[1]Facultad de Química y Biología, Universidad de Santiago de Chile, Santiago, 725475, Chile, [2]Centro para el Desarrollo de la Nanociencia y Nanotecnología (CEDENNA), Santiago, 725475, Chile, [3]Facultad de Ciencias. Universidad de Chile, UCH. Las Palmeras 3425, Santiago 7800024, Chile, [4]Departamento de Química - ICEx, UFMG, Campus Pampulha, 31270-901 Belo Horizonte, MG, Brazil, [5]Universidade Federal dos Vales do Jequitinhonha e Mucuri (UFVJM), Campus JK, 39100-00 Diamantina, MG, Brazil, [6]Facultad de Química, Pontificia Universidad Católica de Chile, Santiago Chile.

ABSTRACT

Nanomagnetite-zeolite composites with controlled particle sizes were prepared, with potential to be used as a magnetic adsorbent material to remove anions from water. The individual components forming the composite and the composite itself were further characterized in an attempt to assess details of their particle size distribution and surface area, along with their chemical composition, saturation magnetization values, powder x-ray diffraction patterns, scanning electron microscopy images and Mössbauer spectroscopy data. The ability of these composites to adsorb arsenate in aqueous solution was monitored through sorption kinetics and corresponding isotherm parameterization. A stoichiometric and well-crystallized magnetite in these composite samples was synthesized with a particle distribution centered to an averaged particle size of 50 nm. The sorption isotherms indicated that the nanomagnetite enhances the anion sorption capacity, relatively to zeolite alone. The magnetite-zeolite composite with a mass ratio of 0.43:1 presented a similar sorption capacity as that observed for pure magnetite. Furthermore, it was possible to verify that particle size reduction increases the arsenic adsorption capacity. The presence of magnetite enables the spent magnetic composite to be easily removed from the water medium, in order to be recycled, cleaned, and reused.

Keywords: arsenic, iron oxides, magnetite, remediation

1. INTRODUCTION

If any specific geological characteristics of a given natural area or anthropogenically-induced changes, as those resulting from mining ore resources, are sources of anions, the consequences may be a real threat to the environment through contamination of running or ground water. Actually, the increasing level of arsenic on the Earth surface has been resulting not only in serious environmental problems, but these is also a high concern about their direct effects on individuals in remote communities or in densely populated urban areas. In northern Chile, especially in the Antofagasta (23^o 39' 7.75'' S 70^o 23' 43.07'' W) region, the occurrence of arsenic in ground and underground fresh water is steadily increasing, as a consequence of the intensive mining activities in that area.

Different remediation treatments have been used in an effort to remove or mitigate anionic pollutants from water bodies. However, these treatments very hardly lead to a reduction of pollutant concentrations to levels below the maximum concentrations that are accepted as safe, according to recommendations by the World Health Organization.

This paper explores composites of modified zeolite with iron oxides as a promising alternative for efficiently removing inorganic anions from aqueous media. Nanomagnetite-zeolite composites were prepared and chemically evaluated to obtain an economically interesting and technologically efficient adsorbent material to remove arsenate from water bodies. The efficiency of arsenate adsorption by these samples of zeolite-based materials was evaluated by varying the mean particle sizes of the zeolite and the proportion of magnetic iron oxides in the composite.

2. MATERIALS AND PROCEDURES

A zeolite sample was collected from a mine located in mid-southern Chile (geographical coordinates of the sampling site, 36º 16' S 71º 40' W). The sample was milled at four different times (20, 40, 60 and 120 min), using a steel ball mill. The resulting materials were then treated so that the individual particles were coated with a layer of magnetite corresponding to magnetite:zeolite mass ratios of 0.07:1, 0.20:1, 0.30:1 and 0.43:1 (the samples were accordingly labeled MtZ-7%, MtZ-20%, MtZ-30% and MtZ-43%), by converting ferrous sulfate in an alkali media containing a suspension of the zeolite under N_2 atmosphere, following the synthesis method described by Schwertmann and Cornell (2000). The composite samples were characterized with respect to their particle size distributions and to surface areas, along with chemical analysis, magnetometric measurements, powder x-ray diffraction, scanning electron microscopy and 298 K-Mössbauer spectroscopy.

3. DATA AND ANALYSIS

3.1 Zeolite and Composite Characterization

Results from chemical analyses indicate that the zeolite contains silicon and aluminum at a Si:Al ratio of 5:1 and 2.0 mass% iron. The XRD patterns (Figure 1 a) indicate that zeolite corresponds to rehydrated mordenite with exchangeable calcium cations corresponding to the chemical formula $Ca_{3.4}Al_{7.4}Si_{40.6}O_{96}(H_2O)_{31}$

Mössbauer spectra for the zeolite, composite (MtZ-7% and MtZ-43%) and this synthetic magnetite are shown in Figure 1 b. As a general pattern, Mössbauer spectra for composites show spectral features of a stoichiometric well-crystallized magnetite, with a particle distribution around an average size of 50 nm (Figure 1b).

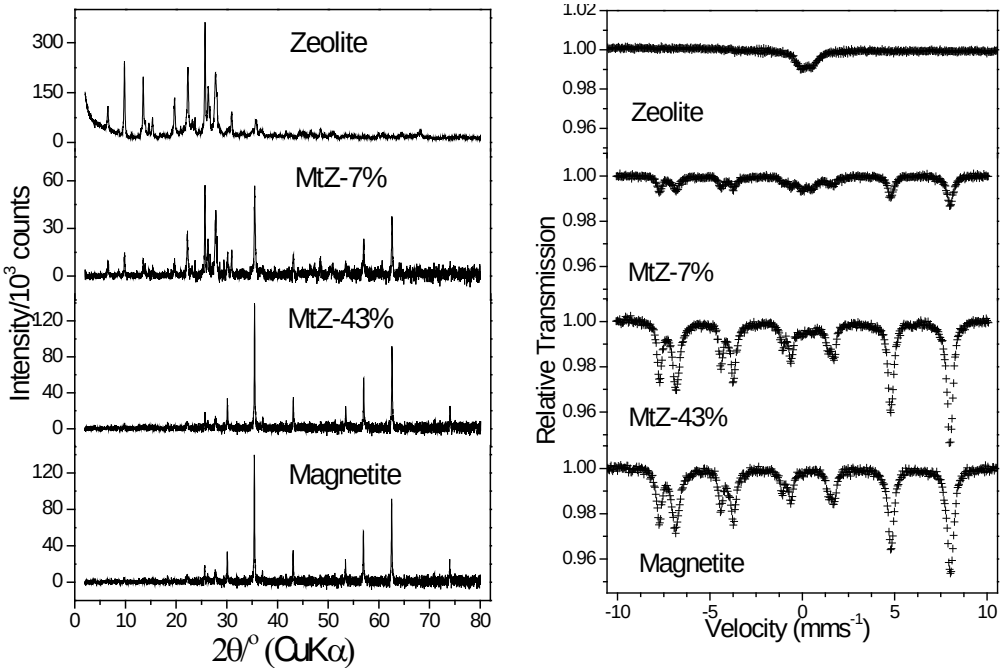

(a) (b)

Figure 1. XRD (a) and 298 Mossbauer spectra (b) for zeolite, magnetite and composites.

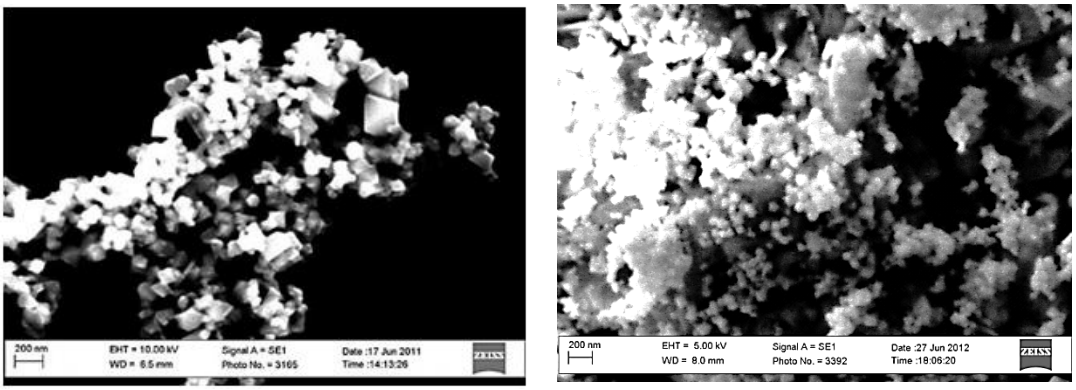

(a) (b)

Figure 2. SEM images for magnetite (a) and for the magnetite-zeolite composite MtZ-43% (b).

3.2 Effect of Proportion on Magnetic Iron Oxides in the Composites

Figures 3 and 4 show the sorption kinetic and isotherm curves for the zeolite (milled during 20 min), and for the composites prepared with the lowest and highest contents of magnetite (samples MtZ-7% and MtZ-43%, respectively). Significant differences in sorption of arsenic are observed when magnetite content is higher in the composites. In contrast with MtZ-43%, the natural zeolite sorption kinetic and isotherm curves (Figures 3 and 4) indicate that a relatively low amount of arsenic is adsorbed, while MtZ-43% has a similar adsorption capacity to that observed for pure magnetite. By fitting data to the Langmuir isotherm model, the maximum sorption values for the MtZ-43% composite was found to be 3.4 mg/g^{-1}. The sorption isotherm for MtZ-7% composite was similar to that of pure zeolite. Furthermore, the presence of magnetite significantly increases the ability of the magnetic composite on the removal of arsenic from water.

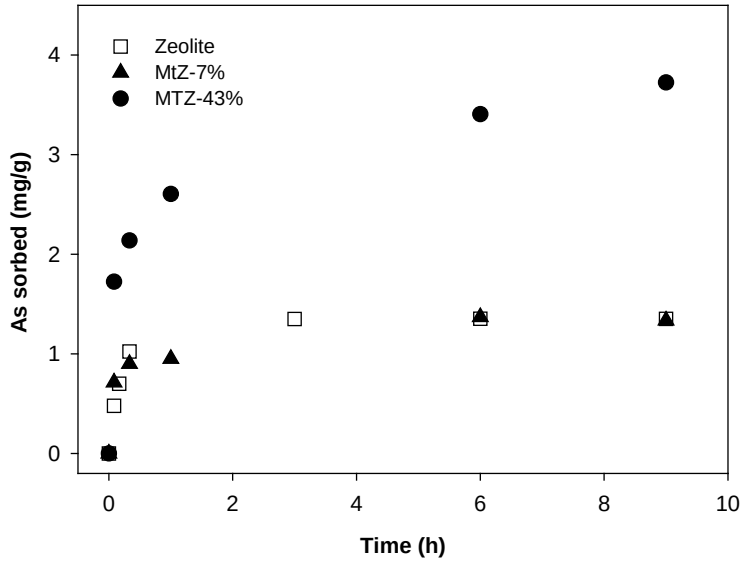

Figure 3. Arsenic sorption kinetic data for natural zeolite and for composites with magnetite:zeolite mass ratios of 0.07:1 and 0.43:1 (MtZ-7% and MtZ-43%, respectively).

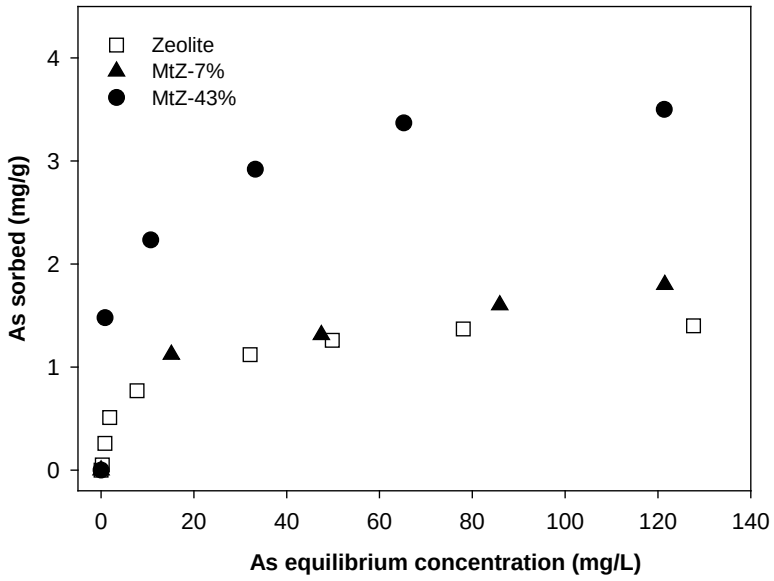

Figure 4. Arsenic sorption isotherm for natural zeolite and for composites with magnetite:zeolite mass ratios of 0.07:1 and 0.43:1 (MtZ-7% and MtZ-43%, respectively).

3.3 Effect of the Variation in the Mean Particle Sizes of the Zeolite

From Table 1, it is possible to observe the effect of zeolite milling. The granulometric fraction in major proportion corresponds to that with particle sizes in the range of 20 μm >◻> 2 μm for both the milled zeolite and the composites MtZ-30% at all milling times. As a result of the composite preparation, the proportion of the finest fraction (<2 μm) of the composite decreased by 90.8 % and 78.0 %, for 20 min and 120 min of milling, respectively, leading to corresponding higher proportions of fractions with bigger particles.

Table 1. Granulometric breakdown for zeolite and MtZ-30% composite samples at different milling time.

Fraction	Mass%			
Particle sizes (ϕ/μm)	20 min		120 min	
	Zeolite	Composite	Zeolite	Composite
>53	29.5 ± 0.0	34.2 ± 0.0	18.1 ± 01	32.1 ± 0.1
53–20	9.0 ± 0.3	20.9 ± 0.0	5.4 ± 0.0	13.1 ± 0.2
20–2	37.7 ± 0.2	42.7 ± 0.0	44.3 ± 0.2	47.8 ± 0.0
<2	23.8 ± 0.0	2.2 ± 0.0	32.2 ± 0.1	7.1 ± 0.0

3.4 Kinetic and sorption isotherms

The arsenic sorption kinetic (for milled samples, Figure 3) is well described by the pseudo-first order model (Kalavathy et al., 2005). The model relates the adsorbed concentration as a function of time by the equation: $q_t = q_0 - e^{(\ln(q_0) - k1 \times t)}$, where q_t and q_e are the adsorbed arsenic at time (t) and the concentration at the initial time (t_0), respectively, and k_1 is the first order kinetic constant. Table 2 shows kinetic parameters for MtZ-30%.

Table 2. First order kinetic constant for the pseudo-first order model for the zeolite sample milled during 20 and 120 min, and for MtZ-30% composite.

Parameter	20 min		120 min	
	Zeolite	Composite	Zeolite	Composite
k_1	0.07±0.00	0.08±0.00	0.04±0.00	0.08±0.00
r^2	0.99	0.98	0.99	0.98

The As sorption isotherms (Figure 4), can be described through the Langmuir approach (Langmuir 1918). The model relates the adsorbed concentration as a function of the equilibrium concentration by the equation: $q = \frac{q_m K_L C}{1+CK_L}$, where q and q_m are the amount of the adsorbed (mg g^{-1}) arsenic and the maximum adsorption capacity (mg g^{-1}), of arsenic respectively; K_L is the Langmuir constant and C

equilibrium concentration (mg L^{-1}) of arsenic. Table 3 show Langmuir parameters for MtZ-30% composite.

Table 3. Parameters for the Langmuir isotherm for the zeolite sample milled during 20 and 120 min, and for MtZ-30% composite.

Parameters	20 min		120 min	
	Zeolite	Composite	Zeolite	Composite
q_m (mg g^{-1})	1.40 ± 0.04	3.81 ± 0.21	2.25 ± 0.01	5.11 ± 0.26
K_L	0.20 ± 0.04	0.32 ± 0.15	0.24 ± 0.11	8.01 ± 0.96
r^2	0.90	0.95	0.94	0.96
R	0.03	0.11	0.05	0.02

The parameter qm indicates that the maximum adsorbed arsenic capacity increases about 61% of mass when milling time increases from 20 to 120 min for zeolite, whereas it increases 172% mass and 265% mass for composites prepared with zeolite milled for 20 and 120 min.

Parameters obtained from fitting data to the Langmuir approach confirms that the arsenic sorption capacity increases with milling time for the zeolite, in relation to an increase of the whole surface area.

4. CONCLUSION

These results show that nanomagnetite enhances the adsorption capacity of natural zeolite. In addition to the high affinity of Fe-As, higher iron contents are expected to increase the availability of positive charges on the surface of particles of the composite, which enhance, in general terms, the adsorption of anions. A consequent secondary effect is the ability of the composite to be easily removed from the liquid medium with a magnet. Moreover, it is possible to establish that the particle size reduction on milling increases the arsenic adsorption capacity of arsenic.

5. REFERENCES

Kalavathi H.M., Karthikeyan T., Rajagopal S., and Miranda L.R. 2005. Journal of Colloid and Interface Science. 292, 354-362.

Langmuir L. 1918.. The adsorption of gases on plane surfaces of glass, mica and platinum. Journal of the American Chemical Society. 40(9), 1361-1403.

Schwertmann and Cornell. 2000. Irox oxides in the laboratory. Wiley-VCH. Germany. 2nd Edition, Pp. 210.

Acknowledgments: Work financially supported by DICYT-USACH 021242PA, CEDENNA FB-0807 (Chile), CNPq (Brazil; grants # 302479/2010-4 and PROSUL # 490096/2010-7) and FAPEMIG (Brazil; including # PPM 00419-10). CAPES (Brazil) grant the Visiting Professor PVNS fellowship to JDF at UFVJM.

Part IV: Hydrocarbons

Chapter 5

FORMATION OF OIL-LIKE PRODUCTS BY HYDROUS PYROLYSIS OF SCRAP TIRES AT TEMPERATURES FROM 150 ^{O}C TO 350^{O}C

Ahmed I. Rushdi[1,2,§], Abdulgader Y. BaZeyad[1], Abdurahman S. Al-Awadi[3], Khalid F. Al-Mutlaq[1] and Bernd R. T. Simoneit[1,4]

[1]Chair of Green Energy Research and Plant Protection Department, College of Food and Agricultural Sciences, King Saud University, P.O. Box 2460, Riyadh 11451, Saudi Arabia, [2]Department of Geosciences, Oregon State University, Corvallis, OR 97331, U.S.A.,[3]Department of Chemical Engineering, College of Engineering, King Saud University, Riyadh 11451, Saudi Arabia, [4]Department of Chemistry, Oregon State University, Corvallis, OR 97331, U.S.A.

ABSTRACT

Disposal of scrap tire waste in landfills and other sites can be a threat to the environment. Pyrolysis is considered a useful method for recycling scrap tires. Hydrous pyrolysis experiments were conducted to assess the effects of water on product composition and yield from scrap tire rubber. Two sets of experiments were conducted at temperatures ranging from 150 ^{o}C to 350^{o}C with contact periods of 48 hours. The reaction mixtures of the first set included only shredded scrap tire rubber and water, whereas the second set also contained oxalic acid to provide excess hydrogen to enhance reduction of rubber. The chemical compound compositions of the alteration products from two different pyrolysis conditions were determined by gas chromatography-mass spectrometry. The yields of the total alteration products both increased with temperature in the presence and absence of oxalic acid, and were higher with oxalic acid. Hydrocarbon concentrations

[§]Corresponding author: Ahmed I. Rushdi, King Saud University, P.O. Box 2460, Riyadh, 11451, Saudi Arabia, 0096614676175, arushdi@ksu.edu.sa

increased in the temperature range of 250 ^{o}C-350^{o}C for both experiment sets. The products confirm that alteration of scrap tire rubber in aqueous medium occurs rapidly and efficiently under reductive pyrolysis conditions above 150^{o}C.

Keywords: hydrous pyrolysis, vehicle tire rubber, hydrocarbons, UCM, PAHs.

1. INTRODUCTION

Disposal of scrap tire waste (STW) in the environment, e.g. landfills, can create serious problems. The composition of passenger vehicle tires is about 55% synthetic rubber (polybutadiene) and 45% natural rubber (latex) (RMA, 2009). Organic matter (OM) of scrap tires can be converted into useful products for energy generation (Clark et al., 1993; RMA, 2009).

Pyrolysis is considered a useful recycling technology for treatment of biomass wastes, incuding scrap tires (Laresgoiti et al., 2004; Barbooti et al., 2004; Kaminsky and Mennerich, 2001; Ucar et al., 2005). It produces volatiles and gases, liquid product (oil and tar) and solid carbonaceous materials (char). Recent pyrolysis experiments of STW included thermogravimetric analysis (Williams and Besler, 1995; Teng et al., 1995), fluidized bed pyrolysis (Kaminsky and Sinn, 1980), vacuum pyrolysis (Benalla et al., 1995; Chaala and Roy, 1996; Darmstadt et al., 1995; Mirmiran et al., 1992; Roy et al., 1995) and fixed bed reactors (Cunliffe and Williams, 1998; de Marco et al., 2001; Laresgoiti et al., 2000). The different studies of scrap tire pyrolyses have focused on various factors such as temperature, time, size of the starting material, and sometimes the associated additives upon the products. Recent studies have shown that the yields and product characteristics for pyrolysis depend on feedstock and operating conditions of the experiments, as well as the size and the type of the reactor (Laresgoiti et al., 2004); therefore, various results by different researchers are expected to vary. The different experiments have illustrated that the pyrolysis temperature and experimental conditions affected the yields and characteristics of the products, and varied from one experiment to another (Cunliffe and Williams, 1998; Laresgoiti et al., 2004).

Lewan (1997) has demonstrated that water plays a significant role in pyrolysis experiments of OM. The presence of water in catagenetic experiments facilitates ionic mineral reactions and regulates Eh and pH of the aqueous system (Eugster, 1986; Leif et al., 1992; Shock, 1990; Seewald, 2001). Therefore, the presence of water is believed to be essential during the thermal alteration of OM. Rushdi et al. (2013) studied the hydrous pyrolysis of scrap tire and found that the product yields increased with an increase of temperature. They observed that the maximum yields of hydrous pyrolysis products were in a temperature window from 250^{o}C to 350^{o}C.

Therefore, the main purpose of this paper is to investigate and assess the temperature effects and different experimental conditions of hydrous pyrolysis on the yields and alteration products from STW. Passenger tire scrap was heated under confined aqueous media at different experimental conditions.

2. EXPERIMENTAL PROCEDURES

2.1. Vehicle Tire Samples

Scrap passenger tires (Bridgestone, Tubeless 195/90-R14) were collected from local puncher shops in the city of Riyadh, Saudi Arabia. The tire samples utilized in the experiments was shredded into small pieces (< 2 mm^3), washed with distilled water, dried at 70^oC and kept at room temperature until use in experiments. The material was analyzed with a CHN analyzer for its elemental content by the College of Sciences, King Saud University.

2.2. Tire Sample Extraction

About 50 mg of the shredded scrap tire sample was extracted with 20 mL of dichloromethane/methanol (3:1, v/v) mixture for 45 minutes using ultrasonic agitation in a 50 mL pre-cleaned beaker. The suspended particles were removed using a filtration unit containing an annealed glass fiber filter. Then, the filtrate was concentrated on a rotary evaporator and reduced using a stream of dry nitrogen gas to a volume of approximately 50 μL. The volume was then adjusted to 100 μL exactly by addition of the solvent mixture before analysis by gas chromatography-mass spectrometry (GC-MS). An aliquot of the total extract was also treated with *N,O*-bis(trimethylsilyl)trifluoroacetamide (BSTFA) with 1% trimethylchlorosilane prior to GC-MS to elucidate the polar compounds.

2.3. Pyrolysis Experiments

Similar 316 stainless steel vessels as utilized by Rushdi et al. (2013) were used (Fig. 1). The vessels were constructed with Sno-Trik high-pressure couplings (Leif and Simoneit, 1995; Rushdi and Simoneit, 2004; 2011; Rushdi et al., 2003) specifically to study the alteration products of vehicle tire rubber under hydrous pyrolysis conditions. The vessels are capable of handling system pressure to 60,000 psi (413,682 kPa, Sno-Trik Company). The internal capacities of the vessels were 480 ± 20 μL. Before each experiment, the reaction vessels, shredded tire rubber and

solid oxalic acid were placed in a glove bag and flushed with N_2 for about 5 min. Two experimental sets were prepared for particular reaction conditions (Rushdi et al., 2013). Experiment set 1 was a mixture of doubly distilled water and about 30 mg of scrap tire. The addition of pre-extracted solid oxalic acid dehydrate (99.5 %, EM Science) to experiment set 1 gave experiment set 2.

Blank experiments (i.e., without scrap tire) were carried out with all reactants to insure that the alteration products were not impurities originating from oxalic acid, doubly distilled water or vessels. A weight of 0.03 g of scrap tire was added to the reaction vessel and filled to capacity with doubly distilled water. For reductive hydrous pyrolysis experiments, 4 mg of oxalic acid was added before the addition of water. After filling with water, the vessels were sealed and placed immediately into an oven for 48 hours at temperature settings of 150^{o}C, 250^{o}C, 300^{o}C and 350^{o}C for the two experiment sets. The vessels were cooled to room temperature upon removal from the oven and then gradually and carefully opened in order to release pressure due to CO_2 and other gases generated during the oven firing.

The sample products were immediately transferred to a glass vial using a Pasteur pipette. Each vessel was rinsed three times with dichloromethane/methanol (3:1 v/v), which was added to the vial, giving a total volume of approximately 2 mL. Each sample was then concentrated under nitrogen flush at room temperature to approximately 50-100 µL before GC-MS analysis. Aliquots of these extracts were treated with BSTFA prior to GC-MS to elucidate the polar compounds.

2.4. Instrumental Analysis

The alteration products and external standards were analyzed by GC-MS, which was an Agilent 6890 GC coupled to a 5975C Mass Selective Detector using a DB-5 (Agilent) fused silica capillary column (30 m x 0.25 mm i.d., 0.25 µm film thickness) and helium as carrier gas. The GC temperature was programmed from 65^{o}C (2 min initial time) to 300^{o}C at 6^{o}C min^{-1} (isothermal for 20 min final time). The electron impact mode of the MS was set at 70 eV ion source energy. The data was acquired with an Agilent Chemstation. Compounds were identified by the GC retention index and by comparison of mass spectra with those of authentic standards, literature and library data, and characterized mixtures. Unknown compounds were characterized by interpretation of the fragmentation pattern of their mass spectra.

Quantification was performed from the GC-MS total ion current (TIC) profiles using the external standard method with authentic compounds of each homologous series (Rushdi et al., 2006). All quantifications were based on the compound peak areas derived from TIC or key ion fragmentograms.

3. DATA AND ANALYSIS

3.1. Elemental Composition of Tire Rubber

The elemental analysis of the scrap tire showed that it consisted of 86.31% carbon, 7.84% hydrogen, 0.10% nitrogen, and 3.95% sulfur. The atomic ratios are: H/C = 1.09, N/C = 0.02, and S/C = 1.47.

3.2. Extract of the Pyrolized Samples

The salient features of the GC-MS data for the total extracts of tire samples and pyrolysate extracts for the experiments are shown in Figure 2. The major compound groups are listed in Table 1. The extract of the tire was comprised of lipid compounds from mainly natural and synthetic organic rubber components, as well as hydrocarbons and additives. They included n-alkanes, n-alkanoic acids, methyl n-alkanoates, hopane biomarkers (fossil fuel tracers), (Simoneit, 1986; Peters and Moldowan, 1993), phenolic antioxidants, resin acids, steroids, and an unresolved complex mixture (UCM) of branched and cyclic compounds. The composition of the n-alkanes, UCM and biomarkers is typical of petroleum additives of tar/heavy oil (Simoneit, 1986; Didyk et al., 1983) and they are added to the tire polymer as softening/sticking agents. For the pyrolysis products, the total concentrations of extracted organic compounds increased with increasing temperatures from 150^{o}C to 350^{o}C and the availability of oxalic acid. In the absence of oxalic acid, the total yields increased from 12.1 mg g^{-1} for the starting tire sample to a maximum of 495.0 mg g^{-1} at 350^{o}C. In the presence of oxalic acid, the total yields increased to a maximum of 560.9 mg g^{-1} at 350^{o}C (Table 1). The pyrolysis products were comprised primarily of n-alkanes, n-alkanoic acids, methyl n-alkanoates, UCM, plasticizers, polycyclic aromatic hydrocarbons (PAHs), and traces of phenols (Fig. 2).

The percentage of n-alkanes in the total product yields increased with rising temperature to a maximum of 25.65% in the absence of and to 28.16% in the presence of oxalic acid, both at 300^{o}C. These percentages decreased to 5.41% and 4.24 % at 350^{o}C in the absence and presence of oxalic acid, respectively (Fig. 3).

The n-alkanoic acids (e.g, Figs. 2 and 3) disappeared at temperatures above 350^{o}C. The carbon number maximum (C_{max}) was mainly at 16 and/or 18 in the absence and presence of oxalic acid (Fig. 2). Their percentages in the total product yields were nil in the starting sample and increased to a maximum of 33.85% at 200^{o}C in the absence of oxalic acid and 24.64% with oxalic acid (Table 1). They decreased to 9.36% and 0.88% at 300^{o}C without and with oxalic acid, respectively (Fig. 3). Methyl n-alkanoates with C_{max} at both 16 and 18 (as alkanoic acid) were

detected in both samples of experimental media, ranging from C_{14} to C_{18} at temperatures below 300°C. Their fractions in the total product yields increased from 0.32% in the initial tire extract, to a maximum of 6.96% at 150°C in the absence of oxalic acid.

Hopane biomarkers ranged from C_{27} to $C_{35,}$ with a maximum concentration at C_{30} in the unheated sample and C_{29} for heated samples. The percentage in the initial sample was 4.6%, which decreased to 0.51% and to 0.56% in the absence and presence of oxalic acid, respectively. These biomarkers were detected as traces at 350°C.

Phenols, mainly phenol and methylphenols, were detected in trace amounts only in the total extracts from the scrap tire pyrolysis. Quinolines were also minor compounds in these total extracts and included methylquinolines.

PAHs were detected only in the pyrolyzed samples, increasing in total yields with higher temperatures, i.e. from 0.00% at 150°C to 25.75% and 26.35% at 350°C, without and with oxalic acid, respectively (Table 1). The major compounds were the naphthalene group including dimethyl- and trimethyl-naphthalenes.

The UCM of the branched and cyclic compounds in the initial tire extract was 60% of the total yield (Table 1). The UCM increased with increasing temperature to a maximum of 68.14% at 350°C in the absence of oxalic acid and 69.49% in the presence of oxalic acid (Fig. 3 and Table 1). The change in UCM with increasing temperature is attributed to the release of bound hydrocarbon products from the polymer at higher temperatures, as well as various reactions from the diverse compounds in the rubber mixture. The presence of hopane biomarkers, UCM and n-alkanes in the total extracts was likely from additive components of petroleum tar/oil in the tire rubber, as well as from minor road asphalt and vehicle exhaust that may be absorbed in the tire with time.

The products of hydrous pyrolysis experiments indicate that the major compound classes are: n-alkanes, UCM, n-alkanoic acids and their derivatives, polar hetero-aromatic compounds, and PAHs, where the first four generally decreased at higher temperatures (Rushdi et al., 2013). The major trends of the reactions are: (1) reduction products increased at temperatures between 250 °C - 350°C (n-alkanes, Fig. 3), especially in the presence of oxalic acid, and (2) the overall oxidation products (mainly dehydrogenation) (e.g, PAHs) increased in all experiments with increasing temperature above 250°C.

The increased concentrations as a function of temperature are obvious in both experiment sets, but the presence of oxalic acid clearly increased the yield by a factor of 1.73 at 250°C, then it decreased to 1.13 at 350°C. The conversion of tire rubber to oil increased with increasing temperature and acidity of the reaction mixture in the temperature range of 150 °C -300°C, indicating that pyrolysis under reducing conditions (with additional hydrogen) is more effective in converting rubber OM to oil-like products at lower temperatures. This study also confirms that

the conversion of tire rubber OM to oil-like products is more efficient and feasible in aqueous media (Rushdi et al., 2013). Furthermore, the yields from hydrous pyrolysis are much higher compared to the yields obtained by others for bulk phase at lower temperatures (< 350^{o}C). For example, de Marco et al. (2001) showed that the yields increased from 4.8±3.9% at 300^{o}C to 38+1.8% at 500^{o}C, Cunliffe and Williams (1998) reported a yield for liquid products of 58% at 450-470^{o}C, and the same yield (57.5±0.75% at 450 ^{o}C -460^{o}C) was obtained by Barbooti et al. (2004). Our results showed that the yields increased from 2.75% at 150^{o}C to 41.95% at 350^{o}C, and slightly decreased to 39.36% at 400^{o}C in the absence of oxalic acid. With oxalic acid, the yields increased from 3.51% at 150^{o}C to 47.53% at 350^{o}C, and slightly decreased to 42.71% at 400^{o}C.

4. CONCLUSION

The results of hydrous pyrolysis of STW OM demonstrate that the yields of products increased with an increase in temperature in both the presence and absence of aqueous oxalic acid. The increase in the conversion rate by a factor of 1.3-1.7 in the temperature range from 150 ^{o}C -250^{o}C with oxalic acid indicates that hydrous pyrolysis is more effective under reducing conditions in converting rubber OM to oil-like products. The concentrations of the various neutral compound groups (e.g, hydrocarbons) and PAHs increased with rising temperature to a maximum yield at 250^{o}C for n-alkanes and PAHs above 300^{o}C. The data also shows that: (1) oxygenated products decrease at temperatures from 150 ^{o}C -250^{o}C; (2) the major products of hydrous pyrolysis are n-alkanes and UCM at 200 ^{o}C - 300^{o}C; and (3) reduction products increase with temperatures above 350^{o}C.

Table 1. The products of scrap tire rubber by hydrous pyrolysis in the absence and presence of oxalic acid at different temperatures for 48 hours.

	Ambient	**150°C**		**200°C**		**250°C**		**300°C**		**350°C**	
		-OA	**+OA**	**-OA**	**+OA**	**-OA**	**+OA**	**-OA**	**+OA**	**-OA**	**+OA**
Yield (mg g^{-1})	1.21	31.88	40.69	66.15	81.72	124.81	215.45	308.48	390.63	494.97	560.91
n-Alkanes (%)[a]	25.95	25.65	8.83	14.82	10.83	25.65	28.16	13.92	18.55	5.41	4.2
n-Alkanoic acids (%)[a]	0	2.5	20.22	33.85	24.64	30.68	23.94	9.36	0.88	0.4	0
Methyl n-alkanoates (%)[a]	0.32	2.6	6.96	0.56	0.09	0.17	0.12	0.37	0.3	0	0
Hopane biomarkers (%)[a]	4.58	4.26	1.01	1.47	1.65	0.66	1.12	0.51	0.56	0	0
Phenolic compounds (%)[a]	ND	ND	ND	T	T	T	T	T	T	T	T
Quinoline compounds (%)[a]	ND	ND	ND	ND	T	T	T	T	T	T	T
PAH (%)[a]	0	0	3.5	5.39	5.6	9.94	7.72	11.39	17.01	25.78	26.35
UCM (%)[a]	69.81	65	59.48	44.44	57.27	32.76	39.66	64.92	63.53	68.14	69.46
Ratio (+OA/-OA)[b]		1.3		1.2		1.7		1.2		1.1	

ND = not detected

T = trace

a = % of the total yield

b = Ratio of the product yields in presence -to-absence of oxalic aci

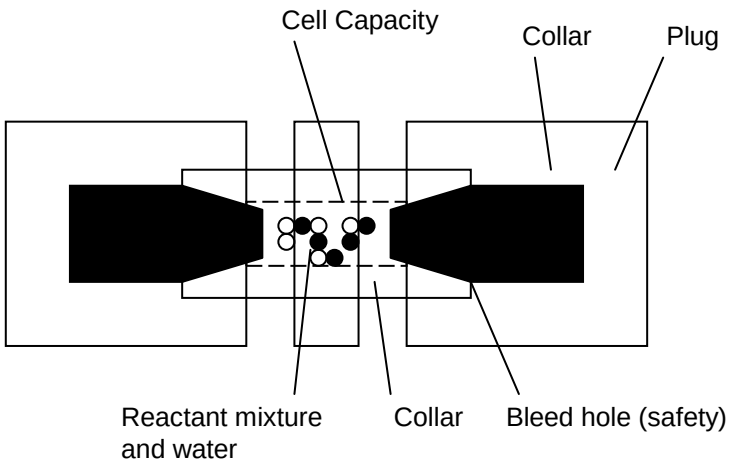

Figure 1. Schematic of the confinement vessel for hydrous pyrolysis experiments.

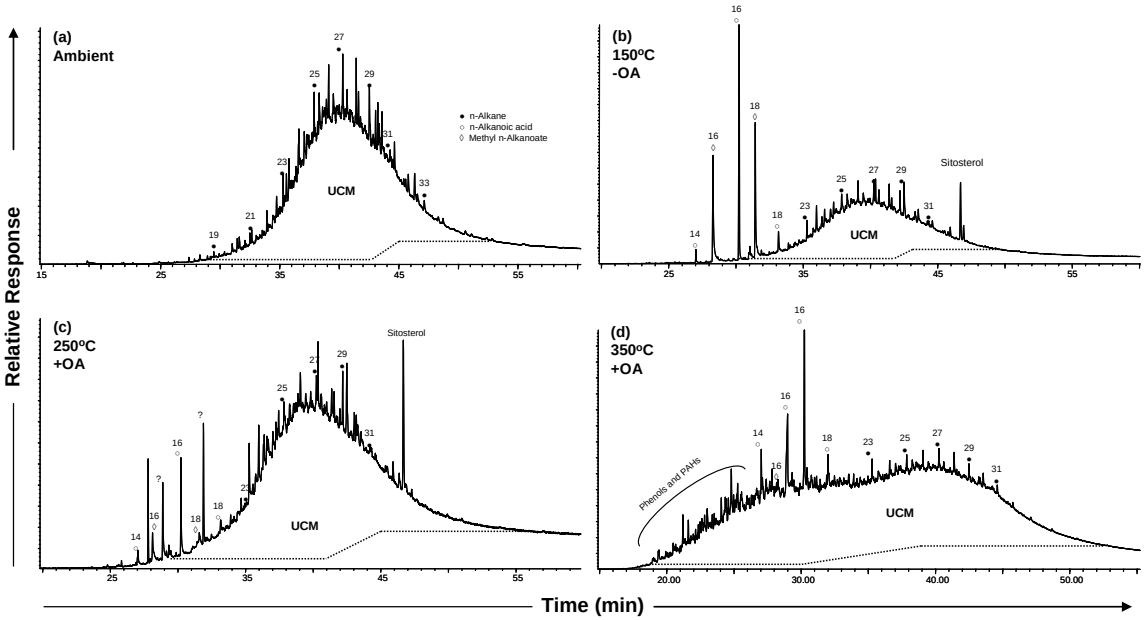

Figure 2. GC-MS total ion current (TIC) traces for: (a) the total extract of the unheated scrap tire sample and (b-d) hydrous pyrolysis products from the scrap tire with (+) and without (-) oxalic acid (OA) at different temperatures (b) 150°C; (c) 250°C and (d) 350°C.

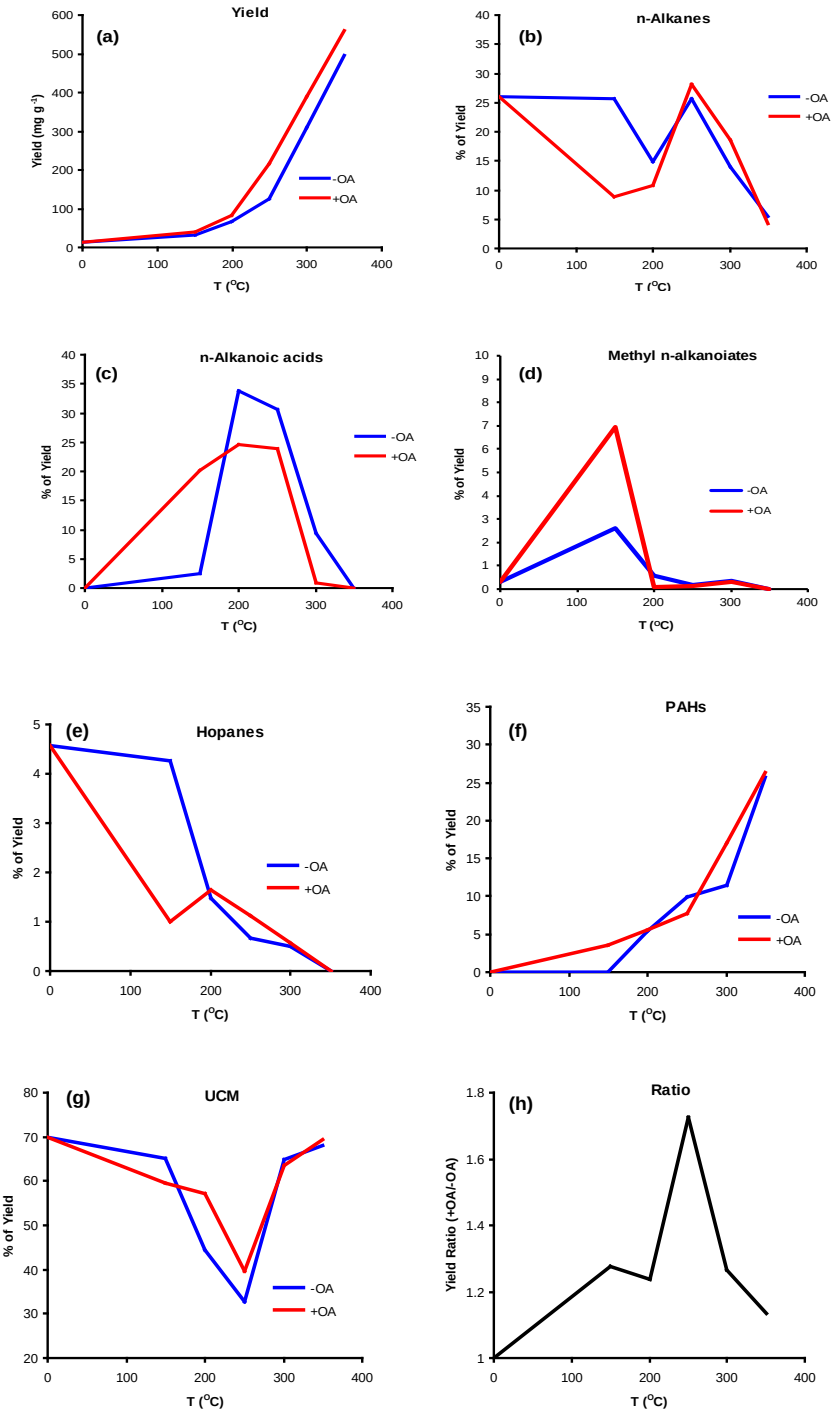

Figure 3. Concentration and % of various compound groups versus temperature plots for the total yields, n-alkanes, n-alkanoic acids, methyl n-alkanoates, hopanes, PAHs, UCM, and +OA/-OA ratio.

5. REFERENCES

Barbooti, H.M., Mohamed, T.J., Hussain, A.A. and Abas, O.F. 2004. Optimization of pyrolysis conditions of scrap tires under inert gas atmosphere. Journal of Analytical and Applied Pyrolysis. 72, 165-170.

Benalla, B., Roy, C., Pakdel, S., Chabot, S. and Poirier, M.A. 1995. Characterization of pyrolytic light naphtha from vacuum pyrolysis of used tires comparison with petroleum naphtha. Fuel. 74, 1589-1995.

Chaala, A. and Roy, C. 1996. Production of coke from scrap tire vacuum pyrolysis oil. Fuel Proc. Tech. 46, 227-239.

Clark, C., Meardon, K. and Russell, D. 1993. Scrap Tire Technology and Markets. Noyes Data, Park Ridge, NJ.

Cunliffe, A.M. and Williams, P.T. 1998. Composition of oil derived from the batch pyrolysis of tyres. Journal of Analytical and Applied Pyrolysis 44, 131-152.

Darmstadt, H., Roy, C. and Kaliaguine, S. 1995. Characterization of pyrolytic carbon blacks from commercial tire pyrolysis plants. Carbon. 33(10), 1449-1455.

de Marco, I., Laresgoiti, M.F., Cabrero, M.A., Torres, A. Chomon, M.J. and Caballero, B. 2001. Pyrolysis of scrap tyres. Fuel Process.Tech. 72, 9-22.

Didyk, B.M., Simoneit, B.R.T. and Eglinton, G.E. 1983. Bitumen from coalport tar tunnel. Organic Geochemistry. 5, 99-109.

Eugster, H.P. 1986. Minerals in hot water. Am. Mineral. 71, 655-673.

Kaminsky, W. and Mennerich, C. 2001. Pyrolysis of synthetic tire rubber in fluidized-bed reactor to yield 1,3-butadiene, styrene and carbon black. Journal of Analytical and Applied Pyrolysis. 58-59, 803-811.

Kaminsky, W. and Sinn, H. 1980. Pyrolysis of plastic waste and scrap tyres using a fluidised bed process. In: Thermal Conversion of Solid Wastes and Biomass. (Jones, J.L. and Radding, B. (Eds.)). ACS Symposium Series 130, American Chemical Society, Washington, DC.

Laresgoiti, M.F., Caballero, B.M., de Marco, I., Torres, A., Cabrero, M.A. and Chomón, M.J. 2004. Characterization of liquid products obtained in tyre pyrolysis. Journal of Analytical and Applied Pyrolysis. 71, 917-934.

Laresgoiti, M.F., de Marco, I., Torres, A., Caballero, B.M., Cabrero, M.A. and Chomón, M.J. 2000. Chromatographic analysis of the gases obtained in tyre pyrolysis. Journal of Analytical and Applied Pyrolysis. 55, 43-54.

Leif R.N., Simoneit, B.R.T and Kvenvolden, K.A. 1992. Hydrous pyrolysis of n-$C_{32}H_{66}$ in presence and absence of inorganic components. Amer. Chem. Soc., Div. Fuel Chem. Preprints. 21(4), 1748-1753.

Leif, R.N. and Simoneit, B.R.T. 1995. Ketones in hydrothermal petroleums and sediment extracts from Guaymas Basin, Gulf of California. Organic Geochemistry 23, 889–904.

Lewan, M.D. 1997. Experiments on the role of water in petroleum formation. Geochimica et Cosmochimica Acta. 61, 3691-3723.

Mirmiran, S., Pakdel, H. and Roy, C. 1992. Characterization of used tire vacuum pyrolysis oil: Nitrogenous compounds from the naphtha fraction. Journal of Analytical and Applied Pyrolysis. 22, 205-215.

Peters, K.E., and Moldowan, J.M. 1993. The Biomarker Guide, Prentice Hall, Englewood Cliffs, NJ, 363pp.

Rubber Manufacturers Association (RMA). 2009. Scrap Tire Characteristics. Accessed from http://www.rma.org/scrap_tires/scrap_tires_and_the_environment/

Roy, C. Rastegar, A., Kaliaguine, S., Darmstadt, H. and Tochev, V. 1995. Physicochemical properties of carbon black from vacuum pyrolysis of used tires. Plast. Rubber Compos. Proc. Appl. 23, 21-30.

Rushdi, A.I., and Simoneit B.R.T. 2004. Condensation reactions and formation of amides and nitriles under hydrothermal conditions. Astrobiology. 4, 213-226.

Rushdi, A.I., and Simoneit, B.R.T. 2011. Hydrothermal alteration of sedimentary organic matter in the presence and absence of hydrogen to tar then oil. Fuel. 90, 1703-1716.

Rushdi, A.I., Al-Zarban, S. and Simoneit B.R.T. 2006. Chemical compositions and sources of organic matter in fine particles of soils and sands from Kuwait city. Environmental Monitoring and Assessment. 120, 537-557.

Rushdi, A.I., Ritter, G., Grimalt, J. O. and Simoneit, B.R.T. 2003. Hydrous pyrolysis of cholesterol under various conditions. Organic Geochemistry. 34, 799-812.

Rushdi, A. I., Abdulgader Y. BaZeyad, Abdurrahman S. Al-Awadi, Khalid F. Al-Mutlaq and Bernd R. T. Simoneit 2013. Chemical characteristics of oil-like products from hydrous pyrolysis of scrap tires at temperatures from 150 to 400^{o}C. Fuel. 107, 578-584.

Seewald, J. 2001. Aqueous geochemistry of low molecular weight hydrocarbons at elevated temperature and pressures: Constraints from mineral buffered laboratory experiments. Geochimica et Cosmochimica Acta. 65, 1641-1664.

Shock, E. 1990. Geochemical constraints on the origin of organic compounds in hydrothermal systems. Origins of Life and Evolution of Biospheres. 20, 331–367.

Simoneit, B.R.T. 1986. Cyclic terpenoids of the geosphere. In: Biological Markers in the Sedimentary Record. (Johns, R.B. (Ed.)), Elsevier Science Publishers, Amsterdam. P.p. 43-99.

Teng, T., Serio, M.A., Wojtowicz, M.A., Bassilakis, R. and Solomon, P.R. 1995. Reprocessing of used tires into activated carbon and other products. Ind. Eng. Chem. Res. 34, 3102-3111.

Ucar, S., Karagoz, S., Ozkan, A. and Yanik, J. 2005. Evaluation of two different scrap tires as hydrocarbon source by pyrolysis. Fuel. 84, 1884-1892.

Williams, P.T. and Besler, S. 1995. Pyrolysis-thermogravimetric analysis of tyres and tyre components. Fuel. 74, 1277-1283

Acknowledgements:

Financial support from the National Plan for Sciences and Technology (09-ENV658-02) of Saudi Arabia is gratefully acknowledged.

Chapter 6

TREATMENT OF 1,4-DIOXANE IN GROUNDWATER

Randy Putnam[§1] and Susan Welt[2]
[1]*EnviroGroup, A Geosyntec Company, 7009 S. Potomac Street, Suite 300, Centennial, CO, 80112*
[2]*EnviroGroup, A Geosyntec Company, 26 Century Hill Drive, Suite 205, Latham, NY, 12110*

ABSTRACT

With increased concern regarding 1,4-Dioxane (dioxane) in groundwater over the last few years, the State of Colorado has required the removal of dioxane, in addition to volatile organic compounds (VOCs), specifically chlorinated VOCs, at a site in Colorado.

The treatment of dioxane is very complex. There are few methods, if any, that can reduce the concentrations to the standards currently being adopted, i.e., 10^{-6} cancer risk based on the Integrated Risk Information System (IRIS) cancer slope factor. Most typical treatment systems, such as activated carbon or air stripping, are ineffective in removing dioxane. The increasingly stringent removal requirements make it even more difficult to meet standards. The process used at this site is an advanced oxidation process (AOP) that is capable of reducing the dioxane concentration to non-detect levels under the right conditions, but this is likely not achievable for many groundwater matrices. This paper presents the treatment requirements and lessons learned from using the advanced oxidation system, as well as the approaches taken to determine the most effective treatment option.

Keywords: 1,4-Dioxane; Treatment; Groundwater; Lessons Learned

[§] Corresponding Author: Randy Putnam, EnviroGroup Limited, 7009 S. Potomac Street, Suite 300, Centennial, CO, 80112, 303-790-1340, rputnam@envirogroup.com

1. INTRODUCTION

Dioxane[2] is present in many products, either as an additive or a byproduct of production. Its primary use is as a stabilizer in chlorinated solvents, especially methyl chloroform[3], at up to 8% by volume (Mohr 2001: 1). It is a byproduct of the production of resins, surfactants, textiles, and plastics (Mohr 2001) and is used as a solvent in a number of different processes (Department of Health and Human Services 2011). Dioxane can also be found in concentrations as high as two percent in many consumer products, such as household aerosols, and even anti-freeze.

Dioxane is considered a probable human carcinogen by the United States Environmental Protection Agency (EPA) (EPA 2010) and reasonably anticipated to be a human carcinogen by the National Toxicology Program (Department of Health and Human Service 2011). As such, it has come under increasing scrutiny as an emerging contaminant, and EPA recently promulgated an update to the unregulated contaminant monitoring regulation (UCMR) to include dioxane (EPA 2012).

The United States production of dioxane is estimated to have peaked at 50 million pounds per year (Mohr 2010: 79) before 1994, when the use of chlorinated solvents began to be phased out. However, through consumer products or the manufacturing process, releases to the environment have resulted in a widespread presence, although at low concentrations (e.g., one milligram per liter [mg/L] or less) of dioxane in surface[4] and groundwater[5]. Due to its chemical properties[6], dioxane plumes often spread further and wider than associated chlorinated solvent plumes (Walsom and Tunnicliffe 2002). It

[2] Dioxane is a cyclic di-ether with three isomers: 1,2-dioxane (o-dioxane), 1,3-dioxane (m-dioxane) and 1,4-dioxane (p-dioxane, CAS No. 123-91-1). Of these three isomers the most common one is 1,4-dioxane and it is also the one that is regulated. Reference to dioxane in this paper refers to 1,4-dioxane.

[3] Methyl chloroform is also known as 1,1,1-Trichloroethane (TCA).

[4] One study of the presence of dioxane in surface water in Japan showed concentrations ranging from 0.02 to 0.49 µg/L (Abe 1999). Mohr (2010: Chapter 2) has reported dioxane in effluent discharges from sewage treatment plants into Lake Michigan at 1 µg/L or greater , and found it in the Haw River in North Carolina (ATSDR, 2012: 165) and in the lower Mississippi River (Zenker 2003).

[5] Analyses of groundwater sources, including drinking water sources, have detected dioxane. California studies of drinking water showed levels up to 47 µg/L (Mohr, GRA 2010). Levels up to 31,000 µg/L have been reported in Illinois groundwater (ATSDR 2012: 165).

[6] Dioxane is miscible in water, does not sorb well onto soils, and does not readily degrade. Due to these properties, dioxane in water creates a larger plume than when compared to chlorinated solvents, as the chlorinated solvents will be sorbed onto soil particles, thus retarding their migration.

has been found in rivers, lakes, groundwater and drinking water, with several water supplies exceeding the health-based limits (e.g., the drinking water risk-based standard based on 10^{-4} cancer risk (35 µg/L, microgram per liter). Due to the potential health effects from dioxane exposure, states are adopting more stringent standards for dioxane in water (see Figure 1).

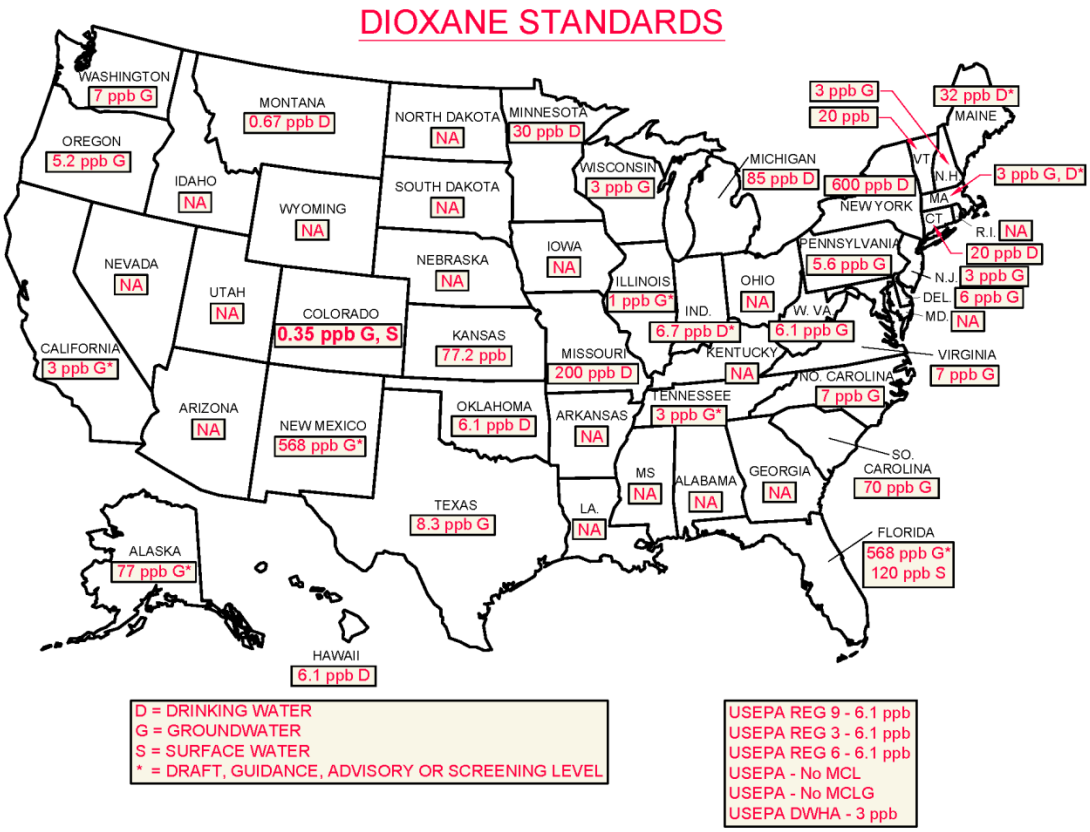

Figure 1. Current Dioxane Standards.

MCL – Maximum Contaminant Level
MCLG – Maximum Contaminant Level Goal
DWHA – Drinking Water Heath Advisory Level

As shown In Figure 1, Colorado has adopted a very low health-based standard (0.35 µg/L[7]) based on a 10^{-6} cancer risk[8] for both groundwater and surface water.

Treatment of dioxane is complicated by its characteristics. It neither strips well from water to air, nor does it sorb well onto activated carbon. The standard biological processes are also ineffective. As presented in Table 1, which summarizes key treatment options, the most effective treatment methods involve advanced oxidation processes (AOPs).

[7] Colorado groundwater standards for dioxane have changed rapidly in the last few years. The standard was 6.1 µg/l from September 2004 until March 2012. It was then reduced to 3.2 µg/L, and further reduced to 0.35 µg/L in January 2013 (CDPHE 2013) based on the EPA IRIS report on dioxane, revised August 2010 (EPA 2010).

[8] Due to these low health-based standards, the analytical method used to detect dioxane is important. EPA Method 522, which is a drinking water method, can detect dioxane to below 0.1 µg/L; the other methods (e.g., Methods 8260 and 8270) can only detect dioxane down to 1 µg/L. (BBL 2006; Florida DEP 2010)

Table 1. Treatment Options.

Treatment Method	Description	Pro	Con	Efficiency	Comments
Chlorination	Chlorine reacts with dioxane		Toxic reactants and byproducts		
Air Stripper	Water comes in contact with air to remove volatile contaminants	Simple to operate, effective in removing volatile contaminants	Not effective for removal of dioxane	<35%	More effective at higher air/water ratios
Ultraviolet Light-Titanium Oxide (UV-TiO_2)	TiO_2 catalyzes a reaction where UV produces hydroxyl radicals	High removal efficiency	Plugging of the TiO_2 recycle loop	65%	
Activated Carbon	Activated carbon adsorbs dioxane	Proven technology, may be able to be regenerated on-site	Not very effective for hydrocarbon removal	72 – 96%	Higher efficiencies may be due to co-metabolism
Persulfate	Persulfate in water produces hydroxyl radicals	Effective, can be introduced in-situ	Chemical costs	90 – 97%	
UV-Peroxide	Peroxide in conjunction with UV produces hydroxyl radicals	High removal efficiency	Lamp life, chemical addition	90 – 100%	

Table 1. Treatment Options (Cont.)

Treatment Method	Description	Pro	Con	Efficiency	Comments
Ozone/peroxide	Ozone and peroxide react with water to produce hydroxyl radicals	Effective	Ozone must be generated on site, very corrosive, toxic	90 – 100%	
Bioreactor	Bacteria digest the dioxane	Low energy, simple to operate	Long retention times required, may require a co-metabolite	95 - 98%	
Fenton's Reagent	Iron and peroxide react to form hydroxyl radicals	Effective	Longer residence times	~100%	
Dow Resin	Resin adsorbs dioxane	Effective	Time to recycle, expensive, little field experience	100%	Lab scale to pilot plant stage

This paper presents the methods used and lessons learned during treatment of dioxane in groundwater at an environmental clean-up site in the City of Denver, Colorado.

2. CASE STUDY

At an environmental clean-up site in Colorado where chlorinated solvents were used, the underlying groundwater is impacted by chlorinated solvents and dioxane. The remedial program is overseen by the Colorado Department of Public Health and Environment (CDPHE). The groundwater within the containment area has levels of chlorinated VOCs and dioxane above the clean-up levels; but originally the contaminants of concern were only the VOCs. To meet the regulatory requirements for VOCs and dioxane in groundwater, a

groundwater treatment system has been designed and implemented, as discussed below.

The site is located within the geologic region known as the Denver Basin. Typical subsurface conditions include loess deposits consisting of clays and silts, with intermittent sand lenses; alluvial deposits consisting of clays, silts, and sands; and gravels deposited by ancestral streams that cut into and formed channels in the bedrock of the Denver Formation. The contact between alluvial deposits and the Denver Formation represents an erosional unconformity. The upper portion of the Denver Formation consists of weathered claystones, siltstones, and sandstones and is located between 10 and 35 feet below ground surface (bgs). The typical depth to groundwater across the site varies from 20 to 25 feet bgs. Groundwater flows through the alluvial materials and weathered bedrock across the site toward the bedrock channel. Hydraulic conductivity in the alluvium ranges from 1×10^{-3} cm/sec to 6×10^{-2} cm/sec downstream from the containment area.

A three-part remediation strategy is being implemented at the site: a groundwater containment system with a pump and treat process; remediation of the groundwater outside of the containment system; and a bedrock remedy intended to reduce the contaminant concentrations leaching from the bedrock. Treatment of dioxane is only required within the containment system. Dioxane concentrations within the containment system range up to 600 µg/L, averaging 110 µg/L in the treatment system influent.

The containment system consists of 21 groundwater extraction and 26 groundwater injection wells. Currently, there are 16 active extraction wells[9] and 16 active groundwater injection wells. Although not all extraction wells deliver the same amount of water to the treatment system, as shown in Figure 2, the daily average flow rate is 11 gallons per minute (gpm).

[9] A typical extraction well depth is 59 feet, with some as shallow as 52 feet.

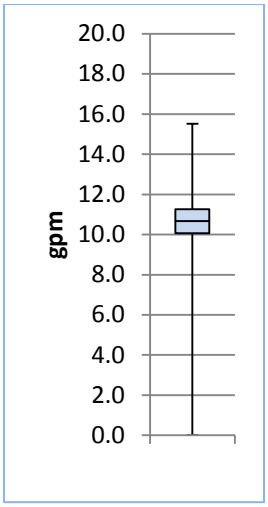

Figure 2. Box and Whiskers[10] 2012 Daily Average Flow (gpm).

With a treatment system influent groundwater concentration averaging 110 µg/L and a state discharge standard of 0.35 µg/L, the required Destruction or Removal Efficiency (DRE) is 99.7% (log 2.50 removal)[11]. The influent concentration is a blend of the various concentrations and flows from the extraction wells.

To try to meet these clean-up standards within the containment system, the groundwater is extracted, air stripped to remove chlorinated solvents, treated to reduce dioxane, and then re-injected to create a hydraulic containment barrier. Although enhancements to the treatment system have been made, the concentration of dioxane has not significantly decreased over the last 5 years indicating either little or no natural attenuation, or a continuing source. The average influent concentration has remained at about 100 to 110 µg/L since 2007.

2.1 Current Groundwater Treatment System

As stated above, the groundwater within the containment area has levels of chlorinated VOCs and dioxane above clean-up levels, but originally the

[10] In a box and whiskers diagram, the bottom of the box is the lower quartile, the line in the middle of the box is the median and the top of the box is the upper quartile. Maximum and minimum values are shown as "whiskers."

[11] Log removal is calculated using the formula: $DRE_{log} = -\log(1- C_e/C_i)$. C_e is the effluent concentration and C_i is the influent concentration. The advantage of the log removal is that the efficiencies are additive; thus, if the first stage has a log removal of 1 (90%) and the second stage has the same log removal, the overall log removal is the sum of the two stages (i.e., 2 or 99%).

contaminants of concern were only VOCs. To reduce the concentrations of VOCs, an air stripper was installed in the pump-and-treat system after the appropriate discharge permits were obtained. Although the site has a surface water discharge permit, all treated groundwater has been re-injected into the ground for the past several years under an Underground Injection Control (UIC) rule authorization from EPA. EPA has determined that an UIC permit is not necessary at this time.

The site is subject to state hazardous waste division oversight, and the current surface discharge permit and UIC authorization overseeing the discharge of treated water do not contain dioxane limits. However, to comply with state-wide standards for dioxane in groundwater, the groundwater treatment system is being modified to improve dioxane removal efficiency.

The air stripper was found to be very effective in removing chlorinated VOCs, reducing the concentrations to below detection levels; however, it is not very effective in removing dioxane. The air stripper has demonstrated that it can remove about 25% (log 0.12 removal) of the dioxane.

Once dioxane was identified as a contaminant of concern, various options to reduce the dioxane concentration were considered. Two systems were evaluated: one using ultraviolet (UV) light with titanium oxide (TiO_2), and the other using ozone-peroxide. For UV to be effective, the water to be treated needs to be relatively transparent to the frequency of the UV lamps. Samples of untreated raw influent and influent after the air stripper and filters were analyzed. The transmittance was 90% before and 91% after at 254 nanometers (nm, 10^{-9} meters). The ozone-peroxide system was eliminated from consideration due to a concern that it would create bromate from naturally-occurring bromine compounds and bromine tracer chemicals. Bromate is also regulated with very low discharge limits (0.05 µg/L) (CDPHE 2013).

A UV-TiO_2 process was initially installed. The UV-TiO_2 system consisted of a bank of UV lamps (128 lamps at 70 watts each) and a TiO_2 recycle loop. The recycle loop removed the TiO_2 nanoparticles using a ceramic filter. The lamps provided a UV dosage of 13.6 kilowatt-hours per thousand gallons (kWh/kgal).

2.2 UV-TiO_2 Treatment

The UV-TiO_2 process uses a reaction where ultraviolet light reacts with water in the presence of TiO_2 to produce hydroxyl radicals. These radicals are extremely reactive[12] and effective in destroying organic chemicals. The TiO_2[13] is recovered by a ceramic filter and recirculated through the process.

[12] The observed rate constant is on the order of 8.7 x 10^{-3}/sec (Stefan 1998).

[13] The TiO_2 used is Degussa TiO_2 P25, which has a nominal particle size of 21 nm, and is over 75% anatase with a minor amount of rutile (25%) (Saggioro et al, 2011: 10381).

As depicted in Figure 3, before the AOP treatment, the groundwater is stripped to remove volatile organics (and some dioxane). It is also filtered to remove any particles that may interfere with AOP operation, i.e., decrease the transmissivity of the ultraviolet light.

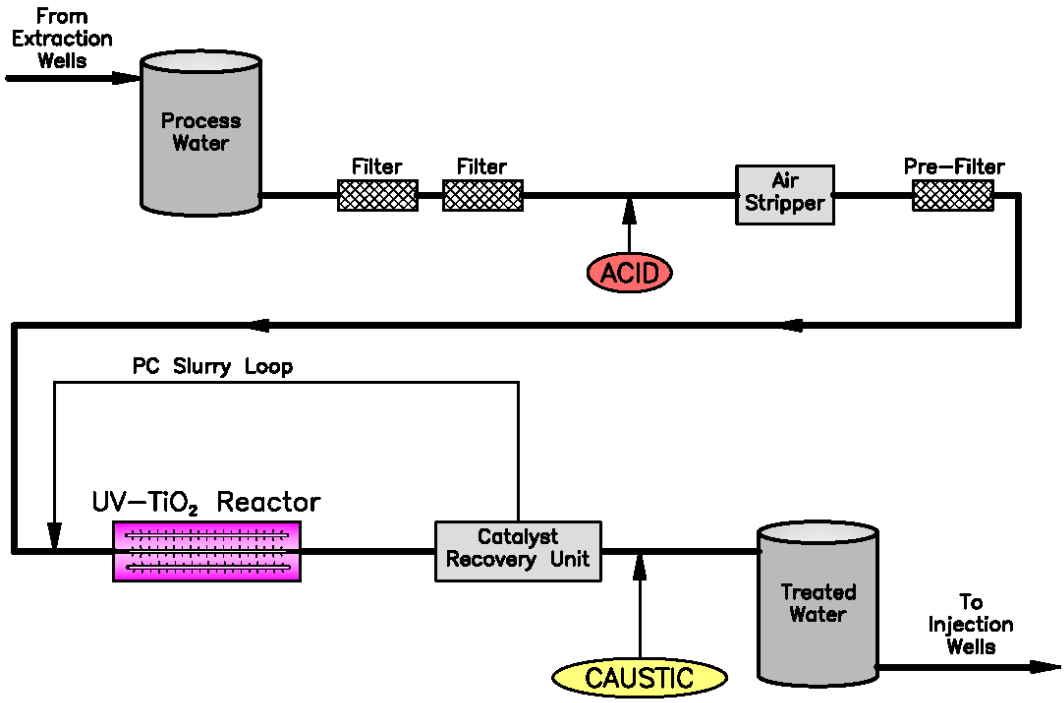

Figure 3. Initial UV-TiO_2 Treatment System.

The overall efficiency of the UV-TiO_2 system is insufficient due to low removal efficiencies and plugging in the TiO_2 recycle loop. Since the TiO_2 particle size is very small, on the order of 21 microns, the filter in the recycle loop had to be able to recover particles that small. The UV-TiO_2 process soon showed a tendency to plug repeatedly and often. Once plugged, the filter unit would be cleaned using acid and alkali solutions. A complete cleaning would take up to 8 hours. Plugging could occur in as few as 4 hours after cleaning and at no point did the system operate for more than 15 days without plugging. The plugging appeared to be caused by dissolved solids precipitating onto the filter unit. The typical concentrations of inorganic constituents in the groundwater are shown in Table 2. Removing these materials would reduce the plugging problem, but treatment to remove dissolved inorganic materials, for example by softening, would be cost-prohibitive.

Table 2. Inorganic Analyses of Water to be Treated (µg/L**).**

Parameter	**Result**
Alkalinity	330,000
Hardness, total, as $CaCO_3$	1,000,000
Dissolved Solids	2,000,000
Suspended Solids	8,300
Iron	180
Manganese	620
Chloride	290
Fluoride	0.93
Potassium	3,000
Sodium	470,000
Sulfate	1,300
UV Transmissivity at 250 nm	91%

To resolve the plugging problem, several approaches were tried. Acid was added to reduce the pH to about 4.5 Standard Units to keep groundwater contaminants in the solution. Sulfuric acid and hydrochloric acid were used at different times to keep the contaminants in the solution. Sequestering agents (e.g., HEDP[14]) were also tried unsuccessfully.

Due to the recycle loop plugging, the best removal efficiency demonstrated was 65% (log 0.46 removal), and average removal was 35% (log 0.19 removal).

2.3 UV-Peroxide

Since it was apparent that the UV-TiO_2 process was not a viable approach, alternate treatment testing (trials) was performed using hydrogen peroxide and the UV light system of the UV-TiO_2 process. Various combinations and concentrations of UV, peroxide, TiO_2, pH, and flow rates were tried. It is important to note that peroxide is listed by the Department of Homeland Security under the Chemical Facility Anti-Terrorism Standard (CFATS) (Department of Homeland Security 2007) at concentrations over 35%; to avoid being subject to this regulation, peroxide is purchased in 25% solutions.

For this treatment system (see Figure 3), the peroxide is added using a peristaltic pump. Such pumps have the advantage of linearity by changing the rate of rotation and they are easy to repair, often requiring a simple change of the tube through the pump.

[14] HEDP: 1-hydroxyethylidene-1,1-phosphonic acid

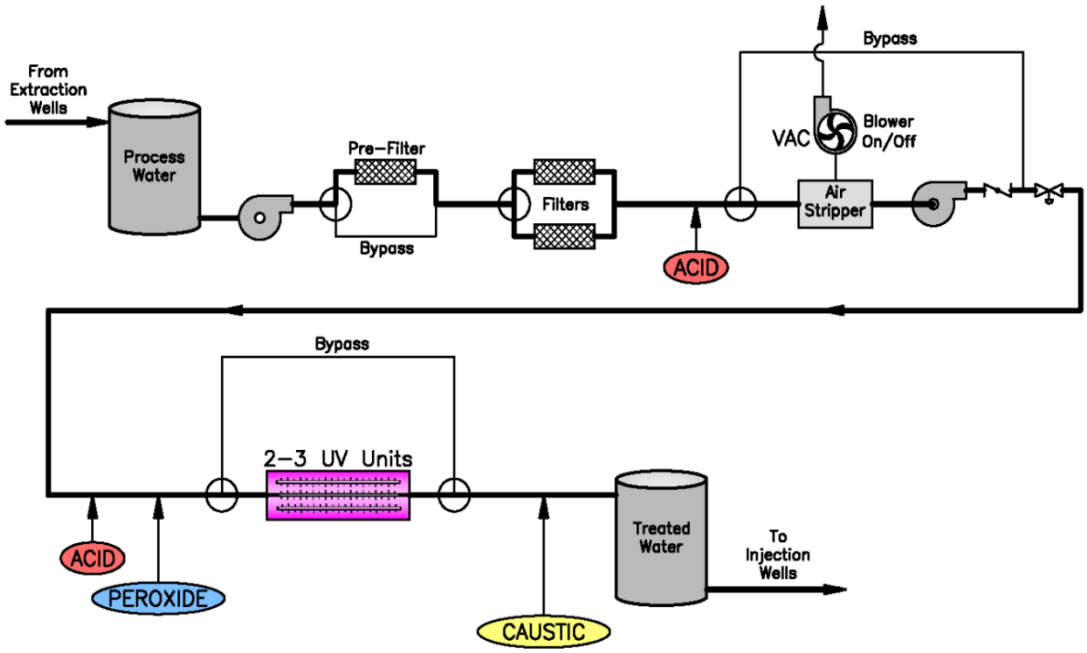

Figure 4. Upgraded Treatment System.

The UV light is added by use of lamps, and the number of lamps is determined based on the additive nature of log removal. However, it was determined that more than the theoretical number of lamps was required to achieve the desired removal efficiency since as the concentration of dioxane decreases, the probability of the reactive species (hydroxyl radical and dioxane) coming in contact to react also decreases.

Figure 5 depicts this theory; showing the DRE decreasing as the influent concentration is decreasing. The rate of reaction is a function of a rate constant and the concentrations of the reactants[15]. As the dioxane is destroyed it uses up a hydroxyl radical, so the rate of reaction decreases as the concentration of dioxane decreases.

[15] R = k*[dioxane]*[hydroxyl radical]. R is the rate of reaction, k is the reaction constant, and [dioxane and hydroxyl radical] are the concentrations of the two chemical species.

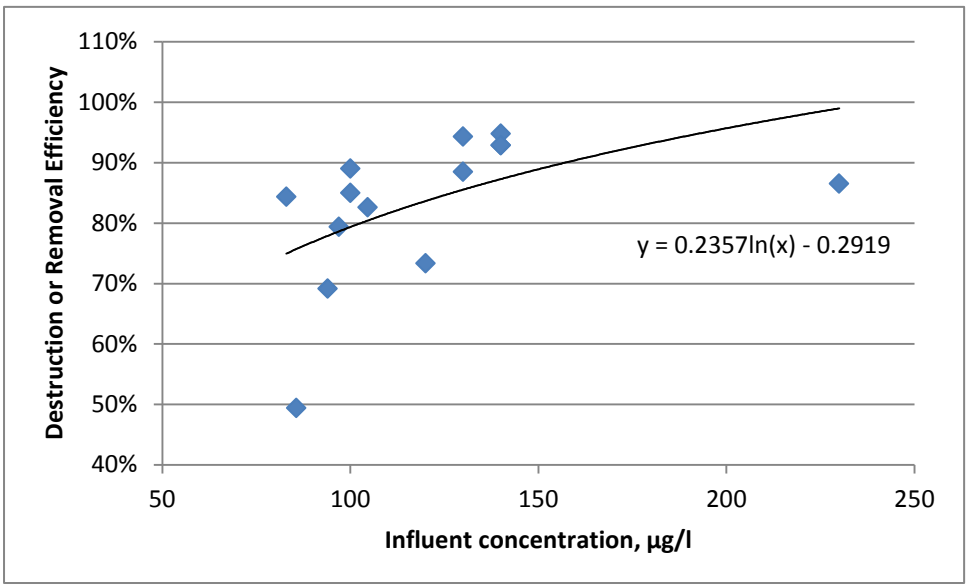

Figure 5. DRE versus Influent Concentration.

The experiments conducted to compare the effects of various parameters, including residence time (flow rate), with or without TiO_2, pH, and peroxide, indicated that the combination of peroxide dosage and UV dosage is key to the DRE. However, as shown in Figures 6 and 7, the data did not demonstrate a correlation between either peroxide dosage or UV dosage and DRE. It should be noted that the UV dosage for the UV-TiO_2 system was estimated as it was not apparent that the lamps were burning out until each lamp was inspected.

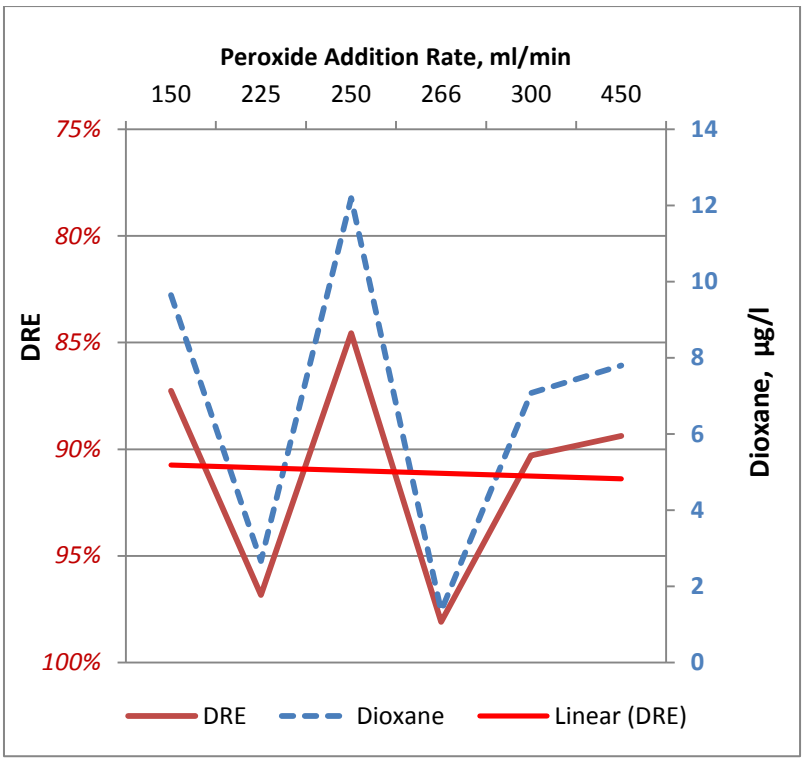

Figure 6. Correlation of Destruction or Removal Efficiency and Peroxide Dosage.

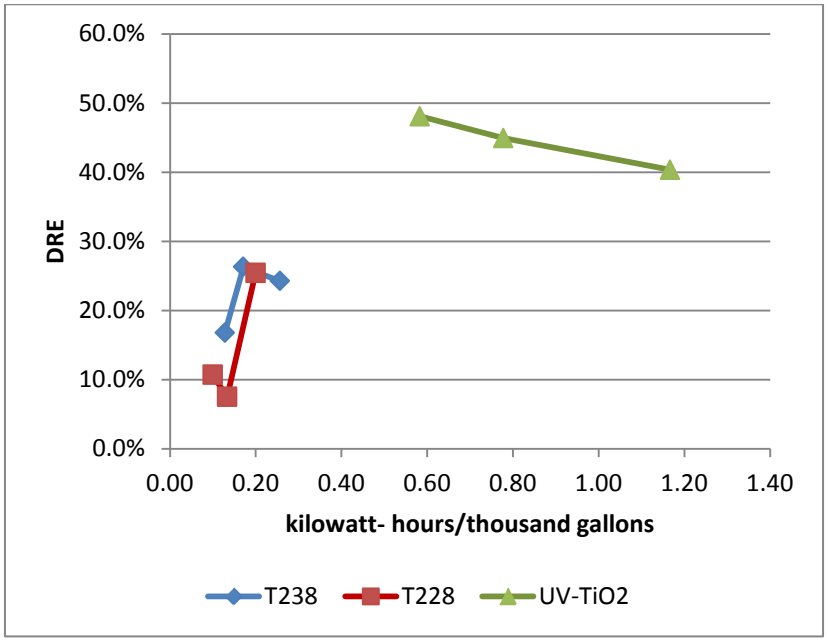

Figure 7. Correlation of Destruction or Removal Efficiency and Ultraviolet Light Dosage.

2.4 Destruction or Removal Efficiency

During the alternate treatment tests (trials), the DRE averaged 95% (log 1.3 removal), with one test resulting in a non-detect (method detection limit [MDL] 1 µg/L) result. With those results, it was clear that a UV-peroxide system could provide treatment that meets the discharge criteria, but that it may take more than one system in series.

It is important to note that operational issues (e.g., sediment collecting in the wells plugging the filters when the extraction pumps are off) required a number of unscheduled trips to the site to do maintenance such as changing filters or restarting the compressor. Thus, the treatment system is currently being upgraded to include additional filtration prior to the air stripper. As shown in Figure 4, the pre-AOP part of the treatment system will include a gross filter (circa 100 µ) to remove this sediment, followed by two finer filters (circa 10 µ) in parallel with a pressure differential sensor to automatically switch to the other filter when it senses one is plugging up. The goal of this redesigned system is to reduce trips from weekly, at a minimum, to monthly, at a minimum.

3. LESSONS LEARNED

The treatment of dioxane in water is very complex and trial and error in the field is part of the process. Key lessons learned to date from this site are highlighted below:

- The quality of the water being treated is critical in determining the type of treatment used. Since dioxane is often found in conjunction with chlorinated solvents, the treatment system needs to be able to treat both contaminants. Often, this is done using multiple processes, e.g., air stripping, followed by AOP, or activated carbon followed by AOP.
- Since the AOP requires water that is transparent at the UV frequencies emitted by the lamps, filtration is required to remove fines such as sediment and bacteria.
- A thorough knowledge of the chemical and physical properties of the water to be treated is essential. At a minimum, we recommend conducting an analysis of the concentrations of the contaminants to be reduced. Testing for any potentially interfering compounds, such as bromine, chlorine, alkalinity, transmittance, sediment, and/or metals, is also recommended. Particle size analysis can be useful in determining the degree of filtration required. Softening removes anions and cations that can interfere with treatment. In addition, air stripping can be effective in reducing carbonate and bicarbonate alkalinity.
- Each clean-up site has unique requirements. It is important to understand the remedial action/clean-up levels. In addition, state or federal regulators may modify the treatment requirements to meet site-specific action levels.

Standards differ by state for groundwater and surface water. Mixing zones and other factors will also impact the allowable discharge limits. If a site can discharge to a municipal or industrial wastewater treatment plant, then the discharge standards may allow for additional treatment or dilution from that treatment.

- Treatment processes may need to be applied in a series to attain the discharge limits. The ability of any system to consistently achieve the new Colorado groundwater standard of 0.35 µg/L, particularly for groundwater containing elevated dissolved solids, has not been established at any site to the authors' knowledge. This may require the setting of site-specific standards, as acknowledged by the Colorado Water Quality Control Commission (5 CCR 1002-41, sections 41.5.B.6 and 41.7.F; Statement of Basis and Purpose, August 13, 2012 Rulemaking, Section 1).
- Drinking water test methods (i.e., EPA method 522) may resolve to levels that are adequate to demonstrate compliance with the lower (less than 1 µg/L) health-based cleanup standards, although, site-specific groundwater matrices may result in elevated reporting limits due to interferences with the test method.
- Whether the discharge is to surface water, groundwater or a sewer system, a permit will be required. Wastewater treatment authorities can dictate discharge requirements. States generally have the authority to set surface water discharge limits and EPA-regulated underground injection. In each case, higher limits requiring less treatment can often be negotiated with the appropriate authorities. Good relationships with the controlling authority are a must.

4. SUMMARY

The treatment of dioxane is very complex. There are few methods that can reduce the concentrations to the standards currently being adopted, i.e., 10^{-6} cancer risk based on the IRIS cancer slope factor (EPA, 2010: II.B.1.2)[16]. Most typical treatment systems, such as activated carbon or air stripping, are ineffective in removing dioxane. The increasingly stringent removal requirements make it even more difficult to meet standards. The treatment approach used at this site is an advanced oxidation process that has the capability to reduce the dioxane concentration to non-detect levels under the right conditions, but this may not be possible at most sites. Further, a correlation between the UV dosage and removal efficiency cannot be made, thereby preventing prediction of the dosage required to attain a specific DRE. As the regulations and discharge limits evolve, the treatment system also needs to evolve. At the beginning of this project, there were no dioxane discharge limits and the initial AOP was installed to meet the 6.1 µg/L

[16] The drinking water risk is 2.9 x 10^{-6} per µg/L.

standard for dioxane. With adoption of the new lower cleanup standard of 0.35 µg/L for both surface water and groundwater discharges, it was necessary to improve the AOP operation. During trials to enhance dioxane removal, operational problems prevented the standard from being met; a 90% DRE was achievable. Additional experiments (pilot field tests) are underway to determine whether the standard can be met with the existing system or whether a new system, one that is practicable and repeatable, is required.

5. REFERENCES

Abe, A. (1999). Distribution of 1,4-Dioxane in relation to possible sources in the water environment. *Science of the total environ.* 227(1), 41-47.

Agency for Toxic Substances and Disease Registry (ATSDR) (2012) Toxicological profile for 1,4-Dioxane. Division of Toxicology and Environmental Medicine/Applied Technology Branch. April 2012.

BBL Environmental Services, Inc. (2006) 1,4-Dioxane comparative analysis study – EPA methods 8260B, 8270C and 8270 with Isotope dilution.

Colorado Department of Public Health and Environment (2013) The Basic Standards for Groundwater, 5 CCR 1002-41, Regulation No. 41. Water Quality Control Division. Denver, CO.

Department of Health and Human Services (2011) *12th Annual Report in Carcinogens* Available: <http://ntp.niehs.nih.gov/?objectid=03C9AF75-E1BF-FF40-DBA9EC0928DF8B15> Last accessed 14 Feb 2013.

Department of Homeland Security (2007) U.S. Code of Federal Regulations, Chemical Facility Anti-Terrorism Standards, 6 CFR 27.

Environmental Protection Agency (2010) *Integrated Risk Information System*. Available: <http://www.epa.gov/IRIS/subst/0326.htm> Last accessed 14 February 2013.

Environmental Protection Agency (2012) Unregulated Contaminant Monitoring Rule, (UCMR-3). 77FR26072. May 2, 2012.

Florida Department of Environmental Protection (2010) Technical Bulletin: Analytical Methods and Recommendations for the Analysis of 1,4-Dioxane. Bureau of Laboratories.

Mohr, T.K.G. (2001) 1,4-Dioxane and other Solvent Stabilizers White Paper. Santa Clara Valley Water District. San Jose, CA. 14 June 2001.

Mohr, T.K.G. (2010) Environmental Investigation and Remediation: 1,4-Dioxane and Other Solvent Stabilizers. Boca Raton, FL: CRC Press.

Mohr, T.K.G. (2010) 1,4-Dioxane in California's groundwater: A Growing Concern. Groundwater Resources Assoc. California (GRA), 19th Annual Con. Meeting. September 15 – 16, 2010.

Saggioro, E., Oliveira, A., Pavesi, T., Maia, C., Ferreira, L., and Moreira, J. (2011) Use of Titanium Dioxide Photocatalysis on the Remediation of Model Textile Wastewaters Containing Azo Dyes. Molecules, 16, 10370-10386.

Stefan, R., and Bolton, J. (1998) Mechanism of the Degradation of 1,4-Dioxane in Dilute Aqueous Solution using the UV/Peroxide Process. *Environmental Science and Technology*, 32(11), 1588 - 1595.

Walsom, D., and Tunnicliffe, B. (2002) 1,4-Dioxane – A Little Known Compound: Changing the Investigation and Remediation of TCA Impacts. *Environ. Science and Engin.*

Zenker, M., Borden, R., and Barlaz, M. (2003) Occurrence and Treatment of 1,4-Dioxane in Aqueous Environments. *Environmental and Engineering Science*. 20(5), 423 – 432.

Part V: Metals

Chapter 7

TRACE METAL CONTENTS OF FERTILIZERS MARKETED IN LEBANON

Isam Bashour[§], Rita Wakim, Nay Dia and Jessica El Asmar
Agricultural Sciences Department, Faculty of Agricultural and Food Sciences, American University of Beirut, Lebanon

ABSTRACT
This study was conducted to assess the content of trace metals (As, Cd, Cr, Co, Ni and Pb) in 69 synthetic fertilizers sources, collected from the Lebanese market between the years 2009 and 2011. Fertilizers used in Lebanon, except for Single Super Phosphate (SSP) and Triple Super Phosphate (TSP), are imported from Europe and the Middle East. The results support the general hypothesis that phosphate fertilizers contain varying levels of trace metals and non-phosphate bearing fertilizers do not contain high amounts of trace metals and therefore should not be considered significant sources of trace metals. At the present rates of fertilization of various crops in Lebanon, the annual loads of As, Cd, Co, Cr, Ni and Pb from fertilizer application correspond to 7.1, 0.98, 10.05, 5.47 and 1.94 μg/kg, respectively. These values are lower than the tolerance limits in soils of Washington State and Canada.

Keywords*:* Commercial fertilizers, synthetic fertilizers, non-nutritive elements, heavy metals.

1. INTRODUCTION

Phosphate fertilizers produced from rock phosphate have been identified as a major source for trace metals in commercial fertilizers (Raven and Loeppert, 1997). A gradual increase in trace metal concentrations of agricultural soils over the past 100 years has been reported in several countries. Long term application of phosphates to agricultural land in New Zealand, where phosphate with about 100 mg/kg Cd was applied, led to the increase of Cd in the soil from two to tenfold within 50 years (McBride and Spiers, 2001). In Australia, near Sydney, vegetables were found to contain higher concentrations of Cd than the Australian maximum permitted levels of

[§] Corresponding Author: Isam Bashour, Agricultural Sciences Department, Faculty of Agriculture and Food Sciences, American University of Beirut, Lebanon, 009613247820, ib02@aub.edu.lb

Cd (Jinadasa et al., 1997) due to fertilization with pacific phosphate sources that are high in Cd.

In Lebanon, fertilizers are commonly applied at high rates by farmers attempting to obtain maximum yields. At present, there are no regulations governing fertilizer application rates. Public concern is increasing about the possible contamination of soil, water and ultimately food with trace metals from excessive and continuous usage of commercial fertilizers in agriculture. Many trace metals are not essential for plant growth, but are absorbed by plants and passed through the food chain and eventually cause health problems whenever they are in high concentrations (Oliver, 1997).

Commercial fertilizers in Lebanon are less than 10% produced locally and about 90% are imported from European and Middle Eastern countries. According to available information, only one study about trace metals (non-nutritive elements) in fertilizers marketed in Lebanon was conducted in 2000 (Bashour et al., 2004). The present study was initiated to assess, once again, the content of the following trace metals, As, Cd, Co, Cr, Ni and Pb, in commercial fertilizer materials marketed in Lebanon from different origins. This information will help evaluate the risk of potential accumulation of trace metals in soils.

2. MATERIALS AND METHODS

Between 2009 and 2011, 69 fertilizer samples were collected from the market. A sample of dry material of approximately 500 grams or 500 mL of liquid sources was taken and placed in clean and labeled containers. Representative subsamples were removed and, when necessary, ground into powder using acid-washed porcelain mortar and pestle. The samples were analyzed for their contents of As, Cd, Co, Cr, Ni and Pb according to the methods of analysis of the Association of Official Analytical Chemists (Latimer, 2010).

A 1.0 g sample was dissolved in a 5 mL concentrated HCl in 25 mL beaker covered with watch glass, boiled for 10 minutes and then evaporated to near dryness. After cooling, the contents were boiled with 10 mL 0.1M HCl and quantitatively transferred into a 25 mL volumetric flask after filtration through Whatman No. 42 filter paper.

The filtrates were analyzed for As, Cd, Cr, Co, Ni and Pb using Inductively Coupled Plasma-Mass Spectrophotometer (ICP-MS). For instrument performance and data integrity, Certified Reference Material (CRM) was analyzed applying the same methodology of the unknown samples. Samples were analyzed in duplicates and known standards were placed among the analyzed tubes to ensure accuracy and instrument stability. The detection limit of the instrument for the analyzed trace metals is 0.2 μg/L.

3. RESULTS AND DISCUSSION

The soil application of fertilizers containing high levels of trace metals could possibly lead to toxicities in plants or animals and may reach the human food chain (Westfall et al., 2005). However, not all trace metals reach the human food chain through fertilizer application to soil; indeed, a good portion is anthropogenic in origin. Concentrations of trace metal contaminants in micronutrient fertilizer sources were not included in this study because micronutrients application rates are low (less than 10 kg/ha). Therefore, soil contamination by trace metals from micronutrient sources are negligible.

Trace metals tend to accumulate in some leafy vegetables more than in cereals and their concentrations are generally lower in grains than in vegetative parts of the crops (Mortvedt et al., 1981). Plant uptake of trace metals from P-fertilizers varied with plant species, soil texture and soil acidity. Bioavailability is usually highest in acidic, sandy soils (Mortvedt, 1996).

The concentrations of As, Cd, Co, Cr, Ni and Pb in the fertilizer samples are presented in Tables 1, 2, 3 and 4 and Figures 1, 2, 3 and 4. The data confirmed the previous work (Bashour, 2000) and show that the concentrations of trace metals are highest in granular phosphate fertilizers (SSP, TSP, DAP and MAP), followed by liquid phosphate fertilizers. The water-soluble powder fertilizers, N-fertilizers and K-fertilizer, generally contain low concentrations of trace metals.

3.1. Nitrogen fertilizers

The major nitrogen sources that are used in Lebanon are $(NH_4)_2SO_4$ (21% N), NH_4NO_3 (33% N) and urea $CO(NH_2)_2$ (46% N). Results of analyses (Fig.1 and Table 1) indicate that the three N-sources are very low in As, Cd, Co and Cr. However, measurable low concentrations of Ni and Pb were found in $(NH_4)_2SO_4$ and NH_4NO_3. These results are in agreement with the reported values in Lebanon (Bashour, 2000) and Saudi Arabia (Al-Modaihish and Al-Sewailem, 1998). As expected, urea contained the lowest concentrations of trace metals because it is an organic synthetic source.

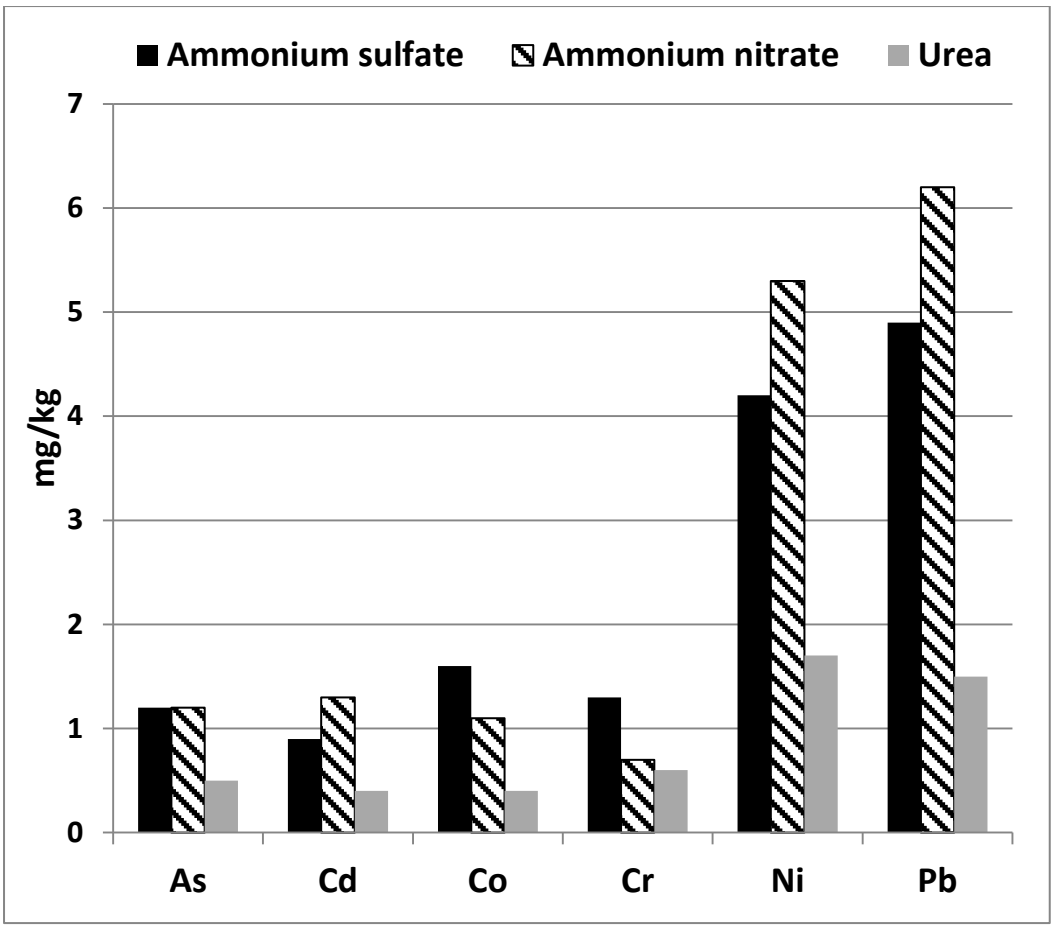

Figure 3. Means of trace metal concentrations in N-fertilizers.

Table 3. Trace metal concentrations (mg/kg) in Nitrogen fertilizers.

Type	**Form**	**Origin**	**As**	**Cd**	**Co**	**Cr**	**Ni**	**Pb**
Ammonium sulfate 21% N	Powder	Germany	1.0	0.6	1.8	1.9	3.4	4.9
		Italy	0.9	0.9	0.6	0.5	5.0	4.3
		Italy	2.0	1.1	1.8	2.0	2.5	10.0
		Italy	1.4	1.3	0.9	1.2	7.4	4.5
		USA	0.5	0.5	3.1	1.1	2.9	0.7
Mean			**1.2**	**0.9**	**1.6**	**1.3**	**4.2**	**4.9**
Ammonium nitrate 33.5% N	Prill	Romania	1.2	1.6	1.4	0.3	4.2	8.7
		Europe	1.5	1.1	0.6	1.0	4.8	4.8
		Ukraine	0.8	1.5	1.4	0.3	4.2	8.8
		Russia	1.2	1.0	0.9	0.9	5.5	6.7
		Europe	1.2	1.3	1.3	1.0	7.8	2.2
Mean			**1.2**	**1.3**	**1.1**	**0.7**	**5.3**	**6.2**
Urea 46% N	Prill	Iraq	0.9	0.4	0.9	0.6	1.8	2.4
		Ukraine	1.1	0.9	0.6	1.9	5.0	3.4
		Saudi Arabia	0.1	0.2	0.1	0.2	0.5	0.5
	Granular	Saudi Arabia	0.1	0.3	0.2	0.3	0.7	0.8
		Qatar	0.1	0.3	0.2	0.1	0.4	0.6
Mean			**0.5**	**0.4**	**0.4**	**0.6**	**1.7**	**1.5**

3.2. Phosphate Fertilizers

Results of the analyses are presented in Fig. 2 and Table 2, and show that phosphate fertilizers contained higher concentrations of trace metals than nitrogen and potassium fertilizers. The data showed that granular P-fertilizers contained higher quantities of trace metals than liquid P fertilizers except for Cd and Ni. The liquid P-fertilizers contained higher concentrations of trace metals than the soluble powder fertilizers. The locally produced phosphate fertilizers from Syrian rock phosphates are granular single super phosphate (SSP, 17% P_2O_5), granular triple super phosphate (TSP, 48% P_2O_5) and green phosphoric acid (H_3PO_4, 52% P_2O_5). The majority of the locally produced P-fertilizers are exported outside the country and only about 5% (about 10,000 tons per year) of production is used locally.

Granular diammonium phosphate (18-46-0) is imported from Jordan, Morocco and Tunisia. Water-soluble powder diammonium phosphate (DAP, 20-51-0) and monoammonium phosphate (MAP, 12-61-0), in addition to granular and powder NPK grades are imported from Europe, Jordan, Saudi Arabia and The United Arab Emirates. The powder water soluble and liquid P-

fertilizers are usually applied through the irrigation system (fertigation), while granular P-fertilizers are usually applied directly to the field.

The concentrations of trace metals in liquid P-fertilizers are variable because of variation in the trace metal concentrations in H_3PO_4. The concentration of trace metals in solid SSP, TSP and DAP was higher than the concentration of trace metals in solid powder P-sources. P-Fertilizer sources imported from North African countries contain much higher trace metals than the ones produced locally from Syrian rock phosphate, or imported from Jordan or Europe.

The Cd concentration in phosphoric acid imported from the US was much higher than the locally produced H_3PO_4 (Table 2). In manufacturing H_3PO_4, most of the trace metals of the original rock phosphate are usually found in the gypsum by-products.

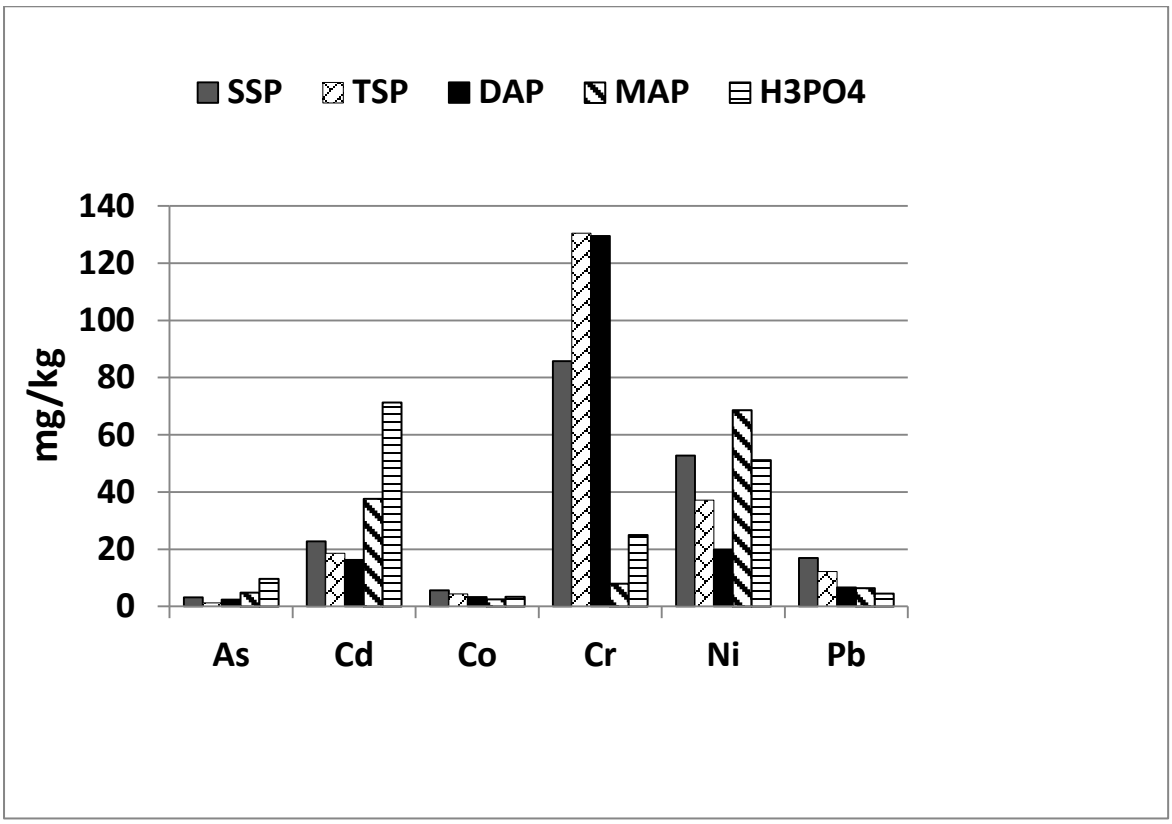

Figure 4. Means of trace metal concentrations in P-fertilizers.

Table 4. Trace metal concentrations (mg/kg) in Phosphorus fertilizers.

Type	Form	Origin	As	Cd	Co	Cr	Ni	Pb
SSP (0 - 18 - 0)	Powder	Lebanon	1.2	6.9	2.3	72.1	26	6
			1	3.2	0.6	76	16	3.5
			7	42	11	101	82	25
			3.7	39	8.4	94	87	33
Mean			**3.2**	**22.8**	**5.6**	**85.8**	**52.8**	**16.9**
TSP (0 - 48 - 0)	Granular	Lebanon	1	3.8	1.8	189.1	19.2	6.2
			2.1	35	9	80.1	55.5	16.8
			1.2	33.3	5.6	86.1	61.6	18
TSP (0 - 46 - 0)		Tunisia	1	2.1	1	166.5	12.4	7.8
Mean			**1.3**	**18.6**	**4.4**	**130.5**	**37.2**	**12.2**
DAP (18 - 46 - 0)	Granular	Tunisia	5.2	27.1	2.2	84.8	21.2	1.7
			1	8.3	1.7	205.1	11.6	3.2
			3	21	5.2	77.3	40	12
		Morocco	4	32.5	7.2	348	18.2	9.1
		Jordan	0.5	7.3	2.2	60.9	21.7	5.3
DAP (18 - 44 - 0)	Powder	Dubai	0.8	1.3	1.4	1	5.8	8.2
Mean			**2.4**	**16.3**	**3.3**	**129.5**	**19.8**	**6.6**
MAP (11 - 52 - 0)	Powder	Europe	13	110	4	20	200	3
MAP (12 - 61 - 0)	Granular	France	1	1	2.3	1.6	2.7	7.4
		Italy	0.6	1.7	1.1	2.5	3	8.7
Mean			**4.9**	**37.6**	**2.5**	**8.0**	**68.6**	**6.4**
H_3PO_4 (52% P_2O_5)	Liquid	USA	11	137	4.1	0	118	3
			13	70	3	0	2.5	2.2
		Lebanon	5	7	3	75	33	8.2
Mean			**9.7**	**71.3**	**3.4**	**25**	**51.2**	**4.5**

3.3. Potassium Fertilizers

The major source of granular potassium fertilizers is potassium sulfate (K_2SO_4, 50% K_2O). Potassium chloride (KCl, 60% K_2O) is banned from entering Lebanon because of its high chloride content.

The powder forms of potassium sulfate (K_2SO_4, 0-0-50), monopotassium phosphate (MKP 0-52-34) and potassium nitrate (KNO_3, 13-0-45) are used in fertigation, mainly for vegetables and fruit trees.

The results of analysis (Fig. 3 and Table 3) show that the content of trace metals in the analyzed K-fertilizers is low for Cr, very low for Ni and Pb and almost negligible for As, Cd and Co. The concentrations of trace metals in granular and powder K_2SO_4 fertilizers were close and differences were due to the origin of the fertilizer rather than to the form

Type	**Form**	**Origin**	**As**	**Cd**	**Co**	**Cr**	**Ni**	**Pb**
Potassium Sulfate (0 - 0 - 50)	Granular	Europe	3.2	3.8	24.1	0.1	7.2	12.0
			5.2	2.8	19.0	0.1	6.1	11.0
			6.0	4.1	18.3	0.1	5.0	14.0
Mean			**4.8**	**3.6**	**20.5**	**0.1**	**6.1**	**12.3**
Potassium Sulfate (0 - 0 - 50)	Powder	Europe	6.2	11.2	16.2	0.1	2.5	2.5
			4.8	10.0	11.1	0.1	5.6	6.8
			5.1	8.6	10.0	0.1	1.9	5.7
			7.1	13.2	12.1	0.1	3.1	4.3
Mean			**5.8**	**10.8**	**12.4**	**0.1**	**3.3**	**4.8**
Potassium Nitrate (13 - 0 - 45)	Powder	Europe	3.8	7.1	6.3	0.1	0.9	4.3
			6.1	9.1	4.9	0.1	1.3	5.0
			0.9	1.1	1.2	0.8	6.7	9.9
			3.0	6.0	9.9	0.2	1.5	3.4
Mean			**3.5**	**5.8**	**5.6**	**0.3**	**2.6**	**5.7**
Potassium Chloride (0 - 0 - 61)	Granular	USA	0.5	0.2	3.8	0.0	2.1	0.3
		Jordan	2.0	0.3	2.1	0.2	2.3	0.5
Mean			**1.3**	**0.3**	**3.0**	**0.1**	**2.2**	**0.4**

Figure 5. Means of trace metals concentrations in K-fertilizers.

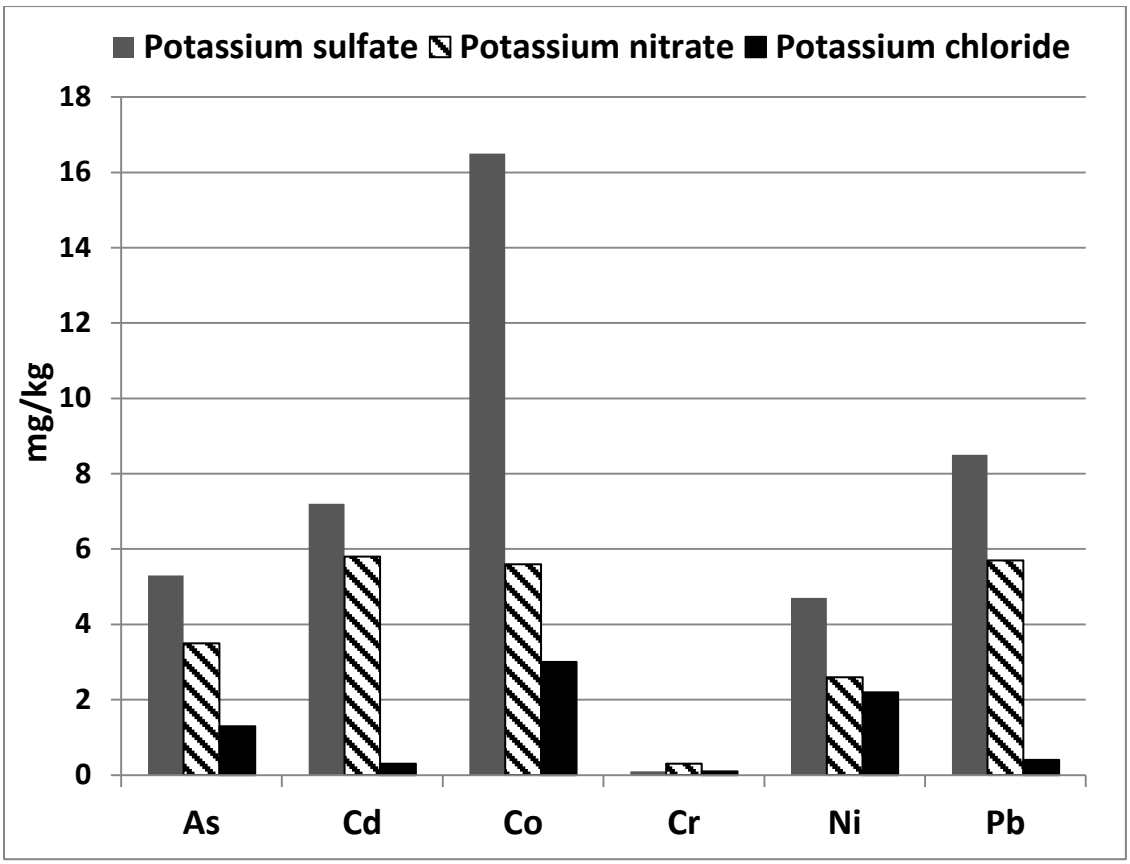

Table 5. Trace metals concentrations (mg/kg) in Potassium fertilizers

3.4. Compound fertilizers

In Lebanon, part of the soluble powder and liquid compound fertilizers are formulated locally using imported raw materials and all the NPK granular fertilizers are imported from Europe and Middle Eastern countries. The results (Fig. 4 and Table 4) show that trace metals concentrations in granular NPK fertilizers are higher than their concentrations in liquid and were lowest in soluble powders. P-containing sources are the main source of trace metals in NPK compounds.

The average annual rates of fertilizer application per hectare in irrigated vegetable fields are about 700 kg of N-fertilizers, 500 kg of P-fertilizers and 200 kg of K-fertilizers (Bashour, 2000). The results of analyses as presented (Figures 1-4 and Tables 1-4) indicate that the sources of trace metals are mainly the P-containing formulas (Table 5).

Trace metals in fertilizers applied to soil for many years may accumulate in soil and become a source of contamination for plants (Williams and David, 1976). McLaughlin, *et al* (1996) reported that Cd accumulation in soil from applied fertilizers is faster than that of Pb. This fact alerted soil researchers and special attention was paid to Cd in soil chemistry and plant

uptake research. Similar to previous work (Bashour *et al*, 2004), the results indicate that trace metals are mainly present in P-fertilizers. Cd ranged between 2.1-110 mg/kg (mean: 26.5) in granular phosphates and 7-137 mg/kg (mean: 71.3) in liquid phosphates. For powder P-fertilizers, the Cd concentration ranged between 1-42, with a mean of 12.25 mg/kg (Table 2).

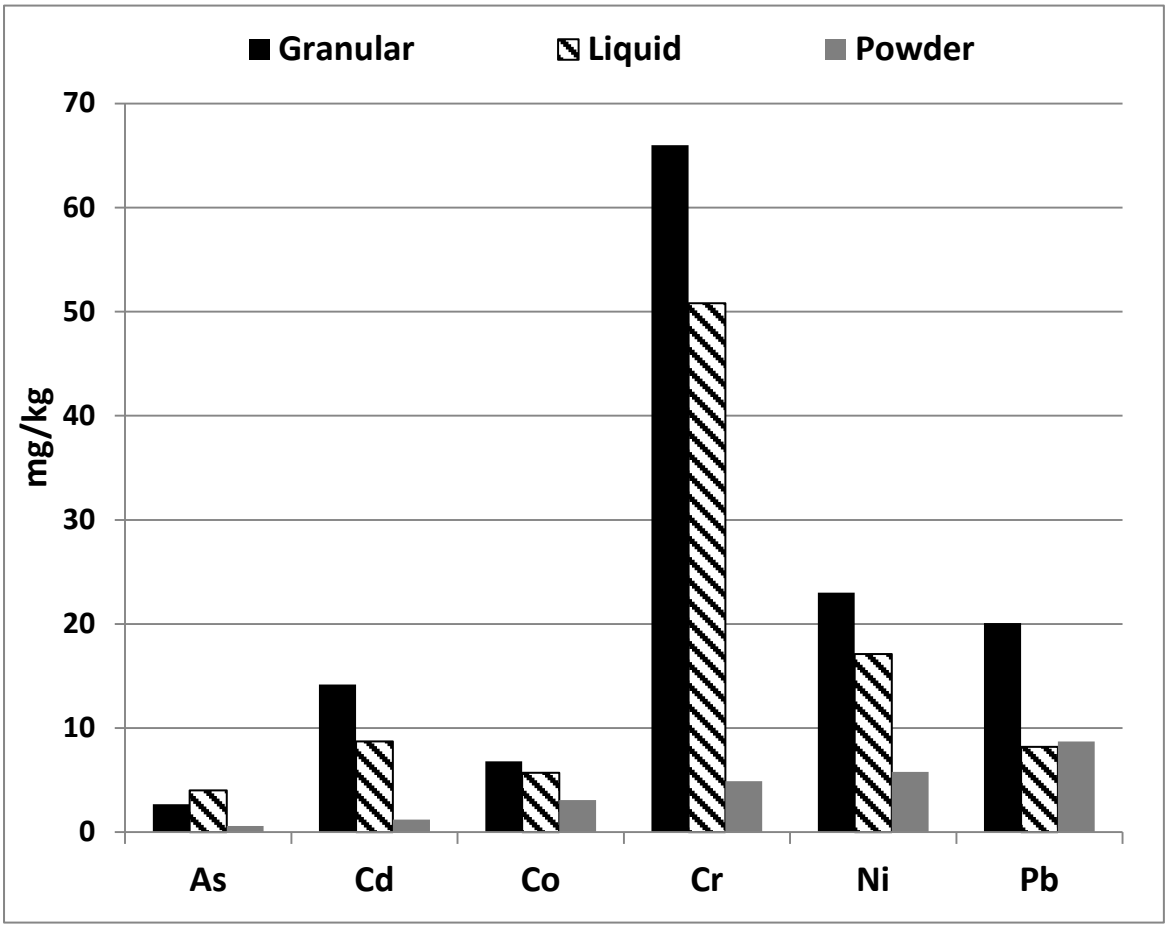

Figure.6. Means of trace metals concentrations in NPK-fertilizers.

Table 6. Trace metals concentrations (mg/kg) in NPK compound fertilizers.

Type	Form	Origin	As	Cd	Co	Cr	Ni	Pb
17 - 17 - 17	Granular	East Europe	2.4	4.4	0.3	112.0	8.4	8.3
		Europe	1.0	1.5	2.1	1.0	7.0	10.5
		Europe	3.0	22.0	19.0	60.0	30.0	15.0
18 - 18 - 18		Europe	2.0	14.0	5.0	80.0	34.0	44.0
		Europe	6.0	28.0	12.0	106.0	55.0	72.0
12 - 12 - 17		Belgium	1.0	1.5	2.0	11.6	13.3	5.3
20 - 20 - 15		Saudi Arabia	2.0	3.8	3.0	59.0	9.0	5.0
30 - 10 - 10		Saudi Arabia	1.0	2.2	2.2	31.0	6.6	4.1
15 - 15 - 15		Europe	6.0	18.0	10.0	78.0	32.0	28.0
		Europe	3.0	31.0	12.0	62.0	28.0	20.0
16 - 40 - 6		Saudi Arabia	2.3	30.0	7.0	125.0	30.0	9.0
Mean			**2.7**	**14.2**	**6.8**	**66.0**	**23.0**	**20.1**
25 - 25 - 18	Liquid	Saudi Arabia	1.0	2.6	1.5	58.0	8.4	4.8
		Jordan	2.0	15.0	9.0	30.0	30.0	15.0
24 - 24 - 18		Europe	1.0	14.0	8.0	31.0	18.0	8.0
0 - 52 - 34		Saudi Arabia	3.0	6.0	3.0	70.0	20.0	6.0
2 - 52 - 8		Saudi Arabia	13.0	6.0	7.0	65.0	9.0	7.0
Mean			**4.0**	**8.7**	**5.7**	**50.8**	**17.1**	**8.2**
20 - 20 - 20	Powder	Jordan	0.4	2.0	8.2	6.0	5.3	8.1
		Saudi Arabia	0.5	1.0	1.4	3.2	3.6	4.4
		France	0.5	0.7	1.2	2.2	2.3	3.9
15 - 30 - 15		Saudi Arabia	0.6	1.1	2.5	9.9	2.8	7.2
13 - 40 - 13		Europe	1.1	1.2	2.0	3.0	15.0	19.9
Mean			**0.6**	**1.2**	**3.1**	**4.9**	**5.8**	**8.7**

3.5. Trace Metals Accumulation

The average annual application of fertilizers per hectare for irrigated agriculture is about 700 kg of N-sources, 500 of kg P-sources and 200 of kg K-sources (Bashour, 2000). The average Cd concentrations are 0.9 mg/kg in N-sources, 29.5 mg/kgin granular P-sources and 6 mg/kgin K-sources (Table 5). Therefore, about (700*0.9) + (500*29.5) + (200*6) = 16.58 g Cd/ha/yr is expected to be applied to the Lebanese agricultural soils with inorganic commercial fertilizers. Assuming that all the Cd stays in the top soil layer (0-

30 cm) with a soil mass = 4400 tons/ha, then the increase in Cd concentration in the top soil layer would be about 3.7 μg/kg/year. This value is much lower than the tolerance limit in Canada and Washington State 20 mg Cd/kg (Pan, Stevens & Labao, 2001).

Table 7. Ranges and means of trace metal concentrations in mg/kg for 69 fertilizer samples collected from the Lebanese market.

Product		**As**	**Cd**	**Co**	**Cr**	**Ni**	**Pb**
N - Fertilizer	Range	0.1 - 2	0.2 - 1.6	0.1 - 3.1	0.1 - 2	0.4 - 7.8	0.5 - 10
	Mean	0.9	0.9	1.1	0.9	3.7	4.2
P - Fertilizer	Range	0.5 - 13	1 - 137	0.6 - 11	0.1 - 348	2.5 - 200	1.7 - 33
	Mean	3.8	29.5	3.9	87.1	41.9	9.4
K - Fertilizer	Range	0.5 - 7.1	0.2 - 13.2	1.2 - 24.1	0.1 - 0.8	0.9 - 6.7	0.3 - 14
	Mean	4.1	6	10.7	0.2	3.6	6.1
NPK -Fertilizer	Range	0.4 - 13	0.7 - 31	0.3 - 19	1 - 125	2.3 - 55	3.9 - 72
	Mean	2.5	9.8	5.6	47.8	17.5	14.5

Repeating the same calculations for As, Co, Cr, Ni, and Pb using the means reported in Table 5, the average annual increase in As, Co, Cr, Ni, and Pb from fertilizer application in Lebanon will correspond to 7.1, 0.98, 10.05, 5.47 and 1.94 μg/kg. All these values are much lower than the tolerance limits set by Washington State and Canada (Table 6).

Table 8. Comparing possible trace metal accumulation in Lebanese soils from commercial fertilizer; in addition to the acceptable levels in Washington State and Canada (Pan *et al*. 2001)

Element	**Trace Mineral Addition**			**Acceptable Levels of Trace Metal Additions in Canada and Washington State**	
	mg/kg/yr	g/ha/yr	Kg/ha/45 yrs	g/ha/yr	Kg/ha/45 yrs
As	7.1	31.24	1.4	330	15
Cd	3.7	16.28	0.73	89	4
Co	0.98	4.02	0.18	667	30
Cr	10.05	44.22	1.99	-	-
Ni	5.47	24.08	1.08	800	36
Pb	1.94	8.54	0.38	2222	100

The soils in the region are generally calcareous and alkaline in nature. Therefore, trace metals present as impurities in commercial fertilizers may precipitate with carbonates, or may be adsorbed by Fe and Mn oxides and co-precipitate as soil particles. Kabata-Pendias and Pendias (2001) reported that As, Co, Cd, Ni and Pb have a very high affinity for carbonates. Therefore, the commonly present free $CaCO_3$ in the soil will capture the trace metals to form carbonate compounds such as $CdCO_3$ which is not soluble in alkaline soil solution. The concentrations of trace metals are much lower than the tolerance limits in Washington State and Canada (Table 6). This indicates that there is no danger from the contamination of soils with trace metals from fertilization. However, it is recommended that less liquid P-sources (H_3PO_4) be imported from the U.S. and less solid phosphate fertilizer sources to be imported from North African countries. P-sources should be encouraged to be imported from Jordan or be locally produced using Syrian rock phosphate, which contains low Cd levels (5 mg/kgCd) and its Cd/P ratio (36-38) is among the lowest in the world (McLaughlin et al., 1996). The international regulations for concentrations of metal impurities in fertilizers are quite different from one country to another. The limits of Cd in P-fertilizers range from 0 in England to 450 mg/kgCd in Australia while the limits for Pb are 500 mg/kgfertilizer (McLaughlin et al., 1996). Contamination of soils with trace metals may come from other sources such as manure, sewage sludge and areal deposition.

4. CONCLUSION

Sixty-nine (69) fertilizer samples that represent the majority of fertilizers marketed in Lebanon and neighboring countries were analyzed. The results from the analysis of the samples show that the risk of food chain contamination with As, Cd, Co, Cr, Ni, and Pb from commercial fertilizers is very low because the concentrations of these trace metals are much lower than the limits acceptable in many countries. Although the concentrations of trace metals in the analyzed fertilizers are lower than the international limits and the soils in the region are calcareous and alkaline in nature, it is imperative that countries legislate for trace metal contents of fertilizers and application rates.

Long-term studies for the accumulation of trace metals from organic and inorganic sources on agricultural land are also needed to determine the acceptable loading limits of trace metals under local agricultural conditions. The implementations of such research work will be beneficial for decision makers and more importantly for the consumers of locally produced products. It is important to keep in mind that “the dose makes the poison”.

5. REFERENCES

Al-Modaihish, A.S., and Al-Sewailem, M.S., 1999. Heavy metals content of commercial inorganic fertilizers used in the Kingdom of Saudi Arabia. Proceedings of the 4th International Conference on Precision Agriculture, University of Minnesota, Minnesota, USA, July 19-22, Pp. 1745-1754.

Bashour, I. 2000. Plant nutrient management for intensification of food production in the Near East Region. Agriculture, Land and Water Use Commission for the Near East. FAO Regional Conference, Beirut, Lebanon, March 25-27, Pp. 1-15.

Bashour, I., Hannoush, G., and Kawar, N. 2004. Trace metal content of commercial fertilizers marketed in Lebanon. In: *Environmental Impact of Fertilizer on Soil and Water*. W.L. Hall Jr. and W.P. Robarge (Eds). American Chemical Society, Washington D.C., Pp. 90-99.

Jinadasa, K. B. P. N., Milham, P. J., Hawkins C. A., Cornish, P. S. D., Williams, P. A., Kaldor, C.J., and Conroy, J. P. 1997. Survey of cadmium levels in vegetables and soils of greater Sydney, Australia. *J. Environ. Qual*. 26 (4), 924–933.

Kabata-Pendias, A., and Pendias, H. 2000. Trace Elements in Soils and Plants. (3rd Edition), CRS Press, New York, USA.

Latimer, G. (Ed). *Official Methods of Analysis of AOAC International*, AOAC, 18th edition, 2010.

McBride, M.B., and Spiers, G.A. 2001. Trace elements content of selected fertilizers and dairy manures by ICP-MS. *Comm. Soil Sci. Plant. Anal. 32* (1, 2), 139-156.

McLaughlin, M.J., Tiller, K.G, Naidu, R., and Stevens, D.P. 1996. Review: The behavior and environmental impact of contaminants in fertilizers. *Aust. J. Soil Res. 34* (1), 1-54.

Mortvedt, J. J., Mays, D. A.; and Osborn, G. 1981. Uptake by wheat of cadmium and other heavy metal contaminants in phosphate fertilizers. *J. Environ. Qual. 10* (2), P.p. 193-197.

Mortvedt, J. J. 1996. Heavy metal contaminants in inorganic and organic fertilizers. *Fertilizer Res*. *43*, 55-61.

Oliver, M.A. 1997. Soil and human health: a review. *European Journal of Soil Science. 48* (4), 573-592.

Pan, W.L., Stevens, R.G., and Labao, K.A. 2001. Cadmium and Lead uptake by wheat and potato from phosphate and waste-derived Zinc fertilizers. 222nd American Chemical Society meeting, Chicago, USA, Aug. 26-31.

Raven, K.P., and Loeppert, R.H. 1997. Trace element analyses of fertilizers and soil amendments. *J Environ. Qual. 26* (2), 551-557.

Westfall, D.G., Mortvedt, J.J., Peterson, G.A., and Gangloff, W.J. 2005. Efficient and environmentally safe use of micronutrients in agriculture. *Comm. Soil Sci. Plant. Anal. 36* (1-3), 169-182.

Williams, C.H., and David, D.J. 1976. The accumulation in soil of cadmium residues from phosphate fertilizers and their effect on the cadmium content of plants. *Soil Sci. 121*: 86-93.

Chapter 8

IS IT CHROMIUM III OR CHROMIUM VI? ARE YOU SURE?

Robert Wellbrock[§], and Anthony Rattonetti

Southeast Laboratory San Francisco Public Utilities Commission, 750 Phelps Street, San Francisco, CA, 94124

ABSTRACT

The 2000 movie "Erin Brockovich" brought increased public attention to the public health threat that is posed by hexavalent chromium (Cr(VI)) in well water from Hinkley, California. This interest was renewed after the 2008 release of toxicity studies by the Department of Health and Human Service's National Toxicology Program. In California, most of the detected Cr(VI) is in Los Angeles, San Bernardino, and Fresno counties, and there has been increased monitoring throughout California due to these studies. For Cr(VI), the current State of California Detection Limit for Reporting (DLR) is 1.0 µg/L, and the California Environmental Protection Agency has established a Public Health Goal (PHG) of 0.02 µg/L in drinking water.

Methods for the determination of Cr(VI) concentrations range from selective solvent extraction to chromatography. The only EPA approved method capable of achieving the PHG is EPA 218.7, which uses ion chromatography for species separation followed by UV/Vis detector for quantitation. Three requirements must be met for accurate measurement of trace amounts of Cr(VI): (1) proper preservation and holding time (these have been issues of contention and continue to be so), (2) reagents and apparatuses must be free of significant chromium contamination, and (3) "real world" certified reference materials (CRMs) must be used to validate findings..

In lieu of available CRMs, a second independent analytic method is needed. A High Pressure Liquid Chromatography - Inductively Coupled Plasma- Mass Spectrometry (HPLC-ICP-MS) procedure for a Collision/Reaction Cell equipped ICP-MS has been developed for this purpose. It is described here, with discussion of its capabilities and limitations.
Keywords: HPLC-ICP-MS, hexavalent chromium

1. INTRODUCTION

Chromium is a naturally occurring element originating from the earth's crust as the mineral chromite ($FeCr_2O_4$), with detectable levels having been

[§] Corresponding Author: Robert Wellbrock, Southeast Laboratory San Francisco Public Utilities Commission, 750 Phelps Street, San Francisco, CA, 94124, 415-920-4967, rwellbrock@sfwater.org

found in soil, water, and air (ATSDR, 2012). Background concentrations of chromium exist in all forms of media. Natural weathering processes release chromium from minerals into the dust, soil, air and water of locations where the chromite mineral is found (ATSDR, 2012). Chromium also has several industrial applications, including smelting, metallurgy, electroplating, and tanning (Gomez and Callao, 2006; Wolf et al, 2007). Due to releases from these anthropogenic sources, chromium can be found in the environment at greater than normal background concentrations.

This paper focuses on chromium in water samples. In aqueous systems, chromium occurs in two predominant oxidation states: trivalent chromium (Cr(III)) and hexavalent chromium (Cr(VI)) (McNeill et al, 2012). Trivalent chromium is generally non-toxic (Zhitkovich, 2011) and has historically been considered to be an essential nutrient in the human diet, although that designation has been recently reconsidered (McNeil et al. 2012). In contrast, hexavalent chromium is a likely carcinogen. Studies have indicated that chronic exposure to hexavalent chromium may result in cancer (Zhitkovich, 2011). Non-carcinogenic adverse exposure effects, including respiratory, cardiovascular, gastrointestinal, hematological, hepatic, renal, and neurological, have been documented (ATSDR, 2012). Research that provides evidence for these health effects has been compiled by the U.S. Department of Health and Human Services Agency for Toxic Substances and Disease Registry (ATSDR, 2012).

Due to the health concerns associated with hexavalent chromium exposure and the technical challenges of quantifying the hexavalent form, total chromium concentration in drinking water is regulated on both the federal and state level. The United States Environmental Protection Agency has established a non-enforceable Maximum Contaminant Level Goal (MCLG) and an enforceable Maximum Contaminant Level (MCL) for total chromium in drinking water systems. The MCLG is determined based on the level of contaminant that will be likely to cause health problems in consumers. The MCL is determined based on the cost and available technology required to address the contamination. Together these two USEPA levels establish the national standard for total chromium in drinking water systems. Currently, the USEPA MCLG and MCL are identical, both set at 100 µg/L (100 ppb) for total chromium (McNeill et al, 2012). There is no MCL specific to hexavalent chromium.

The total chromium standard for the State of California is more stringent than the national standard. The enforceable MCL for total chromium in California drinking water systems is currently 50 µg/L (McNeill et al., 2012). As of July 2011, the Office of Environmental Health Hazard Assessment (OEHHA) of the California Environmental Protection Agency established a Public Health Goal (PHG) specific to hexavalent chromium at 0.02 µg/L. This PHG is equivalent to the USEPA MCLG because it is determined solely via health-protection without consideration of cost and technology (OEHHA, 2011). The final PHG by the OEHHA has initiated the

process for establishment of a hexavalent chromium specific MCL by the California Department of Public Health (CDPH). This MCL is expected to be implemented between July 2014 and July 2015 (CDPH, 2012).

It is fair to say that increased regulation of hexavalent chromium is being considered on both the state and federal level. With the CDPH considering the new low PHG, a likely outcome will be a lower MCL for hexavalent chromium. Although hexavalent chromium is not specifically regulated on the federal level, the USEPA has begun monitoring levels of hexavalent chromium in public water systems. Hexavalent chromium was recently added to the list of contaminants tested for in the third version of USEPA's Unregulated Contaminant Monitoring Regulation for Public Water Systems, released in May 2012. Regulations regarding acceptable levels of hexavalent chromium are currently in development.

The current preferred analysis method for trace level hexavalent chromium uses ion chromatography: EPA Method 218.7 entitled "Determination of Hexavalent Chromium in Drinking Water by Ion Chromatography with Post-Column Derivatization and UV-Visible Spectroscopic Detection" (USEPA, 2011). This method offers two buffer options designed to prevent both reduction of Cr(VI) and oxidation of Cr(III). In other words, the goal of the buffer is maintain the concentrations of each chromium species as they are at the moment of sample collection. Ion chromatography does achieve detection levels that would satisfy the requirements of the new PHG. Method 218.7 identifies Lowest Concentration Minimum Reporting Levels (LCMRL) ranging from 0.012 to 0.036 μg/L and a method detection limit (MDL) ranging from 0.0044 to 0.015 μg/L (USEPA, 2011). Similar results have been achieved using EPA 218.7 by McNeill et al. (2012), who reported a LCMRL of 0.0089 μg/L and an MDL of 0.0067 μg/L, and a Minimum Reporting Limit of 0.02 μg/L.

Our laboratory has begun research on an independent method for hexavalent chromium speciation, detection, and quantification that would be capable of achieving the detection levels that might be required in a new low MCL. Separation of the chromium species using High Pressure Liquid Chromatography (HPLC) and detection using Inductively Coupled Plasma-Mass Spectrometry (ICP-MS) is one alternate method that has been previously researched with varying degrees of success.

For the separation of Cr(III) and Cr(VI) using HPLC, it is important to consider the ionic complexes in the environment in which these two oxidation states exist. Cr(III) exists as an cationic or neutral species (Cr^{+3}, $CrOH^{+2}$, $Cr(OH)_2^{+}$, $Cr(OH)_3^{0}$) and Cr(VI) exists as an anionic species ($HCrO^{-}$ and CrO_4^{-2}) (McNeill et al, 2012). The ionic chromium species present will depend on redox conditions, pH, and water composition (ATSDR, 2012). These factors also affect the conversion between the Cr(III) and Cr(VI) oxidation states. To put it very generally, Cr(VI) species are more likely to dominate in basic conditions, while Cr(III) are more likely to dominate in acidic conditions (ATSDR, 2012). EPA Method 218.7 uses a buffer to raise

the pH to alkaline conditions in an effort to prevent species interconversion. Our study method does not use a buffer, but instead focuses on developing analysis methods that obviate the need for buffers.

Some studies that were particularly useful for this research have been listed in Table 1. One issue that became evident in the literature search is that the previous studies did not use the equipment that is available to our lab. Particularly, our HPLC column has been rarely used in other independent studies. The packing for this column is polymethacrylate polymer that was developed for anion exchange functionality. The column used by Byrdy et al. (1995) also has a polymer packing useful for ionic separation.

The subject of the column brings up another important issue. As mentioned previously, Cr(III) ions are cationic and Cr(VI) ions are anionic. The anionic exchange columns will not retain cationic species and will only retain the Cr(VI) species. To perform simultaneous analysis of the two oxidation states using an anionic column, Cr(III) must be chelated to form an anionic species. A popular chelator is ethylenediaminetetraacetic acid (EDTA). One issue that we have with using EDTA to chelate Cr(III) is that water must be heated to higher than ambient temperatures to initiate the reaction. One of our goals is to avoid any additions such as a buffer or EDTA. Therefore, our focus is to isolate and quantify Cr(VI) species.

Table 1. Previous research investigating chromium analysis using HPLC-ICPMS.

Reference	**Mobile Phase**	**Method Detection Limit (µg/L)**	
		Cr(III)	**Cr(VI)**
Byrdy et al, 1995	35 mM $(NH_4)_2SO_4$, pH 9.2 with NH_4OH	0.4	1.0
Chang and Jiang, 2001	0.6 mM EDTA, 2 mM TBAP, 2% v/v methanol, pH 6.9	0.063	0.061
Wolf et al, 2007	2 mM TBAOH, 0.5 mM EDTA, 5% methanol, pH 7.6	0.09	0.06
McNeill et al, 2012	350 mM HNO_3	N/A	0.03

Table. 2 Interference Concerns (Byrdy et al, 1995; Seby et al, 2003).

^{52}Cr	$^{36}Ar^{16}O$, $^{40}Ar^{12}C$, $^{35}Cl^{16}OH$, $^{37}Cl^{14}NH$, $^{35}Cl^{17}O^+$
^{53}Cr	$^{36}Ar^{16}OH$, $^{40}Ar^{13}C^+$, $^{37}Cl^{16}O^+$, $^{35}Cl^{18}O$, $^{40}Ar^{12}CH$

A feature the ICPMS instrument used in our study has in common with instruments used in previous research is the operation of a collision/reaction cell. Chromium has 2 major stable isotopes at mass 52 (83.8%) and mass 53 (9.5%) (Seby et al., 2003). Polyatomic ions with the same nominal mass as the chromium isotopes may form due to reactions between components of the plasma and sample. These polyatomic ions may interfere with chromium detection. Common polyatomic ions that will interfere with these chromium isotopes are listed in Table 2. While the exact function of this collision cell will depend on the particular instrument manufacturer, the overall goal is to remove interfering ions that would impact the response of a desired analyte such as hexavalent chromium.

The literature search revealed several different options for mobile phase solutions. We chose an experiment with several mobile phase components and concentrations to minimize background noise and optimize response The goal of this project is to develop an HPLC-ICPMS procedure to separate chromium species to quantify low level hexavalent chromium concentrations in drinking water samples by applying speciation techniques from the literature with a collision/reaction cell equipped ICPMS

2. EXPERIMENTAL

2.1 Reagents and Standards

All water was deionized (18MΩcm) and prepared by passing through a NanoPure treatment system (Barnstead).

Chemicals used in the mobile phase were of analytical reagent grade. Two types of ethylenediaminetetraacetic acid (EDTA) were used. The first was EDTA-2Na Ultrapure Bioreagent (J.T. Baker, Avantor Performance Materials, Center Valley, PA). The second was EDTA-2Na for HPLC ≥ 99.0% (Fluka, Sigma-Aldrich, Germany). Sodium sulfate (Na_2SO_4, A.C.S Reagent) was purchased from J.T. Baker (Avantor Performance Materials, Phillipsburg, NJ). The sodium phosphate used was sodium phosphate monobasic monohydrate ($NaH_2PO_4 \cdot H_2O$, A.C.S. Reagent), purchased from J.T. Baker (Avantor Performance Materials, Center Valley, PA). The sodium hydroxide (NaOH) was in the semi-conductor grade 99.99% trace metals in pellet form (Sigma-Aldrich, St. Louis, MO).

The second mobile phase used ammonium sulfate ($(NH_4)_2SO_4$), Fluka TraceSelect for trace analysis ≥ 99.9999% (Sigma-Aldrich, Germany). Ammonium hydroxide (NH_4OH), 20% v/v, Ultrex Ultrapure was purchased from J.T. Baker (Avantor Performance Materials, Center Valley, PA).

The third mobile phase had the same ammonium hydroxide as the second mobile phase. The sulfuric acid (H_2SO_4) Omnitrace 95.5%-95.6% was purchased from EM Science (Merck KGaA, Darmstadt, Germany).

Cr(III) standards were prepared from chromium nitrate nonahydrate ($Cr(NO_3)_3 \bullet H_2O$) (Alfa Aesar, Ward Hill, MA). Cr(VI) standards were prepared from potassium chromate (K_2CrO_4) (J.T. Baker, Avantor Performance Materials, Center Valley, PA).

Mobile phase solutions were prepared fresh when used. No interconversion between Cr(III) and Cr(VI) was observed in standards. Working level standards were prepared fresh when used.

3. EQUIPMENT

3.1 Vials

Agilent 1 mL crimp/snap polypropylene vials (PN 5182-0567) were used. Samples were capped with Agilent Snap Caps, 11 mm (PN 5182-0542).

3.2. HPLC Conditions

An Agilent 1200 series HPLC equipped with a binary pump, autosampler, and vacuum degasser was used for this work. The samples were injected at ambient temperature so there was no need for a column to be heated. The column used was the Agilent Chromium Speciation column for ICP-MS. This separation column is an anion exchange column (4.6 mm i.d. x 30 mm polyhydroxymethacrylate base resin). An Agilent Bio Compatibility Kit (PN 5065-9972) with PEEK tubing was installed, as well as an Agilent Bio-Inert MultiDraw Kit(PN G5667-68711). See Table 3 for HPLC operating conditions.

3.3 ICPMS Conditions

An Agilent 7500ce ICP-MS was used for chromium detection. Chromium isotopes ^{52}Cr and ^{53}Cr were monitored according to the method settings. The use of collision/reaction cell technology was employed using helium as the reaction gas. See Table 4 for ICPMS operating conditions.

Table 3. HPLC equipment and operating conditions.

HPLC Instrument	Agilent 1200
- Sample Volume	**0.300 mL**
- Column	**Cr Speciation G3268-80001**
- Pump Speed	**0.700 mL/min**
- Mobile Phase Composition	**50 mM $(NH_4)_2SO_4$, pH = 7.5**

Table 4. ICP-MS equipment and operating conditions.

ICP-MS Instrument	Agilent 7500ce
Plasma Conditions	
- Rf Power	**1550 W**
- Carrier Gas	**1.05 L/min**
- Make up Gas	**0.30 L/min**
- Nebulizer Pump	**0.20 rps**
- S/C Temperature	**2 deg C**
Mass Spectrometer Settings	
- Monitoring Mass	**^{52}Cr, ^{53}Cr**
- Integration Time	**2.0 sec**
- Acquisition Time	**355 sec**
Collision Cell Parameters	
- He reaction gas flow	**5.0 mL/min**

ŧ Notice: the mention of trade or commercial products does not constitute endorsement or recommendation for use by the San Francisco Public Utilities Commission.

3. RESULTS AND DISCUSSION

The mobile phase composition was the condition that was given the most attention. The first mobile phase was recommended by the manufacturer. There were four components to this mobile phase: NaH_2PO_4, Na_2SO_4, EDTA-2Na (ethylenediaminetetraacetic acid), and NaOH with at pH 7. This mobile phase successfully separated Cr(III) and Cr(VI); however, the main issue with this mobile phase was the amount of background noise present during a run. The lowest level with a discernible peak was at 0.25 ppb. Although efforts were made to purchase pure components, analysis of the individual components revealed that chromium contamination was present in each product. The combination of contamination in the individual components resulted in an excessive amount of background noise which makes it difficult for trace level analysis. An attempt to use a chelation product to remove the contamination had limited success and was not pursued further.

The components of the second mobile phase are also used for one of the eluents in EPA Method 218.7: $(NH_4)_2SO_4$ and NH_4OH (USEPA, 2011). These same mobile phase components were also recommended by Byrdy et al. (1995). However, research performed by Byrdy et al. (1995) concluded that a

mobile phase with high salt concentration can lead to salt deposition and clogging of the ICP-MS, with the end result being a loss of sensitivity. Therefore, the 35 mM $(NH_4)_2SO_4$ concentration suggested by Byrdy et al. (1995) was chosen over the 250 mM $(NH_4)_2SO_4$ EPA ion chromatography eluent. To make this mobile phase, powdered $(NH_4)_2SO_4$ was diluted with nanopure deionized water and brought to pH 7.5 with NH_4OH. This mobile phase was immediately more successful than the previously used mobile phase. The background abundance dropped from 1500 to 500 counts. Using this mobile phase, the response of Cr(VI) was detectable down to 0.050 ppb. Altering the concentration and the pH of the mobile phase changed the peak shape and location, but did not have a large effect on the background noise or response. A concentration of 50 mM $(NH_4)_2SO_4$ was eventually settled upon with no salt deposition or negative effects on the ICP-MS.

The final mobile phase was based on the success of the 50 mM $(NH_4)_2SO_4$. However, this mobile phase was made using ultrapure H_2SO_4 and NH_4OH instead of reconstituting from the solid state. The background abundance for this mobile phase was between 150 and 200 counts. Similar to the previous mobile phase, the signal of Cr(VI) was detectable down to 0.050 ppb. At this point, we increased carrier gas flow and nebulizer gas flow, which increased the sensitivity of the mass spectrometer, but also increased the background abundance to 250 to 300 counts. Cr(VI) standards of 0.025 ppb could be detected using these conditions, but the peak could not be quantified. At this point, we received and installed a new sample loop that allowed us to increase the sample size to 300 µ/L. The gas flows were adjusted to lower the background noise back down to 200 counts, and the tripling of the sample size allowed for 0.025 ppb to be detected at a quantifiable level.

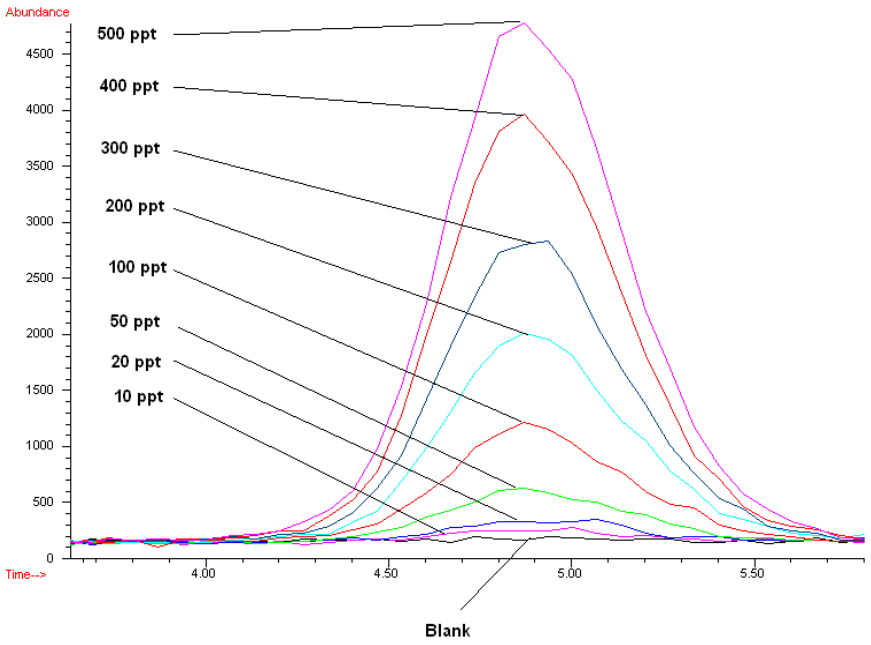

Figure 1. Calibration points.

The instrument was calibrated with Cr(VI) standards and a calibration curve was created. To demonstrate the analytical capabilities of the HPLC-ICP-MS using the final mobile phase and instrument conditions, seven replicates of spiked laboratory blanks were run at the desired minimum reporting limit (MRL). To demonstrate the precision and accuracy of the analysis, seven replicates of laboratory control spikes (LCS) were run at a level in the middle of the calibration range. Following the example provided by McNeill et al. (2012), the precision and accuracy of the tap water was also tested. Five replicates of tap water were initially analyzed for Cr(VI) concentration, and then the samples were spiked at the same levels as the MRL and the LCS. Seven replicates of the Cr(VI) spiked tap water were run for both the MRL level and the LCS level.

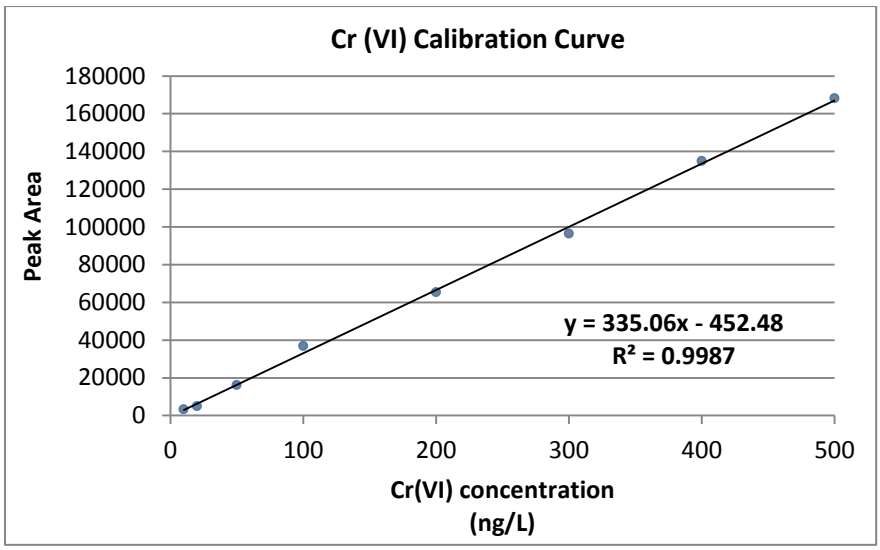

Figure 2. Cr(VI) calibration curve.

The regression analysis resulted in a well-fitting linear calibration curve (Figure 1). The calculated MDL is 5.41 ng/L. Although we are satisfied with this MDL, we believe that the current system could support a lower MDL. The MRL study results indicate that we achieved our goal of a 20 ng/L reporting limit. The MRL was validated based on the EPA Prediction Interval of Results study (Table 5).. The results for the 99% two-sided confidence interval are well within the required quality control interval of recovery of 50% to 150%. MRL study results are summarized in Table 5.

Table 5. Summarized MRL results.

MRL Results		
MRL Average	19.57	ng/L
Standard Deviation	1.72	ng/L
RSD	8.79	%
MDL	5.41	ng/L
HR_{PIR}	6.82	ng/L
Upper HR_{PIR}	131.96%	≤ 150% (PASS)
Lower HR_{PIR}	63.76%	≥ 50% (PASS)
$t_{(6,1-\alpha = 0.99)} = 3.143$		

5. CONCLUSION

The final instrument operating conditions and mobile phase composition have successfully been used to analyze laboratory spiked blanks and tap water samples. This method has the potential to be used for analysis of hexavalent chromium concentrations as low as the new PHG; however there is room for improvement. Particularly, the next phase of research will focus on verifying the lack of interference, potential for use with the 218.7 buffer, other potential storage methods, and analysis of real world samples to verify the methods used for a less predictable matrix.

6. REFERENCES

Agency for Toxic Substances and Disease Registry (ATSDR). 2012. Toxicological profile for Chromium. U.S. Department of Health and Human Services, Public Health Service, Atlanta, GA.

Byrdy, F. A., L. K. Olson, N. P. Vela, and J. A. Caruso. 1995. Chromium speciation by anion-exchange high-performance liquid chromatography with both inductively coupled plasma atomic emission spectroscopic and inductively coupled plasma mass spectrometric detection. Journal of Chromatography. 712: 311-320.

Chang, Y. L. and S. J. Jiang. 2001. Determination of chromium species in water samples by liquid chromatography-inductively coupled plasma-dynamic reaction cell-mass spectrometry. Journal of Analytical Atomic Spectrometry. 16: 858-862

Gomez, V. and M. P. Callao. 2006. Chromium determination and speciation since 2000. Trends in Analytical Chemistry. 25(10), 1006-1015.

California Department of Public Health (CDPH). 2012. Chromium-6 in drinking water: MCL update. Available at: http://www.cdph.ca.gov/certlic/drinkingwater/Pages/Chromium6.aspx Accessed March 14, 2013.

McNeill, L., J. McLean, M. Edwards, and J. Parks. 2012. State of the science of hexavalent chromium in drinking water. Water Research Foundation, Denver, Colorado.

Office of Environmental Health Hazard Assessment (OEHHA). 2011. Public health goal for hexavalent chromium (Cr VI) in drinking water. Pesticide and Environmental Toxicology Branch, California Environmental Protection Agency. Available at: http://oehha.ca.gov/water/phg/072911Cr6PHG.html Accessed March 14, 2013.

Séby, F., S. Charles, M. Gagean, H. Garraud, and O. F. X. Donard. 2003. Chromium speciation by hyphenation of high-performance liquid chromatography to inductively coupled plasma-mass spectrometry - study of the influence of interfering ions. Journal of Analytical Atomic Spectrometry. 18, 1386-1390.

United States Environmental Protection Agency (USEPA). 2011. Method 218.7: determination of hexavalent chromium in drinking water by ion chromatography with post-column derivatization and UV-Visible spectroscopic detection. US EPA, Washington, DC.

Wolf, R. E., J. M. Morrison, and M. B. Goldhaber. 2007. Simultaneous determination of Cr (III) and Cr (VI) using reversed-phased ion-pairing liquid chromatography with dynamic reaction cell inductively coupled plasma mass spectrometry. Journal of Analytical Atomic Spectrometry 22:1051-1060.

Zhitkovich, A. 2011. Chromium in drinking water: sources, metabolism, and cancer risks. Chemical Research in Toxicology 24:1617-1629.

Part VI: Modeling

Chapter 9

MODELING OF CONTAMINANT TRANSPORT IN POROUS MEDIA UNDER FLUCTUATING WATER TABLE CONDITION USING COMSOL MULTIPHYSICS® PLATFORM

S. Lukman and M.S. Al-Suwaiyan[§]

Department of Civil and Environmental Engineering, King Fahd University of Petroleum & Minerals, Dhahran 31261, Saudi Arabia

ABSTRACT

Groundwater pollution from leaking underground storage tanks (USTs) is a wide spread environmental problem. Dissolved contaminant plumes that affect groundwater quality result from the slow dissolution of leaking organic products. The present study is intended to study and assess enhanced dissolution and accompanying contaminant plume evolution due to the existence of a light non-aqueous phase liquid (LNAPL) in saturated porous media under fluctuating water table conditions. A quantitative approach was developed that aids in the prediction of the transport of dissolved LNAPL in the saturated zone under water table fluctuation (WTF). WTF causes an increase in the dissolved phase concentration and residual LNAPL through an increase in the smear zone.

The effect of WTF is incorporated into the model by systematically varying the inflow and outflow boundary conditions using a sine function. The model makes use of several useful COMSOL Multiphysics 3.5 features such as: multiphysics coupling between fluid flow and transient solute transport analysis in addition to the ALE Moving Mesh application for static analysis. Presence of continuous LNAPL pool and discontinuous ganglia are considered for the advective-dispersive transport. Numerical simulations of the developed 2-D model were carried out using COMSOL Multiphysics® platform. Moving Mesh ALE determines the initial water table location, while the parameter function varies the water table position as the contaminant dissolution progresses.

[§] Corresponding Author: M.S. Al-Suwaiyan, KFUPM # 1979, Dhahran, Saudi Arabia, 31261, msaleh@kfupm.edu.sa

Simulations were performed under both constant and fluctuating water table conditions. The results revealed significant spreading in the longitudinal and vertical directions after 2 days. However, the longitudinal spreading and dissolved phase concentration were observed to be higher in the case where the water table fluctuates.

Dispersion plays a significant role in contaminant spreading, while ganglia entrapment due to water table fluctuation, promotes LNAPL mass loss through enhanced dissolution. An experimental investigation using a sand box physical model of is already under way to validate the proposed model.

In conclusion, adding a source dissolution term within the area of the water table fluctuation in COMSOL Multiphysics® predicts the behavior and transport of the contaminant plume in saturated porous media.

Keywords: Groundwater, pollution, water table fluctuation, COMSOL

1. INTRODUCTION

The quality of subsurface waters could be affected by naturally occurring processes as well as anthropogenic activities. Some of the general ways in which the composition of groundwater may be altered include natural processes, non-point agricultural and urban runoff, waste disposal practices, and hydrocarbon spills from storage sites or during transportation, leakage from waste disposal or underground storage tanks (UST) or from industrial facilities and other unintentional releases (Bedient *et al.*, 1999).

Light non-aqueous phase liquids (LNAPLs) are immiscible organic products which are lighter than and only slightly soluble in water, therefore forming a separate oily phase in the subsurface. LNAPL migration is affected by buoyancy, gravity and capillary forces. Due to the variation in the chemical composition of LNAPLs, they exhibit variable solubility and potential for volatilization.

Subsurface releases of crude oil, gasoline, jet fuels, diesel, heating oil and kerosene are frequently treated as LNAPL release (Bedient et al., 1999, USEPA, 1995). Upon release of LNAPL into the environment, migration occurs generally downward under the force of gravity and capillarity. As it moves through the unsaturated zone, a fraction of the organic mass will be retained as residual blobs or ganglia in the soil pores, thereby depleting the LNAPL mass until it is completely retained. If sufficient LNAPL is released, it will continue to migrate until it reaches near the water table. Once the capillary fringe is reached, it may remain on the water table as a pool or move laterally as a continuous free-phase (Bedient et al., 1999, USEPA, 1995). Along the vertical above the water table, the three fluids: water, LNAPL and

air, coexist at various proportions depending on the distance from the water table.

The vertical fluctuation of the water table affects the volume of residual and mobile LNAPL, increases the concentration of the dissolved phase components and enhances biodegradation (Dobson, 2007). Recharge, the uptake by vegetation and groundwater withdrawal, which vary over time, result in water table fluctuation (Zhang, 1998). In addition, variations may also occur for a short period of time due to changes in the surface water elevations in nearby water bodies such as lakes, tidal marine waters, and rivers (Williams and Oostrom, 2000).

A number of studies examining the effects of water table fluctuations on LNAPL dissolution, biodegradation, saturation and entrapment have been conducted. These studies range from laboratory scale (1-D, 2-D, 3-D) to field-scale investigations. The quantification of air and LNAPL entrapment under fluctuating water table conditions was first undertaken by Lenhard et al. (1993). From a numerical point of view, Reddi et al. (1998) predicted enhanced dissolution and biodegradation of LNAPL in systems subject to cyclic WTF. Marinelli and Durnford (1996) developed a semi-analytical model which predicts LNAPL thickness in monitoring wells considering the effects of saturation hysteresis and air/LNAPL entrapment under WTF. A field study by Lee et al. (2001) was carried out on a contaminated shallow aquifer which was subjected to an annual WTF exceeding 2 m in response to groundwater recharge/discharge events.

The main aim of this research is to model dissolved phase concentration under fluctuating water table conditions using the COMSOL Multiphysics® platform. COMSOL Multiphysics® (or simply COMSOL), which was formerly known as FEMLAB. COMSOL is a finite element analysis and solver software package for various physics and engineering applications, particularly coupled phenomena referred to as multiphysics (COMSOL, 2008). Main transport mechanisms considered are advection, dispersion and dissolution.

2. MATERIALS AND PROCEDURE

2.1 Model Development

The flow is driven by the total hydraulic head gradient, H, which can be written as:

$$H = H_P + y \qquad (1)$$

Where:
H_P = pressure head (L); y = elevation head (L).

The specific discharge is obtained using Darcy's law,

$$\boldsymbol{q} = -K\boldsymbol{\nabla}H \qquad (2)$$

A zero flux Neumann condition gives impermeable boundaries at AF, BC and DE.

$$K\boldsymbol{\nabla}H = 0 \qquad (3)$$

At the water table, the Neumann boundary condition is again used to model in the absence of any recharge, since *y* is still unknown and H_P is zero. Hence,

$$K\boldsymbol{\nabla}H = 0 \qquad (4)$$

The ALE Moving Mesh application determines *y* given that H_P is zero at the water table. The application starts with an arbitrary straight line water table geometry which deforms until the shape conforms to the zero pressure head contour (COMSOL, 2008).

Fig. 1 depicts the conditions for the solute transport. Because the aquifer is initially uncontaminated, initial concentrations equal zero. A contaminant with a relative concentration of 1.0 is applied over the interval G < x < H for the given duration. When the contaminant source is removed, the concentration along this segment is dropped to zero. Contaminant migration is modeled by advection and dispersion in the aquifer. The parameters associated with this problem are given later in Table 1.

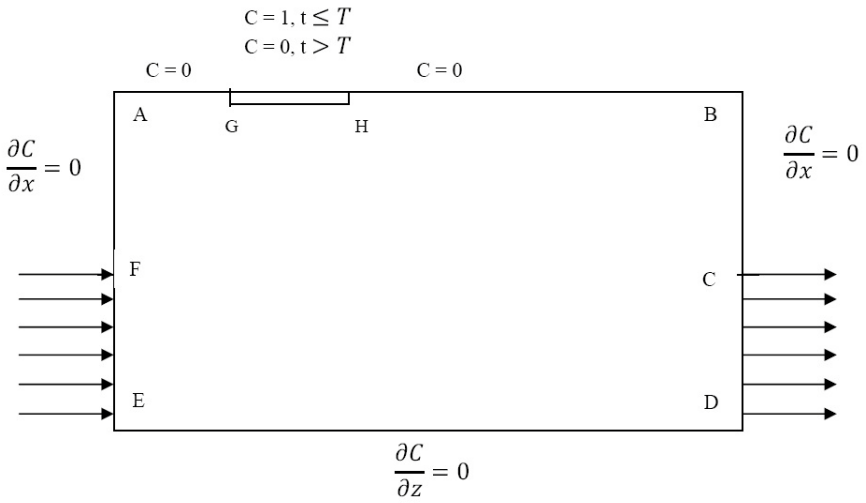

Figure 1. Solute transport domain, boundary and initial conditions.

Transient solute transport advection-dispersion equation which incorporates dissolution of ganglia as a source term derived by Bedient et al. (1999), Lesage and Brown (1994), and Sulaymon and Gzar (2011) is:

$$\frac{\partial(nC)}{\partial t} = \boldsymbol{\nabla}.(\theta \boldsymbol{D} \nabla C) - \boldsymbol{\nabla}.(\boldsymbol{q}C) + k(C_e - C) \qquad (5)$$

Where:

n = effective porosity;
θ = moisture content;
D = hydraulic dispersivity.

For boundary and initial conditions, the Neumann conditions are used at the water table where C(x, H, t) = 0, except for the segment between x = A and x = G, where, the solute flux is given by the Cauchy boundary condition which applies to the zero flux boundaries (AF, DE, BC).

$$-(\theta \boldsymbol{D} \nabla C) + (\boldsymbol{q}C) = 0 \qquad (6)$$

The initial condition specifies that the aquifer is originally pristine, i.e.

$$\mathrm{C}(x, y, 0) = 0 \qquad (7)$$

Since the solute concentration at face CD will generally be the calculated solute concentration along CD, it will be treated as a free mass outflow boundary.

2.1 Effect of Water Table Fluctuation

Effect of water table fluctuation is incorporated into the model by systematically varying the inflow and outflow boundary conditions. This is applicable to boundaries with constant hydraulic head or inflow rate. For instance, in the case of a constant hydraulic head, a sinusoidal function in terms of time may be formulated depending on the extent of the fluctuation.

$$\mathrm{f(t)} = a\ \mathrm{Sin}(\alpha t) \qquad (8)$$

Where:

a = amplitude of the sine wave; α = angle in radians; t = time parameter.

For the problem presented in Figs. 1 and 2, the inflow and outflow boundary conditions are replaced with a constant hydraulic head given by the new boundary condition:

$$\mathrm{H(x = E, y, t)} = \mathrm{H(x = E, y, 0)} + a\mathrm{Sin}(\alpha t) \qquad (9)$$

The parameter function was used to determine the water table position at different times, while a Moving Mesh (ALE) application was used to determine the initial water table position based on zero pressure head contour.

For every rise of fall of the water table, a smear zone entrapping the LNAPL ganglia is formed.

These ganglia serve as additional sources of contaminants and increase the interfacial area of contact between the LNAPL and the aqueous phase, thus enhancing dissolution. This extra dissolution flux resulting from the entrapment of ganglia due to fluctuating water table conditions may be modeled using the dissolution flux:

$$J_{dissolution} = k_L(C_e - C) \qquad (10)$$

Where $J_{dissolution}$ = mass transfer flux ($ML^{-2}T^{-1}$) between aqueous phase and LNAPL; C_e = effective equilibrium aqueous concentration of the constituent (ML^{-3}); C = average concentration dissolved in the aqueous phase at that location (ML^{-3}); k_L = 1st order rate coefficient of mass transfer between LNAPL-water interface (LT^{-1}).

Finally, experimental validation of the developed mathematical model results are underway using a 2-D aquifer model for the simulation of LNAPL contamination, and subsequent monitoring and measurement of the dissolved plume concentrations as it moves within the porous media. The solute transport domain described is based on the aquifer model depicted in Fig. 2.

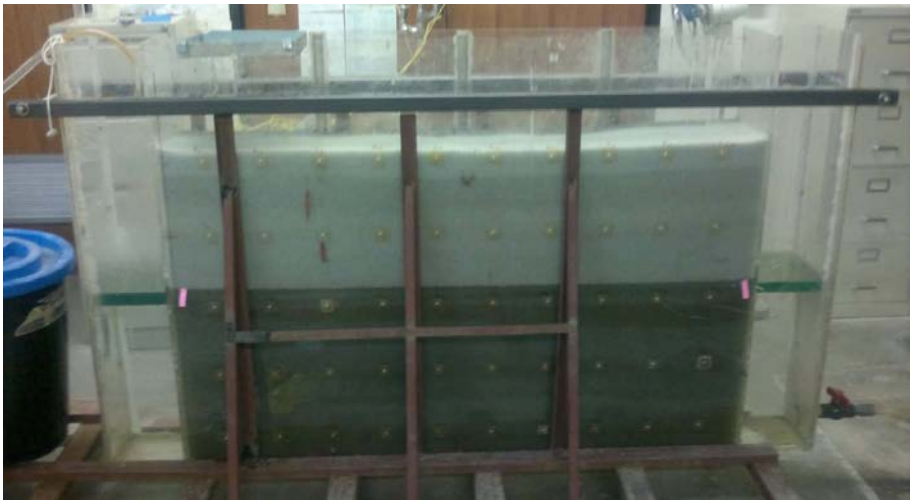

Figure 2. Physical model showing gasoline layers in inlet and outlet sumps.

3. RESULTS AND DISCUSSION

3.1 Input Parameters

This section will present and discuss the results obtained in the application of COMSOL to a case of steady-state fluid flow and transient solute transport whose physical domains and flow boundary conditions were presented earlier. The model input parameters for the simulation are given in Table 1. These values were either obtained from actual measurement or estimated for the model aquifer presented in Fig. 2.

Table 1. Model input parameters.

Parameter	Value
Mean particle size, d_e	$2.03\ mm$
Density, ρ	998.21 kg/m^3
Viscosity, μ	0.001 Pa.s
Water temperature	20 ^{0}C
Effective porosity, n	39 %
Hydraulic conductivity, K	$9x10^{-2}\ m/s$
Longitudinal dispersivity, α_L	0.4 m
Transverse dispersivity, α_v	$0.004\ m$
Relative concentration	1.0
Flow rate	1 mL/s
Specific discharge	1.54 m/d
Hydraulic gradient	6.25 x 10^{-3}
Tortuousity, τ	0.73
Effective molecular diffusion, D_e	$6.86\ x\ 10^{-10}\ m^2/s$

3.2 Constant and Fluctuating Water Table Numerical Simulations

In this case, a constant water table was initially considered and the flow field was computed, followed by solute transport simulation. The flow field in the physical setup shown in Fig. 2 was simulated according to the boundary conditions and initial conditions presented in Fig. 1. The simulation was carried out using the COMSOL Multiphysics' Earth Science Module for steady-state hydraulic analysis. The most important aspect of this stage is the establishment of the velocity field, which is a prerequisite for subsequent solute transport simulation. The streamlines due to the flow of water through the porous media just prior to initiation of the contaminant spill (i.e. t = 0) are shown in Fig. 3. The flow directions are also depicted in Figure 3. The results from the flow field simulation ,specifically, the velocity field, were stored, for subsequent use in the solute transport simulation.

The contaminant (with a relative concentration of 1.0) was applied to the water table at the rate of 2 L/min for 5 min over the interval 225 mm < x < 510 mm of the water table. Transient contaminant migration was modeled by advection and dispersion in the steady-state flow field over the course of 48 hours (2 days). The plume movement and contours for the first 1 hour and 48 hours after the spill under constant WT conditions are shown in Figs. 4 and 6. For the fluctuating WT scenario, the WT was initially raised above the original position, then lowered, and then raised up again beyond the initial position. Amplitude of 2 cm was imposed above and below the water table. Figures 5 and 7 provide an overview of the mean behavior of the contaminant plumes under WTF. Initially, the contaminant dissolved only slightly, but the concentration increased progressively with time. Significant plume spreading in the longitudinal and vertical directions and its accompanying dilution were observed. Regions of high concentration observed just upstream of the spill area (Fig. 4) were a consequence of both the initial plume shape and the vertically downward component of the mean velocity. Figs. 6 and 7 show how the vertical downward component of the mean velocity caused significant dilution in the vertical plane, while the horizontal velocity component caused the plume to migrate to the exit face. The velocity variations greatly affected the shapes of the plume trajectories. The first streamtube, which is located just below the water table (Fig. 3), was observed to have the maximum plume concentration throughout the duration of plume migration. Several interpolations were carried out (not reported here) at different solution times in order to obtain a clearer understanding of the plume movement and its trajectories. Barely 1 hr after the spill, the vertical spread of the plume was found to be about 20 cm and 50 cm for constant (Fig. 4) and fluctuating WT (Fig. 5) respectively. Within the next 48 hours the plume moved about 50 cm and 60 cm down in the vertical direction for constant (Fig. 6) and fluctuating WT (Fig. 7), respectively. About 1 hour after the spill, the plume traversed the entire length of the aquifer (160 cm) while the vertical plume displacement was not remarkable during this time. Conclusively, the longitudinal spreading was observed to be several orders of magnitude greater than vertical spreading.

During the water table rise (Fig. 5), a smear zone above the initial water table position was created within the porous media which entraps LNAPL blobs or ganglia. These ganglia increase the interfacial area between the aqueous phase and LNAPL, thereby enhancing dissolution and reducing the lifetime of the LNAPL due to increased rate of mass loss. Subsequently, aqueous phase concentration is spread within the porous media. When the water table descended below its original level, some of these entrapped ganglia might have been completely consumed by the dissolution.

During the downward movement, regions of non-zero aqueous phase concentrations were smaller than during the water table rise. As such, the rate of mass loss during water table rise was higher than during water table fall, since the mass loss is quantified using the aqueous phase concentration.

Significant spreading of the contaminant also occurs within the porous media due to the smear zone contribution (Fig. 7).

Comparing the constant and fluctuating conditions, it is evident that regions of high concentrations are higher under fluctuating water table conditions than under constant water table conditions, which certainly means that contaminant spreading was higher under the fluctuating condition.

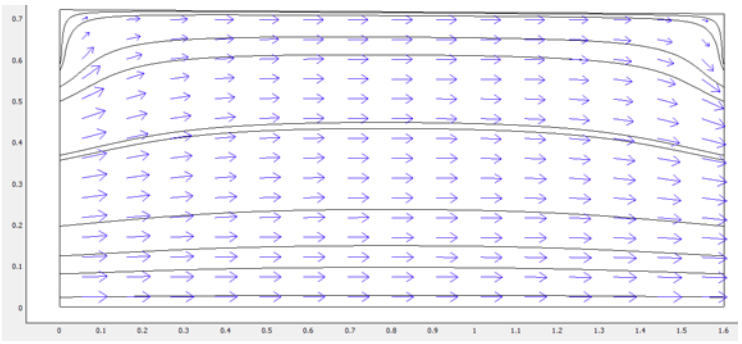

Figure 3. Streamline and flow direction of the velocity field at t = 0.

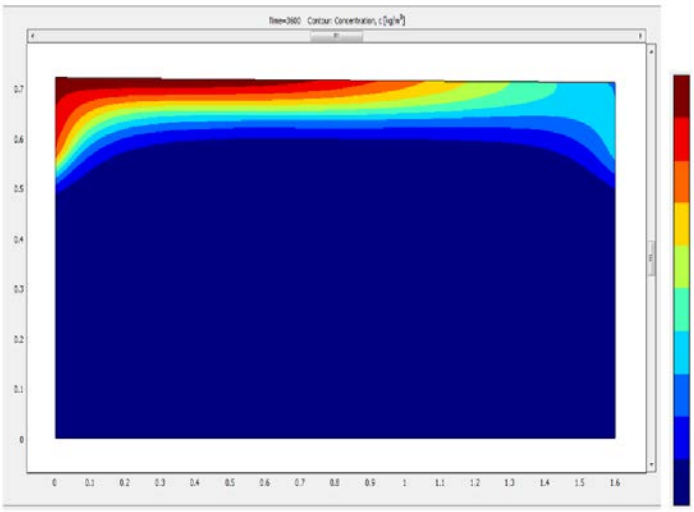

Figure 4. Plume concentration contours, 1 hour after contaminant spill (constant WT).

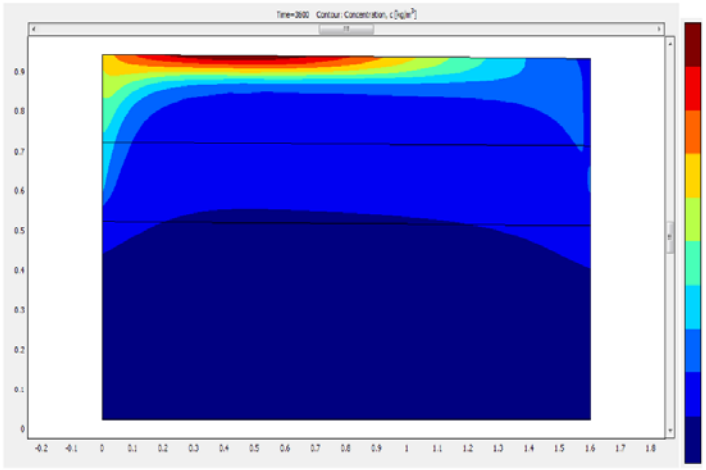

Figure 5. Plume concentration contours, 1 hour after contaminant spill (fluctuating WT).

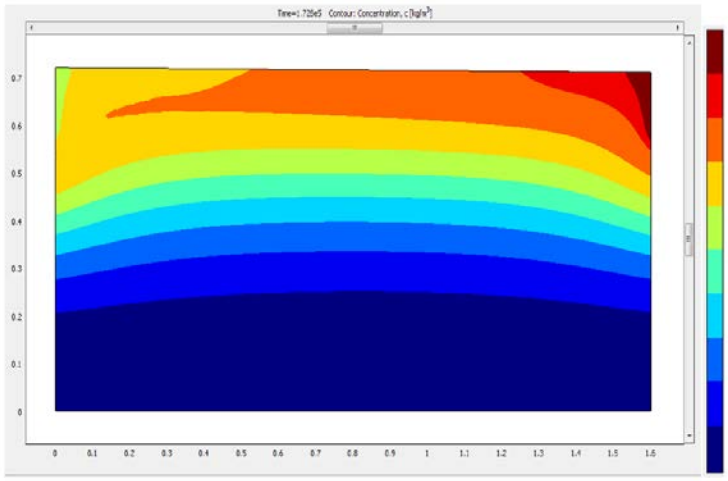

Figure 6. Plume movement and contours, 48 hours after contaminant spill (constant WT).

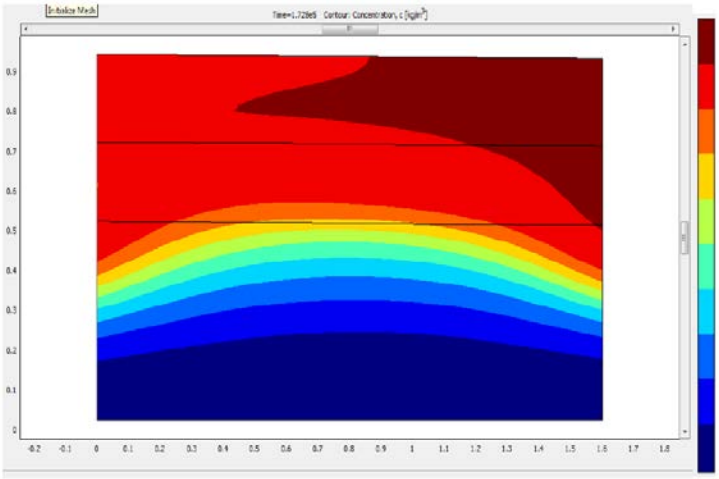

Figure 7. Plume movement and contours, 48 hours after contaminant spill (fluctuating WT).

4. SUMMARY AND CONCLUSION

A quantitative approach was developed for the prediction of the transport of dissolved LNAPL in the saturated zone under water table fluctuation (WTF). Presence of a continuous LNAPL pool and discontinuous ganglia were considered. The relevant domains, boundary and initial conditions were presented and discussed. It may be concluded that LNAPL-contaminated aquifers subjected to water table fluctuations may be expected to result in increased exposure of down-gradient receptors to dissolved LNAPL components. However, in the presence of suitable measures for the prevention of plume migration to receptors, fluctuations in the water table could be employed as an option for the reduction of remediation time of LNAPL-contaminated aquifers. Advection and dispersion play a significant role in contaminant spreading, while ganglia entrapment promotes LNAPL mass loss through enhanced dissolution.

Acknowledgement

The support provided by the Civil and Environmental Engineering Department at King Fahd University of Petroleum and Minerals is highly appreciated.

6. REFERENCES

Bedient P.B., Rifai H.S., and Newell C.J. 1999. Ground Water Contamination: Transport and Remediation. 2. Prentice Hall, Inc.

COMSOL Multiphysics. 2008. Documentation: Aquifer water table calculation. Stockholm: COMSOL AB. Version 3.5a

Dobson R., Schroth M.H., and Zeyer J. 2007. Effect of water-table fluctuation on dissolution and biodegradation of a multi-component, light nonaqueous-phase liquid. J. Cont. Hydro. 94, 235–248.

Lee, C.H., Lee, J.Y., Cheon, J.Y., and Lee, K.K. 2001. Attentuation of petroleum hydrocarbons in smear zones: a case study. J. Env. Eng. 127(7), 639–647.

Lenhard, R.J., T.G. Johnson and J.C. Parker. 1993. Experimental observations of nonaqueous-phase liquid subsurface movement. J. Contam. Hydro. 12, 79-101.

Lesage S. and Brown S. 1994. Observation of the dissolution of NAPL mixtures. J. Contam. Hydrol. 15, 57-71.

Marinelli, F. and Durnford, D.S. 1996. LNAPL thickness in monitoring wells considering hysteresis and entrapment. ground water. 34(3), 405 – 414.

Reddi, L.N. 1998. Mass loss from LNAPL pools under fluctuating water table conditions. J. Env. Eng. 124(12), 1171–1177.

Sulaymon A.H., and Gzar H.A. 2011. Experimental investigation and numerical modeling of light nonaqueous phase liquid dissolution and transport in a saturated zone of the soil. J. Hazard. Mat. 186, 1601–1614.

USEPA (U.S. Environmental Protection Agency). 1995. Light Nonaqueous Phase Liquids. Office of solid waste and emergency response, Washington, DC. EPA/540/S-95/500.

Williams, M.D., Oostrom, M. 2000. Oxygenation of anoxic water in a fluctuating water table system: An experimental and numerical study. J. Hydro. 230, 70–85.

Zhang, M.H., Geng, S., and Ustin, S.L. 1998. Quantifying the agricultural landscape and assessing

Chapter 10

SIMULATION MODELING OF ARSENIC DYNAMICS & REMOVAL IN CONTAMINATED GROUNDWATER

Michael Miyittah [1§], James Jones [2], Samuel Adiku [3], Dean Rhue [4], Craig Stanley [1] and Jack Rechcigl [1]

[1]Gulf Coast Research and Education Center, University of Florida, USA, [#]Department of Environmental Sciences, University of Cape Coast, Ghana, [2]Department of Agriculture & Biological Engineering, University of Florida, USA, [3]Department of Soil Science, University of Ghana, Legon, Ghana, [4]Soil & Water Science Department, University of Florida, USA

Abstract

Groundwater containing arsenic(V) (As(V)) from a contaminated site was used in this experiment. The study simulated As(V) dynamics under a control system of pH <5.0, aided by sorption mechanism in flow calorimetry. The control system is needed to understand the nature and behavior of As(V) dynamics and the removal process. Flow calorimetry provided numerical energetics of As(V) sorption reactions occurring at surfaces on amorphous aluminum oxide (Al-Ox) at point of zero charge (PZC) ~5.6. The study models and simulates As(V) dynamics for sorption onto aluminum oxide under uniform flow rates. A simple mathematical model is presented, and was used to describe the distribution and dynamics of As(V*)* given the initial concentration of As(V) in solution, the sorption capacity of the sorbent, as well as the reaction rates. A numerical technique was used for the simulation. The model simulation results showed As(V) variations with time as the groundwater moves through segmented cells within the sorbent. Results showed that the sorbent final time of exhaustion can be estimated within the confinement parameters of the sorbent. A sensitivity analysis (SA) was conducted on parameters of sorption capacity and on rate of sorption

§ Corresponding Author: Michael Miyittah, University of Cape Coast, Department of Environmental Science, Cape Coast, Ghana, Tel: 233-240336050, Email: m-miyittah@ucc.edu.gh

using Monte Carlo methods. The SA showed rate of sorption to be more influential on As(V) removal than on sorption capacity. The model provides information useful to researchers in comparing the behavior of different sorbing materials under similar or different conditions for arsenic contaminated groundwater treatment and management.

Keywords: simulation modeling, adsorption, As(V), contamination, groundwater and flow calorimetry.

1. INTRODUCTION

Arsenic(V) (As(V)) contamination has been an issue in groundwater pollution and can pose threats to human and ecological health. To attenuate the transport of As(V) through environmental media, several chemical adsorbents containing Fe, Al, and Ca, and ion-exchange adsorbents have been investigated (Kabengi et al., 2006; Miyittah et al., 2011; Awual et al., 2013). However, the transport mechanisms of As(V) and removal may be better understood if the process is simulated. Simulation modeling provides opportunities to explore scenarios which decision makers may use as advisories regarding the degree of the concentration.

Flow calorimeter is a continuous flow process where contaminant-adsorbent reactions can be tracked with time. It consists of a column containing adsorbent that is placed inside a water bath providing stability against temperature changes. Within the column are two thermistors that sense changes due to reactions in the solution. A change in solution temperature produces a differential output voltage that feeds into an instrumentation amplifier and the amplified signal is transmitted into a computer for processing (Rhue et al., 2002; Kabengi et al., 2006).

The above process between a reactant-adsorbent interface may depict As(V)-adsorbent behavior for the groundwater reaction with Al-oxide. The As(V)-adsorption reactions may be tracked to ascertain the efficiency of an adsorbent in removing the contaminant, or the time remaining for the contaminant to be totally removed. The As(V) transport through Al-oxide may be simulated if certain parameters of the process such as concentration of As(V), flow rate of contaminant, adsorbent properties such as sorption capacity and hydraulic behavior of the adsorbent are known. To our knowledge there is no simulation modeling depicting As(V) reactions with adsorbent through the aid of flow calorimetry. The objectives of this study were: 1) to formulate a simple mathematical model that simulates As(V) transport through Al-oxide under a control condition in order to evaluate the dynamics and estimate complete

removal; 2) to evaluate the duration of complete saturation of the adsorbent; and 3) to determine the sensitivity parameters influencing the sorption process.

2. MATERIALS AND METHODS

2.1 Instrumentation

The experimental set up and description of flow calorimetry is given in detail in Rhue et al., 2002; and Harvey and Rhue, 2006. Briefly, contaminated groundwater containing As(V) is allowed to pass through a column adsorbent of Al-oxide. The experiments were carried out using about 100 mg of Al-oxide powder packed into a micro-column. The micro-column is positioned between two thermistors, with inlet thermistor acting as a reference; together the two thermistors detect changes in temperature. Solutions containing As(V) were allowed to pass through the packed column at flow rates between 0.35 and 0.40 $mLmin^{-1}$. Any heat of reaction due to physical or chemical interactions between the reacting fluid and the Al-oxide in the column was sensed as a differential voltage from the differences in the thermistors' signals. The differential voltage is then displayed graphically through amplification to a computer and recorded as a function of time. At the end of the reaction, an area under or above a baseline producing either a positive or negative curve is generated depending on the nature of the reacting solution (Kabengi et al., 2006; Harvey and Rhue, 2008).

2.1.1 Model Development

A simple mathematical model in the form of a differential equation was developed and numerically simulated in Microsoft Excel. In the formulation, it was assumed that the column is subdivided into ten segmented cells (C1 to C10) to enhance the computation.

$$\frac{dC_{i,t}}{dt} = \frac{F}{H_w A \Delta_x}\left[C_{i-1,t-1} - C_{i,t-1}\right] - \left[1 - \frac{B_{i,t-1}}{B_{\max}}\right]\left[C_{i,,t-1} r\right] \qquad \textit{E qn .1.}$$

Where, $_{i=1}$; C_{i-1} = input concentration with time (mM); $B_{i,t-1}$ = sorption with time; F = flow rate ($mLmin^{-1}$); H_w = hydraulic property of adsorbent; A = area of the

column (cm^2); Δx = total distance per column cell (cm); r = rate of sorption (min^{-1}) and B_{max} = sorption capacity of adsorbent (gkg^{-1}).

3. RESULTS AND DISCUSSION

Figures 1 and Figure 2 show As(V) sorption onto Al-oxide with time. Figure 1 shows simulated As(V) moving through segmented cells of the column when specific parameters of the model are provided. For instance, given that the flow rate is 0.36 $mLmin^{-1}$, initial As(V) concentration = 0.5mM, sorption capacity of adsorbent = 2 gkg^{-1}, mass of Al-oxide = 100 mg, rate (r) of sorption = 5 min, delta-T, = 0.025 min, volume of the column = 0.4 cm^3, pH(solution) = 4.8, PZC(Al-oxide) = 5.6, and hydraulic property of adsorbent = 0.5, yield Figure 1 and Figure 2. The graph in Figure 1 indicates the duration for As(V) to reach maximum sorption through each cell. The graph shows that for a continuous flow system of As(V) passing through an adsorbent, each cell reaches a maximum sorption at 2 mg As $cell^{-1}$. Also, at about 140 minutes, maximum sorption would have occurred in the tenth segmented cell leading to a breakthrough. The basic idea of As(V) sorption is that as As(V) is transported through the segmented cells, portions of the concentration are adsorbed within each compartment. The remaining concentration of As(V) moves as output to the next cell. In other words, the output of the first cell becomes the input of the second cell. The repeating scenario goes on until the As(V) solution reaches the final compartment. The simulation suggests that the model may be used to describe the extent of the adsorption process with time when specific parameters are known.

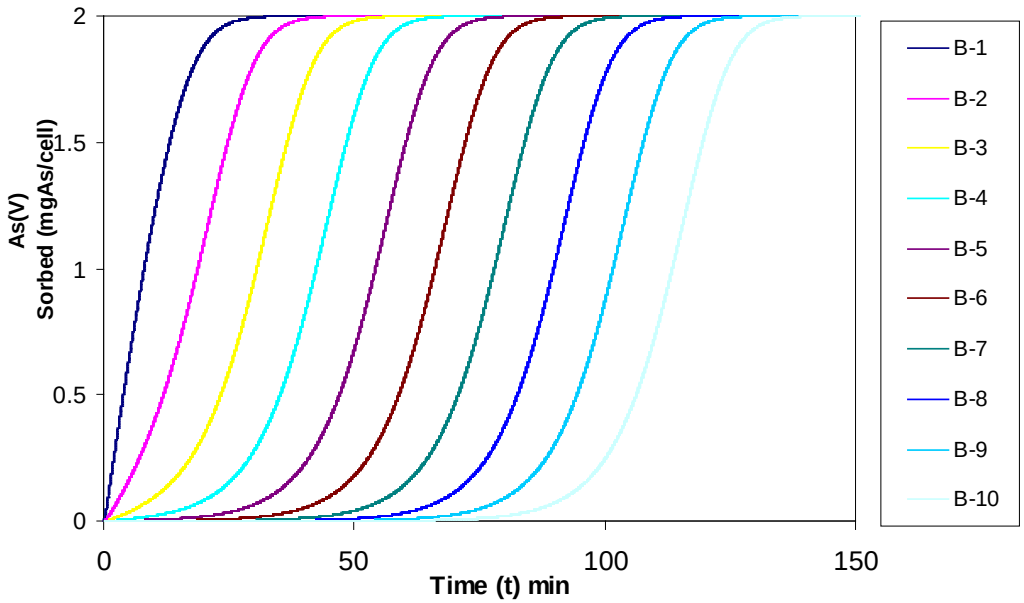

Figure 1. Arsenic(V) sorption through segmented cells one through ten, with each cell reaching maximum capacity at B-1 through B-10

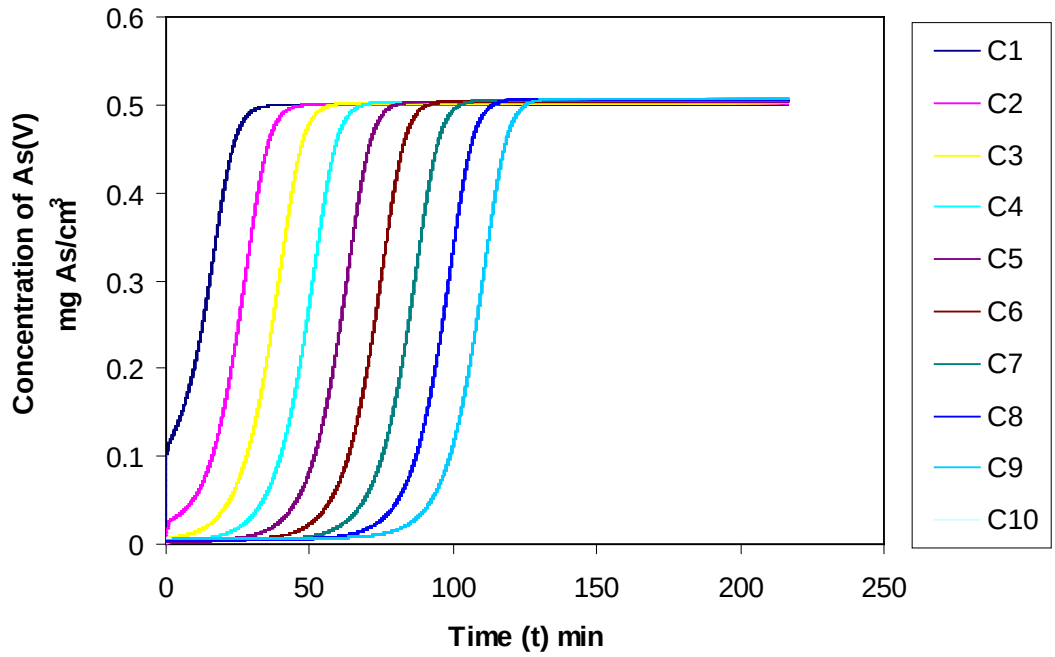

Figure 2. Changes in concentration of Arsenic(V) through segmented cells of the column. The change in concentration is depicted through C1 to C10.

In Figure 2, changes in concentration of Arsenic(V) through segmented cells of the column are demonstrated. The change in concentration is depicted through C1 to C10. At time zero, ~0.1 mg As cm^{-3} was instantly adsorbed. The instant adsorption might be attributable to diffusion and due to the different interface of wetting fronts of a liquid meeting a porous solid material. Afterwards, instant concentration uptake for subsequent cell C2 decreases and reaches zero, thereby allowing the immediate cell to have a smooth flow as the wetting front is eliminated within the column without further resistance. The simulation, therefore, shows that the time for complete breakthrough can be estimated with the aid of the model as concentration of As(V) decreases with time. The application is designed so that whenever a contaminant such as As(V) is moving through an environmental medium such as soil or water and the parameters above are known, it is possible to predict behavior and the dynamics of the contaminant. The predictions may not exactly reflect field conditions, but may be of help to serve as guidance in contaminant transport assessment and management.

3.1 Sensitivity Analysis

A sensitivity analysis is the process of evaluating the impacts of the model input parameters with regards to changes on the simulation model results. A global sensitivity analysis (Monte Carlo) was used with the aid of random variables and probabilities in determining the parameters of significant influence. The simulation utilizes pseudo numbers generated in Excel function = RAND().

Parametric data for r (sorption rate) and B_{max} (sorption capacity of adsorbent) were simulated (data not shown). The result suggests that the parameter r is more sensitive than B_{max}. The implication is that parameter r should have more attention during the As(V) sorption reaction. The practical implication is that kinetic reactions are one of the most important processes controlling sorption due to their dynamic nature as revealed in the simulation model.

4. CONCLUSION

The findings show that a simple simulation model may be of help in depicting sorption of As(V) through environmental media. Flow calorimetry data provided the initial baseline study on the nature of sorption of As(V) through Al-oxide. The input data were used to formulate the model equation. Results from the simulation model show that breakthrough time and extent of sorption dynamics can be evaluated with the aid of simulation model within the limits of the

parameters of the model. However, further work is needed using field experimental data, as this work is based mainly on laboratory data. Also, parameters of the model should be estimated and verified with experimental data. Furthermore, the model may also provide useful information to researchers in comparing the behavior of different sorbing materials under similar or different conditions for contaminant removal process and estimation.

5. REFERENCES

Awual, M.R., Hossain, M.A., Shenashen, M.A. Yaita, T., Suzuki, S., and Jyo, A. 2013. Evaluating of arsenic(V) removal from water by weak-base anion exchange adsorbents. Environ. Sci. Pollut. Res. 20, 421-430.

Harvey, O.R., and Rhue, R.D. 2008. Kinetics and energetics of phosphate sorption in a multi-component Al(III)-Fe(III) hydr(oxide) sorbent system. J. Colloid Interface Sci. 322, 384-393.

Kabengi, N. J., Daroub S. H. and Rhue, R.D. 2006. Energetics of arsenate sorption on amorphous aluminum hydroxides studied using flow adsorption calorimetry. J. Colloid Interface Sci. 297, 86-94.

Miyittah, M.K., Stanley, C.D., Mackowiak, C., Rhue, R.D., and Rechcigl, J.E. 2011. Developing a remediation strategy for phosphorus immobilization: Effect of Co-blending, Al-residual and Ca-Mg amendments in a manure-impacted spodosol. Soil and Sediment Contamination: An Inter. J. 20, 337-352.

Rhue, R.D., Appel, C., and Kabengi, N. 2002. Measuring surface chemical properties of soil using flow calorimetry. Soil Sci. 167, 782-790.

Chapter 11

BIODEGRADATION KINETICS OF PETROLEUM DERIVATIVES IN WASTEWATER THROUGH RESPIROMETRY DATA MODELING

Renato N. Montagnolli[§], Paulo Renato M. Lopes, Ivo S. Tamada, Jaqueline M. Cruz, Mariana L. Sousa, and Ederio D. Bidoia
São Paulo State University, Avenida 24 A, 1515, Rio Claro, SP, Brazil, 13506-900.

ABSTRACT

Petrochemical industry residual contamination by oil and its derivatives damages terrestrial and aquatic ecosystems. Bioremediation technologies are used to remove pollutants from the environment in a safe, economical and harmless way during the treatment of waste, especially with the use of techniques such as biodegradation. Water samples contaminated with a wide variety of petroleum derivatives were studied to evaluate the biodegradability of different types of oils. The objective of this study was to apply a respirometric technique as a biodegradation process monitor, and then use the data to construct mathematical models to characterize and determinate how different types of oils are capable of affecting biodegradation kinetics parameters. The kinetics were evaluated through selected models with a reasonable fit to experimental data. The Bartha and Pramer respirometer was used as a method to accurately measure CO_2 formation in the organic compounds during degradation by microorganisms. Differences in the biodegradation efficiency were compared within different groups of oils using mathematical models fitting the data for the kinetics of biodegradation. Used lubricant automotive oils are more susceptible to the biodegradation process, yielding 509.1 mg of CO_2 after 147 biodegradation days, since their molecular structures have already been altered after use. Gasoline also presented high CO_2 values after undergoing biodegradation processes, producing 371.7 mg of CO_2 in the same time period.

[§]Corresponding Author: Renato Nallin Montagnolli, São Paulo State University, Avenida 24 A, 1515, Rio Claro, SP, Brazil, 13506-900, 55(19)3526-4100, renatonm3@gmail.com

Phenol compounds and crude petroleum samples were less susceptible to biodegradation by microbiota, producing 180.7 and 119.2 mg of CO_2, respectively. The models fitted to data in each of these assays demonstrated different biodegradation rate profiles accurately describing their environmental behavior over time. Highest predicted rates of biodegradation and total CO_2 production are to be expected in automotive lubricant oils rather than any other petroleum derivative.

Keywords: bioremediation, biodegradation, kinetic, respirometer

1. INTRODUCTION

Worldwide transportation and consumption of petroleum products cause hydrocarbon releases into the environment. Such releases can occur in smaller amounts by improper disposal or leakage in storage systems, or large-scale accidental spills by tankers, oil platforms and pipelines. Demand for oil has increased steadily since the beginning of oil exploration in the nineteenth century oil and its derivatives has received an increasing demand due to its rapid acceptance as an energy source. This increases the quantity and circulation of petroleum compounds in the environment (Pala *et al*., 2006). Oil is a viscous liquid that contains thousands of compounds formed mainly from carbon and hydrogen. World oil production is now over 3 billion tons a year, and half that amount is transported by sea. It is estimated that over 2 million tons are lost annually by handling accidents with petroleum (Readman *et al*., 1992), and so, the presence of hydrocarbons in the environment can lead to serious environmental problems (Okoh and Trejo, 2006).

Mechanical removal of hydrocarbons from the environment is expensive, slow and inefficient (Mandri and Lin, 2007). Bioremediation is an alternative to total removal of hydrocarbons from polluted environments. Biotechnology processes using microorganisms for bioremediation are a growing field of study, given the potential for solving environmental problems caused by these contaminants. Biodegradation in aquatic environments is well studied due to its potential application in accidents involving oil disposal directly in the environment, mainly because oil's final destination is almost always water bodies. Petroleum environmental fate and handling is an important subject. Biodegradation has been extensively investigated in many studies in coastal areas (Readman *et al*., 1996), estuarine sediments (Oudot *et al*, 1998) and even marine conditions in the Arctic (Garret *et al*., 2003). Biodegradation has long been one of the main fields of research in microbiology, which includes biodegradation of organic and inorganic

substances. Microorganisms can be great tools for pollutant degradation in soil, water and sedimentt due to its numerous advantages over other processes in processing and degradating substances (Nano *et al*, 2003; Morelli *et al*. 2005; Demnerova *et al*., 2005). Thus, potential bioremediation microorganisms must be screened and evaluated when applied to oil contaminated water restoration.

Large catastrophic accidents involving oil tankers have attracted public attention to the fate of petroleum hydrocarbon in marine environments. In response to this concern, research on petroleum hydrocarbon biodegradation in natural environments has been enhanced. The studies by Atlas and Bartha (1992) and Bragg *et al*. (1994) showed that concentrations of available nitrogen and phosphorus in sea water are factors that influence the growth of hydrocarbon degrading microorganisms. Thus, the addition of these elements stimulates biodegradation of petroleum (Caineau *et al*., 2005). Biodegradation processes occur differently in different petroleum products the cleaning of environments by using bioremediation processes should also exploit microorganisms by understanding how the process occurs in different petroleum products (Van Hamme *et al*., 2003). Some studies have examined the effect of temperature, salinity and nutrients on the kinetics of different oil biodegradation (Atlas, 1981). There are also reports about the biodegradation of specific petroleum constituents, such as polycyclic aromatic hydrocarbons, (PAHs) (Li *et al*. 2008), sulfur compounds and nitrogen (Benedik *et al*., 1998) and anaerobic metabolism of hydrocarbons (Frazer *et al*., 1996). Hence, data regarding biodegradation kinetics of different substances are important for managing the behavior of these substances on the environment.

Feasibility studies are a prerequisite for any planned strategy in bioremediation contaminated environments in order to identify limitations towards biodegradation and to predict remediation performance and thereby rule out technologies that may be inappropriate for the clean-up of the substances of concern. Additionally, the environmental behavior and chemical-physical properties of oils are the basis for new fluid developments and for ecological treatment strategies.

The present study evaluated biodegradation of different petroleum products in a simulated environment, allowing comparison of various data on CO_2 production. The isolation, characterization and profiling of petrol derived oils biodegradation capacity studies are important when deciding the correct bioremediation strategy.

2. MATERIAL AND METHODS

2.1. Biodegradation Respirometry

This study used the respirometric method of Bartha and Pramer (1965) to determine CO_2 concentrations in the micro-atmosphere created inside a respirometer flask. Respirometry allows for weekly monitoring of CO_2 production. The CO_2 produced during microbial respiration processes can be neutralized in a KOH solution located in a side arm connected to the respirometric flask. The absorbed CO_2 amount was analyzed by titration.

Microorganisms capable of biodegradation used in the respirometric assays were pre-selected by a soil contamination simulation though a plastic bag filled with 3 kg of soil, 100 mL of distilled water and 50 mL of a mixture containing equal parts crude oil and petroleum derivatives. The container was then filled with small holes of approximately 1 mm diameter, spaced at one inch each. This interface allowed microbial exchange between outer and inner soil media. Such inoculum preparation followed a L6.350 CETESB (1990) technical standard with some adaptations. After 15 days, it was considered that there was a microbial pool adapted to oil degradation. The soil was then immersed in 1500 mL of water, thus defining the "base aqueous media" to be used in all biodegradation assays.

Afterwards, biodegradation assays were carried out in Bartha and Pramer (1965) respirometric flasks (Figure 1). The respirometer consists of a fully enclosed system with two connected chambers: a major chamber where biodegradation takes place in whichever analyzed effluent (Figure 1, indicated by G), and another chamber where an alkaline solution is placed to neutralize CO_2 produced by microbial respiration (Figure 1, indicated by D).

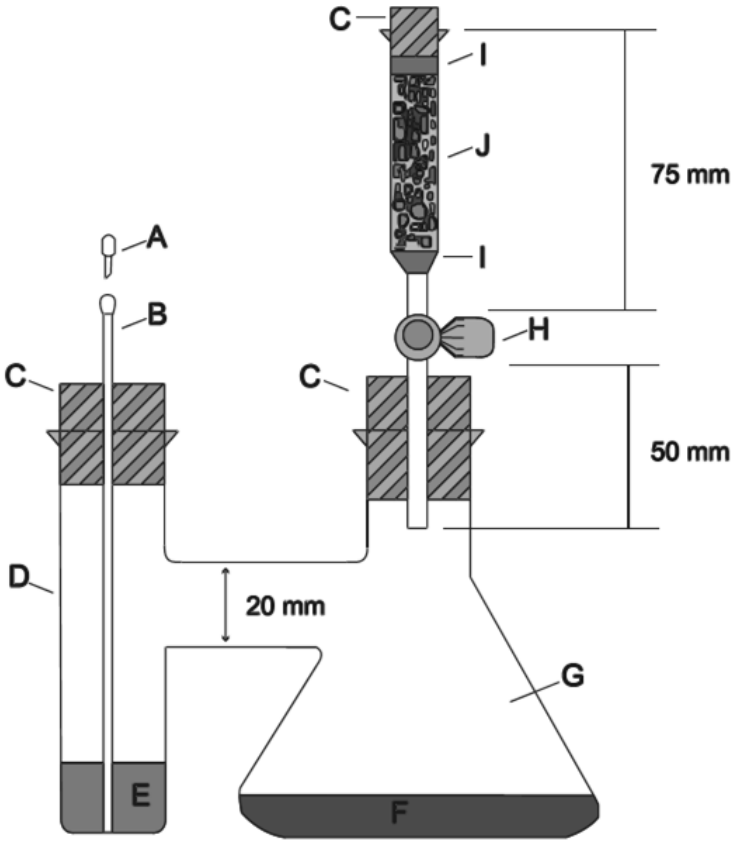

Figure 1. Bartha and Pramer respirometer. A: Cannula cap, B: Cannula (diameter 1-2 mm), C: Rubber cork., D: Lateral arm (diameter 40 mm, height 100 mm), E: KOH solution, F: Medium with aqueous analyte, G: Erlenmeyer flask (250 mL), H: Valve, I: Support (glass, wool or cotton), J: Air filter (diameter 15 mm, height 40 mm).

Respirometry applied to bioremediation studies offers several advantages for obtaining data on CO_2 production that would be otherwise difficult to obtain by other means (Graves *et al*., 1991). This study used a methodology adapted for aqueous medium respirometry (Montagnolli *et al*., 2009) that made it possible to obtain information about a simulated wastewater environment polluted by the following substances: petroleum, automotive lubricant oils, diesel, gasoline, kerosene and phenol. For a bioremediation study, it is necessary to measure biodegradation over time (Wu *et al*., 2004) involving different stages of adaptation, degradation and termination of the biodegrading microbiota. Such data can be immediately related to biodegradation rate and biomass changes over time (Fiuza *et al*., 2004).

Bartha and Pramer (1965) respirometry monitors CO_2 evolution rate through a simple analytical chemistry process. Carbon dioxide evolved during metabolism

is captured in a potassium hydroxide (KOH) solution located on the side arm connected to the respirometric chamber. The CO_2 amount is then neutralized and analyzed by titration of residual KOH with a standard solution of hydrochloric acid (HCl), after the addition of barium chloride ($BaCl_2$) to precipitate carbonate ions. Levels of carbon dioxide produced are then calculated and plotted as a function of incubation time (Balba *et al*., 1998).

2.2. Data Modeling

The whole process of kinetics was modeled according to biodegradation rate. Thus, by measuring CO_2 production, it was possible to plot the biodegradation profile of both diesel and biodiesel.

Carbon dioxide data from respirometry were applied to mathematical models that best described the biodegradation process. Parameterizing models with data allows a better understanding of biodegradation kinetics, thus allowing to predict and optimize the process (Kernanshani *et al*., 2006). Mathematical and statistical tools are effective ways to describe parameters involved pollutants removal during biodegradation (Pala *et al*., 2006). The proposal of different models of biodegradation for each type of substance biodegraded allowed determining how the biodegradation profiles may vary for each substance during biodegradation.

The proposed data-fitted model for CO_2 production was an adapted logistic equation by Schmidt *et al*. (1985) initially used by the author to describe microbial growth in culture media (Equation 1). This equation was tested to provide a prediction of maximum production of CO_2 by microorganisms in biodegradation process. Regarding weekly respirometry curves, another model was adjusted to better describe changes in biodegradation rate over time. This plot presents a more complex profile and thus required a greater number of modeling parameters. The model proposed by Membre *et al*. (1996) for growth and death of microbial communities (Equation 2) was chosen and adapted to the following biodegradation parameters:

$$B = Bmax / (1 + [(Bmax - Bo) / Bo] e^{(-rt)}) \quad \text{Equation (1)}$$

$$B=[((1/K1) * e^{(-m1r)})+((1/K2) e^{m2t})] ^ (-1) \quad \text{Equation (2)}$$

Where: B = CO_2 produced; Bmax = maximum CO_2 production; Bo = initial CO_2 production; r = maximum production rate specified for a particular oil; K1 = production increase constant; K2 = production decrease constant; m1 = rate of Increase in CO_2 production; m2 = rate of decrease in CO_2 production, t = time.

Both models were created to describe microbial growth and assumed a correlation between the microbial population dynamics and CO_2 production, successfully applied to the data set obtained by respirometry.

3. RESULTS

Biodegradation kinetics obtained from respirometers containing each petroleum derivative were evaluated through weekly and total accumulated CO_2 production models.

3.1 CO_2 Production Rate

Each substance presented a distinct biodegradation profile (Figure 2). The models fitted to data in each of these assays demonstrated different biodegradation rate profiles, describing their environmental behavior along time. Figure 2 shows the adjustment of experimental data from weekly CO_2 production with the adjusted fit (Membre *et al*, 1996).

In most cases, respirometric assays reached a maximum of CO_2 production followed by a decline in the production. It was then possible to predict the kinetic behavior expected for each type of oil within their respective rates of CO_2 production per week during the biodegradation process. The maximum rate of biodegradation (BRmax) corresponds to the curve peak in Figure 2. The model precisely calculates maximum CO_2 production time by each substance (BRmaxT). In Figure 2, the time axis has been extended to 400 days, which is greater than the 180 day interval when data was collected from respirometers. We used this kinetic model to predict CO_2 production values from up to 400 days of biodegradation in a set environment.

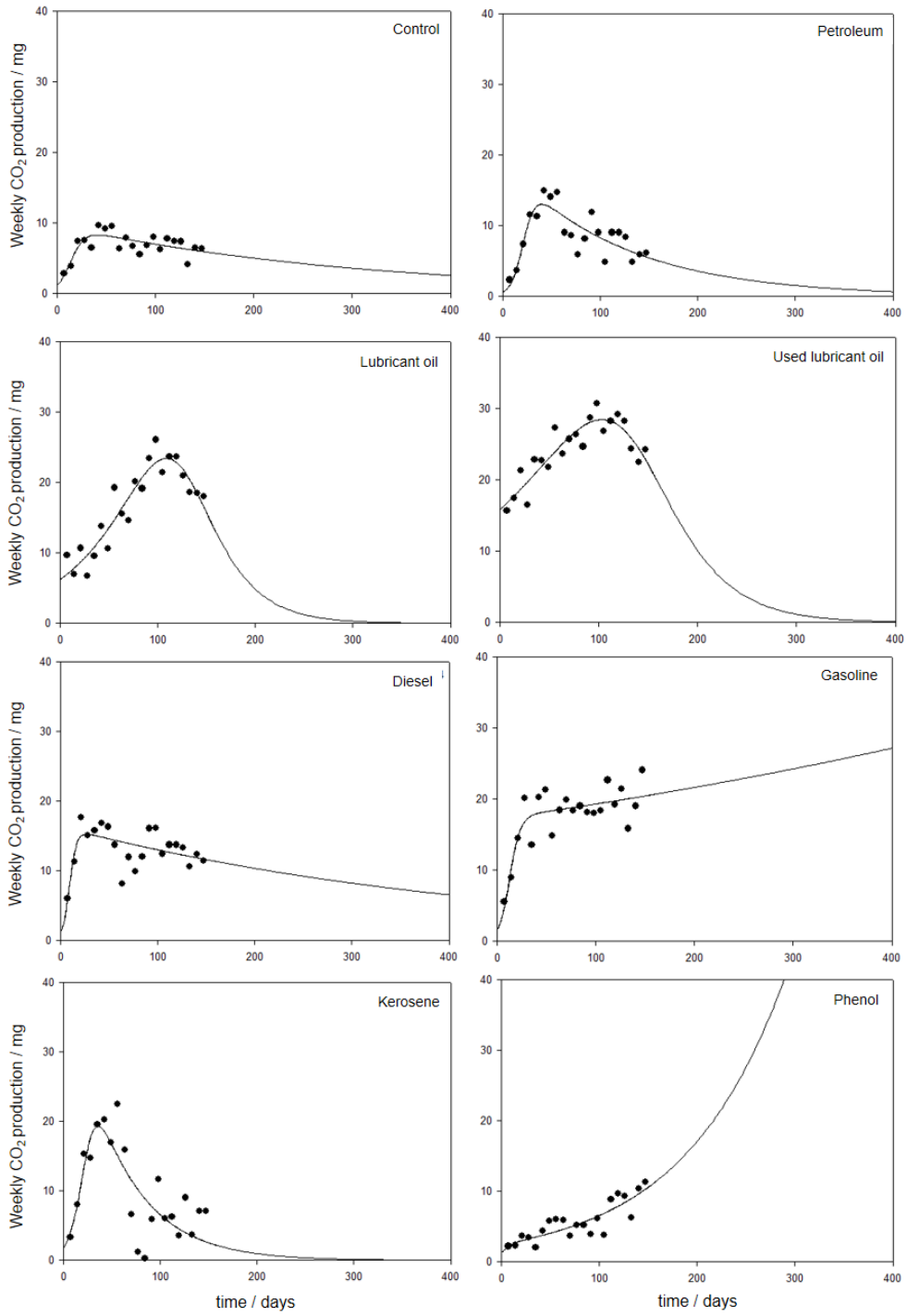

Figure 2. Weekly CO_2 production adjusted curve in petroleum derivatives.

Whereas the mathematical adjustment showed higher values in correlation ($R^2 > 0.8$), it was possible to determine an estimated cease time to biodegradation (BRminT) considering the time that weekly production of CO_2 reach very low values.

As expected, control assays had very low weekly CO_2 production (8.1 mg CO2 average) compared to other assays, except for phenol assays. Control assays only had "base liquid media" as substrate, and there was no further carbon source from petroleum hydrocarbon provided in the medium. However, the least CO_2 producing were phenol assays, which yielded the lowest CO_2 production levels. Their average CO_2 production weekly rate was 5.2 ± 0.8 mg of CO_2. This occurred due to a lower concentration of carbon substrate from phenol (100 mg/L^{-1}), as well as metabolizing difficulties of phenol by microorganisms. An increase in weekly production of CO_2 from phenol occurred only after 120 days. Lower biodegradation in phenol assays may be related to toxic effects.

Certain compounds, such as diesel oil, presented a continuous CO_2 production profile sustaining a mean 17.8 ± 3.8 mg of CO2 throughout the entire process, with a reduced decreasing trend after 60 days. Assays containing kerosene,had a very high initial CO_2 production, peaking at 27.5 ± 2.3 mg. However, an increased biodegradation rate did not remain constant throughout the course of experimentation. After 40 days, the weekly production of CO_2 decreased and ceased soon afterwards.

Modeling was considered unsuitable for gasoline and phenol, as they do not present a coherent adjustment. The mismatch occurs because there is no decline in CO_2 production over time. According to the model, the production of CO_2 is continuous and grows indefinitely in these cases. This statement is not coherent, since it would require an infinite amount of organic matter in respirometers for that to happen. The incorrect fit is because points do not indicate any decreasing trend of CO_2 production after 180 days. Thus, the model is not valid to accurately describe long term kinetics in these substances. However, other assays fitted satisfactorily as modeling parameters of interest. Among all trials that occurred in the adjustments to the model, only diesel oil showed correlation coefficients R^2 slightly lower than 0.75.

3.2 Accumulated CO_2 Production

The accumulated sum of CO_2 produced in each respirometric flask throughout the biodegradation process is presented in Figure 3. Figure 3 shows the adjustment of accumulated CO_2 production via the Schmidt *et al*. (1985) model. The most important parameters are the Expected Maximum Biodegradation (Bmax) and Time of Total Biodegradation (BmaxT). It is possible to predict the

maximum amount of CO_2 that would be produced from each substance biodegradation.

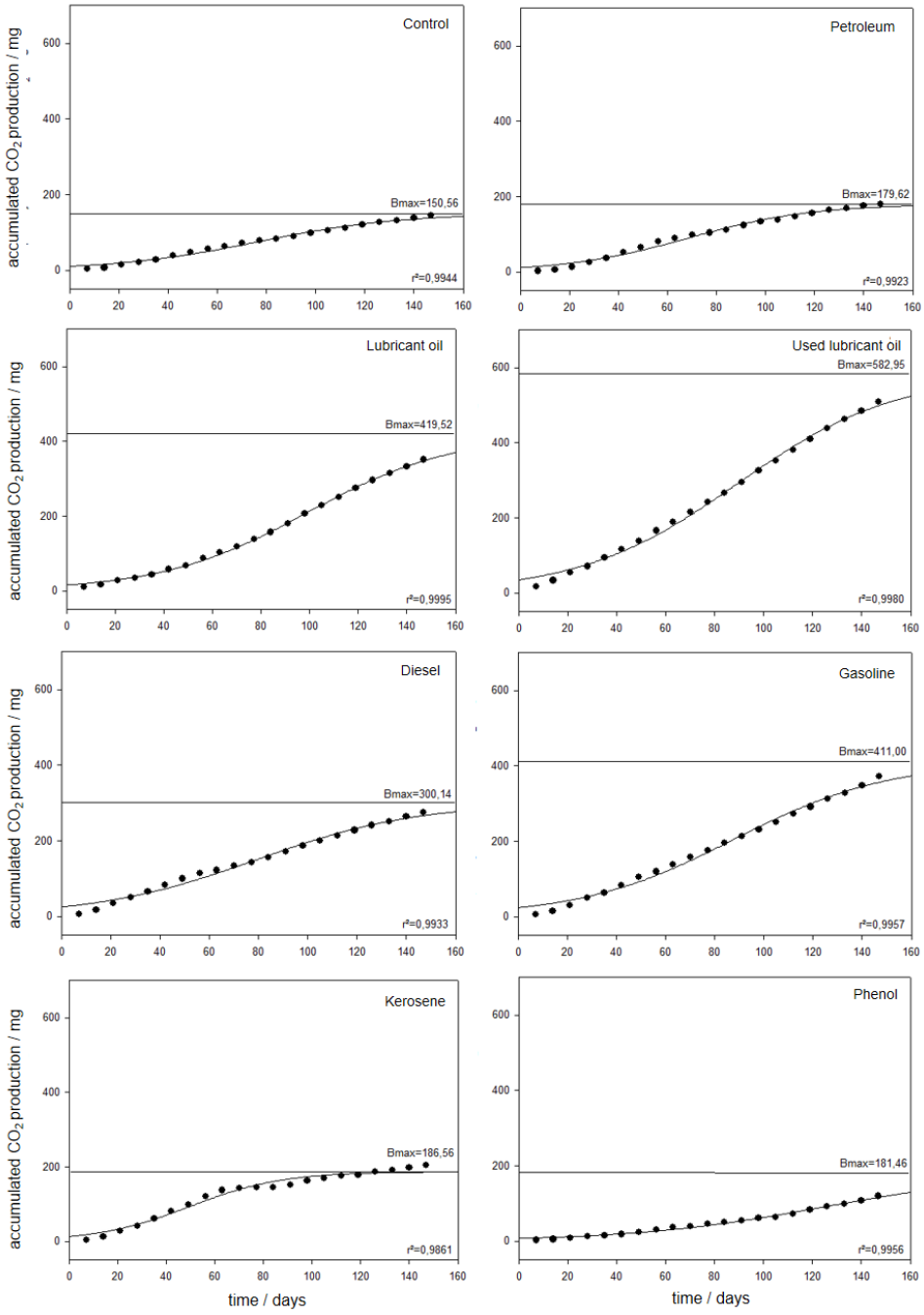

Figure 3. Accumulated CO_2 production adjusted curve in petroleum derivatives.

The maximum production of CO_2 (Bmax) is the expected CO_2 amount yielded from within each respirometric by the time all biodegrading microbial activity ceases. Bmax is established when the curve is stabilized and no longer accrues significant increase in the B parameter (accumulated CO_2 production) over time. Significant increase was defined by values B < 0.99 x Bmax. A horizontal line was inserted to indicate Bmax for each assay. Since B = Bmax time tends to infinity, and the CO_2 production time for Bmax was considered as B = 0.99 x Bmax.

Different Bmax values from each substance indicated where greater CO_2 production was expected. Gasoline and lubricating oils presented the highest extrapolated biodegradation values. The average expected total CO_2 production (Bmax) in these systems reaches 3.05 times greater values than control assays. On the other hand, kerosene and crude petroleum oil presented the lowest accumulated CO_2 values. By further analyzing Bmax parameters, we found some interesting information regarding biodegradation kinetics. According to the proposed model, some substances such as phenol and gasoline will continue biodegradation for about one year (336 and 417 days, respectively) until CO_2 production is over. Therefore, it is noticeable that biodegradation processes produce CO_2 more effectively in certain substances.

3.3 Model Matching

Mathematical models must achieve consistent results in similar parameter estimates to provide reliable and coherent information. As the accumulated CO_2 production slope decreased over time, a decrease in weekly CO_2 production also occurred. The biodegradation end time is expected when both accumulated CO_2 production reaches Bmax value in the Membre *et al*. (1996) model, and the weekly CO_2 production reaches reduced values in the Schmidt *et al*. (1985) model.

The common value allows the two models to be compared to determine if there was an accurate final biodegradation time calculation. To achieve this, BmaxT from Membré *et al* (1996) was compared to the lowest biodegradation rate time (BRminT) in the Schmidt *et al*. (1985) model. The BRminT was considered the time when weekly CO_2 production reached less than 5 mg. A side-by-side comparison of parameters is shown in Table 1.

Most data sets presented in Table 1 had very similar BmaxT and BRminT values. In general, BmaxT was slightly above the one provided by BRminT. Nevertheless, these results are reliable enough to indicate the same situation, coherently pointing toward biodegradation end time. Only gasoline and phenol BRminT values were inadequate to calculate the end time of expected biodegradation.

Table 1. CO_2 parameters fitted to biodegradation data modeling. Comparison between predicted biodegradation cease time between two model parameters (BmaxT and BRminT).

Assay ID	Weekly Respirometry				Accumulated Respirometry		
	BRmax (mg/week^{-1})	**BRmaxT** (days)	**BRminT** (days)	**R^2**	**Bmax** (mg)	**BmaxT** (days)	**R^2**
Control	8,89	42,09	194.13	0,7649	150,56	200,01	0,9944
Petroleum	12,32	38,65	157.12	0,8362	179,62	162,76	0,9923
Lubricant oil	23,74	109,05	198.42	0,9322	419,52	212,69	0,9995
Used lubricant oil	28,74	103,43	231.57	0,8986	582,95	257,20	0,9980
Diesel	15,12	25,56	490.42	0,5714	300,14	271,42	0,9933
Gasoline	---	---	---	---	411,00	285,21	0,9957
Kerosene	19,57	35,89	113.67	0,7741	186,56	121,81	0,9861
Phenol	---	---	---	---	181,46	336,24	0,9956

Diesel assays presented a major difference between the estimated values during the validation process. Such inaccuracy between the two models can be related to a quite low R^2 value (0.5714 and 0.6519, respectively), thus leaving a low accuracy in determining biodegradation end time. A very long biodegradation process may compromise modeling precision and consistency to an exact final biodegradation time. Still, most respirometric assayed substances had an accurately adjusted model that is reliable enough to predict substances behavior in any similar scale respirometric based experiments.

In summary, modeling parameters show that lubricant oils are more likely to reach the highest maximum production of CO_2 than other petroleum derivatives. Furthermore, a higher kerosene weekly CO_2 production in less time may indicate a higher affinity and adaptation of microorganisms compared to diesel oil, whereas kerosene CO_2 production ceased after a peak. Other petroleum compounds presented a continuous biodegradation process that yielded similar Bmax values. However, according to the modeled data, it would take 257.2 days for such a value to be reached in used lubricant oil assays when compared to other assays.

It was also observed that the microbial consortium was unable to further degrade kerosene in the long term, since production of CO_2 ended after 121.81 days. This may be due to the formation of secondary metabolites not biodegradable (Zhengkai and Wrenn, 2008). Continuous biodegradation processes observed in crude petroleum and diesel oil also eventually ceased at a later time according to the modeled predicted values.

4. DISCUSSION

Biodegradation of different petroleum products is influenced by a wide range of variable components, each of those with their own biodegradability (USEPA, 2003; Widdel and Rabus, 2001). It is possible, for example, to infer biodegradability of various derivatives based on the chain length of n-alkanes, branched chains concentration, and / or the presence of polycyclic aromatic hydrocarbons (Feitkenhauer *et al*., 2003; Jovančićević *et al*., 2008).

Oil fractions can be obtained by distillation and refining. In general, there is an average composition for all derivatives being formed by a variety of alkanes, unsaturated chains, aromatic rings and polycyclic structures. Different biodegradation profiles found ranged up to 551.8 mg of CO_2 produced in lubricating oils and a minimum of 181.5 mg of CO_2 for phenol (Table 1). Such variation is attributed to specific biodegradation susceptibility of many compounds, which differ in sizes of carbon chains, and to each individual components present in substances to be biodegraded (Peters *et al*., 2005).

The C7 to C11 chains present in gasoline, for example, have high concentrations of alkene compared to other petroleum products. Biodegradation of gasoline produced a maximum of 371.7 mg of CO_2 in respirometry. Such a value may be because gasoline alkenes are easily biodegraded (Solano-Serena *et al*., 1999). Propylene and ethylene activate specific enzymes (monooxygenases) easily metabolized within microorganisms (Ensign, 2001). Small molecules are reported as more readily biodegraded hydrocarbons, while aromatic compounds are degraded at a rate slower than alkanes in aqueous environments (Sasaki *et al*., 1998). It is also known that n-alkanes with a chain length below C14 are naturally broken down by weathering in aqueous media (Ehrhardt and Weber, 1991).

Diesel oil is a compound denser than gasoline, containing chains in the range of C12 to C15, followed by other kerosene and fuel oils. According to the degradation profiles seen in Figures 2 and 3, the chain length had a great influence in biodegradability of these compounds, which produced 230.7 CO_2.

However, the size of the carbon chains is not the only explanation for greater biodegradability of lubricating oils. Lubricating oils have even longer carbon chains than gasoline, diesel and kerosene. CO_2 production at the end of respirometric monitoring (393.3 mg CO_2) indicated a greater degradation of this oil in comparison to other products. Among petroleum products studied, automotive lubricant oil represented serious environmental harm, since only a small proportion is recycled, and most of it is incinerated or burnt.

The high CO_2 production values found in used lubricating oil (509.1 mg of CO_2) when compared to the non-used lubricant is (350.9 mg of CO_2) were similar to those described by Einsentraeger *et al*. (2002). In their study, it was proposed that the changes in chemical structure of the hydrocarbons occur when used in

lubricants. The high temperatures and pressure of the engine break down the long carbon chains present in this oil, thereby facilitating microbial action.

In this study, no extensive phenol biodegradation occurred. The accumulated CO_2 production in assays containing phenol (99.4 mg) was even lower than the "base aqueous media" control (197.4 mg). Phenolic compounds are common constituents of effluents from oil refineries, but their biodegradation depends on adequate conditions of temperature and specific phenolytic microorganisms. Onysko *et al*. (2000) were able to promote the growth of only one strain of *Pseudomonas putida* to remove a variety of phenolic compounds. Even though the results of this study demonstrated that a microbial consortium was not capable of expressively biodegrading phenol, an increase in phenolytic capacity was observed at the end of respirometry by a slight increase in CO_2 production after 120 days. The adaptation of the microbial community to phenol from an inoculum previously adapted to other substrates should not be discounted, as already reported by Shimp and Pfaender (1987). Prolonged exposure of microorganisms to phenol in an aqueous medium, as occurred in this study yielded a delayed biodegradation in aromatic compounds such as m-cresol, m-aminophenol and p-chlorophenol, explaining the expected CO_2 production values above control assays. This effect was also observed by Gonzalez *et al*. (2001) when submitting a *Pseudomonas* sp strain to phenol in a bioreactor. These results demonstrate the versatility of microorganisms when biodegradating different substances.

It is important to note that biodegradability of petroleum products is not only a function of molecular chain size. As discussed in studies from Leahy and Colwell (1990) to establish levels of biodegradability from a wide variety of components present in petroleum, many factors must be accounted. In general, hydrocarbon biodegradation can be ranked as follows: n-alkanes>branched alkanes>aromatic low molecular weight>cyclo-alkanes>polyaromatic compounds>polar compounds, according to levels established by Peters, *et al*. (2005).

5. CONCLUSIONS

Petroleum product compositions are very complex and their biological properties vary widely. Biodegradation profiles vary between each compound.. It was observed in this study that there is a wide variety of behaviors for different substances released into the environment as they biodegrade. Biodegradability is an important property and must be considered in regard to environmental impact. An improved petroleum biodegradation occurred by a microbial consortium present in the set conditions within respirometric flasks. With the exception of phenol, all substances tested were biodegraded at different intensities. It was possible to mathematically model and predict the behavior of biodegradation of the studied substances. The different biodegradation profiles are found, possibly

related to the specific characteristics of each substance, as the size of the carbon chains and the presence of aromatic rings. Biochemistry associated with oil degrading microorganisms is not uniform and is difficult to establish patterns between substances and microorganisms. There is a wide variety of reactions involved in oil biodegradation that explain these differences, and these reactions can vary depending on environmental conditions and nutrients. Thus, the proposed knowledge and profiling of biodegradation in different substances allows understanding of the environmental behaviour of such substances.

6. REFERENCES

Atlas, R.M. 1981. Microbial degradation of petroleum hydrocarbons: an environmental perspective. Microbiol. Rev. 45, 180-209.

Atlas, R.M., and Bartha, R. 1992. Hydrocarbon biodegradation and oil-spill bioremediation. Adv. Microb. Ecol. 12, 287-338.

Balba, M.T., Awadhi, N., and Daher, R. 1998. Biorremediation of oil–contaminated soil: microbiologics methods for feasibility, assessement and field, evaluation. J. Microbiol. Methods. 3, 155-164.

Bartha, R., and Pramer, D. 1965. Features of flask and method for measurement of the persistence and biological effects of pesticides in soil. J. Soil Sci. 68, 100-102.

Benedik, M.J., Gibbs, P.R., Riddle, R.R., and Wilson, R.C. 1998. Microbial denitrogenation of fossil fuels. Trends Biotechnol. 16, 390–395.

Bragg, J.R., Prince, R.C., Harner, E.J., and Atlas, R.M. 1994. Effectiveness of bioremediation for the Exxon Valdez oil spill. Nature. 368, 413-418.

CETESB (Companhia de Tecnologia e Saneamento Ambiental). 1990. Determinação da Biodegradação de Resíduos – Método Respirométrico de Bartha. São Paulo, Brazil. L6.350.

Chaîneau, C.H., Rougeux, G., Yéprémian, C., and Oudot J. 2005. Effects of nutrient concentration on the biodegradation of crude oil and associated microbial populations in the soil. Soil Biol. Biochem. 37, 1490–1497.

Ehrhardt, M., and Weber, R.R. 1991. Formation of low molecular weight carbonyl compounds by sensitized photochemical decomposition of aliphatic hydrocarbons in seawater. Fresenius' J. Ana. Chem. 339, 772-776.

Eisentraeger, A., Schmidt, M., Murrenhoff, H., Dott, W., and Hahn, S. 2002. Biodegradability testing of synthetic ester lubricants – effects of additives and usage. Chemosphere. 48, 89–96.

Ensign, S.A. 2001. Microbial metabolism of aliphatic alkenes. Biochemistry. 40, 5845–5853.

Feitkenhauer, H., Muller, R., and Markl, H. 2003. Degradation of polycyclic aromatic hydrocarbons and long chain alkanes at 6070°C by Thermus and Bacillus spp. Biodegradation. 14, 367–372.

Fiúza, A.M.A., and Vila, M.C.C. 2004. An insight into soil bioremediation through respirometry. Environ. Int. 31, 179-183.

Frazer, A.C., Coschigano, P.W., Young, L.Y. 1996. Toluene metabolism under anaerobic conditions: a review. Anaerobe. 1, 293–303.

Garrett, R.M., Rothenburger, S.J, and Prince, R.C. 2003. Biodegradation of fuel oil under laboratory and arctic marine conditions. Spill Sci. Technol. Bull. 8, 297–302.

González G., Herrera, G., Garcia, M.T., and Peña, M. 2001. Biodegradation of phenolic industrial wastewater in a fluidized bed bioreactor with immobilized cells of Pseudomonas putida. Bioresour. Technol. 80, 137-142.

Graves, A., Lang, C., and Leavitt, M. 1991. Respirometric analysis of the biodegradation of organic contaminants in soil and water. Appl. Biochem. Biotechnol. 28/29, 813–26.

Jovančićević, B., Antić, M., Pavlović, I., Vrvić, M., Beškoski, V., Kronimus, A., and Schwarzbauer, J. 2008. Transformation of petroleum saturated hydrocarbons during soil bioremediation experiments. Water, Air, Soil Pollut. 190, 299–307.

Kernanshani, A., Kararnanev, D., and Margaritis, A. 2006. Kinetic modeling of the biodegradation of the aqueous p-xylene in the immobilized soil bioreactor. Eng. J. 27, 204–211.

Leahy, J.G., and Colwell, R.R. 1990. Microbial degradation of hydrocarbons in the environment. Microbio. Rev. 54, 305-315.

Li, X., Li, P., Lin, X., Zhang, C., Li, Q., and Gong, Z. 2008. Biodegradation of aged polycyclic aromatic hydrocarbons (PAHs) by microbial consortia in soil and slurry phases. J. Hazard. Mater. 150, 21-26.

Mandri, T., and Lin, J. 2007. Isolation and characterization of engine oil degrading indigenous microorganisms in Kwazulu-Natal, South Africa. Afr. J. Biotech. 6, 23–26.

Membré, J.M., Thurette J., and Catteau, M. 1996. Modeling the growth, survival and death of Listeria monocytogenes. J. Appl. Microbio. 82, 345-350.

Montagnolli, R.N., Lopes, P.R.M., and Bidoia, E.D. 2009. Applied models to biodegradation kinetics of lubricant and vegetable oils in wastewater. Int. Biodeterior. Biodegrad. 63, 297-305.

Okoh, A.I., and Trejo-Hernandez, M.R. 2006. Remediation of petroleum hydrocarbon polluted systems: exploiting the bioremediation strategies. Afr. J. Biotechnol. 5, 2520–2525.

Onysko, K.A., Budman, H.M., and Robinson, C.W. 2000. Effect of temperature on the inhibition kinetics of phenol biodegradation by Pseudomonas putida Q5. Biotechnol. Bioeng. 70, 291–299.

Oudot, J., Merlin, F.X., and Pinvidic, P. 1998. Weathering rates of oil components in a bioremediation experiment in estuarine sediment. Mar. Environ. Res. 45, 113–125.

Pala, D.M., Carvalho, D.D., Pinto, J.C., and Sant'anna, G.L. 2006. A suitable model to describe bioremediation of a petroleum-contaminated soil, Int. Biodeterior. Biodegrad. 58, 254–260.

Peters, K.E., Walters, C.C., and Moldowan, J.M. 2005. The biomarker guide, biomarkers and isotopes in petroleum exploration and earth history. New York. Cambridge Univ. Press.

Readman, J.W., Bartocci, J., Tolosa, I., Fowler, S.W., Oregioni, B., and Abdulraheem, M.Y. 1996. Recovery of the coastal marine environment in the Gulf following the 1991 war-related oil spills. Mar. Pollut. Bull. 32, 493–498.

Readman, J.W., Fowler, S.W., Villeneuve, J.P., Cattini, C., Oregioni, B., and Mee, L.D. 1992. Oil and combustion-product contamination of the Gulf marine environment following the war. Nature. 358, 662-665.

Schmidt, S.K., Simkins, S., and Alexander, M. 1985. Models for the kinetics of biodegradation of organic compounds not supporting growth. Appl. Environ. Microbio. 50, 2, 323-331.

Shimp, R.J., and Pfaender, F.K. 1987. Effect of Adaptation to Phenol on Biodegradation of Monosubstituted Phenols by Aquatic Microbial Communities. Appl. Environ. Microbio. 53, 1496-1499.

Solano-Serena, F., Marchal, M.R., Lebeault, R.J.M., and Vandecasteele, J.P. 1999. Biodegradation of gasoline: Kinetics, mass balance and fate of individual hydrocarbons. J. Appl. Microbio. 86, 1008–1016.

USEPA (United States Environmental Protection Agency). 2003. Aerobic biodegradation of oily wastes - A field guidance book for federal on-scene coordinators. Washington, USA.

Van Hamme, J.D., Singh, A., and Ward, O.P. 2003. Recent advances in petroleum microbiology. Pet. Microbio. 67, 503–549.

Widdel, F., and Rabus, R. 2001. Anaerobic biodegradation of saturated and aromatic hydrocarbons. Curr. Opin. Biotech. 12, 259–276.

Wu, Y., Chiang, C., and Lu, C. 2004. Respirometric evaluation by graphical analysis for microbial systems. Env. Monit. Assess. 92, 137–152.

Zhengkai, L., and Wrenn, B.A. 2008. Effects of ferric hydroxide on the anaerobic biodegradation kinetics and toxicity of vegetable oil in freshwater sediments. Water Res. 38, 3859–3868.

Chapter 12

A QSAR MODEL FOR THE PREDICTION OF DRUG BINDING AFFINITIES TO HUMAN SERUM ALBUMIN

Serli Onlu, Gulcin Tugcu, and Melek Türker Saçan[§]
Bogazici University, Institute of Environmental Sciences, 34342, Bebek, Istanbul, Turkey

ABSTRACT

Drugs are not entirely absorbed by the human body; they are excreted and passed into wastewater and surface water. Human serum albumin (HSA) is an abundant plasma protein with remarkable binding strength. Therefore, drug binding to HSA is an area of considerable research. Developing a computational model using Quantitative Structure–Activity Relationships (QSARs) has been very useful for environmental and pharmaceutical studies. They are advantageous since they rationalize experimental observations, saving time, money and other resources.

The binding affinity to HSA for 90 drug and drug like molecules was modeled with the descriptors calculated solely from their molecular structures using data published by Colmenarejo *et al.* (2001). The dataset was split into training and test sets randomly. A three–descriptor (ALOGP2, C–040, EEig07r) linear model was allocated to the training set. The heuristic method was utilized for this purpose, leading to a good squared correlation coefficient (R^2=0.78). The validation of the model was performed according to the OECD principles (OECD, 2007). The most important variable described by the model (ALOGP2) was evaluated as hydrophobicity, which indicates that binding to HSA is mainly determined by hydrophobic forces. This is in accordance with the x–ray structures of HSA, where the binding regions are mainly composed of hydrophobic residues.

The three–descriptor model without any outliers is statistically better, mechanistically interpretable, and robust when it is compared to QSAR models with many descriptors and outliers for the same data set in literature.

Keywords: MLR, QSAR, descriptor, human serum albumin, drug–binding, model.

[§] Melek Türker Saçan, Bogazici University, Institute of Environmental Sciences, 34342, Bebek, Istanbul, Turkey, msacan@boun.edu.tr

1. INTRODUCTION

Many pharmaceuticals are being used in human health care; however, they are not totally metabolized in the human body and are excreted to some extent. Therefore, they can be detected in sewage treatment plants (STPs) after excretion. Several pharmaceutically active compounds are discharged from STPs into receiving waters and may eventually reach drinking water due to incomplete treatment. Improper disposal of unused medications may be regarded as environmental pollution (Kümmerer 2001; Heberer 2002; Hernando *et al.,* 2006). Experimental trials of drug design and production may also cause additional discharge, especially when conducted as large scale industrial activities. Therefore, computational model development for the prediction of drug pharmacokinetics is important for both the pharmaceutical industry and the environment.

In–silico prediction methods such as Quantitative Structure–Activity Relationship (QSAR) have been very useful in the fields of applied chemistry, environmental science, toxicology, and pharmacology (Hansch 1993; Colmenarejo *et al.,* 2001; Colmenarejo *et al.,* 2003; Hall *et al.,* 2003; Xue *et al.,* 2004; Deeb and Hemmateenejad 2007; Zsila *et al.,* 2011). QSARs are advantageous since they rationalize a considerable number of experimental observations, saving time and money, and also implicitly contributing to environmental pollution prevention (Firestone *et al.,* 2010; Fjodorova *et al.,* 2008; Benigni *et al.,* 2007).

Human Serum Albumin (HSA) is the most abundant protein in plasma, comprising more than half of all blood proteins. It is the most significant plasma component characterized by its astonishing capacity to bind a large variety of drugs. HSA enables solubilization of hydrophobic compounds. In this manner, it provides more homogeneous distribution of drugs through the body and increases their biological lifetime (Colmenarejo *et al.,* 2001; Colmenarejo *et al.,* 2003; Deeb and Hemmateenejad 2007). Comprehensive studies have revealed two main drug–binding sites in HSA, specified as site I and site II. Site I prefers large heterocyclic and negatively charged compounds, site II has a tendency for small aromatic carboxylic acids. These sites were localized at subdomains IIA and IIIA, when the crystal structures of HSA with ligands were available (Colmenarejo *et al.,* 2003; Carter *et al.,* 1994; Sugio *et al.,* 1999).

There are several studies on mathematical models predicting binding affinities of drugs to HSA in literature (Colmenarejo *et al.,* 2001; Colmenarejo *et al.,* 2003; Hall *et al.,* 2003; Xue *et al.,* 2004; Deeb and Hemmateenejad 2007; Zsila *et al.,* 2011; Estrada *et al.,* 2006; Gunturi *et al.,* 2006; Wichmann *et al.,* 2007; Deeb 2010; Chen and Chen 2012). Most of these studies were gathered and reviewed by

Colmenarejo *et al.* (2003). In their previous study, Colmenarejo *et al.* (2001) constructed the first *in–silico* models for the prediction of drug–binding strengths to HSA by using a large and diverse set of (95 compounds) drug and drug–like molecules. The very best model among them is a non–linear, multivariate equation. Different studies have been published by other researchers utilizing different statistical methods using the same data set (Hall *et al.,* 2003; Xue *et al.,* 2004; Deeb and Hemmateenejad 2007). However, some compounds having somewhat large residuals were reported as outliers in the studies of Colmenarejo *et al.* (2001) and Hall *et al.* (2003).

In this study, a statistically valid QSAR model was constructed for 90 drug molecules by selecting from the experimental data of the chromatographic retention index log*K*'HSA of Colmenarejo *et al.* (2001) to predict the binding affinity to HSA with the molecular descriptors.

2. MATERIAL AND METHODS

2.1 Data Set

A data set with 90 structurally diverse drug compounds, having a wide range of physicochemical properties, was selected from the study published by Colmenarejo *et al.* (2001) and displayed in Table 1. The selection was done according to the binding affinity values to represent the entire data range, as well as the structural and physicochemical properties. Five compounds (captopril, ebselen, minocycline, sancycline, and zidovudine) were excluded from the original data set of 95 compounds for a variety of reasons; for instance captopril; due to experimental error and ebselen; for which descriptors could not be calculated.

The experimental binding affinity data were calculated in the logarithmic scale by utilizing the High–Performance Affinity Chromatograhy (HPAC) method as follows: log*K*'HSA = [log/(t - t_0)/t_0], where t and t_0 are the retention times of the drug and nonretained material, respectively (Colmenarejo *et al.,* 2001). The binding affinities in the data set fall within the range of -1.39 for acetylsalicylic acid to 1.34 for clotrimazole.

The whole data set was randomly split into training and test sets for external validation. The training set of 71 compounds was used to construct the model, and the test set of 19 compounds (Table 1) was used to evaluate the predictive power of the model.

Table 1. Experimental and predicted binding affinities of drugs to HSA.

ID	Name	HSA Exp. [a]	HSA Pred. [b]	ID	Name	HSA Exp. [a]	HSA Pred. [b]
1	Acetylsalicylic Acid	-1.39	-1.04	**46**	Camptothecin [c]	-0.08	-0.39
2	Cefuroxime [c]	-1.33	-0.81	**47**	Tetracycline	-0.08	-0.20
3	Amoxicillin	-1.21	-0.84	**48**	Bupropion	-0.05	-0.09
4	Cephalexin	-1.11	-0.82	**49**	Sumatriptan	-0.05	-0.12
5	5-fluorocytosine	-1.11	-0.97	**50**	Warfarin	-0.04	-0.05
6	Cromolyn	-1.07	-0.33	**51**	Bumetanide [c]	-0.03	0.03
7	Caffeine [c]	-0.92	-0.60	**52**	Oxyphenbutazone	-0.02	-0.01
8	Acetaminophen	-0.81	-0.86	**53**	Acrivastine	-0.02	0.55
9	L-tryptophan	-0.78	-0.48	**54**	Phenytoin	0.00	-0.25
10	Methotrexate	-0.77	-0.71	**55**	Doxycycline	0.01	-0.16
11	Propylthiouracil	-0.75	-0.74	**56**	Ketoprofen [c]	0.03	0.03
12	Antipyrine [c]	-0.69	-0.57	**57**	Alprenolol	0.04	0.03
13	Phenoxymethylpenicillinic Acid	-0.69	-0.77	**58**	Prazosin	0.06	-0.12
14	Salicylic Acid	-0.66	-0.85	**59**	Digitoxin	0.13	0.32
15	Cefuroxime Axetil	-0.56	-0.96	**60**	Levofloxacin	0.14	-0.15
16	Etoposide [c]	-0.49	-0.07	**61**	Ciprofloxacin [c]	0.14	-0.25
17	Atenolol	-0.48	-0.49	**62**	Labetalol	0.14	-0.13
18	Chloramphenicol	-0.46	-0.44	**63**	Norfloxacin	0.14	-0.27
19	Cimetidine	-0.44	-0.52	**64**	Phenylbutazone	0.19	0.06
20	Chlorpropamide	-0.44	-0.20	**65**	Naproxen	0.25	-0.18
21	Sotalol [c]	-0.44	-0.30	**66**	Clofibrate [c]	0.27	-0.20
22	Hydrochlorothiazide	-0.42	-0.42	**67**	Propranolol	0.28	0.08
23	Tolazamide	-0.42	0.13	**68**	Tetracaine	0.32	-0.10
24	Hydrocortisone	-0.40	0.04	**69**	Fusidic acid	0.33	0.69
25	Nadolol	-0.40	-0.09	**70**	Novobiocin	0.35	0.10
26	Prednisolone [c]	-0.40	0.04	**71**	Ondansetron [c]	0.37	0.18
27	Scopolamine	-0.34	-0.31	**72**	Droperidol	0.43	0.33
28	Timolol	-0.33	-0.15	**73**	Quinidine	0.44	0.24
29	Metoprolol	-0.29	-0.12	**74**	Indomethacin	0.47	0.24
30	Trimethoprim	-0.26	-0.09	**75**	Quinine	0.49	0.24
31	Dansylglycine [c]	-0.26	-0.26	**76**	Verapamil [c]	0.52	0.98
32	Lidocaine	-0.23	-0.23	**77**	Sulfasalazine	0.56	0.35
33	Methylprednisolone	-0.22	0.13	**78**	Progesterone	0.59	0.49
34	Tolbutamide	-0.22	-0.04	**79**	Desipramine	0.61	0.51
35	Sulfaphenazole	-0.21	0.07	**80**	Estradiol	0.68	0.51
36	Acebutolol [c]	-0.21	-0.32	**81**	Glibenclamide [c]	0.68	0.50
37	Procaine	-0.19	-0.40	**82**	Testosterone	0.74	0.39
38	Terazosin	-0.16	-0.22	**83**	Imipramine	0.75	0.69
39	Oxprenolol	-0.15	-0.05	**84**	Ketoconazole	0.84	0.37
40	Lamotrigine	-0.13	-0.14	**85**	Promazine [c]	0.92	0.57
41	Clonidine [c]	-0.13	0.01	**86**	Itraconazole	1.04	1.66
42	Pindolol	-0.13	-0.07	**87**	Triflupromazine	1.05	0.97
43	Furosemide	-0.13	-0.27	**88**	Chlorpromazine	1.10	0.82
44	Carbamazepine	-0.10	0.18	**89**	Terbinafine [c]	1.17	1.08
45	Ranitidine	-0.10	-0.15	**90**	Clotrimazole	1.34	1.04

[a] Experimental values published by Colmenarejo *et al.*, (2001), [b] Predicted values using the heuristic method in this work, [c] Test set compound.

2.2 Model Development

All of the structural calculations were performed at the semi–empirical PM3 calculation level using SPARTAN software (v. 04, 2004, Wavefunction, Inc., Irvine, CA, USA).

The geometrically optimized structures of molecules were then used to calculate the molecular descriptors by DRAGON software (v. 5.4., 2006, Talete, Milano, Italy). The CODESSA software (v. 2.2, 1996, ©University of Florida, Gainesville, USA) was used for further calculations, since it enables construction of QSARs via the calculation of a large number of descriptors based solely on structural information. Certain geometrical (molecular volume, molecular surface area, etc.) and thermodynamical descriptors (energy of highest occupied molecular orbital (E_{HOMO}) and energy of lowest unoccupied molecular orbital (E_{LUMO})) were calculated separately with the data extracted from SPARTAN 04 output. Constant descriptors were excluded to minimize the volume of information. All of the descriptors were imported into the CODESSA and analyzed with the heuristic option.

The multiple linear regression (MLR) analysis with stepwise selection was employed to model the binding affinity (log*K*'HSA) relationship with the best set of descriptors derived from the heuristic method.

2.3 Model Validation

The Statistical Package for Social Scientists (SPSS) software (v. 17, 2008, SPSS, Inc., Chicago, IL, USA) and the heuristic multilinear regression procedure were utilized to explain the goodness of fit by computing the squared correlation coefficient (R^2) for the training set and the test set, the adjusted squared correlation coefficient (R^2_{adj}), the Fisher statistics (F), and the standard error (SE). The cross–validated (leave–one–out) squared correlation coefficient (R^2_{cv}) was also calculated in the heuristic procedure in order to describe the stability of the regression model.

2.4 Applicability Domain

Since it cannot be expected that a single model will predict the activity of all chemicals, it is essential to define the applicability domain (AD) of the model. The possible outliers were searched and the AD of the model was defined by the leverage approach.

The leverage of a chemical provides a measure of the distance of the chemical from the centroid of its training set. To visualize the outliers in a model (i.e., outliers in both the descriptor space and the response space), a plot of standardized residuals versus leverages (or hat values, h), called the Williams

plot, was used to define AD. Critical hat value (h^*) was set at $3p/n$, where p is the number of descriptors plus one and n is the number of compounds in the model. A compound is identified as a structural outlier if the hat value of that compound is greater than the h^*. If the predicted value is higher than three standardized residuals in MLR models, then the compound is identified as a response outlier (OECD, 2007).

An HP model computer with Windows XP operating system equipped with a 2.20 GHz processor was used for all calculations.

3. RESULTS AND DISCUSSION

In total, 1563 descriptors calculated from DRAGON, SPARTAN, and CODESSA software packages were run under the heuristic procedure for the 71 structures of the training set. The best three–descriptor linear model developed is displayed in Table 2 together with the abbreviations, names and definitions of descriptors appearing in the model. The 95% confidence intervals were also given in parentheses.

The *t*–values for partial correlation coefficients are shown in Table 2 as 9.544, -6.788, and 5.209 for ALOGP2, C–040 and EEig07r, respectively. On the basis of the *t*–values, it can be concluded that ALOGP2, representing hydrophobicity, is the most important descriptor appearing in the model.

The statistical parameters of the model (R^2=0.78, F=79.2, and SE=0.27) are also presented in Table 2. The adjusted squared correlation coefficient R^2_{adj} of 0.77 gave evidence that there was no overfitting. The internal validation of the model was described with the cross–validated squared correlation coefficient R^2_{cv} of 0.74, reflecting the stability of the model.

The predictive power of the model was evaluated by using the test set which comprises chemicals that were not used in the model development. The external validation of the model yielded the R^2_{test} of 0.76, demonstrating that the model is able to predict the response for chemicals (test set) not used in the model development.

The interpretation of the descriptors can illuminate the factors that are likely affecting the binding affinities of drugs to HSA. ALOGP2 explains the molecular hydrophobicity as log P (the logarithm of 1-octanol/water partition coefficient) (Todeschini and Consonni, 2000). This outcome is consistent with the studies of x-ray structures of HSA, which indicate that the binding regions of both sites I and II are mainly composed of hydrophobic residues (Colmenarejo *et al.*, 2001; Colmenarejo *et al.*, 2003; Deeb and Hemmateenejad 2007). In this respect, it can be stated once more that hydrophobicity increases drug binding to HSA. In our previous study, C-040 contributed to toxicity modeling of pharmaceuticals in fish

(Tugcu *et al.*, 2012). In both models, the number of specific fragments reflected by C-040 was found to be inversely correlated with the dependent variable.

Table 2. Descriptors appearing in three–descriptor model for the binding affinity of drugs to HSA.

Descriptor	**Description** [a]	**Type** [a]	***t*-value**
ALOGP2	Square of Ghose-Crippen octanol-water partition coefficient ($logP^2$)	Molecular properties	9.544
C–040	R-C(=X)-X / R-C#X / X=C=X (Atom-centered fragment)	Atom-centered fragments	-6.788
EEig07r	Edge adjacency index	Eigenvalue-based indices	5.209
Model			
log*K*'HSA = 0.042 (± 0.004) ALOGP2 – 0.249 (± 0.037) C–040 + 0.231 (± 0.044) EEig07r – 0.651 (± 0.091)			
$n_{training}$= 71; R^2 = 0.78, R^2_{adj} = 0.77, R^2_{cv} = 0.74, $F_{3,67}$ = 79.2, *SE* = 0.27			
n_{test}= 19; R^2_{test} = 0.76, *AAE* = 0.25			

[a] Todeschini and Consonni, 2000.

The experimental HSA binding affinity values (Colmenarejo *et al.*, 2001) and the corresponding predicted values are displayed in Table 1. The plot of predicted versus observed log*K*'HSA values for the model is shown in Figure 1 for both training and test chemicals.

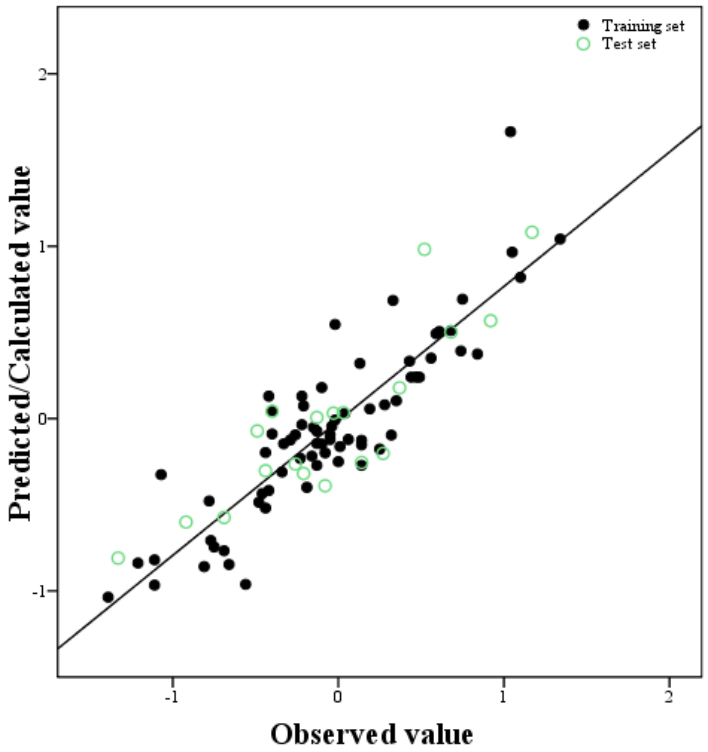

Figure 1. Plot of predicted versus observed log*K*'HSA values of the model.

To visualize the possible outliers, *i.e*., outliers in both the descriptor space and the response space, the Williams plot of standardized residuals versus leverages (or *h*) was drawn and shown in Figure 2. The critical hat value was calculated as *h**=0.17 for 71 compounds for the three–descriptor model.

It can be seen from Figure 2 that cefuroxime axetil and itraconazole have higher leverage values than the critical hat value, which is at 0.17. Cefuroxime axetil and itraconazole are influential chemicals in the model. Cefuroxime axetil has the maximum value for C–040 and itraconazole has the maximum value for ALOGP2 among the training set compounds. On the other hand, there is no apparent molecule as a response outlier. However, Deeb and Hemmateenejad (2007) indicated that itraconazole is different from other molecules with respect to both molecular structure (descriptors) and biologic activity (binding constant). Apart from these, Colmenarejo *et al.* (2001) remarked five compounds as response outliers. In another publication, cromolyn, propylthiouracil, cimetidine, and acrivastine were classified as statistical outliers as well (Estrada *et al.*, 2006).

It is of our interest to compare our model with the literature models. The developed model consists of comparatively fewer descriptors than the reported

models. Additionally, the proposed model was developed and validated according to OECD principles (OECD, 2007).

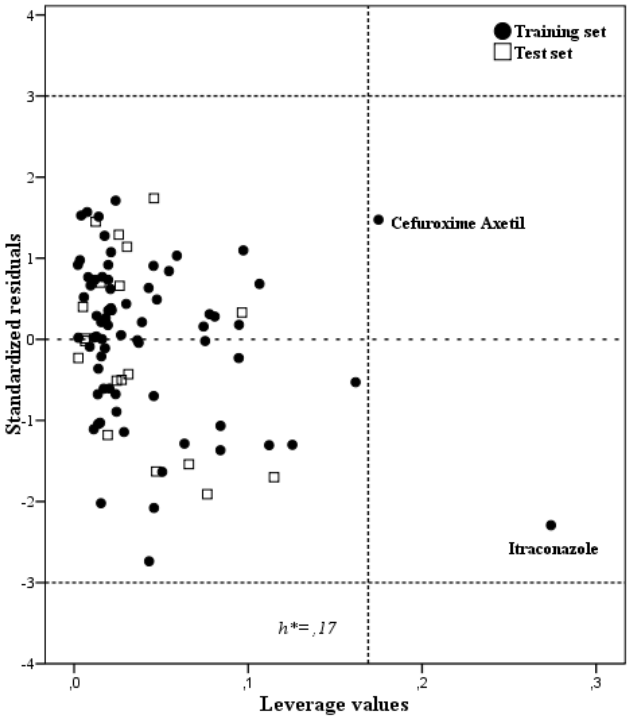

Figure 2. Williams plot of the model (h^* = 0.17).

4. CONCLUSION

When taken into account that drugs are not entirely absorbed by the human body and may eventually be passed into receiving water bodies and drinking water in the long run, this model is useful for both industrial and environmental applications. A linear QSAR was allocated for the prediction of the affinity of a diverse set of 90 drugs binding to human serum albumin based on descriptors calculated solely from molecular structure by the heuristic method. The internal and external validation of the model yielded good statistical parameters, presenting a good predictive power compared to the previously published models. The model was found to be capable of predicting the binding affinities by utilizing only three molecular descriptors. It was indicated by the model that an increase of hydrophobicity is expected to result in an increased drug binding to HSA. Otherwise, the probability of the direct release of drug molecules with low binding affinity to HSA in the environment will be increased.

Acknowledgements: The financial support of Bogazici University Research Fund (BAP) (Project No: 6730) is appreciated. The authors would also like to thank Dr. Tuna Tugcu from The Department of Computer Engineering, Bogazici University for coding the descriptor import module.

5. REFERENCES

Benigni, R., Netzeva, T. I., Benfenati, E., Bossa, C., Franke, R., Helma, C., Hulzebos, E., Marchant, C., Richard, A., Woo, Y. T., and Yang, C. 2007. The Expanding Role of Predictive Toxicology: An Update on the (Q)SAR Models for Mutagens and Carcinogens. J. Environ. Sci. Health C Environ. Carcinog. Ecotoxicol. Rev. 25, 53-97.

Carter, D. C., Chang, B., Ho, J. X., Keeling, K., and Krishnasami, Z. 1994. Preliminary Crystallographic Studies of Four Crystal Forms of Serum Albumin. Eur. J. Biochem. 226, 1049-1052.

CODESSA v. 2.2, 1996, University of Florida, Gainesville, USA.

Colmenarejo, G. 2003. *In Silico* Prediction of Drug-Binding Strengths to human serum albumin. Med. Res. Rev. 23, 275-301.

Colmenarejo, G., Alvarez-Pedraglio, A., and Lavandera, J. L. 2001. Chemoinformatic Models to Predict Binding Affinities to Human Serum Albumin. J Med Chem. 44, 4370–4378.

Deeb, O., and Hemmateenejad, B. 2007. ANN-QSAR Model of Drug-binding to Human Serum Albumin, Chem. Biol. Drug Des. 70, 19-29.

DRAGON v. 5.4, 2006. Talete, Milano, Italy. Chemometrics and QSAR Research Group. Accessed from http://michem.disat.unimib.it/chm/, http://www.vcclab.org/lab/edragon/

Firestone, M., Kavlock, R., Zenick, H., Kramer, M., and the U.S. Environmental Protection Agency Working Group on the Future of Toxicity Testing the U.S. EPA Strategic Plan for Evaluating the Toxicity of Chemicals 2010. J. Toxicol. Environ. Health, Part B. 13, 139-162.

Fjodorova, N., Novic, M., Vracko, M., Kharchevnikova, N., Zholdakova, Z., Sinitsyna, O., and Benfenati, E. 2008. Regulatory Assessment of Chemicals within OECD Member Countries, EU and in Russia. J. Environ. Sci. Health C Environ. Carcinog. Ecotoxicol. Rev. 26, 40-88.

Ghose, A. K., Viswanadhan, V. N., and Wendoloski, J. J. 1998. Prediction of Hydrophobic (Lipophilic) Properties of Small Organic Molecules Using Fragmental Methods: An Analysis of ALOGP and CLOGP Methods. J. Phys. Chem. 102, 3762-3772.

Hall, L. M., Hall, L. H., and Kier, L. B. 2003. Modeling Drug Binding Affinity with E-State Topological Structure Representation. J. Chem. Inf. Comput. Sci. 43, 2120-2128.

Hansch, C. 1993. Quantitative Structure-Activity Relationships and the Unnamed Science. Acc. Chem. Res. 26, 147-153.

Heberer, T. 2002. Tracking Persistent Pharmaceutical Residues from Municipal Sewage to Drinking Water. J. Hydrol. 266, 175–189.

Hernando, M.D., Heath, E., Petrovic, M., and Barceló, D. 2006. Trace-level Determination of Pharmaceutical Residues by LC–MS/MS in Natural and Treated Waters. A Pilot-Survey Study. Ana. Bioanaly. Chem. 385, 985–991.

Kümmerer, K. 2001. Drugs in the Environment: Emission of Drugs, Diagnostic Aids and Disinfectants into Wastewater by Hospitals in Relation to Other Sources-review. Chemosphere. 45, 957–969.

Organization for Economic Co-operation and Development, Guidance document on the validation of (quantitative) structure–activity relationships [(Q)SAR] Models, OECD Environment Health and Safety Publications, Series on Testing and Assessment No. 69. Paris, France, 2007.

SPARTAN v. 04, 2004. Wavefunction Inc, Irvine, CA, USA,
Available at http://www.wavefun.com/products/spartan.html

SPSS v. 17, 2008. SPSS Inc., Chicago, IL. Available at http://www-01.ibm.com/software/analytics/spss/?pgel=ibmhzn&cm_re=masthead-_-products-_-sw-spss

Sugio, S., Kashima, A., Mochizuki, S., Noda, M., and Kobayashi, K. 1999. Crystal Structure of Human Serum Albumin at 2.5 Å Resolution. Protein Eng. 12, 439-446.

Todeschini, R. and Consonni, V. 2000. Handbook of Molecular Descriptors, WILEY-VCH, Germany.

Tugcu G., Saçan M.T., Vracko M., Novic M., and Minovski N. 2012. QSTR Modeling of the Acute Toxicity of Pharmaceuticals to Fish. SAR QSAR Environ. Res. 23(3-4), 297-310.

Xue, C. X., Zhang, R. S., Liu, H. X., Yao, X. J., Liu, M. C., Hu, Z. D., and Fan, B.T. 2004. QSAR Models for the Prediction of Binding Affinities to Human Serum Albumin Using the Heuristic Method and a Support Vector Machine. J. Chem. Inf. Comput. Sci. 44, 1693-1700.

Zsila, F., Bikadi, Z., Malik, D., Hari, P., Pechan, I., Berces, A., and Hazai, E. 2011. Evaluation of Drug–Human Serum Albumin Binding Interactions with Support Vector Machine Aided Online Automated Docking. Bioinformatics. 27, 1806-1813.

Part VII: Site Characterization

Chapter 13

LNAPL INVESTIGATION AND BEHAVIOR IN A SAPROLITE AQUIFER

Christopher J. Mulry, P.G.1[1§] and Don A. Lundy, P.G.[2]
[1]*Groundwater & Environmental Services, Inc., 1350 Blair Drive, Suite A, Odenton, MD, USA, 21113,*
[2]*Groundwater & Environmental Services, Inc., 6655 Peachtree Dunwoody Road, Atlanta, GA, USA, 30328*

ABSTRACT

Operation of a fuel bulk storage and distribution terminal in the Piedmont region of northwestern South Carolina from the 1940s through the late 1980s resulted in a large LNAPL plume, consisting primarily of kerosene/jet fuel, existing at 45 feet below ground surface. A total of over 100 monitoring wells, recovery wells, and small-diameter piezometers have been installed in six or more discrete investigative events over the past three decades. Remediation via total fluids extraction (pump and treat) from 16 extraction wells has been ongoing since the early 1990s. Over 159,000 gallons of fuel have been recovered to date with a clear decline in recovery rate over time.

Recent efforts to clarify regulatory drivers and evaluate site strategy have led to a reappraisal of the LNAPL plume. Issues include the practicality of maintaining current recovery efforts, steps to optimize recovery operations, validity of apparent LNAPL thickness data derived from small-diameter monitoring points, and determining tools and techniques for use in understanding LNAPL behavior.

A recent LNAPL plume evaluation incorporated review of historical recovery data, well-specific yield testing for existing recovery wells, laser-induced fluorescence (LIF) analysis, core collection and lab analysis, and bail-down testing at select locations. These tests were undertaken to determine the extent of LNAPL, smear zone characteristics, and LNAPL mobility and recoverability. Results are presented with discussion of their applicability and utility to this site.

§ Christopher J. Mulry, P.G., Groundwater & Environmental Services, Inc., 1350 Blair Drive, Suite A, Odenton, MD, USA, 21113, 800-220-3606 x3708, cmulry@gesonline.com

For example, LNAPL well thickness was determined to be a poor indicator of recoverability, and oil transmissivity (T_o) proved to be a meaningful basis for gauging relative LNAPL recoverability.

Methods comparing LIF response, bail-down test results, and lab results derived from core analyses are discussed and correlations evaluated to streamline data collection and decision making related to practical management strategies and development of technically defensible remedial endpoints.

Keywords: environment, soil, investigation, direct push, LIF, laser-induced fluorescence, LNAPL, light non-aqueous phase liquids, LCSM, conceptual site model, saprolite

1. INTRODUCTION

Managing sites with Light, Non-Aqueous Phase Liquids (LNAPL) presents a number of challenges to responsible parties and practitioners. Paramount amongst these are the recognition of potential exposure pathways associated with the presence of LNAPL and practical source identification and mitigation approaches. Recent developments in the understanding of LNAPL behavior in real-world environments (API, 2007) have greatly advanced both the underlying theory and practical management techniques and options for handling LNAPL sites – particularly within the context of an overriding LNAPL Conceptual Site Model (LCSM)(ASTM, 2007). As knowledge of the new paradigm promoted for the occurrence, mobility, and limitations on recoverability of LNAPL in geologic media spreads, state regulatory policies are changing. Because such policy changes occur slowly, historical action levels and well-established regulatory policies remain hurdles to implementation of practical and achievable long-term strategies. In addition, application and integration of recently-developed investigative techniques still requires simplification of the relationships and resultant behavior often exhibited by sites with complex hydrogeologic or operational/release conditions and histories. In these cases, experience suggests that empirical data is best used to demonstrate LNAPL behavior characteristics and develop a sound management strategy.

In this paper, a case study is examined that provides examples of various investigative techniques applied to develop a practical and acceptable LCSM. The case study objectives are to prevent further migration of LNAPL and aqueous phase plumes, evaluate LNAPL recoverability and determine the “practical endpoint” of LNAPL recovery. This paper focuses on field methods to evaluate metrics critical to understanding LNAPL behavior and defining LNAPL recoverability. It reveals some benefits as well as limitations to integrating diverse

data sets in the development of a sound LCSM. The investigation methods also demonstrate that correlation of unique data sets is not simple or straightforward, because multiple variables affect LNAPL occurrences in wells and geologic media. LNAPL mobility and recoverability in the regolith (saprolite), which has relic fractures in a fine-grained low-permeability matrix, adds another level of complexity to these analyses. The development of acceptable endpoints for site restoration may be as much an issue of risk perception and tolerance as a technical challenge.

1.1 Site Setting and History

The site encompasses approximately 8 acres and is located in the Piedmont physiographic province of northwestern South Carolina. The geology is comprised of deeply weathered biotite gneiss parent rock with a mantle of regolith, aka “saprolite”. Both the unweathered bedrock and saprolite exhibit a structural fabric aligned southwest to northeast at the regional and smaller scales (Nystrom, 2002). Historical reports indicate that bedrock exists at depths of between 60 and 100 feet of land surface in the site vicinity, but no competent rock has been logged in wells installed at the site within depths of 85 feet. Depths to groundwater range from approximately 10 to 55 feet below ground surface, but exceed 40 feet across most of the site. Groundwater flows in a semi-radial pattern to the north-northeast and southwest (Figure 1) and mirrors surface topography. The land use surrounding the site is industrial and petroleum spills have been reported from three or more nearby properties. No operating water supply wells are known to exist within a half-mile radius of the site.

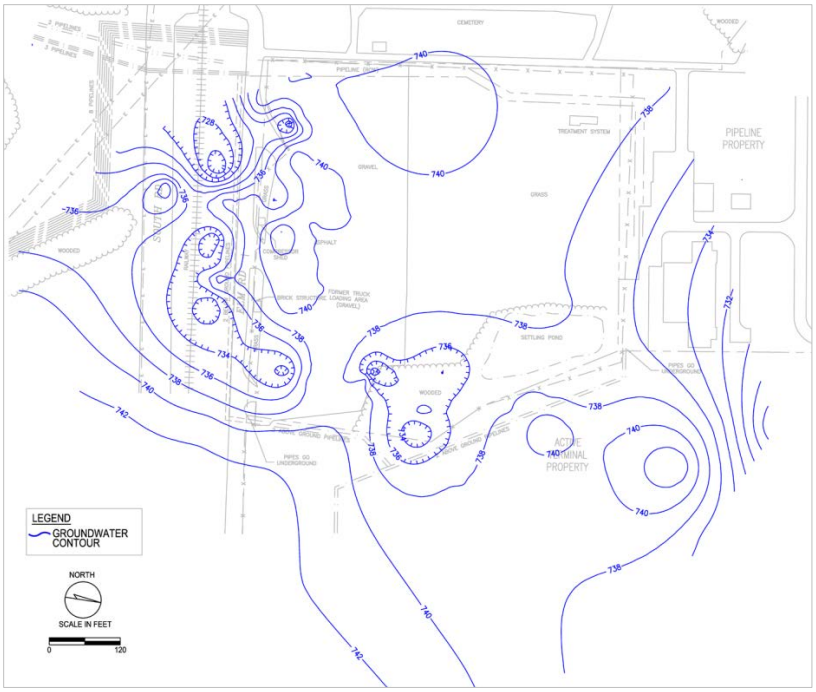

Figure 1. Regional Groundwater Contour Map

The site was operated as a petroleum bulk storage and distribution terminal from the 1940s through the late 1980s when it was closed and all tanks, piping and infrastructure were removed. A total of 53 monitoring wells, 24 recovery wells and 30 small diameter direct push (DP) points are located on or immediately adjacent to the site. The timing and sequencing of their installation is unknown, but most wells were installed from approximately 1987 through 1995 and four wells were installed as part of this updated LNAPL evaluation in 2011. Boring and well construction logs do not exist or are unavailable for review for all but the most recently-installed wells. Additional questions have been raised relative to the accuracy of apparent product thickness data obtained from the DPs as the construction of these points is unknown and it is also unknown whether they were ever developed. Further, as there is no practical means to evacuate LNAPL from the DPs, it has been postulated that they may act as local LNAPL traps as product collected there under variable water table conditions is highly unlikely to flow back into the fine-grained aquifer matrix. This relationship is discussed in a subsequent section of this paper.

A select number of wells and DPs are gauged on a biannual (twice per year) basis and groundwater samples are collected from 13 of these wells in accordance with the current compliance plan. Table 1 presents a synopsis of the

May, 2011 well gauging event where all monitoring wells and DPs were gauged. Anecdotal information indicates that the regional water table has declined in elevation since the inception of this project in the late 1980s. While historical records have not been located to validate this assertion, it is consistent with the large number of dry wells that currently exist across the site. It is also noteworthy that the DPs contain both a higher frequency of LNAPL occurrence and exhibit greater apparent LNAPL thickness relative to 2-inch diameter monitoring wells. This finding may be a function of location relative to the plume center and is also be revisited in Section 3 of this paper.

Table 1. Well Gauging Summary, May 2011

Monitoring wells:

# Wells Gauged (1)	# Wells dry	# Wells with NAPL	# Wells with NAPL > 3ft	Avg NAPL apparent thickness (ft.)
51	24	16 (59%)	9 (33%)	4.14

Direct Push Points (DPs):

# DPs Gauged	# DPs dry	# DPs with NAPL	# DPs with NAPL > 3ft	Avg NAPL apparent thickness
30	2	21 (75%)	19 (68%)	4.99

Recovery wells:

# Wells Gauged	# Wells dry	# Wells with NAPL	# Wells with NAPL > 3ft	Avg NAPL apparent thickness
21	0	5 (24%)	0	1.24

Note: (1) does not include 2 deep wells screened from 80-85 feet below grade

Groundwater and LNAPL recovery operations have been ongoing since approximately 1989. System design and operation has been geared towards prevention of off-site contaminant migration in accordance with a Consent Agreement in place between the property owner and the South Carolina Department of Health and Environmental Control (SCDHEC). Sixteen wells currently contribute total fluids to the recovery system at an aggregate rate averaging nearly 9 gallons per minute. LNAPL recovery has exceeded 159,000 gallons since 1992, and demonstrates a decreasing annual trend (Figure 2). Recent annual totals are on the order of 3,000 gallons per year. Some fluctuation in this value, particularly since 2004, is believed to have resulted from changes in contractor assignments and resultant system operations and maintenance (O&M) performance to include recovery well development and pump maintenance. In addition, recovery well yield testing suggests that nearly all of the on-site LNAPL recovery is occurring from well R-14 at present. The existing recovery system

does not have the capability to isolate or record individual recovery well contribution.

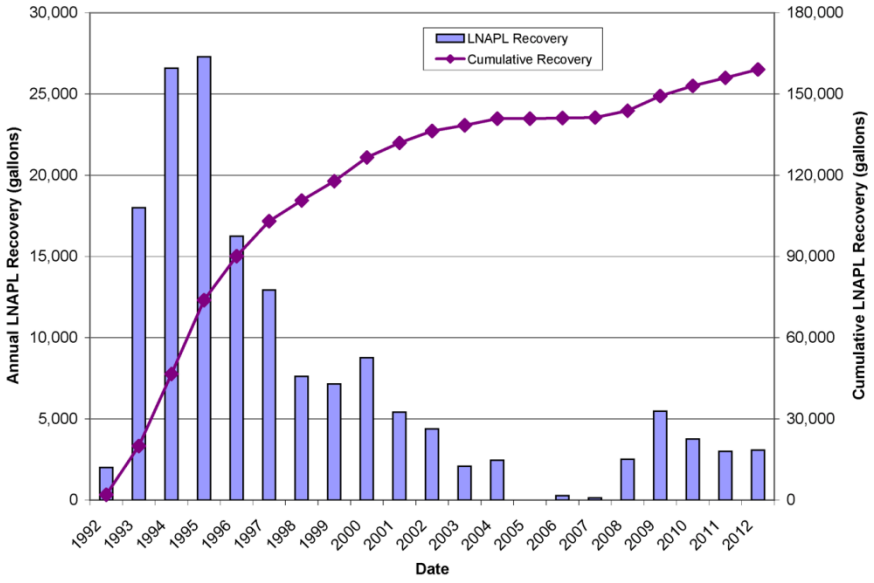

Figure 2. Historical Product Recovery

2. LNAPL OCCURRENCE AND INVESTIGATION

Well and DP gauging data reveal significant fluctuations in apparent product thickness over time and the interpretation of LNAPL extent can differ depending upon whether DP data are included or omitted. Comparison of apparent product thickness data between two-inch diameter monitoring wells and nearby ¾-inch diameter DPs, demonstrates similar overall thickness values and trends near the plume center (Figure 3A), but a disparity in thickness outside of the plume center locations, whereby LNAPL thickness in DPs is 2 to 5 times greater than in nearby wells, while thickness trends showed general agreement (Figure 3B). This finding has implications relative to LNAPL flux in the plume core relative to outer areas and may also point out differences in timing or ability for small diameter wells to reach equilibrium under dynamic fluid conditions. Owing to a number of dry wells existing across the site, the LNAPL plume extent is less well-defined along its western and southeastern edges.

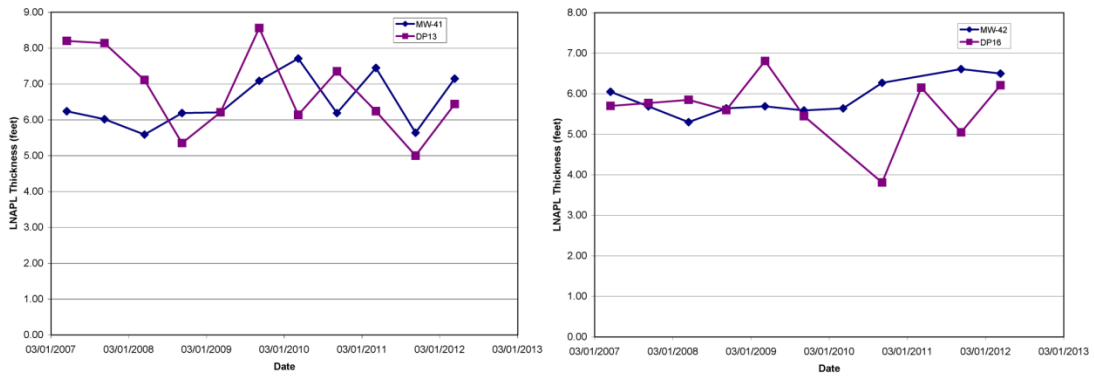

Figure 3A. Well and DP LNAPL Thickness Comparisons – Plume Core

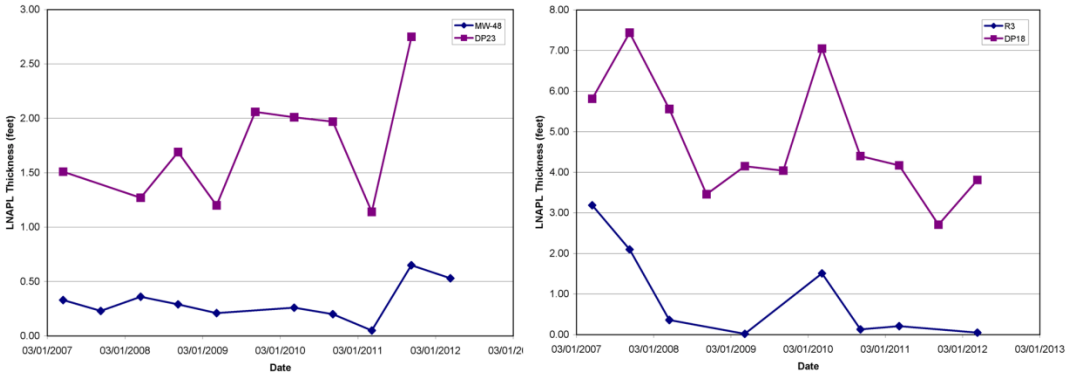

Figure 3B. Well and DP LNAPL Thickness Comparisons – Plume Periphery

Figure 4 shows the interpreted LNAPL plume (utilizing both monitoring well and DP data) as of May, 2012. Comparison of this figure to Figure 5, the LNAPL plume interpretation from September, 1994, indicates that the southern LNAPL plume boundary has contracted, and the plume core has also reduced in size and shifted slightly to the north of its 1994 location. Activation of recovery wells 21 and 22 in the 1995 time frame is believed to have attributed to the reduction in LNAPL south of the site. The apparent plume center movement, while not spatially quantified as per methods used to demonstrate plume stability (Ricker, 2008), does imply dynamic behavior in the plume core.

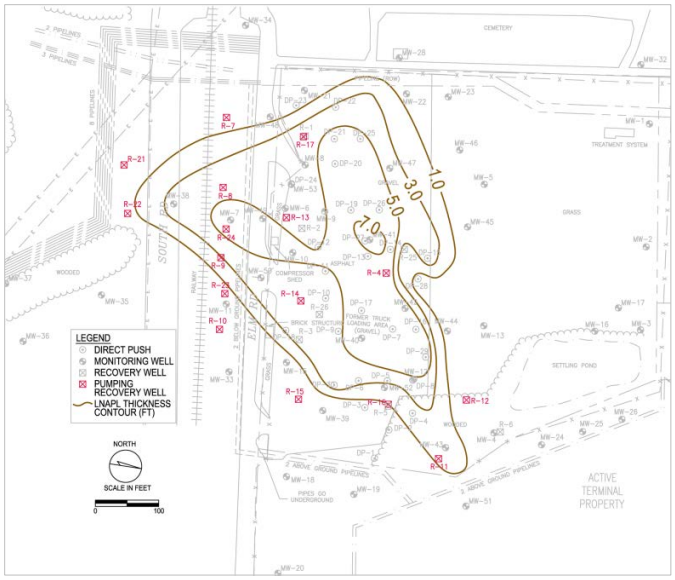

Figure 4. LNAPL Thickness, May, 2012

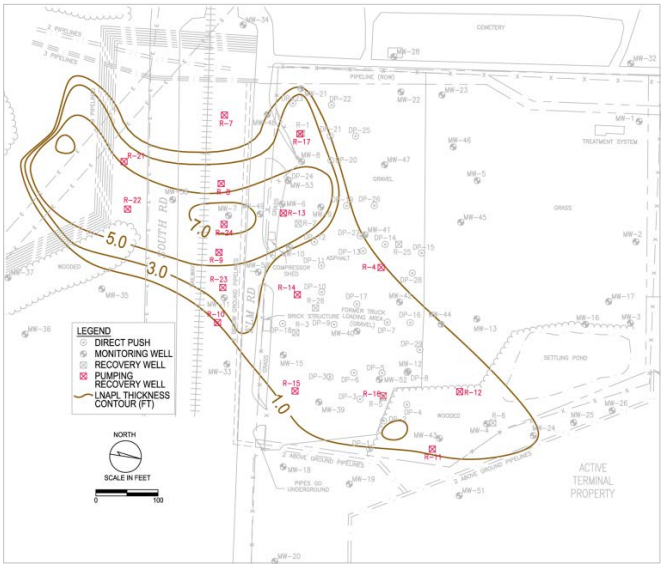

Figure 5. LNAPL Thickness, September, 1994

Historical site documents suggest that the LNAPL plume is comprised primarily of kerosene (or jet fuel) with some mixed weathered diesel. Forensic testing completed in 2004 validated the kerosene profile and little weathering appears to have not affected the LNAPL body. No discrete source has been identified in project documents. There is a relatively compact dissolved BTEX plume that extends beyond the fringes of the LNAPL footprint. Historical and

current gauging data compiled and reviewed indicates that the LNAPL plume is stable or shrinking as discussed above.

3. LIF INVESTIGATION AND FINDINGS

Given the extensive and poorly understood background of the site and data gaps presented through the currently dry wells near LNAPL plume boundaries, a Laser-Induced Fluorescence (LIF) survey was undertaken in 2009 to gain a better understanding of the LNAPL plume extent and configuration. In particular, it was hoped that this effort might shed light on the validity of fluid level data collected from the 30 DPs located across the site.

A total of 28 LIF borings and three additional hydraulic profiling tool (HPT) borings were advanced to depths ranging from 38 to 58 feet below ground surface. LIF data collection was continuous during probe advance and signal response showed significant variability with depth on a fine scale. Most LIF profiles returned responses near depths corresponding to the water table (i.e., in the 35 to 45 foot depth range) and mostly in the kerosene spectrum. However, most borings returning significant LIF instrument responses did so across a relatively narrow range (smear zone) of 5 feet or less, in some cases less than one foot. The LIF responses were characterized by moderate response levels with occasional thinner high levels or "spikes" suggesting a heterogeneous distribution of LNAPL controlled or influenced by relic fractures and/or foliation partings.

While the LIF results provided clarity related to the presence of compounds that fluoresce (typically PAH and aromatic fuel constituents), it is less certain that signal strength can be a reliable indicator of LNAPL mobility. As discussed in Section 4, there is a correlation between LIF response and oil transmissivity, but this relationship bears further investigation. A report by Alostaz and others (2008) indicates that fluorescence intensity is related to matrix physical properties (grain size, porosity and mineralogy), as well as fuel composition and compound presence. Their work indicated that fine-grained matrix materials can interfere with LIF signal response and fuel constituent differences due to weathering can also result in differing LIF responses for like matrices. Therefore, the heterogeneous matrix properties and fluid transport pathways of the saprolite aquifer are likely to impart multi-variant influences upon the LIF signal response.

Due to significant variability in signal response, expressed as the percentage of a reference emitter paste (%RE) on the recorded data plots, an effort was made to normalize the data set by summing all signal %RE responses above background and within a vertical profile in which LIF responses were observed. This was done by summing the four-channel digital response signals and producing one cumulative, dimensionless response value for each LIF boring.

This evaluation method was developed and instituted to reduce the influence of data spikes and impart a larger-scale "filter" to the data set. A contoured interpretation of these cumulative LIF response values is provided in Figure 6 along with oil transmissivity values (described in Section 4). These cumulative LIF response values show a distinct northeast to southwest orientation coincident with mapped bedrock fabric trends and also align closely with interpreted LNAPL thickness maps relative to maximum (plume core) and minimum (plume fringe) values.

Figure 6. Cumulative LIF Response and Oil Transmissivity

Additional findings of note from the LIF investigation include:

- The LNAPL signature as inferred from the LIF signal response spectra is primarily in the kerosene range, but responses correlating to weathered gasoline and weathered diesel were also noted in five or more borings - including three within the "core" LNAPL area.
- Most maximum LIF responses were recorded at depths below 35 feet; several exceptions were noted that indicate a separate fuel signature at more shallow depths. This finding suggests that kerosene is the more mobile NAPL at a site scale, which may be a function of the relative fuel spill volumes. Figure 7 includes LIF logs for borings L-6 and L-21 which provide examples of these findings.
- Extreme signal variation was noted in most LIF logs over short vertical intervals. This is also demonstrated in Figure 7 and may be related to increased oil saturation in small-scale secondary porosity features, fuel weathering in water-washed features, or signal interference from fine-grained particles in the non-fractured (bulk) saprolite matrix.

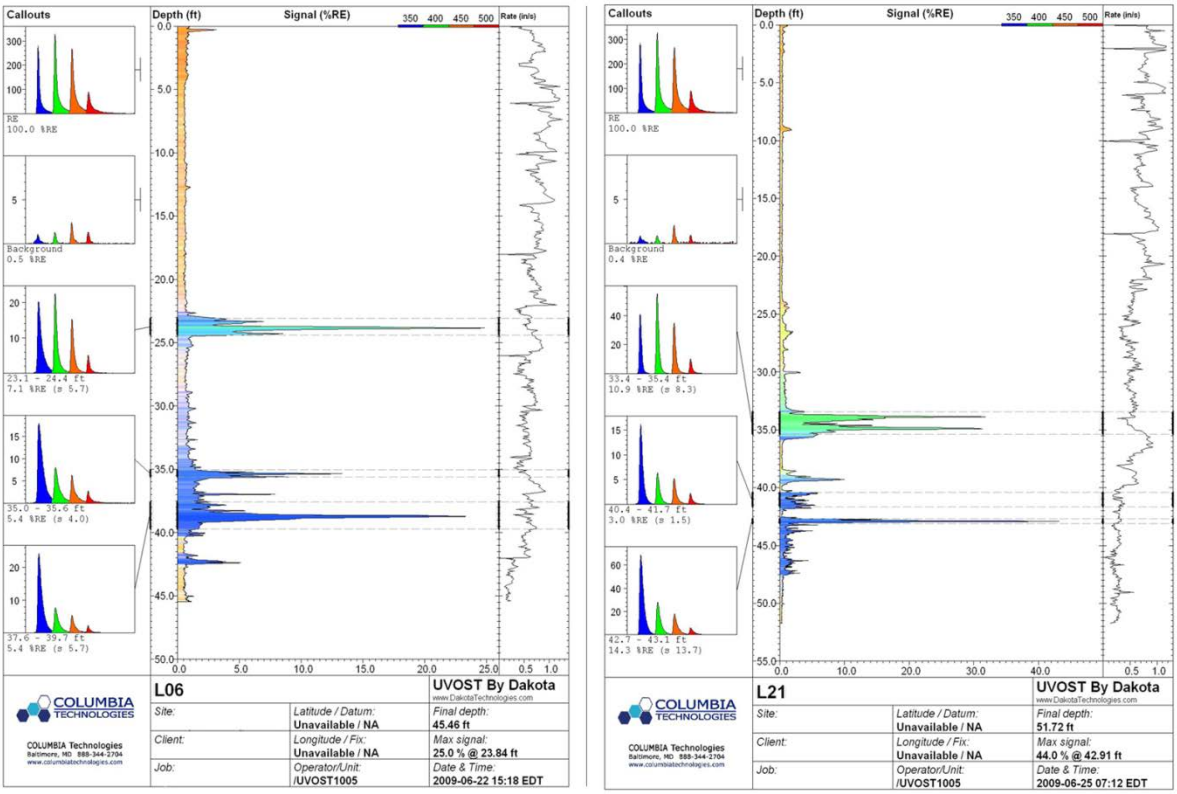

Figure 7. LIF Logs, L-06 and L-21

4. LNAPL TRANSMISSIVITY EVALUATION

LNAPL bail-down testing was completed at eleven (11) selected monitoring wells in June and October 2011 and May, 2012. This work was undertaken to better understand LNAPL mobility and recoverability. Table 2 presents a simplified summary of the data analysis. Calculation of oil transmissivity values, noted as T_o on Table 2, was undertaken utilizing the parametric method of Lundy and Zimmerman (1996), which is explained in greater detail in Lundy (2004) and Lundy (2006). The results for six of the wells fall within the range stated by ITRC to reflect LNAPL mobility, which is 0.1 to 0.8 ft^2/day (ITRC, 2009). Three wells (MW-38, R-25, and MW-50) yielded a T_o result in excess of this range and two (MW-52 and MW-47) returned values below the 0.1 ft^2/day mobility threshold. The top three T_o values of 2.05, 1.60, and 1.53 ft^2/day, respectively for these wells, show a similar spatial relationship to the center-of-mass or "core" LNAPL plume zone demonstrated in the LIF survey results. The well tested farthest to the west, MW-47, yielded the lowest T_o value (0.007 ft^2/day), again corroborating with the overall LIF survey findings. Further, of the nine T_o values calculated to be in the mobile LNAPL range, the lowest two correspond to wells located farthest downgradient (northeast) within the identified plume core. While there is insufficient data to make broad generalizations regarding oil transmissivity beyond these 11 data points, the general correlation with LIF findings suggests that LNAPL at the former Spartanburg terminal is significantly less mobile and recoverable outside of the "core" plume footprint and the spatial distribution is aligned coincident with mapped bedrock fabric. However, the less mobile LNAPL may still slowly drain from the surrounding areas to the linear zone connecting wells with the highest LNAPL transmissivities, if indeed they are fracture controlled as suggested below.

Table 2. Bail-down Test Data Summary

Well #	Test Date	Initial APT (ft)	T_o ft^2/day	T_o Rank	% recovery at 4 hours
MW-38	10/25/2011	2.69	2.050	1	28%
R-25	5/8/2012	3.34	1.600	2	37%
MW-50	6/21/2011	5.09	1.530	3	33%
MW-49	6/21/2011	5.38	0.760	4	48%
MW-41	6/21/2011	6.86	0.600	5	18%
MW-7	6/21/2011	4.55	0.470	6	85%
MW-53	5/8/2012	5.42	0.460	7	22%
MW-40	6/20/2011	4.76	0.460	8	26%
MW-42	6/20/2011	0.92	0.110	9	49%
MW-52	5/8/2012	4.26	0.030	10	11%
MW-47	6/20/2011	3.66	0.007	11	9%

Note: T_o calculated using Lundy & Zimmerman (1996) method and employing API database

Figure 6 provides an overlay of the LNAPL transmissivity and cumulative LIF response values. When compared with Figure 4, this figure reveals a spatial correlation amongst differing metrics for identification of the plume core. Additional bail-down test results from areas outside of the interpreted plume core could be employed to validate or strengthen this correlation. Despite large apparent LNAPL thicknesses, the baild own test and LIF evaluations coupled with historical LNAPL plume mapping and on-going liquid level monitoring, demonstrates that the plume is not expanding. Individual well yield testing indicated that nearly all LNAPL recovery is currently taking place from only one of 16 operational fluid recovery wells, where further strengthens this argument by removing active LNAPL recovery from the plume fringes as a mechanism to impede further LNAPL migration. Further, the most productive recovery well where LNAPL removal has been positively measured (R-14) is located within the plume core as defined by LIF and bail-down testing methods. Well R-14 falls on a line extrapolated from wells MW-38 and MW-50, demonstrating high oil transmissivity, and suggesting that they may be interconnected along a fracture with an approximate N30E bearing, similar to regional structural trends.

5. SOIL CORE ANALYSIS

In an effort to make quantitative evaluations of LNAPL mobility and recoverability and determine if practical correlations between these data and LIF data can be established, undisturbed soil core samples and fluid samples (both LNAPL and water) were collected from the areas near two of the LIF borings that returned the greatest response (L-02 and L-09) in July 2011. Undisturbed soil cores were collected in 3-inch diameter aluminum Shelby tube samplers, sealed, labeled, placed on dry ice (frozen), and shipped to an analytical laboratory for black (UV) light photography and analysis of physical and chemical properties of both the solid matrix and pore fluids. The core intervals selected for analysis were chosen to cover the smear zone and also match the maximum LIF response zones for the adjacent locations probed in 2009.

Six-inch diameter recovery wells (R-25 and R-26) were completed at these coring locations to depths of 59 and 60 feet, respectively. In addition, two-inch diameter monitoring wells (MW-52 and MW-53) were installed near the perimeter of the LNAPL plume core as interpreted by the LIF survey. These monitoring wells were installed in close proximity to DPs with apparent product thicknesses in excess of 3.0 feet in an effort to evaluate the reliability of the LIF data against the DP gauging data to best determine measurable LNAPL presence in the aquifer. These wells were also selected for LNAPL bail-down testing in May 2012. Table 3 presents a compilation of varied data obtained from the LIF survey, well gauging and new well installation activities. Figure 8 presents an

overlay of soil core photography, grain size distribution, and LIF response for the LIF-02 (R-25) and LIF-09 (R-26) locations. As shown on Figure 8 and in Table 3, the soil cores were further subdivided at the laboratory and tested for a range of parameters including grain size distribution, native and residual LNAPL saturation, water saturation and total porosity. These lab results are summarized in Table 4. Soil sub-cores were selected based upon the level of fluorescence noted in the total core via black light photography.

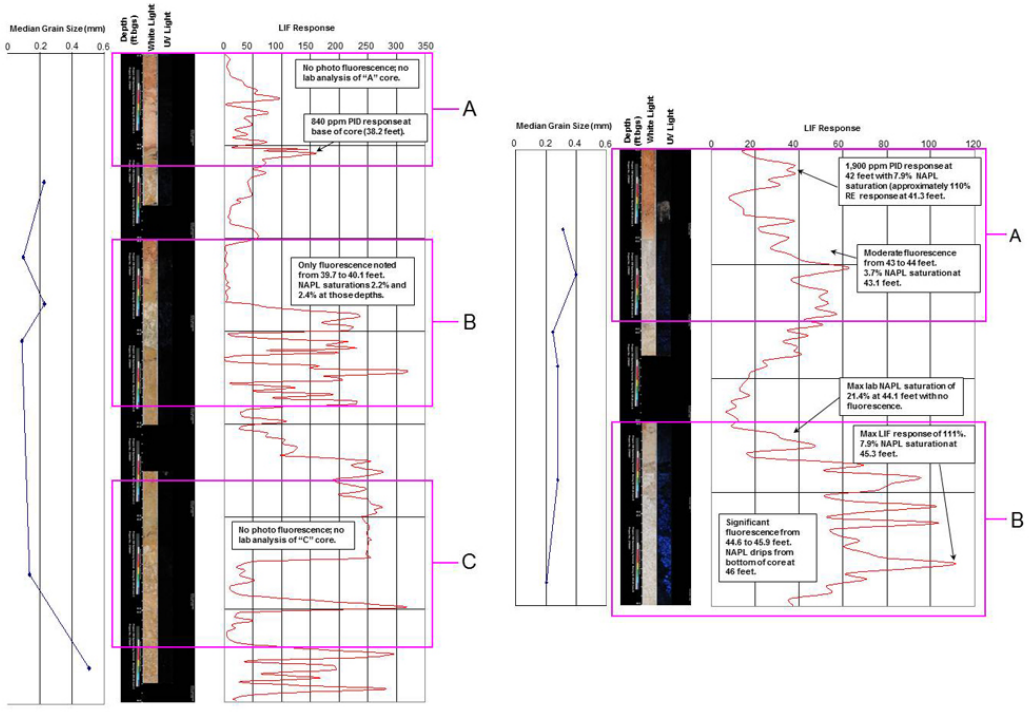

Figure 8. Soil Core and LIF Overlay

Table 3. LNAPL Assessment Data Summary

Well #	Depth	Max PID Response	Core Collection Depth (ft)	NAPL APT 8/9/2011 (ft)	Distance to LIF Boring (ft)	LIF Response (% RE)	Distance to DP well (ft)	NAPL APT in DP well* (ft)
MW-52	25	968	NA	0.71	55	23	5	3.06
ER-25	27	1070		0.88	2		8	4.64
	33	1150						
	38	840	37' - 38'2"			160		
	41.5-42.5	NM	39'- 40'8"			260		
	44.2	NM	41'6" - 43'4"			351		
ER-26	20	438		0.00	2		35	2.86
	30	1560				30		
	35	2130				38		
	40	2470				107		
	42	1900	42' - 43'9"			63		
	45.6	NM	44' - 46'2"			111		
MW-53	20	197	NA	2.38	32	19	10	3.48
	25	640						
	30	117						
	35	338						
	40	422						

Notes: NA - not applicable
NM - not measured
*NAPL apparent thickness (APT) shown from most recent gauging event of 5/6/11, not an average

Table 4. Soil Core Physical Data

Core Location	Center of Subcore Depth (feet)	Mean Grain Size	USDA Class	Median Grain Size (mm)	Native State LNAPL Sat'n (%)	Residual State LNAPL Sat'n (%)	Native State Water Saturation (%)	Residual Water Sat'n (%)	Total Porosity (%)
ER-25 Core A	38.4	Medium sand		0.227	3.7		71.4		45.1
ER-25 Core B	39.2	Fine sand		0.099	3.6		31.1		61.4
ER-25 Core B	39.7	Medium sand	Sandy Loam	0.231	2.2	2.2		38.7	43.2
ER-25 Core B	40.1	Fine sand	Sandy Loam	0.090	2.4	2.4		47.0	49.0
ER-25 Core C	42.6	Fine sand	Sandy Loam	0.140	4.5		80.2		46.4
ER-25 Core C	43.6	Medium sand	Loamy Sand	0.505	2.7		81.3		45.2
ER-26 Core A	42.2	Fine sand	Sandy Loam	0.202	7.9		25.7		61.1
ER-26 Core A	43.1	Fine sand	Sandy Loam	0.277	3.7	3.7		24.6	44.2
ER-26 Core B	44.1	Fine sand	Sandy Loam	0.278	21.4		52.2		48.6
ER-26 Core B	44.4	Fine sand	Sandy Loam	0.246	12.6		63.9		49.1
ER-26 Core B	44.9	Medium sand	Loamy Sand	0.401	10.3		65.0		42.8
ER-26 Core B	45.3	Medium sand	Sandy Loam	0.314	7.9	7.9		22.5	40.9
Averages				**0.3**	**6.9**	**4.0**	**58.9**	**33.2**	**48.1**

Evaluation of Figure 8 along with the data presented in Tables 2, 3 and 4 suggests some unexpected results relative to integration of LIF results, LNAPL measurements and soil core observations. These include:

- Core fluorescence as noted via black light photographs may not correlate directly with maximum LIF response or maximum lab-derived LNAPL saturations. This may be a function of scale, as the sub core is smaller and "interior" to the section of core photographed. Well R-26 clearly demonstrates these disparities.
- Greater emphasis may need to be placed on grain size in determining LNAPL mobility or recovery. Again, Well R-26 demonstrates this as it shows the greatest lab-determined LNAPL saturations (21.4% at 44.1 feet), but this occurs in a fine-grained matrix (0.278 mm average) and does not correspond to an elevated LIF response. No LNAPL has yet been measured in this well despite visual LNAPL presence at the base of the core at the 46 foot depth.
- An extremely high LIF response of over 300% RE from LIF-02 (or R-25) at a depth of 40.5 feet did not produce any noticeable fluorescence from the core photography and yielded a very low native state LNAPL saturation value of 2.4% from lab testing. The median grain sizes for the nearest tested intervals were also very small at 0.09 mm and 0.14 mm relative to an average for all tested core plugs at 0.3 mm. Measurable LNAPL has consistently been detected in Well R-25; bail-down testing completed at this well in May 2012 (10 months after installation and development) resulted in a high T_o value of 1.60 ft^2/day. Thus, LIF and LNAPL bail-down test results show agreement relative to significant mobile LNAPL presence at this location, but the soil core analyses do not support these determinations.

Some additional findings of note determined from evaluation of the field data presented herein include:

- LIF responses vary significantly over short vertical intervals. The elevated signals presumably denote LNAPL transport and are likely related to the presence of fractures or small-scale grain size variations. Accurate depth control is critical when collecting and analyzing these data sets, but directly intercepting such fractures or finding physical evidence of their presence in a core sample may be difficult to achieve in a field investigative program. Lundy and others completed a similar LNAPL investigation in a saprolite aquifer and concluded that one of six soil cores collected demonstrated evidence of having intercepted a transmissive fracture or foliation plane in the smear zone (Lundy, et al., 2004). The data derived from that core interval yielded a difference

in oil transmissivity in excess of an order-of-magnitude related to the balance of the tested sub-core intervals.

- The highest photoionization detector (PID) responses during coring and drilling were obtained from Well R-26, at a depth of 40 feet. A high LIF response (111% RE) was also recorded from R-26 at a depth of 45.6 feet, but no LNAPL has yet been measured in this 6-inch diameter well. LNAPL was visible during core collection at a depth of 46 feet in this borehole. Core analyses performed at the R-26 "Core A" interval (43.1 feet below grade surface (bgs)) and the "Core B" interval (45.3 feet bgs) reported native state LNAPL saturation values of 3.7% and 7.9%, respectively. The corresponding residual LNAPL saturation values for ER-26 "Core A" and "Core B" intervals were identical at 3.7% and 7.9%, respectively, indicating no free LNAPL available to migrate into the well. Again, these apparent data incongruities point out that empirical data (such as bail-down testing) is better suited to explain plume-scale LNAPL behavior.
- As evident in Table 3, maximum PID responses are all found at depths above the water table. PID response may be muted in the smear zone or at the water table depth and may not be a good indicator of LNAPL presence once in a groundwater-saturated regime.
- LNAPL has been detected in both monitoring wells installed (MW-52 and MW-53) as noted in Table 3. LNAPL was first noted approximately three weeks after well installation and development, suggesting low LNAPL migration rates. Maximum LIF responses for points located nearest these well locations were relatively low at 19% RE and 23% RE, respectively.
- R-25 may be the only well where results are as expected relative to LNAPL presence and thickness when compared to LIF results and LNAPL occurrence and thickness in nearby DPs; yet as mentioned above, little core fluorescence was noted. This again points out the difficulty in intercepting transmissive features in a bedrock or saprolite aquifer through the use of small-scale core and laboratory sub-core analysis methods. The probability of intercepting transmissive features would be expected to decrease as the feature becomes closer to vertical in orientation (i.e., steeply-dipping planar features).

6. CONCLUSION

The LNAPL investigation work summarized above represents only part of the full scope of work undertaken at this project site. Several conclusions can be reliably asserted to support LCSM development and focus for future project direction. These include:

- In-well LNAPL thickness is not a reliable means to evaluate product recoverability or mobility. This may be particularly relevant in small-diameter wells in a fine-grained aquifer matrix as evidenced by DP data, which consistently demonstrated LNAPL thicknesses in excess of 3 feet outside of the plume "core" as recently determined via LIF analysis and bail-down testing.
- Reasonable correlations can be made between cumulative LIF and oil transmissivity data to determine a plume core that may benefit from hydraulic recovery methods.
- Large-scale evaluation of plume extent and behavior is not likely to be sufficient for an understanding of recovery system optimization when working in a heterogeneous and/or fine-grained aquifer matrix. Variations in individual well behavior related to geologic structure, grain size or well efficiency can result in order of magnitude variations in the well, or LNAPL behavior that may not be apparent without undertaking individual well testing. These issues can be compounded by aged monitoring and recovery system infrastructure and the lack of or accurate records related to the construction of historical environmental quality data for components thereof.
- Empirical data relative to individual well LNAPL yield, historical LNAPL recovery trends and large-scale plume behavior is vital to LCSM and project strategy development – particularly in complex hydrogeologic environments. In the LCSM context, these data may prove valuable in demonstrating preferential aquifer attributes that may escape small-scale investigative techniques (i.e., coring).
- Grain size and grain size distribution, as well as location and orientation of planar features in fractured media (or saprolite), play a critical role in understanding LNAPL behavior. However, our ability to collect and evaluate these types of data sufficient to the scale of a LNAPL plume may be inadequate for the development of practical remedies as the probability of encountering transmissive features via small-scale core analysis is low. For this reason, plume-scale empirical data derived from well testing or a site-scaled survey to detect LNAPL is recommended.

- Comparison of in-well LNAPL bail-down testing results and LIF survey results using a cumulative data summation approach appears to offer a reasonable correlation for the determination of mobile LNAPL extent. This data also fits the LCSM developed for the project to include preferential flow influence related to aquifer structure and long-term plume recovery and migration history.

To the extent that questions posed for resolution at the outset of this LNAPL evaluation were not adequately answered, this work strengthened the reliance upon empirical data collection and analysis of multiple data sets to resolve uncertainties in data correlation and determination of management priorities. Use of cumulative LIF response data is encouraged for sites where heterogeneity imparts significant signal variation across the vertical zone of interest.

7. REFERENCES

Alostaz, M., Biggar, K..W. Donahue, R., and Hall, G. 2008. Soil Type Effects on Petroleum Contamination Characterization Using Ultraviolet Induced Fluorescence Emission-Excitation Matrices and Parallel Factor Analysis. Journal of Environmental Engineering & Science. 7, 661-675.

Charbeneau, R. and Beckett, G.D. 2007. LNAPL Distribution and Recovery Model, Vol. 1: Distribution of Petroleum Hydrocarbon Liquids in Porous Media. American Petroleum Institute.

American Society for Testing and Materials. 2007. Standard Guide for Development of Conceptual Site Models and Remediation Strategies for Light Nonaqueous-Phase Liquids Released to the Subsurface. Standard E2531-06.

Interstate Technology and Regulatory Council (ITRC). 2009. Evaluating LNAPL Remedial Technologies for Achieving Project Goals, Washington D.C.

Lundy, D. A. 2004. A Methodology for Evaluating LNAPL Conductivity and Transmissivity from LNAPL Bail-down Tests: The Lundy-Zimmerman Approach. Interactive LNAPL Guide. Version 2.0. American Petroleum Institute.

Lundy, D. A., 2006. Field Measurement of LNAPL Mobility and Soil Properties through Parametric Analysis of Product Bail-down Tests. Nat. Groundwater Assoc. Con.and Expo. November, 6-7.

Lundy, D.A., Parcher, M.P., Bennett, M., Brady, M., and Itin, C. 2004. Scale Dependency of LNAPL Occurrence and Migration through Relict Fractures in Saprolite – A Case Study from the Piedmont of North Carolina. NGWA Archives (Previously Groundwater On-Line).

Lundy, D. A. and Zimmerman, L.M. 1996. Assessing the Recoverability of LNAPL Plumes for Recovery System Conceptual Design. Nat.Groundwater Assoc. 10th Ann. Nat. Outdoor Action Con. and Expo.

Nystrom Jr., P.G. 2002. Geologic Map of the Spartanburg Quadrangle, Spartanburg County, South Carolina. South Carolina Geological Survey Open-File Report. OFR-144.

Ricker, J.A. 2008. A Practical Method to Evaluate Ground Water Contaminant Plume Stability. Ground Water Monitoring and Remediation 28(4), 85-94.

Chapter 14

DETERMINATION OF MERCURY IN ENVIRONMENTAL SAMPLES

Anthony Rattonetti[§], Mike Salvato, Grant Mays, Mike Nguyen, and Steven Z. Wen

Southeast Laboratory San Francisco Public Utilities Commission, 750 Phelps Street, San Francisco, California, USA, 94124

ABSTRACT

Hatch and Ott published their cold vapor atomic absorption method for the determination of mercury over 44 years ago. Since then, global interest in mercury in the environment and its reduction have increased enormously. While methods based on Hatch and Ott are still good choices currently, there have been significant advances in analytical methods and instrumentation that have given the environmental chemist more choices in performing the needed analysis of samples for mercury. The development of ICP-MS has been significant. Data is presented demonstrating that ICP-MS is in some cases a much better choice, especially when samples are analyzed for other toxic metals. The authors have also found that gold tetrachloride, a preservative for mercury, interferes with methods based on cold vapor atomic absorption procedures.

Keywords: mercury, soil, tissue, water, amalgam, ICP-MS

1. INTRODUCTION

In 1968, Hatch and Ott published a method for the determination of mercury (Hg) in rock samples (Hatch and Ott, 1968). They were employed by a mining company and needed a reliable and sensitive method to determine mercury in rock samples for exploratory purposes. Their method rapidly became the basis for the methods specifically developed for determination of Hg in environmental samples.

[§]Corresponding Author: Anthony Rattonetti, San Francisco Public Utilities Commission Southeast Laboratory, San Francisco, CA, USA 94124, 415-920-4967, trattonetti@sfwater.org.

It has been over 44 years since the publication of their method and accurate determination of Hg in the environment has become of paramount importance. Hg pollution in the environment has been an issue dating back to at least 1956 when Minamata disease was discovered. It was named after the city of Minamata in Japan. It was caused by the release of methyl mercury in industrial wastewater from the Chisso Corporation's chemical factory into Minamata Bay. It took place during the years 1932–1968, and resulted in the bioaccumulation of Hg in shellfish and fish that were eaten by the local population. Thousands of humans and their animals sickened or died. A settlement was not reached until 2010.

There are now global concerns regarding Hg pollution and the use of Hg and its compounds. Currently in the United States warning signs regarding Hg in seafood being sold are posted in seafood markets. In 1999, the USEPA began a national study on chemical residues in fish tissue (EPA, 2009). Hg was included in the study. Internationally, the Zero Mercury Working Group (ZMWG) was formed in 2005. It is composed of various organizations from 52 countries, and its goal is to reduce Hg in the global environment to a minimum. Domestically, Public Law 110-414 was passed in 2008, referred to as the "Mercury Export Ban Act of 2008." It requires a report to Congress on the Hg compounds that are used in significant quantities in products or processes, and effective 1 January 2013, prohibits the export of elemental Hg from the United States. Hg has been referred to as "Water Quality Enemy Number One" regarding the San Francisco Bay Estuary (Regional Monitoring Program, 2008).

After more than 44 years, are the methods that were developed from the original Hatch and Ott paper still the best to use? Do they always work as written? Have advances in analytical instruments provided more choices for the environmental chemist for the determination of Hg, as they have for the other metals? This paper reviews the methods and discusses these issues based on the authors' experiences in the determination of Hg.

2. EQUIPMENT AND SUPPLIES[†]

The inductively coupled plasma–mass spectrometer (ICP-MS) used was an Agilent 7500ce, with a collision/reaction cell and operated in the helium mode. Hg was measured at masses ^{200}Hg and ^{202}Hg. The data using ^{202}Hg was used for reporting purposes and the ^{200}Hg data used for confirming. Both Hg masses were in agreement. Gold (Au) was measured at ^{197}Au to confirm that it was added as a preservative. The internal standard of platinum (Pt) was measured at ^{195}Pt at a concentration of 50 µg/L. It was fitted with a Burgener Research Mira Mist® all-Teflon® nebulizer. The ICP-MS instrument also contained Au at a concentration

of 2 µg/mL to reduce instrument memory effects. The inductively couples plasma – atomic emission spectrometer (ICP-AES) was a Jobin Yvon 138 ULTRACE and also fitted with a Burgener Research Mira Mist® all-Teflon® nebulizer.

Several types of cold vapor atomic absorption (CVAA) instruments were used: a Varian 220FS with VGA-77 accessory, a CETAC M6000A, and a CETAC M6100. The cold vapor atomic fluorescence (CVAF) instrument used was an automated Brooks Rand MERX® system.

Two types of digestion blocks were used: a SCP Sciences DigiPREP® and an automated Thomas Caine (TC) DEENA®. Both types used a SCP polypropylene digestion vessel, with a nominal volume of 65 mL and dimensions of 30 (D) x 110 (H) mm.

The ICP-MS autosampler was installed, and EPA 3050B digestions and 1631 based sample preparation and digestions were performed in an all plastic HEPA total exhaust fume hood. Industrial waste samples were prepared in a conventional fume hood.

3. REAGENTS AND STANDARDS†

Reagent water met the specification of ASTM Type I water. All acids used to prepare industrial waste water, soil; tissue samples and calibration standards for ICP-AES and CVAA were J. T. Baker Instra-Analyzed ® grade. Acids used to prepare BrCl, ICP-MS and CVAFS calibration standards were J. T. Baker Ultrex® II or SCP Science PlasmaPURE® Plus.

Certified reference materials (CRMs) were purchased from ERA, Arvada, CO, USA; National Institute of Standards and Technology (NIST), Gaithersburg, MD, USA; and National Research Council of Canada (NRCC), Ottawa, Ontario, Canada. CRMs were chosen to include the range of Hg in the samples where possible. Mercury stock solutions were purchased from a variety of manufacturers and diluted as needed.

†The mention of trade names or commercial products in this paper is for illustrative purposes only, and does not constitute a San Francisco Public Utilities Commission endorsement or exclusive recommendation for use.

4. PRESERVATION AND HOLDING TIME

4.1 Nitric Acid (HNO_3)

The standard procedure to preserve water samples based on EPA Methods 245.1 (USEPA 1994a) and 7470A (USEPA 1994b) is to add HNO_3 to water samples to make the pH less than 2. Typically 1 or 2 mL per liter of sample is adequate. The maximum holding time is 28 days from the date of collection; however in the authors view, it is best to determine Hg as soon as practically possible due to the capricious stability of Hg when only preserved with HNO_3

4.2 Bromine Monochloride (BrCl)

The standard procedure to preserve water samples based on EPA Method 1631e (USEPA 2002) is toadd 5 mL/L of BrCl (0.2 N). Samples should turn a pale yellow and maintain the color until analysis. Some samples will require more BrCl. The maximum holding time is 90 days from the date of collection. See also 5.1.2.

4.3 Hydrochloric (HCl) or Sulfuric Acid (H_2SO_4)

These acids are used if methyl mercury is to be determined, according to EPA 1630 (USEPA 2001a). Fresh water samples are to be preserved by adding 4 mL/L of HCl (12N). Saline samples with chlorides >500 mg/L are to be preserved by adding 2 mL/L of H_2SO_4 (9M). According to this method, acid preserved samples are stable for at least six months if kept dark and cool. HCl may also be used to preserve samples for EPA 1631e if methyl mercury is to be determined in the same sample container.

4.4 Gold Tetrachloride ($AuCl_4^-$) Combined with HNO_3

The use of a combination of $AuCl_4^-$ and HNO_3 was developed by NIST (Moody *et al*. 1976) to stabilize Hg and develop Standard Reference Materials (SRM) for Hg. Au, as the tetrachloride, was added at a concentration ten times that of Hg. Initially, it was believed that the Hg would be stable for at least one year. Two SRMs were developed: SRM 1641 (1975, 1.49 µg/mL) and SRM 1642 (1974, 1.18 ng/mL). SRM 1641 was developed for the preparation of calibration solutions or for use as a spiking solution, i.e., to be significantly diluted. A

dilution factor of 1000 is recommended on the certificate. It is currently available as SRM 1641d (issued 2008, 1.557 ug/g) and the amount of Au was reduced to about 1 µg/g. The certificate is valid until 1 October 2014. SRM 1642 was intended to be used as received without dilution or other alteration. It was last issued as SRM 1642b (1982, 1.49 ng/mL) and it is no longer available.

Unfortunately, Au interferes when determining Hg using CVAA and CVAF. See Section 6.0.

4.5 Potassium Dichromate ($K_2Cr_2O_7$) Plus HNO_3

Hg solutions containing 5% HNO_3 and 0.05% $K_2Cr_2O_7$ have been found to stabilize dilute Hg solutions (Feldman, 1974; Lo and Wai, 1975). Standards prepared and stored in glass or Teflon containers will be stable for months.

This preservation method was also the basis for the determination of inorganic and organic Hg with graphite furnace atomic absorption when used as a matrix modifier (Rattonetti, 1980; Keller *et al*, 1984).

4.6 Freezing

The Appendix to EPA 1631 allows solid samples to be stored for up to one year if they are frozen at < -15 °C.

4.7 Sample Contamination or Loss During Storage

Samples collected for trace Hg (ng/L amounts) should only be collected in glass or fluoropolymer bottles. Caps for both should be fluoropolymer or fluoropolymer lined. It is recommended to also follow EPA 1669 to avoid inadvertent contamination (USEPA, 1996a).

5. MATRICES

5.1 Aqueous Samples

The various EPA methods employ two digestion procedures followed by the addition of hydroxylamine hydrochloride ($NH_2OH•HCl$) (or sulfate) and stannous chloride ($SnCl_2•2H_2O$), and one procedure for the direct sample analysis for low turbidity.

5.1.1 EPA 245.1 and 7470A Digestions

Subsamples are heated for 2 hours at 95 °C in a capped vessel after the addition of HNO_3, H_2SO_4, potassium permanganate ($KMnO_4$), potassium persulfate ($K_2S_2O_8$). Prior to analysis, NH_2OH•HCl is added to reduce the excess permanganate. The $SnCl_2$•$2H_2O$ addition may be added automatically by the instrument.

There are generally no problems with the analysis of drinking water or treated wastewater by this procedure; however, industrial waste samples may need modification to the method. The amount of $KMnO_4$ had to be doubled to meet the spike recovery limits of 70 – 130%. The problem samples did maintain the purple color for at least the required 15 min prior to adding the additional $KMnO_4$. Medical center samples were especially problematic. See Table 1.

5.1.2 EPA 1631 Digestions

If samples were initially preserved with HCl, BrCl (0.2N) is added to samples or subsamples and capped. Samples are then digested at room temperature for at least 24 hours. A persistent pale yellow color must be maintained until the samples are analyzed. It is best to add the BrCl directly into the container of the original sample rather than a subsample. The method default amount is 5 mL BrCl per L of sample; however, the authors have found that for treated wastewater effluent samples at least 10 mL/L is needed. If in doubt, the samples can be tested with potassium iodide indicator paper just prior to analysis. Wastewater treatment plant influents may take 100 mL/L or more of BrCl and would best be analyzed by EPA 245.1. Overall, the method works very well so long as contamination is minimized. Instruments that offer automation are clearly preferable to the manual method, as described in the EPA method.

Table 1. Recoveries of Hg spikes at the level of 25 µg/L made to industrial waste samples from medical centers.

Reagents	Study 1	Study 2	Study 3
Conc. H_2SO_4, mL	1.0	1.0	1.0
Conc. HNO_3, mL	0.5	0.5	0.5
5% $KMnO_4$, mL	3.0	6.0	6.0
5% $K_2S_2O_8$ mL	1.6	1.6	3.2
12% NH_2OH•HCl, mL	2.0	4.0	4.0
ID	Conc µg/L / %R	Conc µg/L / %R	Conc µg/L / %R
Medical Center A	22.0	40.7	42.0
Medical Center A Duplicate	10.3	41.2	41.4
Medical Center A Spike	16.4 / 0	62.1 / 86	62.5 / 82
Medical Center A Spike Duplicate	16.7 / 26	61.8 / 82	62.5 / 84
Medical Center B	ND 0.02	0.14	0.14
Medical Center B Duplicate	0.06	0.10	0.14
Medical Center B Spike	15.0 / 60	21.4 / 85	23.4 / 93
Medical Center B Spike Duplicate	16.1 / 64	20.9 / 83	22.8 / 91

Note: The %R of the first spike was calculated using the sample result; however, the spike duplicate used the sample duplicate.

5.1.3 Samples with Low Turbidity

EPA Method 200.8 (USEPA 1994c) allows for the direct determination of metals, including Hg, if the turbidity is < 1 NTU. The only preparation required is

to make the samples 1% in HNO_3, otherwise, samples must be digested using EPA Method 200.2 (USEPA 1994d). Hg is not approved in this instance because of potential loss of organic Hg during heated digestion. Studies conducted by the authors have shown that inorganic Hg spikes are fully recoverable down to at least 0.000025 ug/L (25 parts per trillion). A study was also made using methyl Hg spikes. Unfortunately, recovery was only in the range of 20 – 30% for methyl Hg.

6. SOLID SAMPLES

6.1 Dental Waste Water (DWW)

Hg in DWW is considered to be a significant source for Hg in the environment (SFPUC, 2003; Zhao et al, 2008; Lubick, 2008)

In 2003, the city and county of San Francisco implemented a Dental Amalgam Reduction Program because the San Francisco Regional Water Quality Board's revised 2002 NPDES discharge permit significantly reduced the amount of mercury the San Francisco Bay area treatment plants could discharge into San Francisco Bay. Additionally, the new permit required cities to implement a Hg source reduction program. During 2003-2006, a special study was conducted to evaluate the amount of Hg being discharged by dental offices. The maximum amount of Hg that can be discharged into the San Francisco sewer system is 0.05 mg/L (total). The typical sample size is 1 L. It is unlikely that a subsample in the typical range of 20-100 mL would include an amount of amalgam that weighed only 0.05 mg. To ensure that all of the Hg contributed from the amalgam would be determined, the entire sample was analyzed for Hg using the following modified EPA 7471B (USEPA 2007a) procedure:

The samples were preserved with HNO_3 to pH < 2, typically 2 mL/L upon receipt at the lab. The samples were allowed to stand until the solids settled. The supernatant was carefully decanted without disturbing the solids at the bottom of the bottle. Hg was determined in the supernatant using EPA 245.1. The bottle with sediment was then placed in a 60 $^{\circ}$C oven to dry. After removing from the oven and cooling, the bottle with the dried solids was weighed to the nearest 0.001 g. The Hg concentration in the solids was determined using EPA 7471B. Ten mL of reagent water and 10 mL of aqua regia were added to the samples and they were digested in a water bath for 30 min at 95 $^{\circ}$C. They were removed from the water bath and cooled. The samples were returned to the water bath after adding 100 mL of reagent water and 30 mL of 5% potassium permanganate solution and the 30 min digestion was repeated. After the samples were removed from the water bath and cooled, 25 mL of concentrated HCl was added and then

reagent water added to bring the volume to 500 mL. The purpose of the HCl step is to keep silver (Ag) in the solution and enable its determination since it is also a constituent of amalgam. The solids were allowed to settle overnight. Various soil certified reference materials were also processed to evaluate the accuracy of the digestion procedure. Hg and Ag were then determined by ICP-AES. Samples that contained Hg < 0.1 mg/L were analyzed by CVAA with a Varian 220FS equipped with the VGA-77 Hg vapor generator. It was important to screen on the ICP-AES first because samples with high Hg concentrations caused severe memory effects with CVAA and the VGA-77 would have to be cleaned. The sample bottle is emptied, rinsed and dried for 24 hours at 95 $^{\circ}$C. The weight of the solids that were digested was determined by subtracting the weight of the dried bottle from the weight of the original bottle that contained the dried solids. After the Hg in the solids was determined, it was converted to mg/L in the original volume and added to the amount of Hg in the supernatant. Most all of the Hg was in the solids. For example, a sample contained only 0.0007 mg/L Hg in the supernatant, but when the Hg in the solids was added, the actual concentration of Hg in the sample was 3.11 mg/L.

6.2 Soil Samples

The EPA method 6020A (USEPA 2007b) states: "If Hg is to be analyzed, the digestion procedure must use mixed HNO_3 and HCl through all steps of the digestion. Hg will be lost if the sample is digested when HCl is not present." The method documentation does not present any data from the analysis of certified reference materials (CRM). It does provide data comparing ICP-MS and CVAA from the analysis of heavily contaminated soil; however, there were many significant differences between the data for the two methods.

Several different CRMs at a range of concentration were analyzed using EPA 3050B (USEPA 1996b) digestion procedures. It was modified by including HCl in the beginning of the digestion. The samples were thoroughly mixed and approximately 0.5 g (dry weight) was weighed into polypropylene digestion vessels (SCP). Then 2.5 mL each of HNO_3 and HCl were added. The samples were placed into a non-metallic digestion block, fitted with a plastic watch glass and heated at 95±5 $^{\circ}$C for 30 min, cooled for 15 min, and 2.5 mL of HNO_3 and HCl were added and heated for another 30 min. The samples were then removed from the digestion block and cooled 30 min prior to adding hydrogen peroxide (H_2O_2). Use caution during the addition of H_2O_2 as it can result in a very vigorous reaction. Following the addition of 2 mL reagent water, 0.5 mL of H_2O_2 was added. After 5 min, an additional 0.5 mL of H_2O_2 was added. The H_2O_2 addition was repeated two more times, with a 5 min wait in-between to prevent an overreaction. After the final addition, a 15 min wait was implemented before

proceeding. Samples were placed back into the digestion block and heated for 60 min at 95±5 °C. They were then cooled for 15 min, 2.5 mL of HNO_3 was added, samples were heated for 15 min, cooled for 15 min, and brought to a final volume of 50 mL. Au as the tetrachloride was added to enable long term preservation of the Hg. The digestion procedure is tedious when performed manually, and the use of a robotic type digestion block (such as Thomas Caine, Inc. DEENA) can facilitate it somewhat. Prior to analysis with collision/reaction cell ICP-MS, samples were diluted a factor of ten with reagent water, gold was added to maintain a concentration of 2 µg/mL, and internal standards were added. The dilution was necessary to prevent damage to the ICP-MS cones from the acid and reduce the chloride concentration.

The results using EPA 3050B digestion and 6020A analysis on the various reference materials are in Table 2. Digestion using EPA 7471B is also shown for several of the low concentration CRMs.

6.3 Fish and Other Marine Tissue Samples

6.3.1 EPA 3050B Digestions

Various marine tissues are analyzed yearly to monitor the environmental effects the San Francisco Public Utilities Oceanside Wastewater treatment plant's discharge into the Pacific Ocean 3.5 nautical miles offshore. A modified EPA 3050B digestion procedure was used to prepare samples for the analysis of mercury and other metals in marine tissues. The automated procedure is described:

The % solid was determined on a separate portion of each sample. On day one, homogenized samples were weighed, to the nearest 0.001 g, directly into polypropylene digestion vessels. The wet weight of each sample that has approximately 0.5-1 g of dry weight wasweighed into the digestion vesseland placed into the sample racks. Polypropylene or Teflon® watch glasses, with a hole in the center for reagent dispensing, were placed on each vessel. Five mL each of concentrated HNO_3 and HCl were dispensed into each digestion vessel. After all acids have been dispensed the digestion program pauses to allow room temperature digestion to occur overnight. On day two, the program was started again. Samples were shaken for 15 s then lowered into the digestion block and heated for 30 min at a block temperature that will achieve a sample temperature of 95±5 °C. Do not allow to boil. Samples were then raised out of the block and cooled for 15 min. Then 0.5 mL of H_2O_2 (30%, high-purity grade, and un-stabilized if tin is to be determined) was added to each vessel. The vessels were lowered again into the digestion block and heated for 30 min then raised out of

the block and cooled for 15 min. The H_2O_2 addition with associated heating and cooling was repeated a second time. Then 1 mL of HCl was added to each vessel followed by 1 mL of H_2O_2 and the vessels were lowered into the block and heated for 30 min then raised out of the block and cooled for 15 min. Then the H_2O_2 addition with associated heating and cooling was repeated two more times. Reagent water was then added to bring the final volume to 50 mL.

Au was immediately added at a concentration of 2 µg/mL. Prior to analysis with collision/reaction cell ICP-MS, samples were diluted a factor of ten with reagent water, gold was added to maintain a concentration of 2 µg/mL, and internal standards were added. The results on the various reference materials are in Table 3. The amounts of methyl mercury of the total mercury in the CRMs are 91% (SRM 1946 Lake Superior Fish Tissue), 92% (SRM 1947 Lake Michigan Fish Tissue), 36% (SRM 1566b Oyster Tissue, and 46% (SRM 2976 Mussel Tissue). SRMs 1946 and 1947 are frozen tissue homogenates. SRMs 1566b and 2976 are freeze-dried materials.

Table 2. EPA 3050B sample prep and 6020A analysis results for the determination of Hg in various soil CRMs (mg/Kg).

CRM:	ERAD065-540	SRM 2709	SRM 2711	SRM 1646a	NRCC MESS-3
Value, mg/Kg:	6.8 ±5%	1.40±5.7%	6.25±3%	(0.04)	0.091±9.9%
Method	Conc/%R	Conc/%R	Conc/%R	Conc/%R	Conc/%R
EPA 3050B/6020A	6.59 / 96.9	1.53 / 109	6.45 / 103.2	0.015 / 37.5	0.069 / 75.8
	6.22 / 91.5	1.58/ 112.9	6.46 / 103.3	0.025 / 62.5	0.084 / 92.3
				0.030 / 75	0.111 / 122
				0.060 / 150	0.145* / 159
				0.035 / 87.5	0.108 / 119
EPA 7471B				0.021 / 52.5	0.082 / 90.1
				0.036 / 90	0.071 / 78.0
				0.06 / 150	0.092 / 101

*Analyzed immediately after ERA D065 without additionally rinsing. High concentration samples may need additional rinsing to prevent memory effects.

Table 3. EPA 3050B sample prep and 6020A analysis results for the determination of Hg in various tissue CRMs (mg/Kg).

CRM:	SRM 1946	SRM 1947	SRM 1566b	SRM 2976
Value, mg/Kg:	**0.433 ± 2.1%**	**0.254 ± 2%**	**0.0371± 3.5%**	**0.061± 5.9%**
Analysis Date	**Conc/%R**	**Conc/%R**	**Conc/%R**	**Conc/%R**
June 2011	**0.360 / 83.2**	**0.223 / 87.7**	**0.0380 / 102**	**0.049 / 80.8**
June 2011			**0.0386 / 104**	**0.057 / 93.8**
August 2012	**0.409 / 94.5**	**0.234 / 92.1**	**0.0370 / 99.7**	**0.062 / 102**
August 2012	**0.397 / 91.7**	**0.262 / 103.1**	**0.0380 / 102**	**0.054 / 88.5**
August 2012			**0.044 / 119**	**0.071 / 116**
August 2012			**0.034 / 91.6**	**0.060 / 98.4**

6.3.2 Appendix to EPA 1631 Digestions

During 2007, a small study of mercury in fish conducted by the State of California's Water Resources Control Board's Surface Water Ambient Monitoring Program (SWAMP) found elevated levels of mercury in two trout caught in the Hetch Hetchy Reservoir. In subsequent years, the San Francisco Public Utilities Commission, along with other organizations, conducted a more thorough study. Over 400 trout were caught and analyzed for mercury. The sample preparation procedure was adapted from the Appendix to EPA Method 1631 (USEPA 2001b). The EPA also used this procedure in their national study of chemical residues in lake fish tissue (USEPA, 2000). The EPA omitted the sulfuric acid in their modification. The SFPUC's modified procedure varied primarily in the type of digestion vessel used and the samples were not allowed to boil. The same reagents were used, but the acids were added the day before. The EPA procedure does not specify to use Au as a preservative.

Approximately 0.5 g of sample was weighed into a polypropylene digestion tube, and then 10 mL of a mixture of HNO_3 and sulfuric acid (7/3 ratio) was added to each sample. It was loosely capped and allowed to sit overnight at room temperature. The following morning, the loosely capped tube was heated for 180 min at 95 ^{o}C in the digestion block (SCP). After the digestion was completed, the

solution was brought to a final volume of 40 mL with 0.02 N BrCl and mixed. Gold tetrachloride was added to all samples at a concentration of 2 µg/mL as a preservative. Initially, it was planned to determine mercury using CVAA; however the % recovery of the mercury was very low in the CRMs. That was a surprise since preliminary studies using ICP-MS as the final determinative step found that the CRMs % recovery were in the acceptable range. Therefore, the samples were diluted by a factor of ten with reagent water to prevent the damage to the ICP-MS cones. Au was added to maintain the concentration in the samples at 2 µg/mL . The internal standard was also added at this time. Table 4 shows representative results for SRM 1947 used in this study. To evaluate the effectiveness of Au as a preservative, samples were randomly selected and analyzed many months later. These results are also included in the table. Similar results were also obtained for the analysis and re-analysis of SRM 1947.

Table 4. Appendix to EPA 1631 sample prep and 6020A analysis and re-analysis results for the determination of Hg in SRM 1946n (mg/Kg).

1st Analysis Date	Conc, mg/Kg	% Recovery	2nd Analysis Date	Conc, mg/Kg	% Recovery
3/21/2012	0.399	92.1	1/18/2013	0.405	93.6
3/26/2012	0.460	106.2	1/18/2013	0.434	100.3
3/28/2012	0.425	98.2	1/18/2013	0.417	96.3
4/2/2012	0.383	88.5	1/18/2013	0.411	95.0
4/11/2012	0.459	106.0	1/18/2013	0.445	102.7
4/30/2012	0.442	102.1	1/18/2013	0.470	108.6
5/2/2012	0.418	96.5	1/18/2013	0.425	98.1
5/7/2012	0.405	93.5	1/18/2013	0.410	94.7
5/14/2012	0.453	104.6	1/18/2013	0.451	104.2
5/22/2012	0.408	94.2	1/18/2013	0.388	89.7
5/29/2012	0.472	109.0	1/18/2013	0.417	96.4
6/6/2012	0.354	81.8	1/18/2013	0.411	95.0
Average	0.423	97.7		0.424	97.9
s	0.035	8.2		0.023	5.2

It was suspected that the interference using CVAA was due to the Au preservative. A study was conducted involving the addition of various amounts of Au as the tetrachloride to Hg solutions. The CVAA instrument (CETAC B) was calibrated with BrCl in the calibration standards, but no Au. Au was then added at varying amounts to the calibration standard and it was analyzed as a sample. The concentration was 4 ng/mL since that would be the approximate concentration range for SRM 1946 after it was digested. The gold concentrations in µg/mL were 0.04, 0.1, 0.5, 1, and 2. The % recoveries were 82%, 49%, 19%, 12%, and 9%, respectively.

It was earlier discovered that Au severely suppressed the recovery when a 1631e type of instrument (BR) was used. Method 1631 briefly mentions that gold interferes, but did not give any details. The relatively high concentrations of Hg in the tissue samples would have required significant dilution to lower the concentration into the linear range of the instrument. When an original prepared sample containing Au at the level of 2 mg/L is diluted by a factor of 50, the Hg signal is still suppressed about 20 – 25%, even though the Au concentration was reduced to 0.04 mg/L.

7. CONCLUSIONS

Determination of Hg using methods that are based on Hatch and Ott's chemical reduction of Hg to a vapor still have a place in modern day environmental chemistry; however, for some applications, methods that utilize ICP-MS may be preferable. EPA Methods 245.1 and 7470 are still more appropriate for the determination of Hg in drinking water and industrial waste samples; however, industrial waste samples may require more than the default amount of reagents specified in the methods. In special applications, such as the determination of Hg in DWW or similar type samples, the solids may have to be digested separately from the aqueous phase to accurately determine the amount of Hg in the samples.

EPA Method 3050B digestion and final determination by 6020A are capable of fully recovering both inorganic and organic forms of Hg. This would be the most cost effective and efficient way to determine Hg if other elements are also to be determined in the samples.

If only Hg is to be determined, EPA 7471b may be preferable for soil samples and the Appendix to Method 1631 preferable for tissue samples; however, the scope and application of the appendix method includes soils also.EPA Method 7473 (USEPA 2007c) may also be considered. If gold is used to preserve the samples for later Hg determinations it will cause aninterference if using CVAA or CVAF methods. ICP-MS determinations are not affected by the presence of Au in the samples.

8. REFERENCES

Feldman, Cyrus. 1974. Preservation of Dilute Mercury Solutions. Ana. Chem. 46, 99-102.

Hatch, W.R., and Ott, W.L. 1968. Determination of Sub-Microgram Quantities of Mercury by Atomic Absorption Spectrophotometry. Ana. Chem. 40, 2085-2087.

Keller, B.J., Peden, M.E., and Rattonetti, A. 1984. Graphite-Furnace Atomic Absorption Method for Trace-Level Determination of Total Mercury. Ana. Chem. 56, 2617-2618.

Lo, J.M., and Wai, C.M. 1975. Mercury Loss from Water during Storage: Mechanisms and Prevention. Ana. Chem. 47, 1869-1870.

Lubick, N. 2008. Dental Offices Contribute to Methyl Mercury Burden. Environ. Sci. Technol. 42, 2712.

Moody, J.R., Paulsen, P.J., Rains, T.C., and Rook H.L. 1976. The Preparation and Certification of Trace Mercury in Water Standard Reference Materials. NBS Special Publication 422, Proc. of the 7th Mat. Research Symp., Gaithersburg, MD. 1974, 267-273. (LaFleur, P.D., Ed.).

Rattonetti, A. 1980. Determination of Hg in Water and in Urine by Furnace Atomic Atomic Absorption Spectroscopy. Instrumentation Laboratory, Wilmington, MA. Report No. 12.

Regional Monitoring Program for Water Quality in San Francisco Bay, 2008. The Pulse of the Estuary, Monitoring and Managing Water Quality in the San Francisco Estuary.

San Francisco Public Utilities Commission (SFPUC), 2003. San Francisco Dental Amalgam Reduction Program. September 2003.

U.S. Environmental Protection Agency (USEPA). 1994a. Method 245.1, Revision 3: Determination of Mercury in Water by Cold Vapor Atomic Absorption Spectrometry. In: Methods for the Determination of Metals in Environmental Samples. EPA-600-R-94-111. May 1994.

U.S. Environmental Protection Agency (USEPA). 1994b. Method 7470A: Mercury in Liquid Waste (Manual Cold-Vapor Technique. September 1994. SW-846 on-line (http://www.epa.gov/wastes/hazard/testmethods/sw846/online/).

U.S. Environmental Protection Agency (USEPA). 1994c. Method 200.8, Revision 5.4: Determination of Trace Elements in Waters and Wastes by Inductively Coupled Plasma-Mass Spectrometry. In: Methods for the Determination of Metals in Environmental Samples. EPA-600-R-94-111. May 1994.

U.S. Environmental Protection Agency (USEPA). 1994d. Method 200.2, Revision 2.8: Sample Preparation Procedure for Spectrochemical Determination of Total Recoverable Elemens. In: Methods for the Determination of Metals in Environmental Samples. EPA-600-R-94-111. May 1994.

U.S. Environmental Protection Agency (USEPA). 1996a. Method 1669:Methods for Sampling Ambient Water for the Determination of Metals at EPA Ambient Criteria Levels. USEPA, Office of Water, Office of Science and Technology, Engineering and Analysis Division (403), 401 M Street SW, Washington, DC 20460, April 1995 with January 1996 revisions.

U.S. Environmental Protection Agency (USEPA). 1996b. Method 3050B: Acid Digestion of Sediments, Sludges, and Soils. December 1996. SW-846 on-line (http://www.epa.gov/wastes/hazard/testmethods/sw846/online/).

U.S. Environmental Protection Agency (USEPA). 2000. Quality Assurance Project Plan for Analytical Control and Assessment Activities in the National Study of Chemical Residues in Lake Fish Tissue. Office of Water, Office of Science and Technology, Engineering and Analysis Division, Washington, D.C. 20460. EPA-823-R-02-006. September 2000.

U.S. Environmental Protection Agency (USEPA). 2001a. Method 1630: Methyl Mercury in Water by Distillation, Aqueous Ethylation, Purge and Trap, and CVAFS. Office of Water, EPA-821-R-01-020. Draft January 2001.

U.S. Environmental Protection Agency (USEPA). 2001b. Appendix to Method 1631 Total Mercury in Tissue, Sludge, Sediment, and Soil by Acid Digestion and BrCl Oxidation. EPA-821-R-01-013. January 2001.

U.S. Environmental Protection Agency (USEPA). 2002. Method 1631, Revision E: Mercury in Water by Oxidation, Purge and Trap, and Cold Vapor Atomic Fluorescence Spectrometry. Office of Water, EPA-821-R-02-019. August 2002.

U.S. Environmental Protection Agency (USEPA). 2007a. Method 7471B, Revision 2: Mercury in Solid or Semisolid Waste (Manual Cold-Vapor Technique). February 2007. SW-846 on-line (http://www.epa.gov/wastes/hazard/testmethods/sw846/online/).

U.S. Environmental Protection Agency (USEPA). 2007b. Method 6020A, Revision 1: Inductively Coupled Plasma-Mass Spectrometry. February 2007. SW-846 on-line (http://www.epa.gov/wastes/hazard/testmethods/sw846/online/).

U.S. Environmental Protection Agency (USEPA). 2007c. Method 7473: Mercury in Solids and Solutions by Thermal Decomposition, Amalgamation, and Atomic Absorption Spectrophotometry. February 2007. SW-846 on-line (http://www.epa.gov/wastes/hazard/testmethods/sw846/online/).

U.S. Environmental Protection Agency (USEPA). 2009. National Study of Chemical Residues in Lake Fish Tissue: Study Design. USEPA, Office of Science and Technology, Washington, D.C. EPA-823-R-09-005.

Zhao, Xiuhong, Rockne, K.J., Drummond, J.L., Hurley, R.K., Shade, C.W., and Hudson, R.J.M. 2008. Characterization of Methyl Mercury in Dental Wastewater and Correlation with Sulfate-Reducing Bacterial DNA. Environ. Sci. Technol. 42, 2780-2786.

INDEX

1,4-Dioxane, **80**, **97**
adsorption, **27**, **60**, **61**, **63**, **65**, **66**, **67**, **138**, **140**, **142**, **144**
albumin, **162**, **170**, **171**
amalgam, **194**, **201**, **202**
Aroclor-1260, **1**, **2**, **6**, **7**, **8**, **10**, **11**, **12**, **13**, **14**, **18**
arsenic, **60**, **61**, **63**, **65**, **66**, **137**, **144**
As(V), **137**, **138**, **139**, **140**, **142**
Bioremediation, **1**, **22**, **40**, **43**, **145**, **146**
Commercial fertilizers, **98**, **99**
contamination, **2**, **20**, **22**, **25**, **27**, **29**, **30**, **31**, **33**, **34**, **35**, **36**, **37**, **38**, **39**, **41**, **61**, **99**, **100**, **106**, **110**, **111**, **113**, **114**, **119**, **130**, **138**, **145**, **148**, **161**, **198**, **199**
descriptor, 162, 166, 167, 168, 169, 171
drug–binding, **162**, **163**, **164**
flow calorimetry, **137**, **138**, **139**, **144**
fuel, **26**, **40**, **41**, **42**, **43**, **44**, **46**, **58**, **72**, **157**, **160**, **173**, **180**, **181**, **183**
groundwater, **22**, **42**, **43**, **46**, **47**, **49**, **50**, **54**, **55**, **56**, **57**, **58**, **80**, **81**, **83**, **85**, **86**, **87**, **88**, **89**, **90**, **95**, **96**, **97**, **125**, **126**, **127**, **137**, **138**, **139**, **175**, **176**, **190**
Groundwater, **57**, **58**, **80**, **86**, **87**, **97**, **125**, **126**, **137**, **173**, **175**, **176**, **177**, **193**
heavy metals, **22**, **98**
hexavalent chromium, **113**, **114**, **115**, **117**, **123**, **124**
HPLC-ICP-MS,, **113**
human, 22, 25, 81, 100, 112, 114, 138, 162, 163, 170, 171
hydrocarbons, 13, 25, 27, 28, 36, 38, 39, 40, 44, 45, 46, 56, 57, 58, 69, 72, 74, 79, 136, 146, 147, 157, 160, 161
Hydrous pyrolysis, **68**, **69**, **78**
ICP-MS, **99**, **112**, **113**, **115**, **118**, **119**, **120**, **121**, **194**, **195**, **196**, **202**, **203**, **204**, **206**, **207**
iron, **42**, **48**, **49**, **53**, **54**, **60**, **61**, **62**, **66**
Lessons Learned, **80**
magnetite, **60**, **61**, **62**, **63**, **64**
mixed planting, 25, 29, 30, 31, 32, 33, 37, 39
MLR, 162, 166, 167
model, **63**, **65**, **125**, **126**, **127**, **128**, **129**, **130**, **131**, **137**, **138**, **139**, **140**, **142**, **150**, **151**, **153**, **155**, **156**, **158**, **161**, **162**, **163**, **164**, **166**, **167**, **168**, **169**, **170**, **174**
MTBE, **42**, **43**, **44**, **46**, **47**, **49**, **50**, **51**, **52**, **53**, **54**, **55**, **56**, **58**, **59**
non-nutritive elements, **98**, **99**
organisms, **1**, **2**, **4**, **5**, **10**, **15**, **16**, **17**, **18**
oxides, **60**, **61**, **67**, **110**
oxygenates, **42**, **43**, **44**, **46**, **50**, **56**, **57**, **58**
PAHs, **69**, **72**, **73**, **74**, **77**, **147**, **160**
petroleum, 24, 25, 27, 28, 35, 36, 38, 39, 40, 41, 44, 45, 46, 58, 72, 73, 78, 136, 145, 146, 147, 148, 149, 151, 152, 153, 154, 155, 156, 157, 158, 160, 161, 175, 176
phytoremediation, **2**, **4**, **5**, **22**, **23**, **24**, **25**, **26**, **36**, **39**, **40**, **41**
QSAR, 162, 163, 164, 170, 171, 172
remediation, **3**, **22**, **40**, **42**, **58**, **60**, **61**, **86**, **135**, **144**, **147**
rhizosphere, **1**, **2**, **4**, **5**, **6**, **7**, **8**, **10**, **11**, **12**, **13**, **14**, **15**, **16**, **17**, **18**, **20**, **21**, **22**, **24**, **25**, **26**, **27**, **33**, **34**, **35**, **36**, **37**, **38**, **39**, **40**
rubber, **68**, **69**, **70**, **72**, **73**, **74**, **75**, **78**

serum, **162**, **170**, **171**
simulation modeling, **138**
soil, **1**, **2**, **3**, **4**, **5**, **6**, **7**, **8**, **9**, **10**, **11**, **12**, **13**, **14**, **15**, **16**, **17**, **18**, **19**, **20**, **21**, **22**, **23**, **24**, **25**, **26**, **27**, **28**, **29**, **30**, **31**, **32**, **33**, **34**, **37**, **38**, **39**, **40**, **41**, **81**, **98**, **99**, **100**, **106**, **108**, **110**, **112**, **114**, **126**, **136**, **142**, **144**, **147**, **148**, **160**, **161**, **174**, **185**, **186**, **189**, **194**, **196**, **202**, **204**, **207**
synthetic fertilizers, **98**
tire, **68**, **69**, **70**, **71**, **72**, **73**, **75**, **76**, **78**
tissue, **194**, **195**, **196**, **204**, **205**, **207**
transformer oil, **1**, **2**, **5**, **6**, **10**, **12**, **14**, **17**, **18**, **20**
Treatment, **11**, **12**, **13**, **14**, **22**, **80**, **83**, **84**, **85**, **86**, **87**, **88**, **89**, **91**, **95**, **97**
UCM, **69**, **72**, **73**, **74**, **75**, **77**
vehicle, **69**, **70**, **73**
water, **2**, **3**, **6**, **8**, **9**, **27**, **28**, **42**, **43**, **44**, **46**, **47**, **48**, **49**, **51**, **52**, **54**, **55**, **56**, **58**, **59**, **60**, **61**, **63**, **68**, **69**, **70**, **71**, **78**, **81**, **82**, **83**, **84**, **85**, **86**, **88**, **94**, **95**, **96**, **97**, **99**, **100**, **102**, **113**, **114**, **115**, **116**, **117**, **120**, **121**, **123**, **124**, **125**, **126**, **127**, **128**, **129**, **130**, **131**, **132**, **133**, **135**, **136**, **138**, **142**, **144**, **146**, **147**, **148**, **160**, **162**, **163**, **167**, **168**, **170**, **175**, **176**, **177**, **181**, **183**, **185**, **186**, **190**, **194**, **196**, **197**, **199**, **201**, **202**, **204**, **206**, **207**